FINAL REPORT

NASA CR72642
APS-5327-R

THE DESIGN AND FABRICATION OF THE BRAYTON ROTATING UNIT OPERATING ON ROLLING ELEMENT BEARINGS (BRU-R)

by B. B. HEATH AND R. A. LUTHER

PREPARED BY

AIRESEARCH MANUFACTURING COMPANY OF ARIZONA
(A DIVISION OF THE GARRETT CORPORATION)

FOR

NATIONAL AERONAUTICS AND SPACE ADMINISTRATION
SEPTEMBER 1969

NASA-LEWIS RESEARCH CENTER
CONTRACT NAS3-9428
LLOYD W. REAM, PROGRAM MANAGER

MP-13432

AIRESEARCH MANUFACTURING COMPANY OF ARIZONA
A DIVISION OF THE GARRETT CORPORATION

NOTICE

This report was prepared as an account of Government sponsored work. Neither the United States, nor the National Aeronautics and Space Administration (NASA), nor any person acting on behalf of NASA:

(a) Makes any warranty or representation, expressed or implied, with respect to the accuracy, completeness, or usefulness of the information contained in this report, or that the use of any information, apparatus, method, or process disclosed in this report may not infringe privately owned rights; or

(b) Assumes any liabilities with respect to the use of, or for damages resulting from the use of any information, apparatus, method or process disclosed in this report.

As used above, "person acting on behalf of NASA" includes any employee or contractor of NASA, or employee of such contractor, to the extent that such employee or contractor of NASA, or employee of such contractor prepares, disseminates, or provides access to, any information pursuant to his employment or contract with NASA, or his employment with such contractor.

Requests for copies of this report should be referred to

National Aeronautics and Space Administration
Office of Scientific and Technical Information
Attention: ATSS
Washington, D.C. 20546

NASA CR-72642
APS-5327-R

FINAL REPORT

THE DESIGN AND FABRICATION OF THE BRAYTON ROTATING UNIT OPERATING ON ROLLER ELEMENT BEARINGS (BRU-R)

by

B. B. Heath and R. A. Luther

AIRESEARCH MANUFACTURING COMPANY OF ARIZONA
A DIVISION OF THE GARRETT CORPORATION

Phoenix, Arizona

Prepared for

NATIONAL AERONAUTICS AND SPACE ADMINISTRATION

September 1969

CONTRACT NAS 3-9428

NASA Lewis Research Center
Cleveland, Ohio
Lloyd W. Ream, Project Manager

FOREWORD

This report was prepared by the AiResearch Manufacturing Company of Arizona, A Division of The Garrett Corporation, to describe the work conducted under Contract NAS3-9428, Brayton Rotating Unit Operating on Oil-Lubricated Rolling Element Bearings (BRU-R), for the National Aeronautics and Space Administration, Lewis Research Center, Cleveland, Ohio.

ABSTRACT

The Brayton Rotating Unit with Rolling Element Bearings (BRU-R) consists of a compressor, turbine, and alternator mounted on a common shaft, supported by two 30-mm angular contact ball bearings, gas-cooled and oil-mist-lubricated within a closed-cycle system. A unique bellows face seal with a hydrodynamic gas bearing on the carbon nose isolates each bearing and prevents oil contamination of the Brayton-cycle working fluid. The bearing and seal designs were confirmed in the BRU-R during a 500-hr and 50-hr endurance test. Seal leakage into the Brayton loop during the test was less than the 0.07 lb of oil specified for a 500-hr operation.

TABLE OF CONTENTS

TABLE OF CONTENTS (Contd)

LIST OF FIGURES

LIST OF FIGURES (Contd)

LIST OF FIGURES (Contd)

LIST OF FIGURES (Contd)

LIST OF FIGURES (Contd)

LIST OF TABLES

FINAL REPORT

THE DESIGN AND FABRICATION OF THE BRAYTON ROTATING UNIT OPERATING ON OIL-LUBRICATED ROLLING ELEMENT BEARINGS (BRU-R)

1. SUMMARY

The AiResearch Manufacturing Company of Arizona, A Division of The Garrett Corporation, has designed, manufactured, and tested a prototype Brayton Rotating Unit operating on oil-lubricated rolling element bearings (BRU-R) and the associated equipment to support the bearing and seal system.

The Brayton Rotating Unit with oil-lubricated rolling element bearings (BRU-R) is a backup unit for the Brayton Rotating Unit (BRU) furnished under Contract NAS3-9427 which operates on gas bearings. The turbine wheel and compressor aerodynamic designs and the alternator design are identical for the BRU-R and the BRU. The BRU-R and its lubrication and cooling system are designed for evaluation and test at the NASA Space Power Facility (SPF) at Plum Brook, Ohio.

The Brayton Rotating Unit with oil-lubricated rolling element bearings (BRU-R) has a radial turbine wheel, a radial compressor, and a four-pole alternator rotor assembled as a group, rotating at 36,000 rpm. The assembly is supported by two 30-mm angular contact ball bearings that are gas-cooled and oil-mist-lubricated by a closed-cycle loop, identified as the BRU-R Lubrication and Cooling System (LCS). Each bearing cavity is isolated from the Brayton cycle thermodynamic loop by a hydrodynamic face seal. This seal is a carbon-nose, bellows-supported design with a hydrodynamic gas bearing geometry located on the inside diameter of the carbon nose. The face seal has rubbing contact with the tungsten carbide rotor at speeds below 5000 to 8000 rpm. As the speed increases, the gas bearing will become hydrodynamic and

generate a gas film-thickness of 0.000150 in. at the design speed of 36,000 rpm. To prevent oil from migrating into the Brayton cycle thermodynamic loop while the seal is hydrodynamic and noncontacting, a differential pressure is maintained across the hydrodynamic face seal to promote gas flow into the bearing cavity from the thermodynamic loop. The deviation controller of the BRU-R lubrication and cooling system maintains a set differential pressure of 0.45 psi between the pressure at the hub of the compressor impeller and the bearing cavity.

A radial labyrinth seal is located between each bearing and the alternator cavity to prevent oil-mist from entering the alternator stator section. In addition, the alternator cavity is supplied with clean dry cooling gas from the BRU-R Lubrication and Cooling System at a higher pressure than the bearing cavity, thereby continually purging the alternator cavity through the labyrinth seals.

The BRU-R Lubrication and Cooling System is a closed, hermetically sealed loop that provides a gas and oil-mist mixture to the bearings. The Lubrication and Cooling System utilizes the same gas as the Brayton cycle thermodynamic loop, i.e., a mixture of helium-xenon with a molecular weight of 83.8. A two-stage water-cooled compressor driven by an electric motor compresses the gas and delivers it to the lubricator tank where the flow is split, part going to purge the alternator, and part to an oil injection section where a positive displacement pump injects a controlled amount of oil into the gas stream. These gas flows are delivered to the BRU-R. The gas and oil-mist mixture is drained from the bottom of the BRU-R and passed through two control valves which regulate the bearing cavity pressure. The gas and oil-mist mixture is filtered to remove the oil and the clean gas supplied to the inlet of the compressor to complete the closed loop.

The bearings used in the BRU-R are 30-mm, M-50 tool steel angular-contact ball bearings with a contact angle of 22 deg and are installed in resilient mounts having a stiffness of 30,000 to 40,000 lb/in. The bearings are spring-loaded to maintain an axial preload of 80 to 100 lb. The bearings were evaluated in a test program that included investigation of cooling-gas/oil-mist ratios and 400:1 by weight was selected. Five bearings were tested for a total of 1864 hr at a design speed of 36,000 rpm. This included a final test of 1058 hr with no evidence of wear.

The hydrodynamic face seal design incorporates a Raleigh stepped-sector gas bearing in conjunction with a conventional sealing land on the face of a bellows-mounted carbon nose. The gas bearing feature permits the seal to operate with a very low power loss, a minute controlled leakage and practically zero wear. The conventional sealing land on the nose provides static sealing. The gas bearing geometry consists of 18 equally spaced pads, separated by a radial slot of 1 deg in width and 0.010 in. depth and separated from the sealing land by an annular slot width of 0.020 in. and 0.010-in. depth. The step portion of the geometry has a depth of 0.0002 in. and has a width of 4 deg.

The seal evaluation test program consisted of evaluating a contacting carbon-nose seal as a backup and two designs of hydrodynamic face seals: One with the gas bearing geometry on the inside and the other with it on the outside. The tests of the "backup" rubbing contact design demonstrated that the seal would be adequate for use if necessary and would have an estimated life of 5000 hr. The power loss, however, was approximately five times as high as the gas bearing designs. The hydrodynamic seal test evaluation selected the design with the gas bearing geometry on the inside diameter, with the oil-mist environment located on the outside diameter. A seal of this design with a tungsten carbide rotor was operated at a speed of 36,000 rpm for a period of 1000 hr, including 79 hydrodynamic starts and stops with no measurable wear.

The inspection and acceptance test of the BRU-R and the Lubrication and Cooling System consisted of three separate tests: 500-, 50-, and 5-hr. The 500-hr test was performed with dummy inertial masses replacing the aerodynamic components. The BRU-R was driven with an air turbine motor. An electrical heater was attached to the turbine end to simulate the thermal input equivalent to operation at a 6.0-kw_e power level. The turbine back shroud was maintained at a temperature of 900° to 950°F. The unit was operated for a total of 502.5 hr at a design speed of 36,000 rpm and for 10 min at an overspeed condition of 120 percent; 68 starts were made during the test. Seal leakage measurements were performed by withdrawing gas samples from the turbine cavity and analyzing the samples on an infrared spectrophotometer with a 10-meter gas cell. These measurements showed oil leakage less than the maximum permissible of 0.070 lb during 500 hr, with no measurable wear on disassembly inspection.

The BRU-R was reassembled with new bearings and seals and the 50-hr test was performed. As in the 500-hr test, dummy inertial masses were substituted for the aerodynamic components, and the BRU-R was driven at a speed of 36,000 rpm. The electrical heater was not used in this test. Seal leakage measurements were again performed by drawing a gas sample from the turbine cavity. Analysis on the infrared spectrophotometer revealed that there was no measurable oil leakage past the hydrodynamic face seal. The BRU-R was reassembled with the turbine wheel and compressor impeller and operated at design speed of 36,000 rpm for 5 hr. The BRU-R was then operated for 10 min at a design overspeed condition of 120 percent.

2. INTRODUCTION

This report, submitted by the AiResearch Manufacturing Company of Arizona, A Division of The Garrett Corporation, describes the results of a program performed under NASA-Lewis Research Center, Contract NAS3-9428.

Originally, the program was directed toward the design and fabrication of a radial-flow turbocompressor and the provision of a set of research compressor components. The radial-flow turbocompressor was to operate in a Brayton cycle, using argon as the working fluid with a turbine inlet temperature of 1950°R. The design consisted of a radial-flow turbine wheel and compressor impeller mounted on the same shaft and supported by oil-lubricated rolling-element bearings. During the early design stages, the program was redirected to provide a Brayton Rotating Unit with oil-lubricated rolling element bearings (BRU-R)--a backup for the Brayton Rotating Unit (BRU) which operates on gas bearings (NASA Contract NAS3-9427). The second major task of the contract was the set of research compressor components to provide an improved impeller design with backward curved exit blading and a scroll to retrofit the Compressor Research Package fabricated under NASA Contract NAS3-2778.

The turbine and compressor aerodynamic and the alternator designs are identical for the BRU-R and the BRU. However, the BRU-R has two angular contact ball bearings that are gas-cooled and lubricated with a MIL-L-7808 oil mist. There are two seals that isolate each bearing cavity and prevent the oil-mist from entering the alternator cavity and the Brayton cycle thermodynamic loop. A maximum of 0.07 lb of oil leakage into the Brayton cycle thermodynamic loop in 500 hr of operation was permitted. The oil-mist and gas-cooling was provided to the BRU-R in a closed-loop Lubrication and Cooling System (LCS).This system consists of a compressor, an oil injection system, filters, and associated controls to deliver 0.0011 lb/min of oil to each bearing. The

design requirements of the BRU-R are shown in Table I. The BRU-R and its lubrication and cooling system is intended for operation at the NASA Space Power Facility (SPF) at Plum Brook, Ohio.

Appendix A describes the preliminary mechanical design and bearing analysis that had been performed on the radial flow turbocompressor before that program was redirected toward a Brayton Rotating Unit with oil-lubricated rolling element bearings.

Appendix B documents the design history of the closed-cycle lubrication and cooling system.

Appendix C details the design of the backward-curved compressor impeller for the retrofit of the Compressor Research Package.

Appendix D contains drawings of the BRU-R Lubrication and Cooling System, the Carbon Nose Seal, and the thermocouple locations.

TABLE I

SYSTEM REQUIREMENTS

	Condition A	Condition B	Condition C
Alternator output, kw_e	2.25	6.0	10.5
Cycle working fluid	Helium-Xenon with molecular weight of 83.8		
Mass flow rate, lb/sec	0.418	0.796	1.32
Turbine inlet temperature, °R	2,060	2,060	2,060
Turbine pressure ratio	1.73	1.75	1.75
Turbine inlet pressure, psia	13.7	25.8	43.2
Compressor inlet temperature, °R	540	540	540
Compressor pressure ratio	1.88	1.9	1.9
Compressor inlet pressure, psia	7.6	14.2	23.7
Design operating life, years	5	5	5
Test operating life (TBO) (bearings and seals), hr[b]	500	500	500
Speed capability, % design	0 to 120[a]		
Speed at design, rpm	36,000	36,000	36,000
Bearing lubricant and coolant	MIL-L-7808 or equivalent		
Alternator and turbine seal coolant	Dow Corning - 200		
Temperature (supply), °R	530	530	530
Flow, lb/hr max	To be determined by contractor		
Bearing lubricant objectives			
Flow, lb/hr max	To be determined by contractor		
Exit temperature, °R max	836	836	836
Internal leakage		c	

[a]Sustain 20 percent overspeed for 5 min at end of 500 hr of test operation (a design objective).

[b]Refers only to minimum bearing and seal life before replacement is required (a design objective).

[c]The unit will be designed with the objective of obtaining the lowest possible leakage of lubricant into the cycle working fluid. Total accumulated leakage of MIL-L-7808 oil into the cycle working fluid shall not exceed 0.07 lb of oil maximum for the 500 hr of operating-life of the bearings and seals.

3. BRU-R CONFIGURATION

The Brayton Rotating Unit with Rolling Element Bearings (BRU-R) consists basically of a compressor, a four-pole alternator, and a turbine mounted on the same shaft and supported on gas-cooled, oil-mist-lubricated angular contact ball bearings. The BRU-R is shown in Figure 1; the disassembled structure in Figure 2; and the cross-section in Figure 3. The BRU-R is similar to the BRU with gas bearings. In fact, the turbine and compressor aerodynamic designs and alternator designs are identical for the BRU-R and the BRU.

3.1 BRU-R Rotating Group

The BRU-R rotating group (Figure 4) consists of an alternator rotor that is straddle-mounted between ball bearings with the radial-flow compressor impeller overhung at one end of the shaft and the radial-flow turbine wheel overhung at the other end. The compressor impeller and the turbine wheel are attached to the alternator rotor through 1.06-in. dia curvic couplings and secured with a tie-bolt and self-locking nut. The bearing on each end of the alternator rotor is held against a shoulder on the alternator rotor with a "round nut" that is locked to the rotor with a retaining ring. The round nut also secures the seal rotor. A soft copper rotor spacer is placed between the seal rotor and the round nut to prevent distortion of the seal rotor under the clamping force. The "arm" of the retaining ring must be inserted through one of the four holes in the alternator rotor and into one of the six slots of the round nut. This installation requires that the copper rotor spacer must be lapped to achieve this alignment. The assembled BRU-R rotating components are shown in Figure 5.

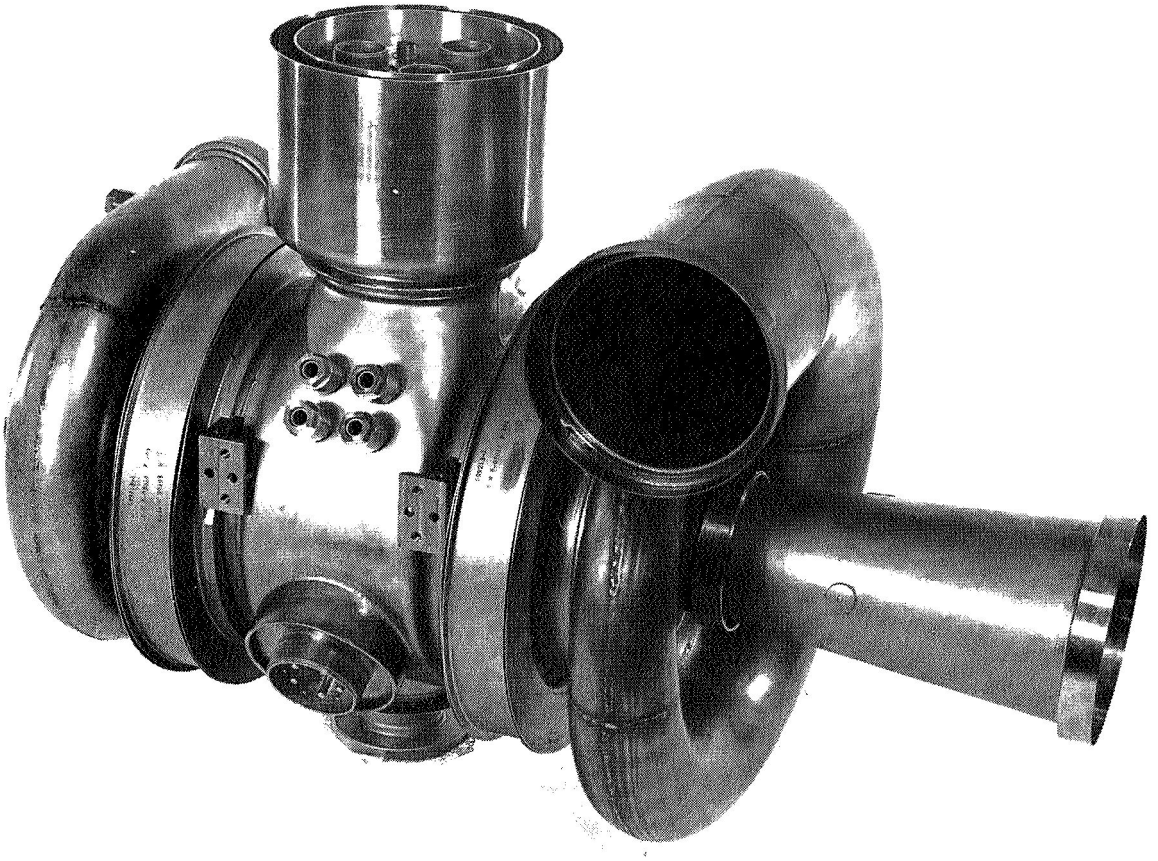

BRAYTON ROTATING UNIT WITH
ROLLING ELEMENT BEARINGS (BRU-R)

FIGURE 1

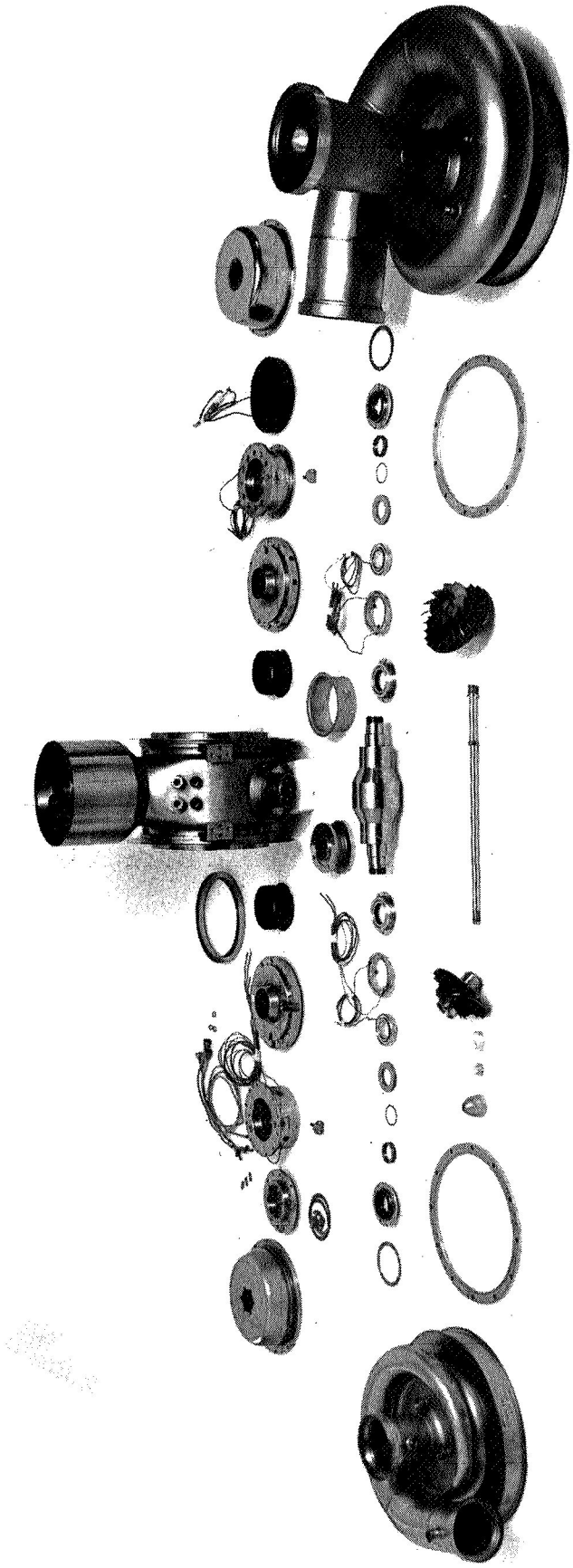

DISASSEMBLED BRU-R PARTS

FIGURE 2

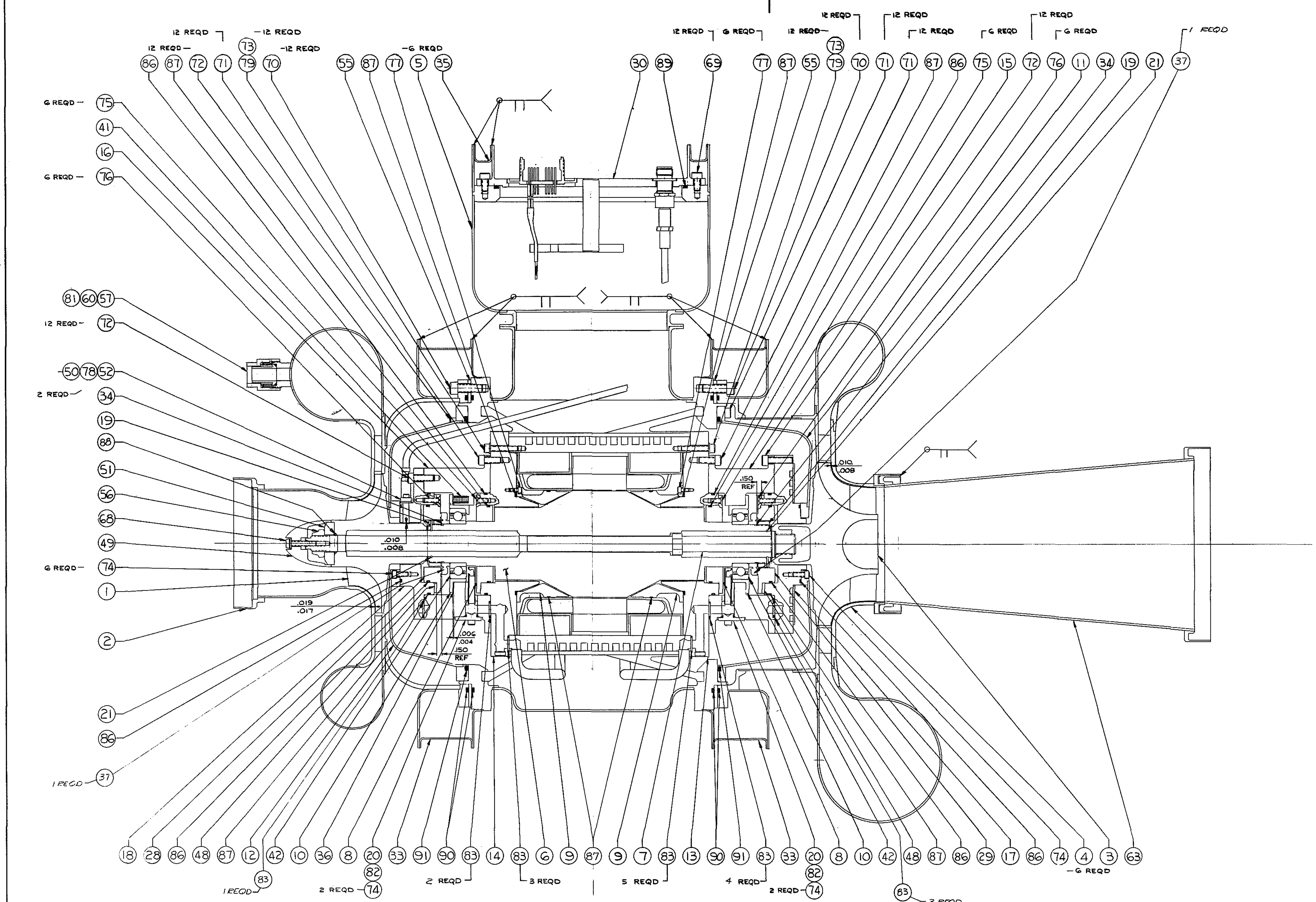

SECTION A-A

QTY REQD -11	QTY REQD -1	ITEM NO.	PART NO.	DESCRIPTION
	2	91	362-557-9003	GASKET
	4	90	NAS1593-174	PACKING, "O" RING
	1	89	NAS1593-162	PACKING, "O" RING
	1	88	NAS1593-014	PACKING, "O" RING
	8	87	NAS1593-041	PACKING, "O" RING
	7	86	NAS1593-035	PACKING, "O" RING
	2	85	NAS1593-015	PACKING, "O" RING
	2	84	NAS1593-013	PACKING, "O" RING
	19	83	NAS1593-012	PACKING, "O" RING
	2	82	NAS1595-3	PACKING, "O" RING
	6	81	S8057-AP-173	PACKING, "O" RING
	3	80	S8057-AP-260	PACKING, "O" RING
	24	79	NAS620C8	WASHER, FLAT
	6	78	NAS1352-04H6P	SCREW, CAP, SOCKET HEAD
	12	77	NAS1352C04H4	SCREW, CAP, SOCKET HEAD
	12	76	S8806-632-8	SCREW, FLAT HEAD, 100°
	12	75	S8806-632-6	SCREW, FLAT HEAD, 100°
	16	74	MS24676-2	SCREW, CAP, SOCKET HEAD
	24	73	MS24674-11	SCREW, CAP, SOCKET HEAD
	36	72	NAS1351-3H10P	SCREW, CAP, SOCKET HEAD
	36	71	MS24673-2	SCREW, CAP, SOCKET HEAD
	28	70	MS24675-22	SCREW, CAP, SOCKET HEAD
	12	69	MS24673-1	SCREW, CAP, SOCKET HEAD
	1	68	655-601-9212	SCREW, SELF LOCKING
	2	67	MS21318-7	SCREW, DRIVE, ROUND HEAD
		66	SEE NDC699180-1	PLATE, IDENTIFICATION
		65		
		64		
	1	63	699899-1	DIFFUSER ASSY, TURBINE
		62		
	3	61	699871-1	NUT, TUBE COUPLING
	6	60	699870-1	NUT, TUBE COUPLING
		59		
	3	58	699798-1	ADAPTER, TUBE
	6	57	699797-1	ADAPTER, TUBE
	1	56	699776-1	NUT, SELF LOCKING
	2	55	699762-1	SPACER, SCROLL
		54		
		53		
	3	52	699746-2	PROBE OUTLINE, CAPACITANCE
	1	51	699739-1	WASHER, THRUST
	3	50	699735-1	SPACER, PROBE
	1	49	699705-1	SPINNER, IMPELLER
	A/R	48	699645-1,2,3,4,5	SPACER, SEAL
10		47	S9053-1-013	INSULATION, SLEEVING
20		46	S9051-5-016	INSULATION, SLEEVING
20		45	699181-15	SOCKET
20		44	699181-13	WIRE, STRANDED
	10	43	699181-11	THERMOCOUPLE ASSY, CONTACT
	2	42	358546	BEARING, BALL, ANGULAR CONTACT
	12	41	114834	SPRING-HELICAL, COMPRESSION
		40		
		39		
		38		
	2	37	699225-1	ROTOR, SEAL
	A/R	36	699216-1,2,3	SHIM
	1	35	699215-1	CHANNEL, SEALING
	2	34	699214-1	SPACER, ROTOR
	2	33	699213-1	SEAL, SCROLL
	1	32	699212-1	SEAL, DRAIN
	1	31	699211-1	FLANGE ASSY, DRAIN
	1	30	699209-1	COVER ASSY, INSTRUMENTATION
	1	29	699208-1	SEAL ASSY (C.C.W)
	1	28	699207-1	SEAL ASSY (C.W)
	2	27	699206-3	ADAPTER, TUBE
	2	26	699206-2	ADAPTER, TUBE
	2	25	699206-1	ADAPTER, TUBE
	2	24	699205-3	NUT, TUBE COUPLING
	2	23	699205-2	NUT, TUBE COUPLING
	2	22	699205-1	NUT, TUBE COUPLING
	2	21	699204-1	RING, RETAINING
	2	20	699203-1	NOZZLE ASSY, LUBE
	2	19	699202-1	NUT, ROUND
	1	18	699201-1	CARRIER ASSY, SEAL, COMPRESSOR
	1	17	699200-1	CARRIER ASSY, SEAL, TURBINE
	1	16	699199-1	CARRIER ASSY, BRG, COMPRESSOR
	1	15	699198-1	CARRIER ASSY, BRG, TURBINE
	1	14	699197-1	END BELL ASSY, COMPRESSOR
	1	13	699196-1	END BELL ASSY, TURBINE
	1	12	699195-1	SHROUD ASSY, COMPRESSOR
	1	11	699194-1	SHROUD ASSY, TURBINE
	2	10	699193-1	MOUNT ASSY, BEARING
	2	9	699192-1	SHROUD, ROTOR
	2	8	699011-1	SEAL, RADIAL
	1	7	699189-1	SHAFT, TENSION
	1	6	699188-1	ROTOR, ALTERNATOR
	1	5	699186-1	HOUSING ASSY, ALTERNATOR
	1	4	699185-1	SCROLL ASSY, TURBINE
	1	3	699184-1	WHEEL, TURBINE
	1	2	699183-1	SCROLL ASSY, COMPRESSOR
	1	1	699182-1	IMPELLER, COMPRESSOR

LIST OF MATERIAL

AIRESEARCH MANUFACTURING COMPANY OF ARIZONA
A DIVISION OF THE GARRETT CORPORATION
PHOENIX, ARIZONA

BRAYTON ROTATING UNIT ASSEMBLY, ROLLING ELEMENT BEARINGS

SIZE J | CODE IDENT NO. 99193 | DWG NO. 699181

SCALE 1/1 | SHEET 1 OF 1

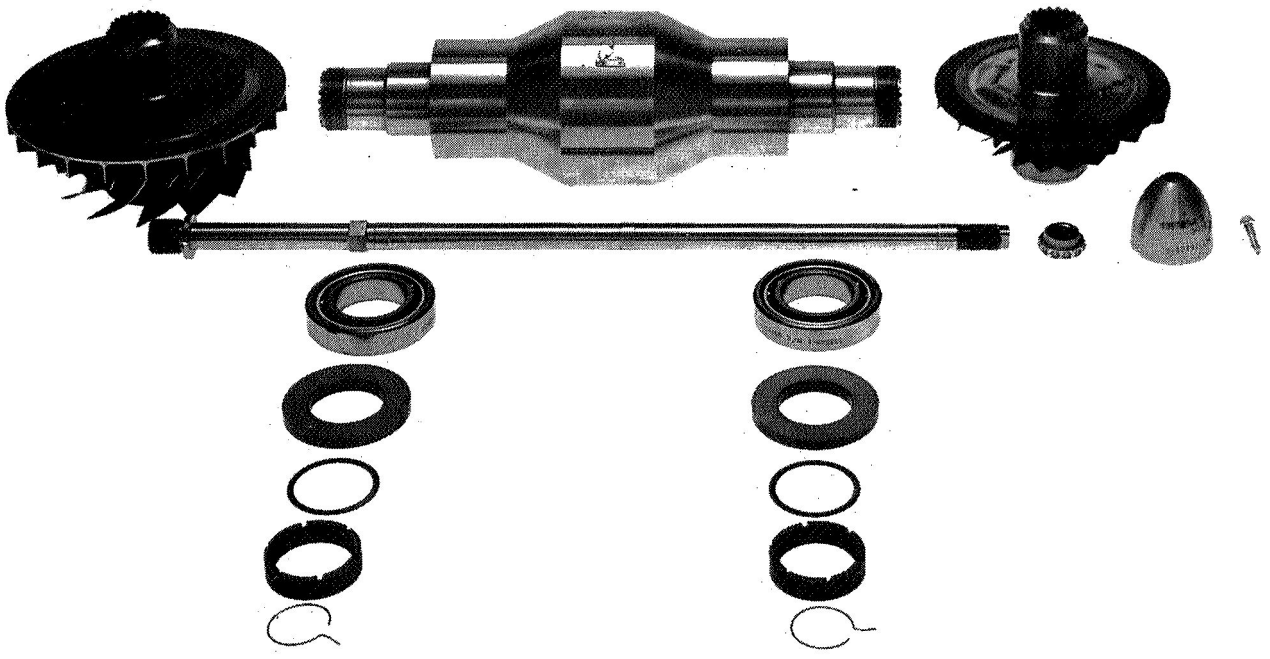

BRU-R ROTATING COMPONENTS

FIGURE 4

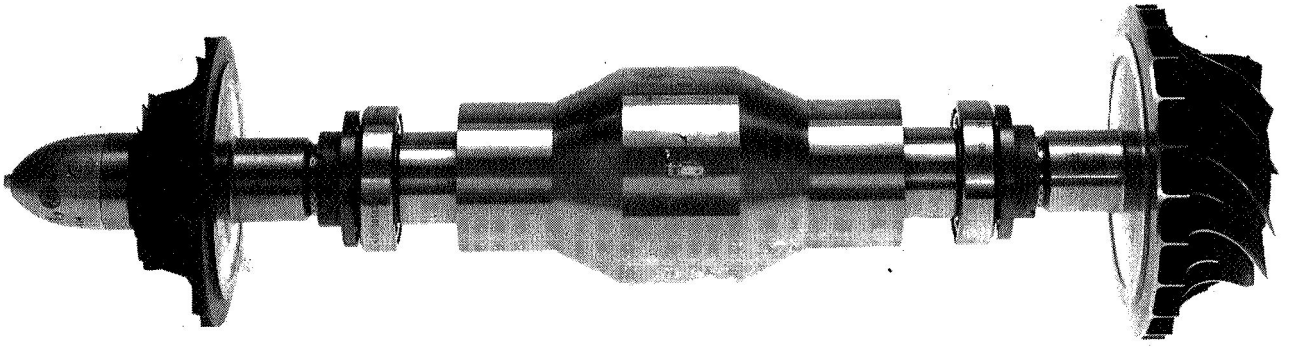

ASSEMBLED BRU-R ROTATING GROUP

FIGURE 5

MP-22569

3.2 Turbine and Compressor

The turbine wheel is a 4.97-in.-dia radial-flow wheel operating over a pressure ratio of 1.87, has a demonstrated performance of 90 percent, and is assembled with a blade clearance between the wheel and the scroll of 0.008 to 0.010 in. This blade clearance increases by 0.0135 to 0.0153 in. due to thermal expansion as the BRU-R is operated to the thermodynamic cycle conditions of the system requirements. For example, if the blade clearance is initially set at the nominal value of 0.009 in. during assembly, the blade clearance will increase to 0.0225 in. when the BRU-R is operated to a system condition of 2.25 kw_e with a turbine inlet temperature of 2060°R. As will be discussed in Paragraph 3.4, the turbine end bearing is "fixed" while the compressor end bearing is "free" to float and accommodate thermal expansion.

The compressor impeller has a 4.25-in. diameter and backward-curved blades. The design pressure ratio is 1.9, and the impeller has a demonstrated maximum efficiency of 82 percent at design corrected speed. The compressor impeller is assembled with a blade clearance of 0.017 to 0.019 in. This decreases by 0.0076 to 0.0095 due to thermal expansion as the BRU-R is operated under "hot" conditions. For example, if the compressor blace clearance is initially set at the nominal value of 0.018 in., the decrease will be to 0.0103 in. when the BRU-R is operated to a system condition of 2.25 kw_e with a turbine inlet temperature of 2060°R and a compressor inlet temperature of 540°R.

3.3 Alternator

The BRU-R four-pole alternator utilizes a solid rotor (Figure 6). The stator has a conventional three-phase ac winding, with two stationary field coils located outside. The magnetic flux generated by the field coils passes into the rotor across a secondary air gap at the end, through the north pole of the machine, around the magnetic frame, and re-enters the rotor at the south pole. Then it passes again across

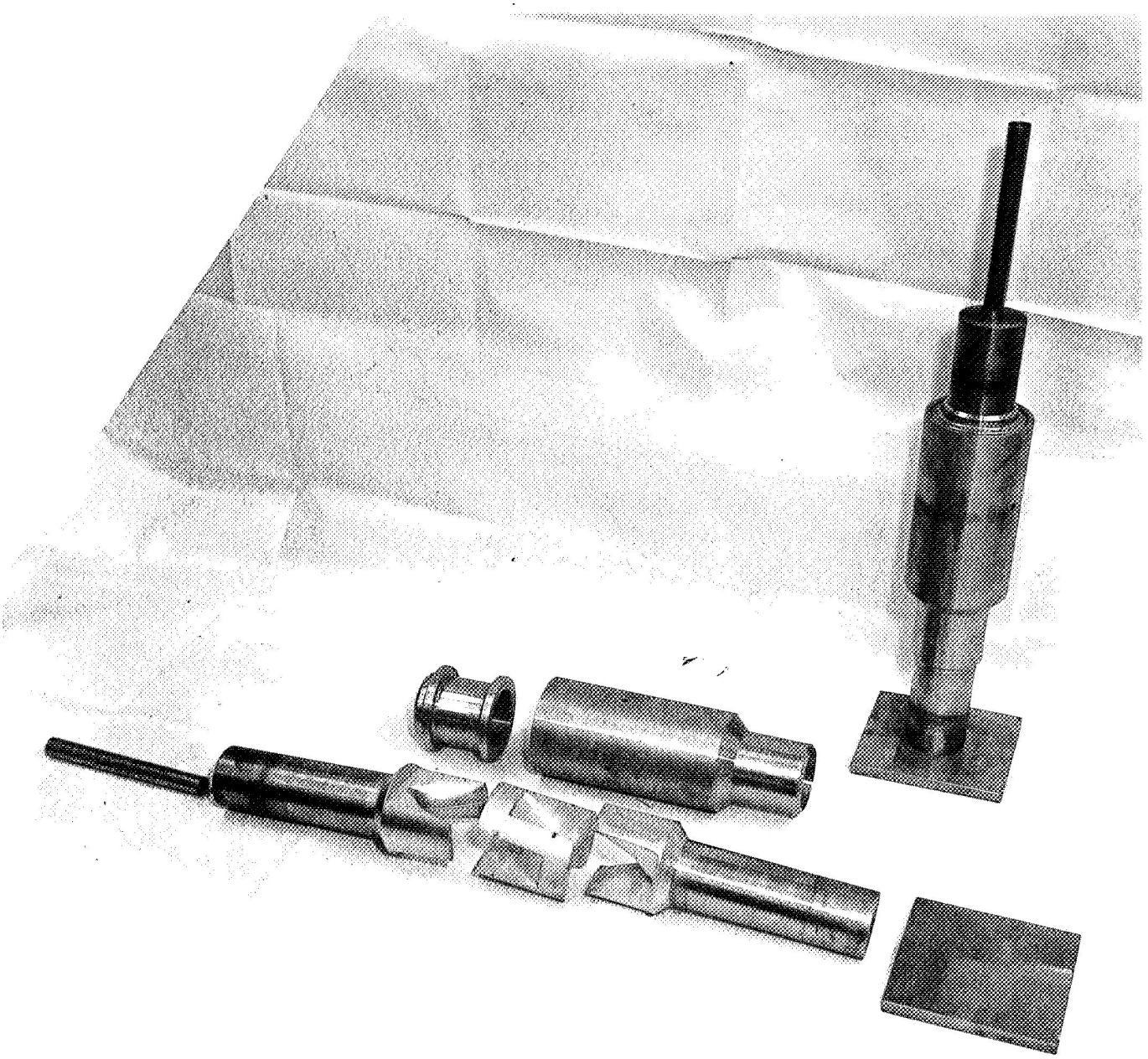

BRU-R ALTERNATOR ROTOR CONSTRUCTION

FIGURE 6

a secondary air gap at the end of the rotor to complete the flux circuit. The construction of the rotor consists of two sections of SAE 4340 steel and a center segment of precision cast Inconel 718. The three pieces are positioned by the use of special tooling, while the center rotor segment is brazed into place.

3.4 Bearings and Seals

The BRU-R operates on two gas-cooled, oil-mist-lubricated angular contact ball bearings. Each bearing is resiliently mounted in a four-lobe flex-mount. The turbine end bearing in the flex-mount is fixed in relation to the alternator housing, and the compressor end bearing in its flex-mount is "free" to move axially to account for thermal expansion. The resilient mount adjacent to the compressor is spring-loaded to provide an axial preload of 80 to 100 lb on both bearings. The axial preload is established during assembly, realizing that thermal expansion will decrease the preload as the BRU-R is operated to the thermodynamic cycle conditions. The thermal expansion at the compressor bearing is 0.0089 to 0.0104 in. for power levels of 2.25 to 10.5 kw_e. The springs that provide the preload have a rate of approximately 700 lb/in. Thermal expansion would produce a maximum preload reduction of 7.28 lb. As discussed in Section 5, as the preload decreases, the ball spin/roll ratio increases with a greater tendency for skidding and subsequent wear. However, the preload design range was recommended to be 60 to 100 lb, but in order to compensate for thermal expansion, assembly procedures were established to give preloads on the high side of this range; that is, 80 to 100 lb.

Each bearing is individually cooled and lubricated by a gas and oil-mist mixture circulated through a closed-loop lubrication and cooling system. Each bearing is provided with 0.0011 lb/min of MIL-L-7808 oil. The gas and oil-mist is scavenged from each bearing cavity and through a duct at the bottom of the BRU-R. Two noncontacting seals surround each bearing cavity to prevent the oil-mist from entering the alternator cavity and the Brayton cycle loop, as shown in Figure 7.

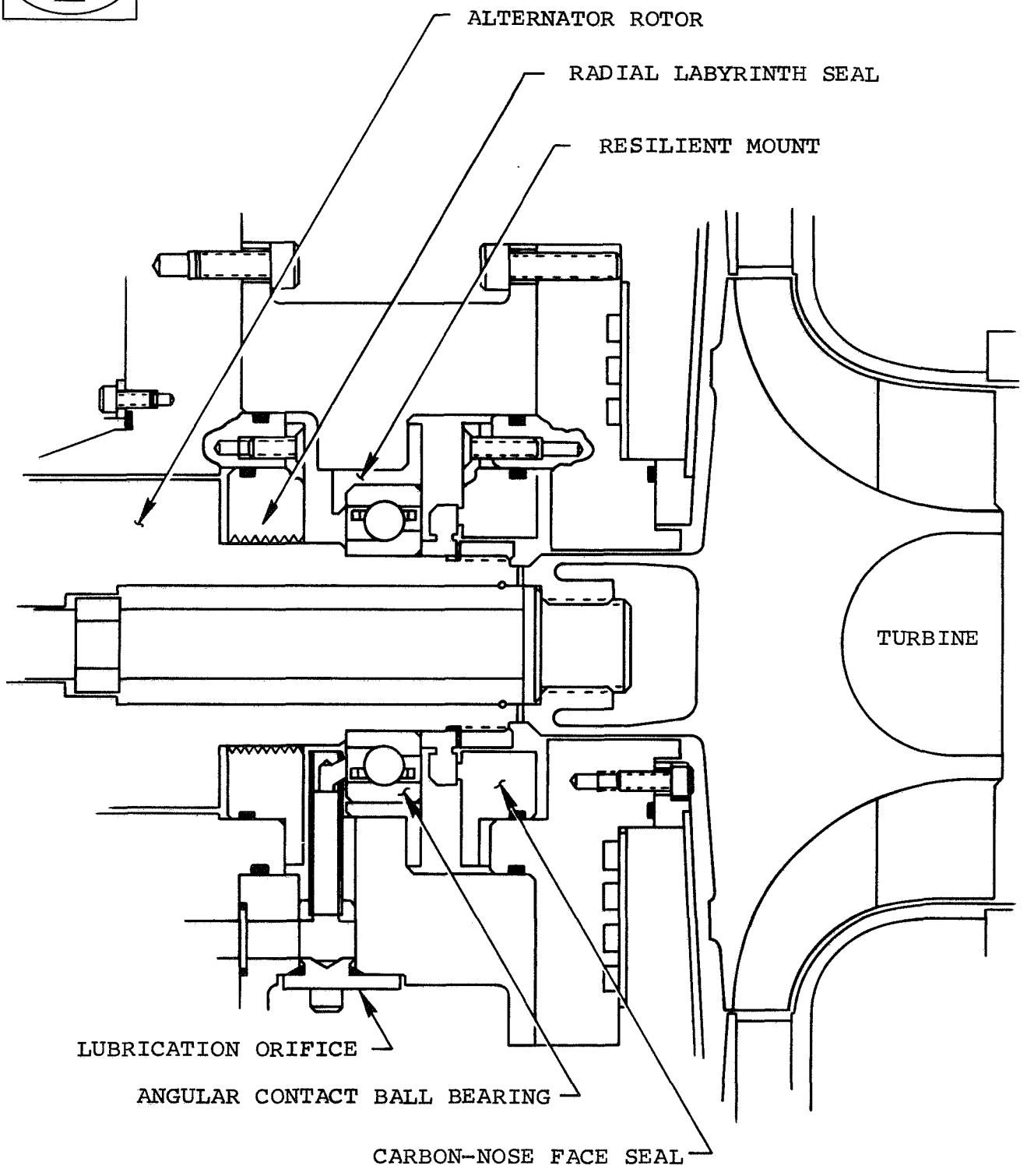

BRU-R TURBINE BEARING AND SEAL CONFIGURATION

FIGURE 7

The angular contact bearings have a bore diameter of 30 mm, an outside diameter of 55 mm, and a width of 13 mm. M-50 tool steel is used in the ring and the balls. The ball diameter is 9/32 in. The inner- and outer-race curvatures are 56 and 54 percent, respectively, of the ball diameter. The angular contact ball bearing and the resilient mount are shown in Figure 8. The bearing resilient mount has a stiffness of 30,000 to 40,000 lb/in.

There are two seals that isolate each bearing and prevent leakage into the Brayton cycle loop: one is a radial-gap labyrinth seal and the other is a carbon-nose bellows face seal. Separating each bearing cavity from the alternator cavity is a radial gap seal, a nonrotating labyrinth type with a fixed-radial clearance (Figure 9). The pressure in the alternator cavity is higher than that in the bearing cavity, resulting in a "controlled leakage" from the alternator across the radial gap into the bearing cavity. The seal located between the compressor impeller and the adjacent bearing, as well as that between the turbine wheel and its adjacent bearing, is a carbon-nose, bellows face seal. This seal and its rotor are shown in Figure 10. A Rayleigh stepped-sector gas bearing is incorporated in the carbon nose of the face seal. The seal differential pressure control of the lubrication and cooling system controls the pressure in the bearing cavity to give a pressure that is less than that at the compressor impeller hub. The pressure at the turbine wheel hub is slightly higher than that at the compressor impeller, so that there is always a "controlled leakage" across the face seal into the bearing cavity.

3.5 Alternator Housing Assembly

The alternator housing assembly contains the instrumentation receptacle housing, the alternator stator and field coils, the power output receptacle, all coolant supply fittings, and all pressure tap fittings. The alternator housing is the nucleus to which all structural ties are made. The compressor end is shown in Figure 11. To

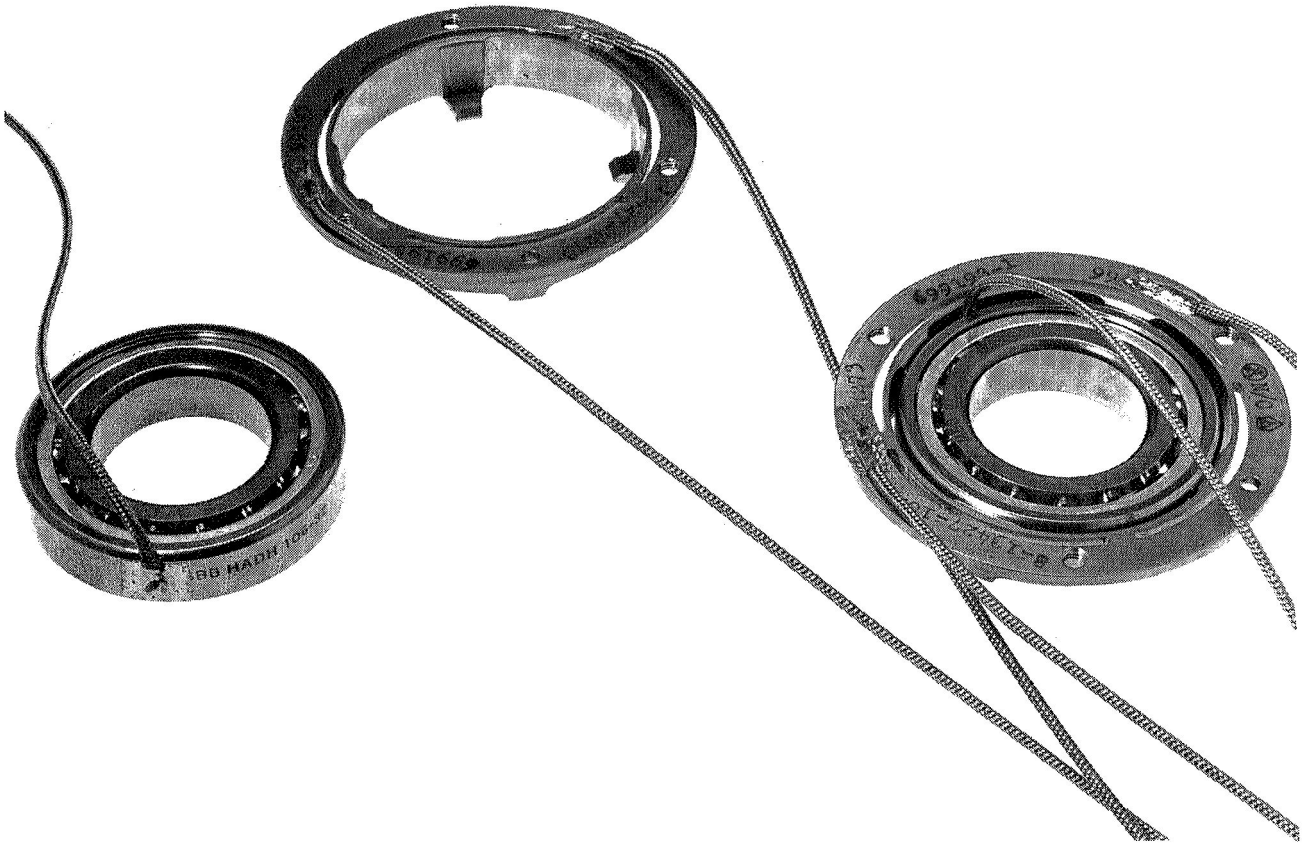

ANGULAR CONTACT BALL BEARING AND
RESILIENT MOUNTING

FIGURE 8

LABYRINTH SEAL-KAPTON LANDS

FIGURE 9

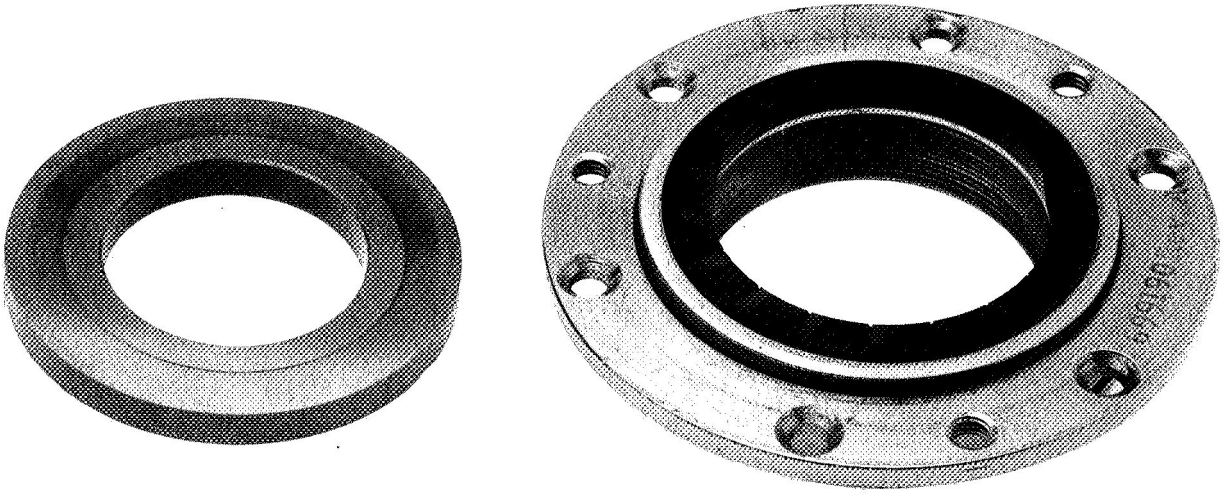

HYDRODYNAMIC FACE SEAL

FIGURE 10

MP-21107

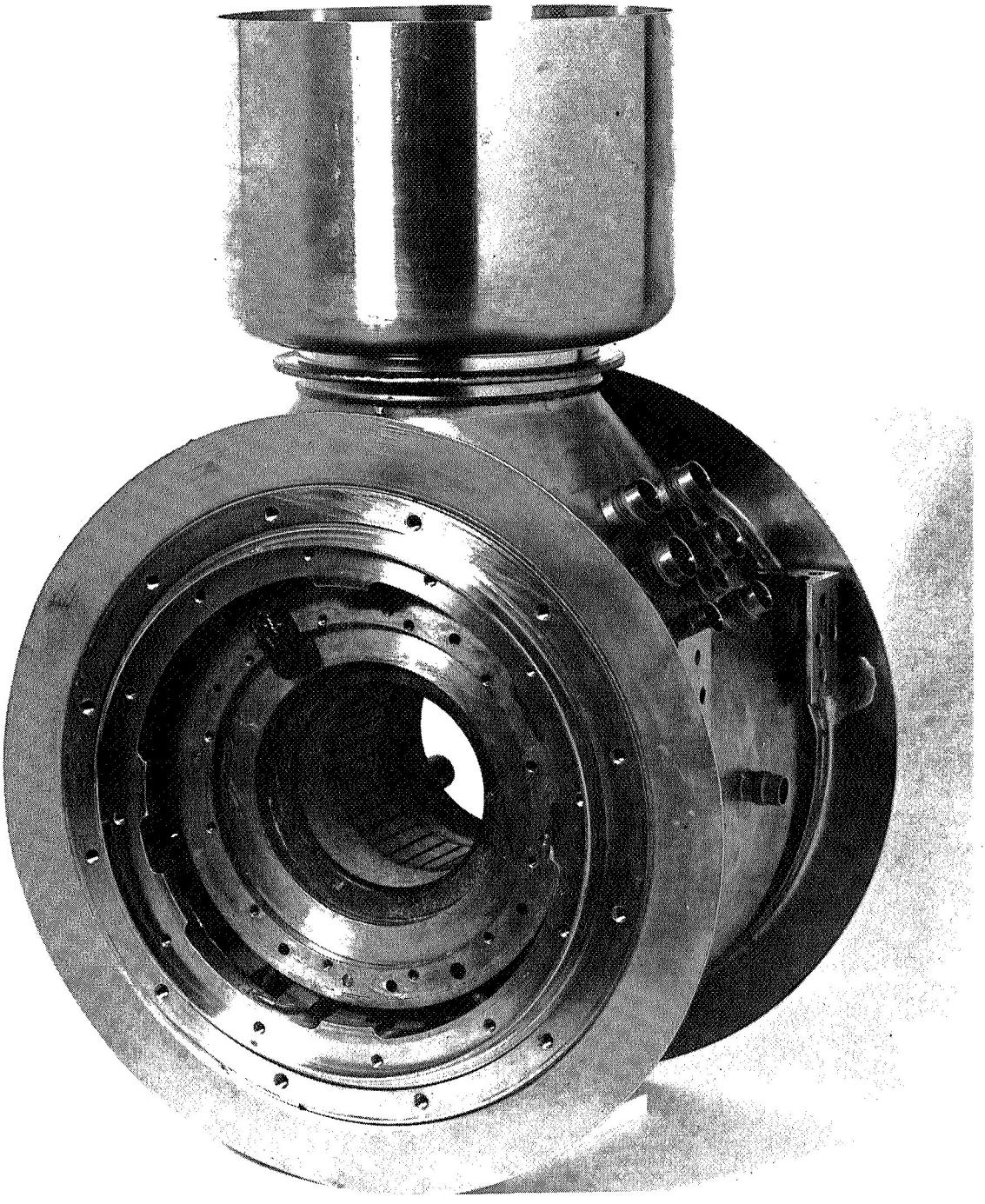

ALTERNATOR HOUSING ASSEMBLY
(COMPRESSOR SECTION)

FIGURE 11

each end, an ingot iron end-bell is bolted to complete the flux path of the alternator. To these, the bearing carrier assemblies, providing the support and positioning of the alternator rotor, are bolted. The seal carrier assemblies that position the carbon-nose seals are bolted to the bearing carrier assemblies. The turbine seal carrier assembly has internal cooling passages for extraction of heat from the turbine side. The housing assembly has piloted diameters for positioning the turbine and compressor scrolls. The blade clearances for the scrolls are obtained by machining scroll spacers. Flanges are provided on the alternator housing and on the scrolls for the attachment of sealing channels. The provision for these sealing channels is also made at the instrumentation receptacle housing and at the bearing drain flange and are welded to the flanges during final preparation for test operation.

The BRU-R is instrumented with 32 thermocouples (Figure 12) and three capacitance probe speed pickups. These are located at the compressor end of the BRU-R (Figure 12).

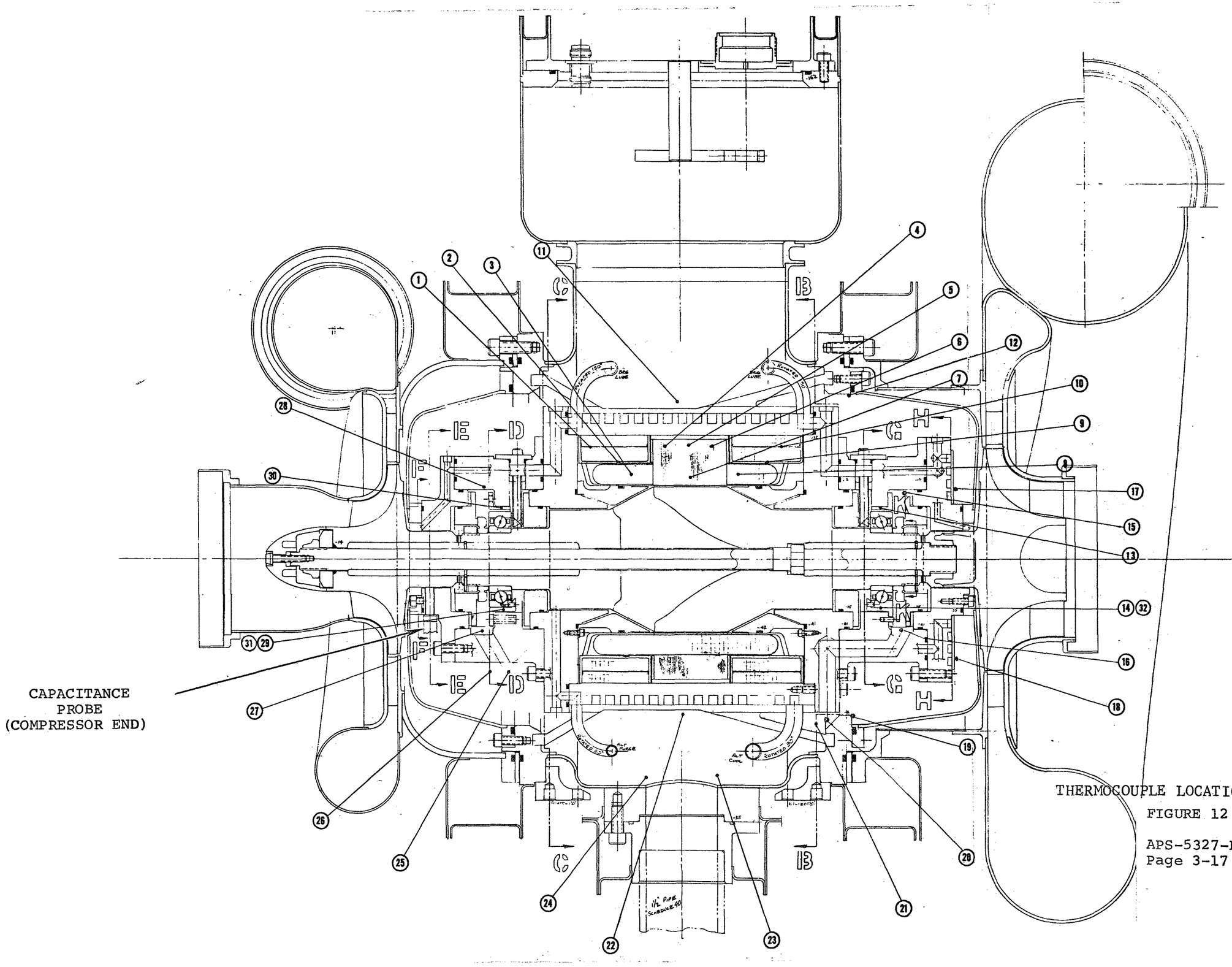

THERMOCOUPLE LOCATIONS BRU-R

FIGURE 12

4. BRU-R LUBRICATION AND COOLING SYSTEM

Each bearing of the BRU-R is lubricated and cooled by a gas and oil-mist mixture that is circulated in a closed, hermetically sealed loop. The design of the BRU-R Lubrication and Cooling System (LCS) evolved from several preliminary design configurations, as detailed in Appendix B. This section discusses the final design that was used in the test program reviewed in Section 10.

The BRU-R Lubrication and Cooling System consists of a two-stage water-cooled compressor driven by an electric motor, a positive displacement oil-lubricator pump and reservoir, a seal differential pressure control, loop instrumentation and control panels, and associated filters, heat-exchangers, and valves. The Lubrication and Cooling System injects a controlled amount of oil into a gas stream and directs this oil-mist and gas mixture to the bearings. The system also provides clean dry purging gas to the alternator cavity. The seal differential control regulates the pressure of the bearing cavity lower than the compressor hub, preventing oil-mist from migrating into the Brayton cycle. The system filters the oil from the gas stream, compresses the gas, filters it again, and returns the gas to the oil injector. The BRU-R and the Lubrication and Cooling System are designed for operation at the NASA Space Power Facility (SPF) at Plum Brook.

4.1 Lubrication and Cooling System Description

A schematic of the Lubrication and Cooling System is shown on Drawing 699220 in Appendix D. The major components are the compressor tank, the lubricator tank, the seal differential pressure control, and the control panels. In the NASA Space Power Facility, the Lubrication and Cooling System will contain the same gas as used in the Brayton cycle loop--a helium-xenon mixture of molecular weight 83.8. During development testing, argon was employed as the working fluid.

Referring to Drawing 699220, the gas and oil-mist mixture enter the compressor tank through the water-cooled heat-exchanger HX-1 where it is cooled to approximately 100°F and then passed to the sump area. The oil-mist entrained in the gas is filtered out in the polyfoam filter (F-2) and drips into the sump. The relatively clean gas is drawn into the compressor (C-1) through a coarse filter (F-5). The gas leaving the compressor is cooled to approximately 100°F by the heat-exchanger (HX-2) and passed through an automatic drain vortex filter (F-3) to remove any oil picked up during compression. The gas passes to the receiver where a motorized remote-control back-pressure regulator (R-2) maintains a pressure of approximately 80 psia. The gas passes from the receiver through the filters (F-1), where the remaining traces of oil are removed, and the clean gas is then pumped through the wall of the space chamber to an electrically heated heat-exchanger where the gas is raised to approximately 100°F.

The gas enters the lubricator tank and is again filtered by an automatic drain filter and regulated to approximately 66 psia by a motorized remotely controlled regulator (Reg-1). The gas at this point can bypass around an oil-mist injector (positive displacement pump, L-1) or through it at the option of the operator. Solenoid valves (V-4 and V-5) provide this feature. From the downstream side of Reg-1, clean gas is also passed through a sonic orifice to the alternator cavity of the BRU-R. The sonic orifice serves to limit the flow of helium-xenon gas to the alternator cavity to 0.2 lb/min under all conditions of operation The gas that bypasses around or through the lubricator is ducted to the BRU-R bearing cavities through two sonic orifices, which serve to limit the flow to each bearing to approximately 1.90 lb/min. After passing through the bearings, the cooling gas and oil-mist is drawn from the bottom of the BRU-R and ducted back through the space chamber wall to control valves V-1 and V-2. These valves are part of an automated control system to maintain a fixed-differential pressure between the cavity back of the BRU-R compressor impeller (P_1) and the bearing cavity

pressure (P_2). The differential pressure is required to prevent leakage of oil-mist into the Brayton cycle thermodynamic loop. As the gas leaves the V-1 and V-2 valves and returns to the compressor tank, the lubrication and cooling loop is closed. The thermocouple locations in the lubrication and cooling system are shown in Appendix D, Drawing 303913.

4.2 Seal Differential Pressure Control

The automatic regulation of the bearing cavity pressure is accomplished with the seal differential pressure control. A block diagram of the control is shown in Figure 13.

The transmitter (Figure 14) senses the differential pressure in a liquid-filled diaphragm-sealed element and exerts a force on a pivoted beam. The movement of the beam varies the reluctance of a force-balance-detector until the feedback transducer mounted on the pivoted beam exerts an equal balancing force.

The deviation indicating controller (Figure 15) is basically an analog computer that compares the milliamp signal received from the differential pressure transmitter to a set-point, indicates the deviation, and supplies a milliamp output signal from an operational amplifier. The amplifier relates the input to the output signal through a feedback path regulated by adjustable responses. The controller can be set to maintain a set differential pressure between 0.0 to 0.75 psi and can be operated in either an automatic or a manual mode. The normal setting is the automatic mode with a set point or a process control value of 60 percent. This results in a controlled differential pressure of 0.45 psi.

In the electropneumatic transducer (Figure 16), the air pressure is regulated to provide a pneumatic output signal proportional to the milliamp input signal. The pneumatic signal powers the valve positioners and control valves shown in Figure 17.

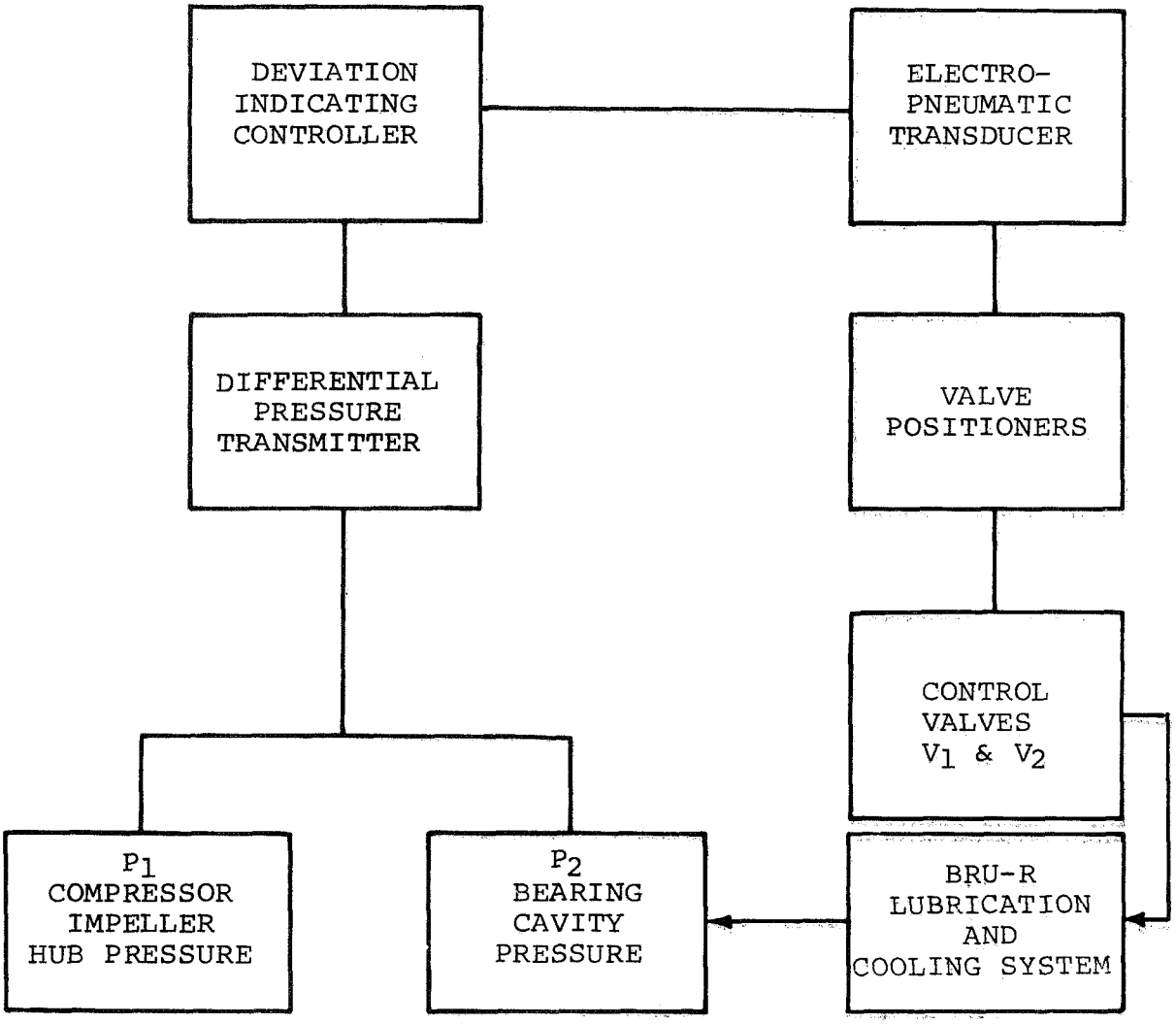

SCHEMATIC OF BEARING SEAL DIFFERENTIAL PRESSURE CONTROL SYSTEM

FIGURE 13

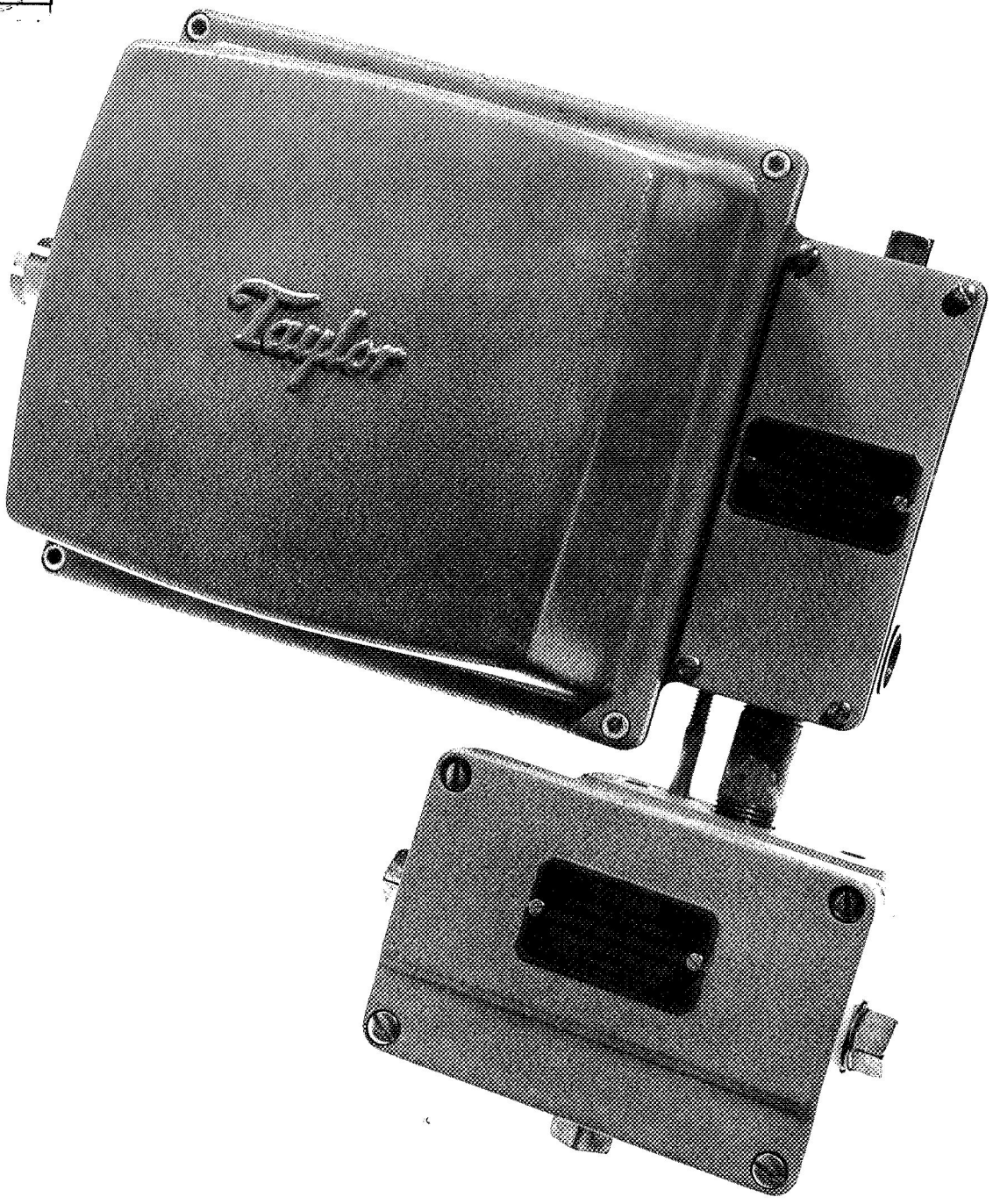

DIFFERENTIAL PRESSURE TRANSMITTER
TAYLOR INSTRUMENT CO.
PART 752-TD-22401, S/N 695

FIGURE 14

MP-21675

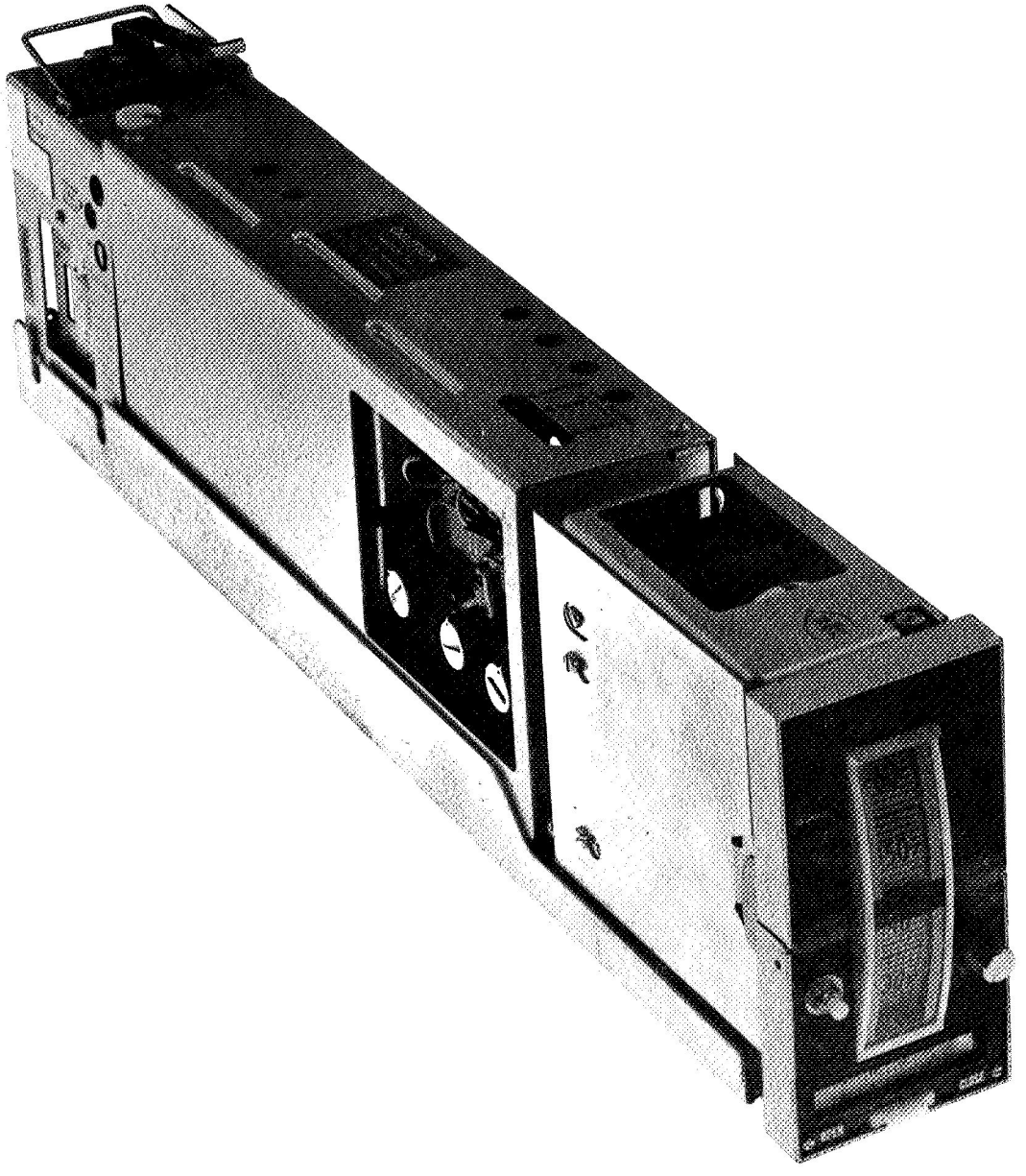

DEVIATION CONTROLLER

FIGURE 15

MP-21271

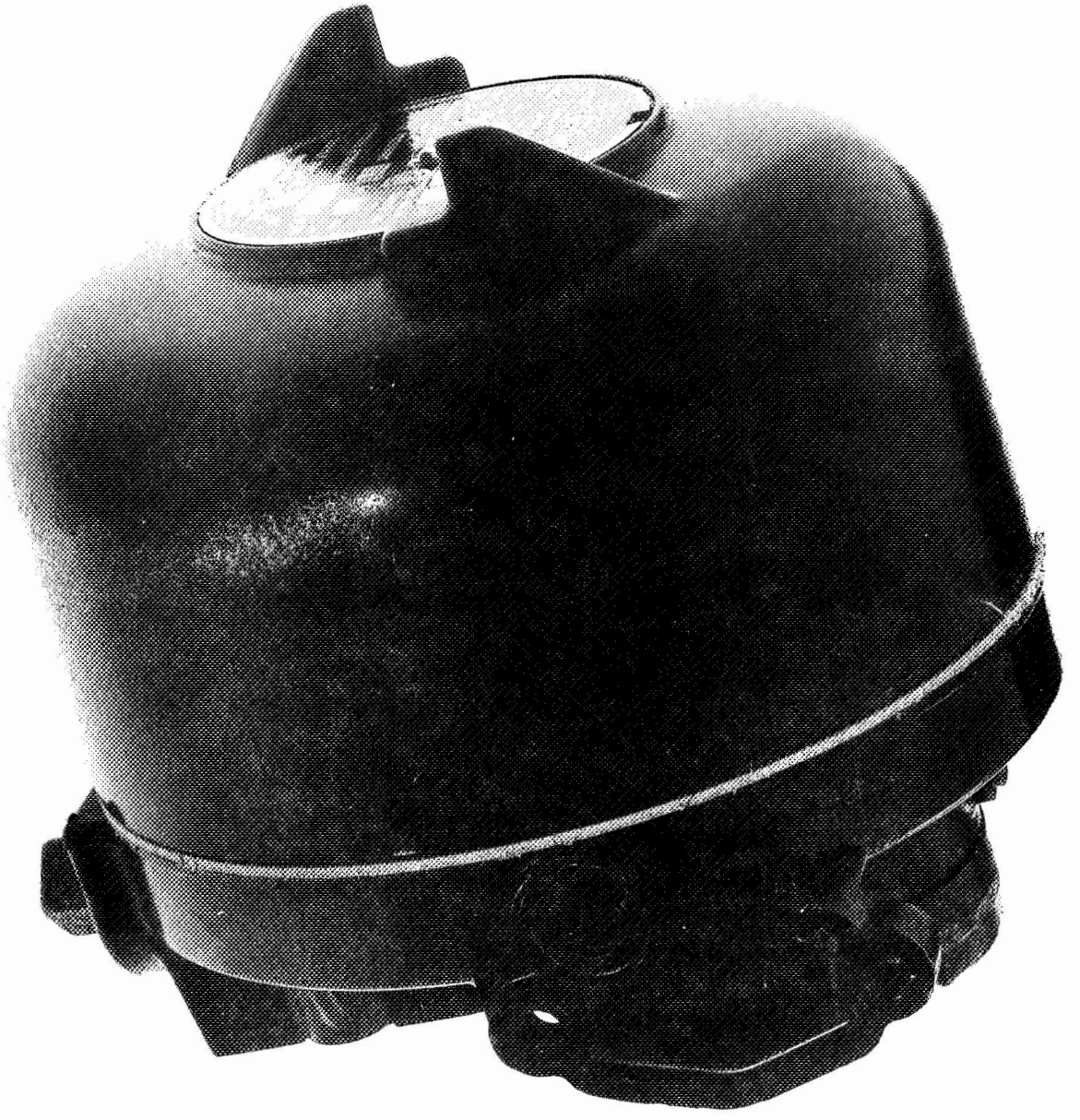

ELECTRO-PNEUMATIC TRANSDUCER

FIGURE 16

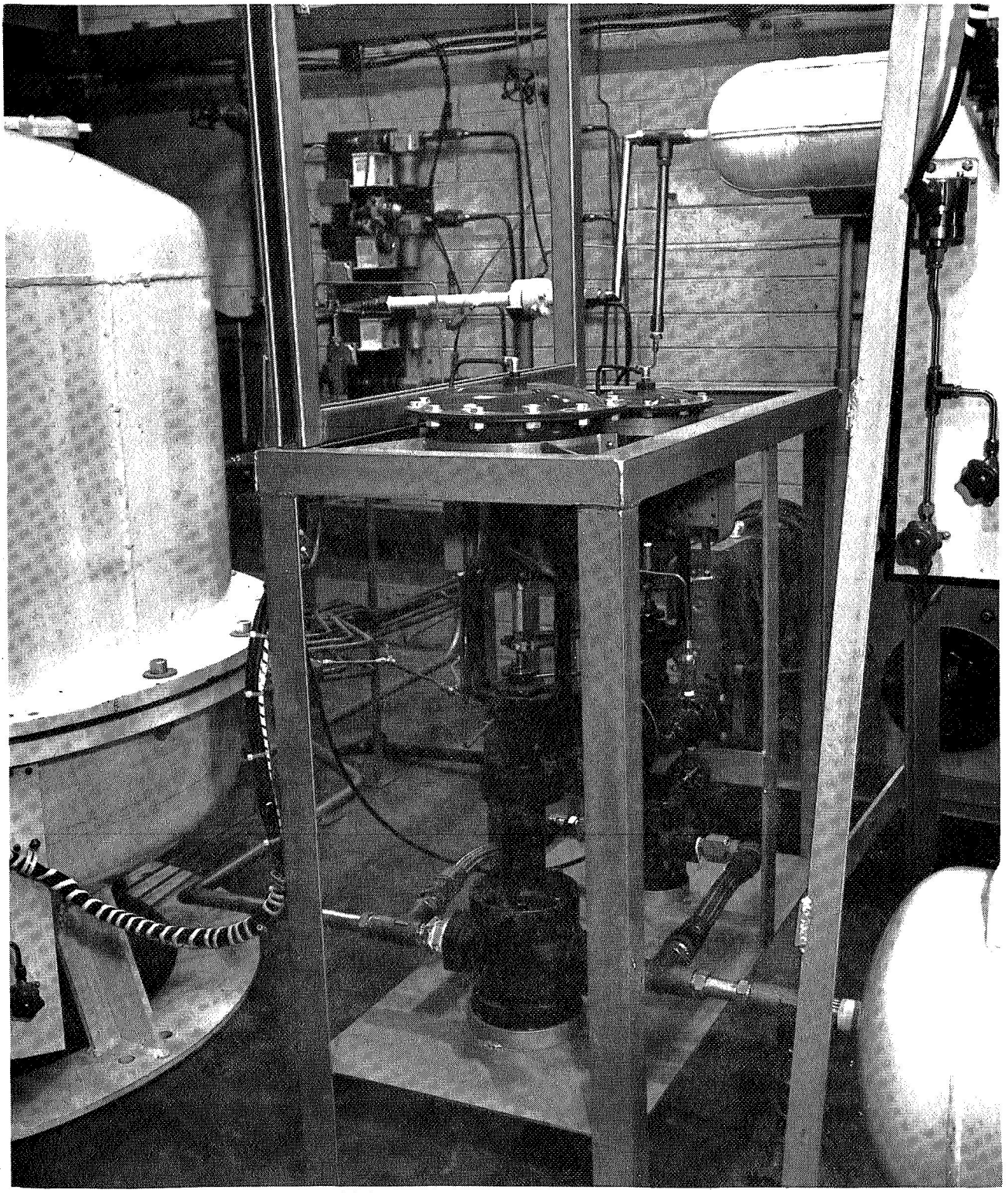

VALVE POSITIONERS AND CONTROL VALVES

FIGURE 17

TAYLOR CONTROL VALVES

PHOTO NO. P-36628-11

AIRESEARCH MANUFACTURING COMPANY
A DIVISION OF THE GARRETT CORPORATION
PHOENIX, ARIZONA

4.3 Compressor Tank

The compressor tank contains the gas compressor and the primary gas clean-up mechanism. The compressor tank is shown in Figure 18 and with the cover removed in Figure 19. The compressor tank has a fitting with a pressure rupture diaphragm rated at 20 to 25 psi; this fitting is for attachment to the NASA gas clean-up system.

The components within the compressor tank are a compressor and motor, three water-cooled heat-exchangers, four filters, and a gas receiver with a motorized remote control back pressure regulator. There are two filters (F-1) outside the tank connected in parallel (Figure 20). The motorized regulator is similar to that shown in Figure 23.

4.4 Lubricator Tank

The lubricator tank contains the mechanism for providing the oil-mist to the helium-xenon gas flow. The lubricator tank is shown with the cover removed in Figure 21.

The components of the lubricator tank are an electrically-heated heat-exchanger (located outside of the tank), an automatic drain filter (Figure 22), a remotely controlled motorized regulator, two solenoid valves, a positive displacement metering pump, a check valve, a pressure transducer, a venturi mixing section, and an oil reservoir. The remotely controlled motorized regulator is shown in Figure 23. There are two solenoid valves in the lubricator tank; one is a normally closed valve and the other a normally open valve. A typical valve is shown in Figure 24.

The oil is injected into the gas stream with a positive displacement lubrication system shown in Figure 25. This system consists of a metering pump, a pressure transducer, a check valve, and a venturi

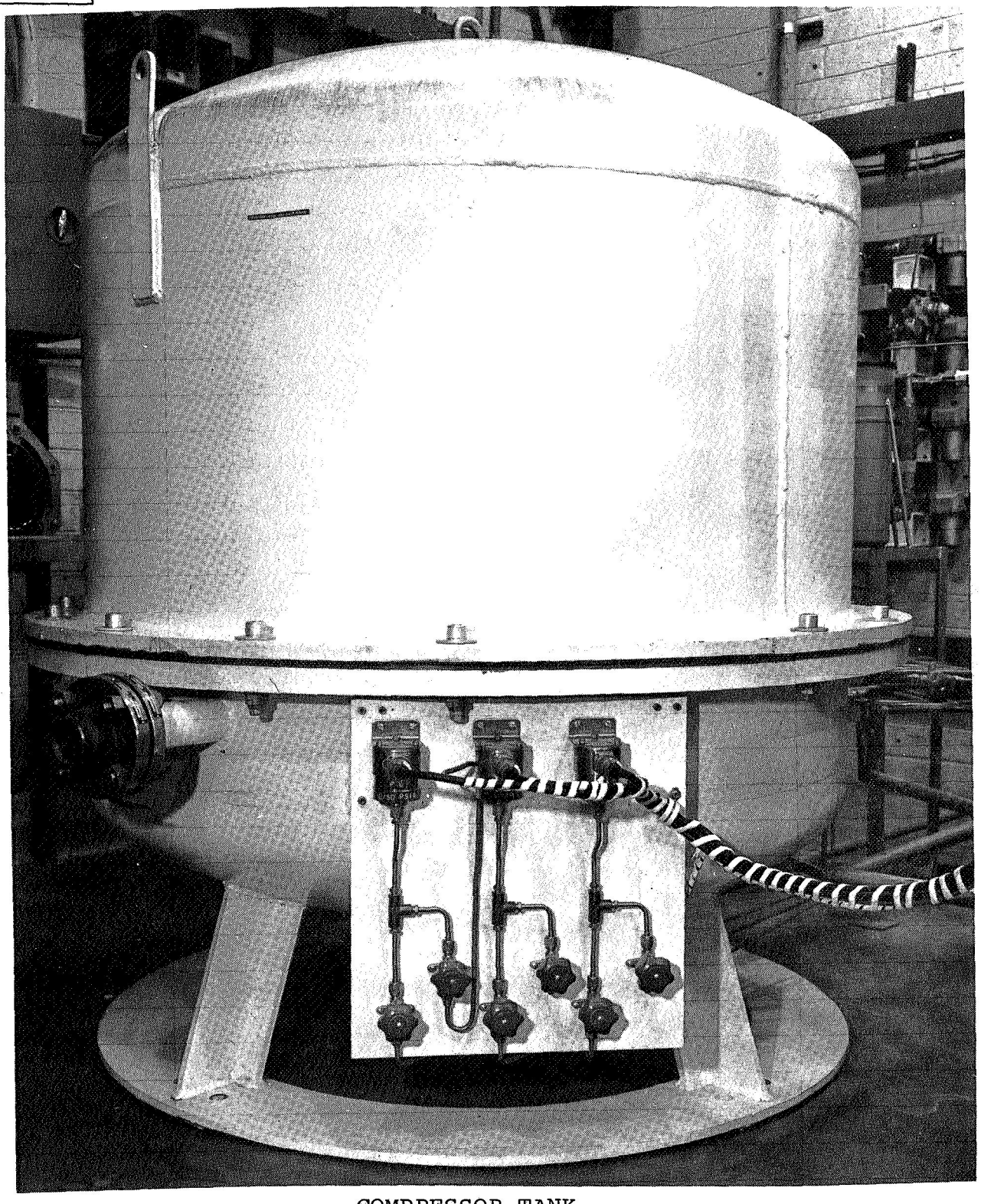

COMPRESSOR TANK

FIGURE 18

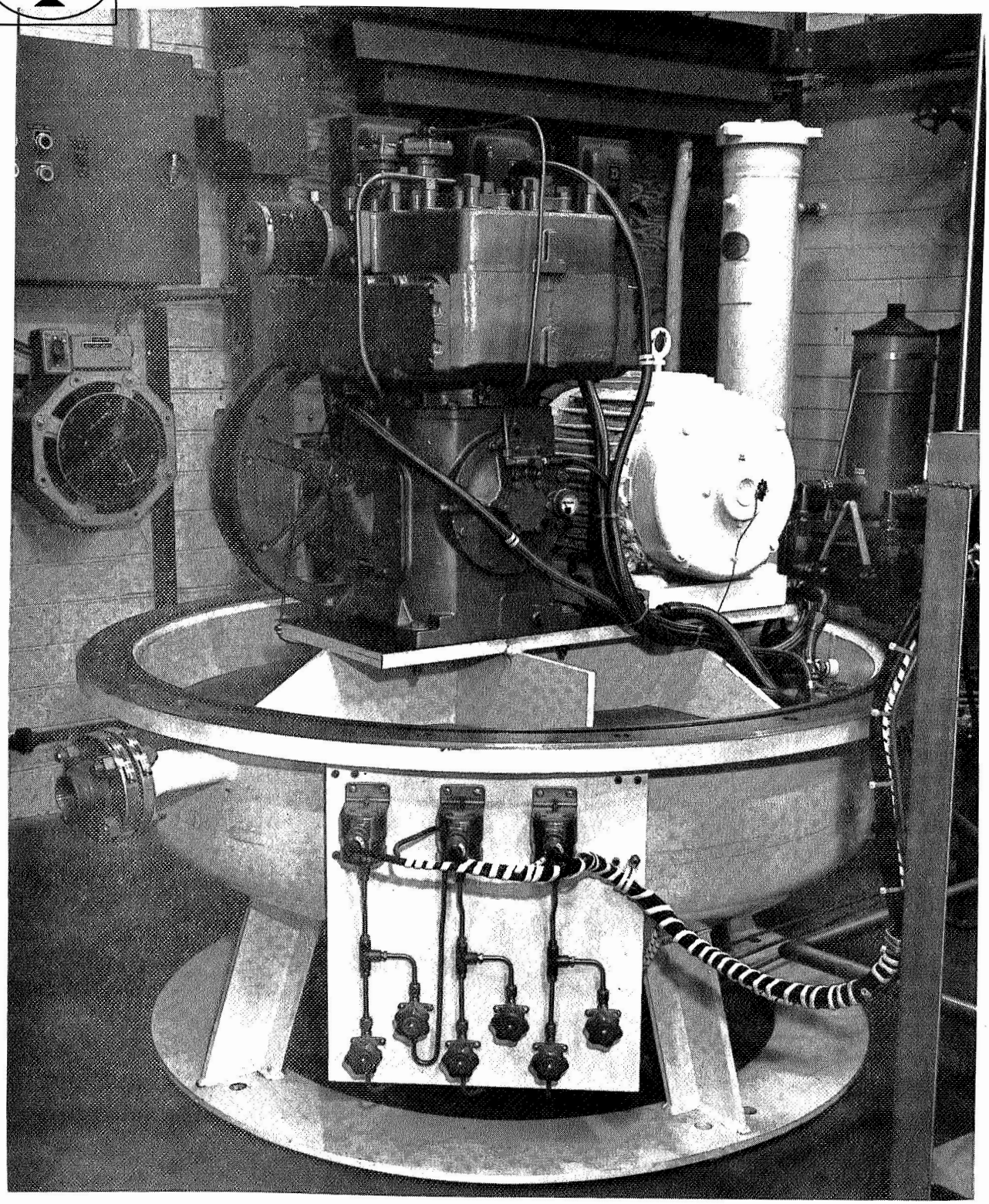

COMPRESSOR TANK WITH COVER REMOVED

FIGURE 19

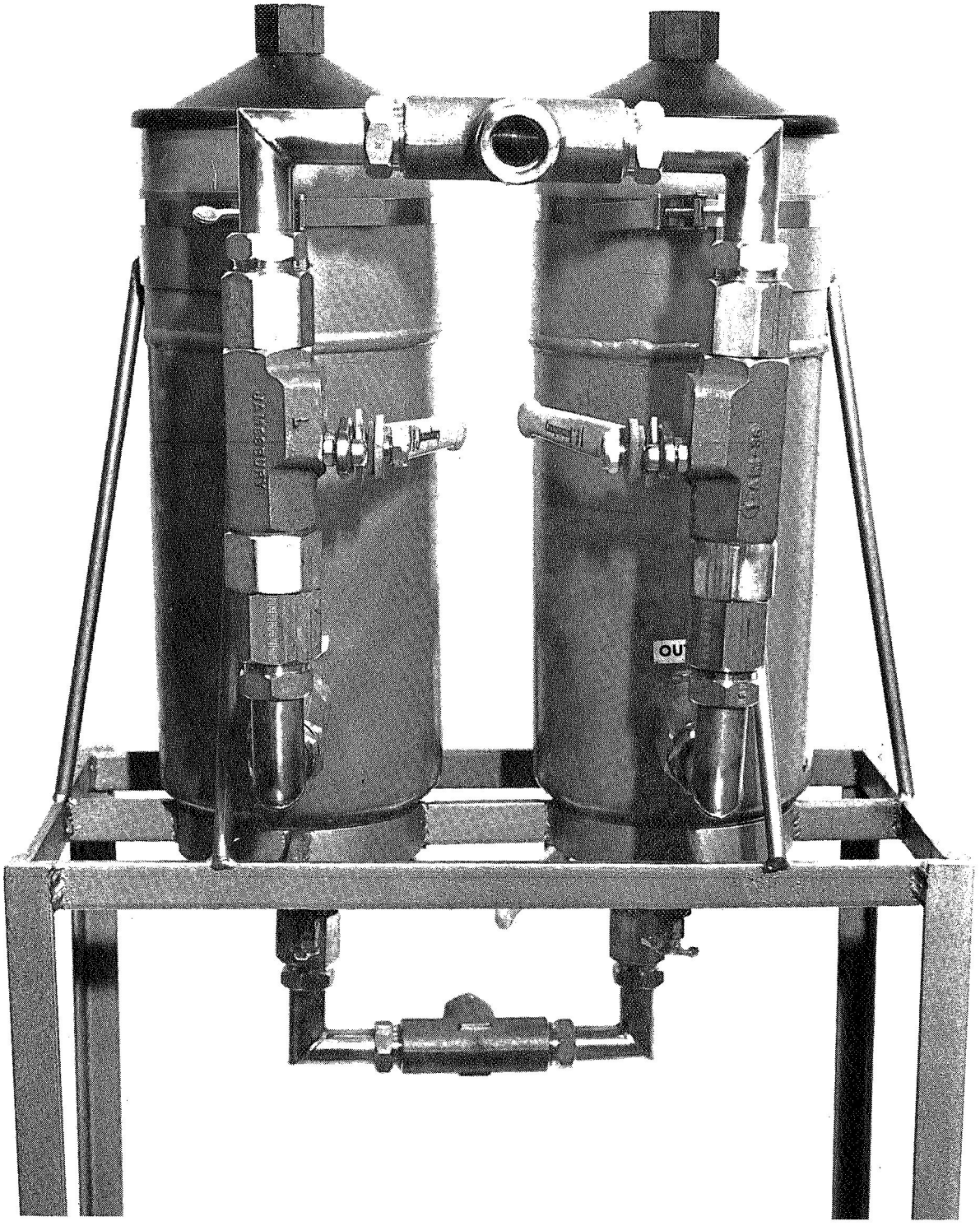

FRAM AIR GARD FILTERS

FIGURE 20

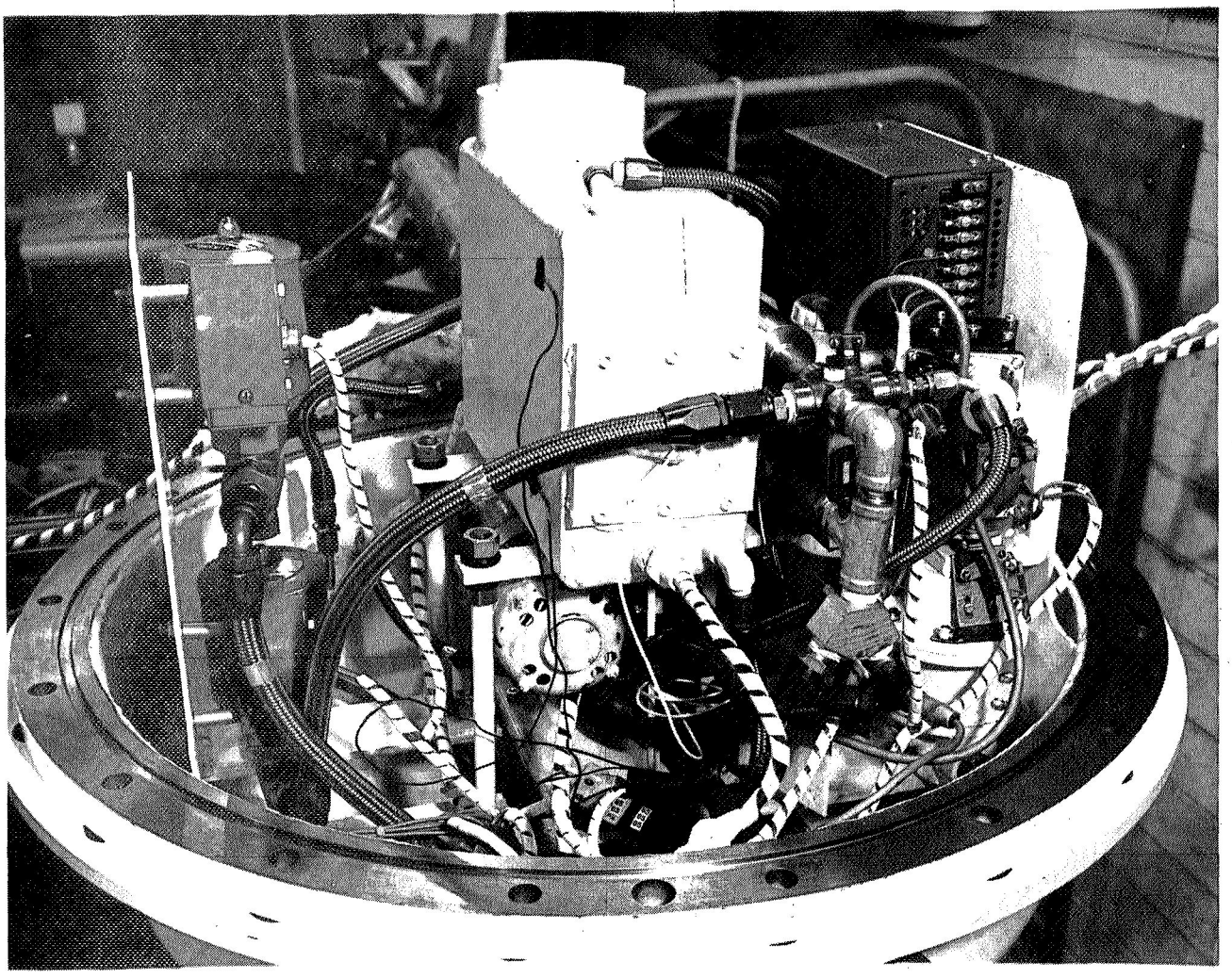

LUBRICATOR TANK

FIGURE 21

AUTOMATIC DRAIN FILTER

FIGURE 22

MP-21328

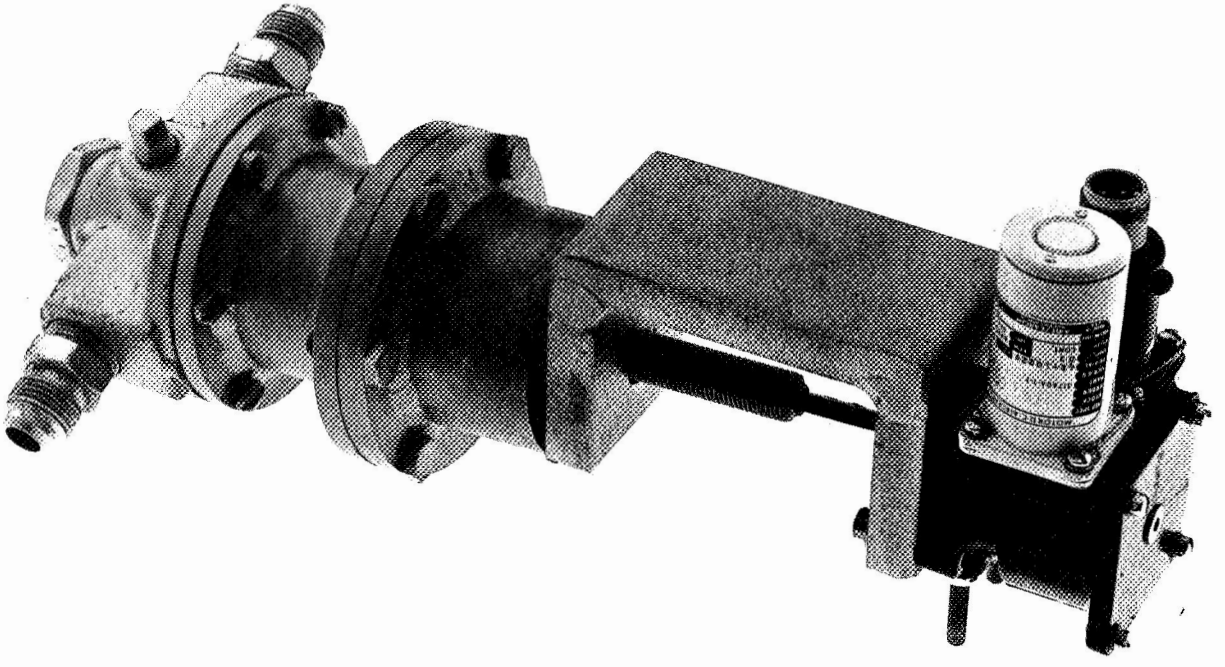

MOTORIZED REGULATOR

FIGURE 23

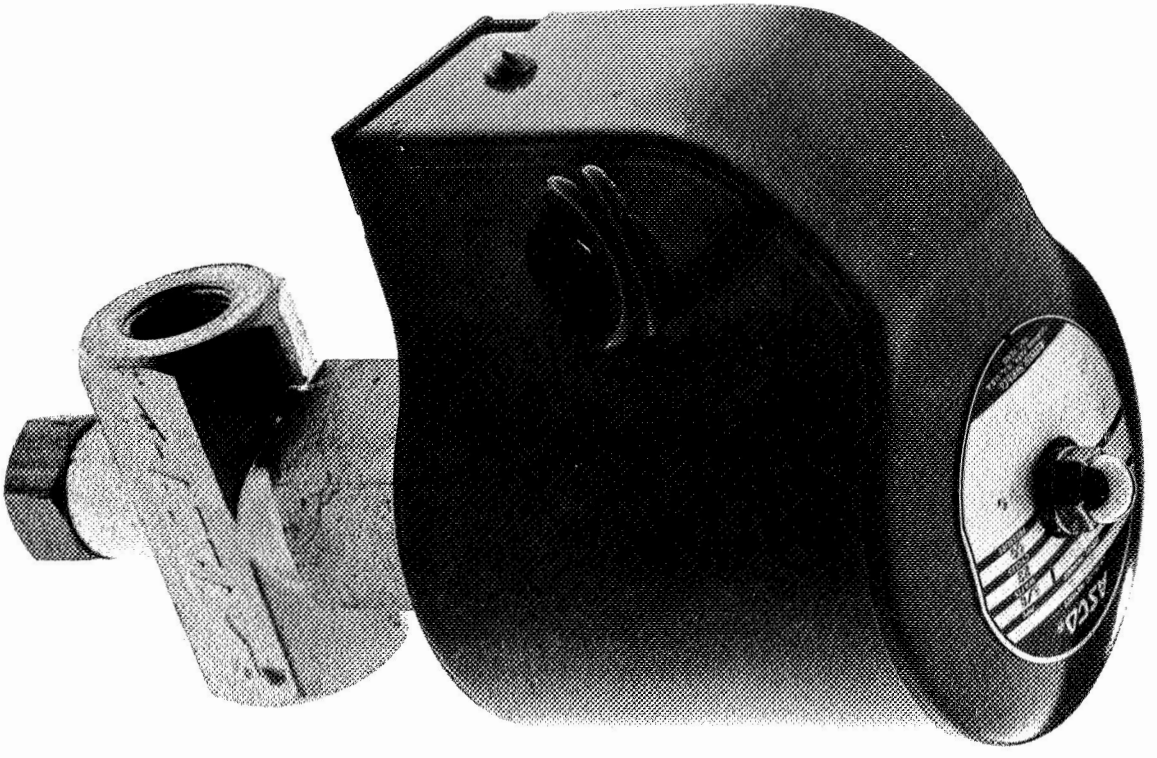

ASCO SOLENOID VALVE

FIGURE 24

MP-21269

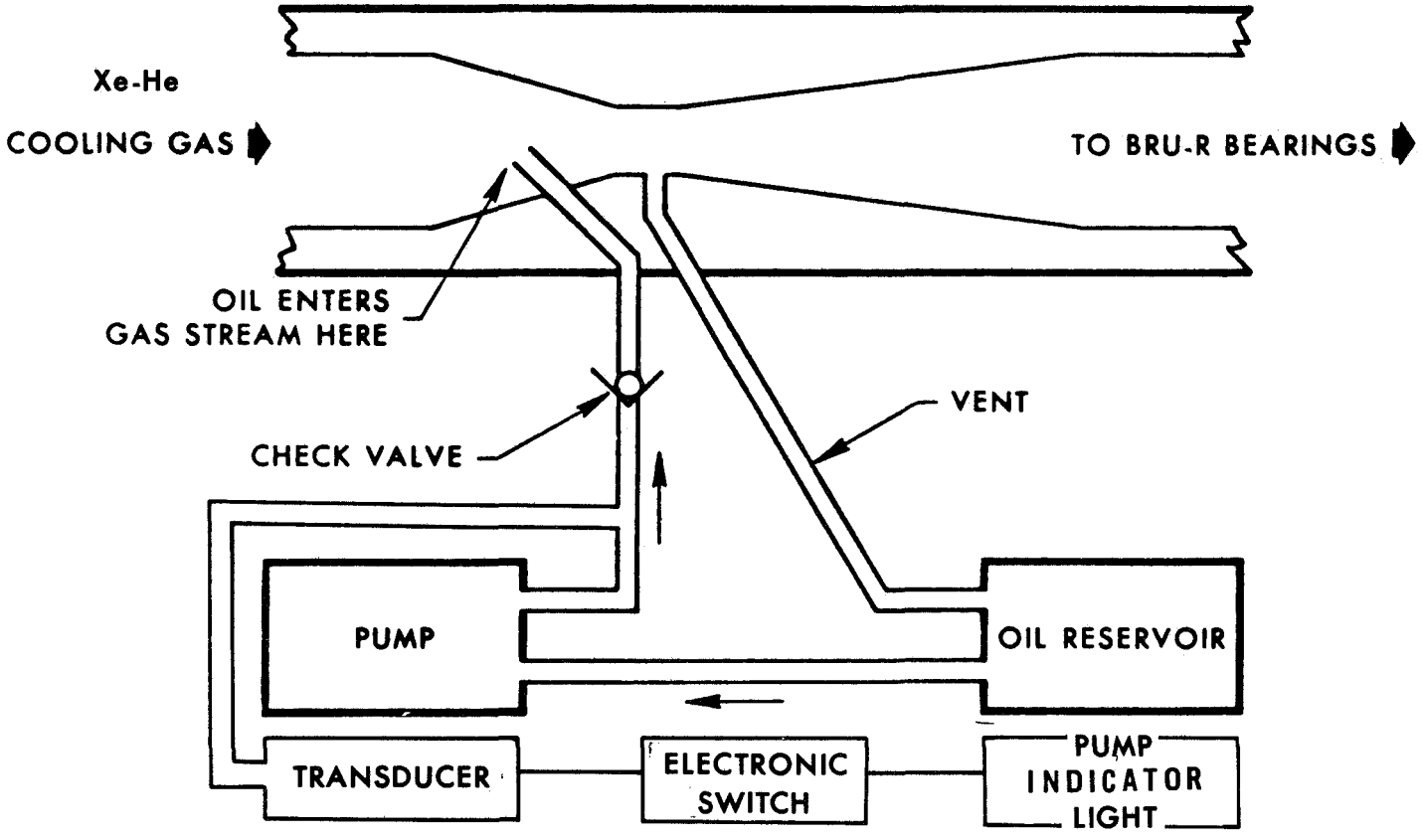

POSITIVE DISPLACEMENT LUBRICATION SYSTEM

FIGURE 25

section. The positive displacement metering pump is shown in Figure 26. Mounted on the discharge of the pump is the pressure transducer and poppet check valve. The transducer senses the pressure build-up of the pump and provides an input signal to an electronic switch that blinks a light on the lubricator control panel. This light will blink approximately 30 times a minute when the pump is properly supplying oil to the gas flow. The poppet check valve provides a positive discharge pressure to allow the pump's internal check valves to seat and thereby provide precise flow control. The oil from the discharge of the check valve is injected into the upstream side of a venturi section. Then it is carried away from the injector, accelerated in the venturi section, atomized, and thoroughly mixed with the helium-xenon gas flow. The last component of the lubricator tank is an oil reservoir fitted with an oil level indicator and an electrical heater regulated with a thermostat. The oil level is displayed on the lubricator control panel with a digital voltmeter. The oil capacity of the reservoir is sufficient for approximately 26 hr of testing. A remote oil-fill should be provided to replenish the reservoir. This supply can consist of a solenoid valve, a pump, and a large oil reservoir that can be set up at a convenient location outside of the lubricator tank.

4.5 Control and Instrumentation Panels

There are two control panels and three instrumentation panels for the BRU-R lubrication and cooling system. These panels contain the controls for the differential pressure, the compressor tank, the lubricator tank, and the indicators of the loop pressure transducers.

The two control panels are for the gas-flow and the lubricator. The cooling gas flow and the controllable pressures can be regulated from the gas flow control panel (Figure 27). The switch labeled "Bearing Cooling Flow V-4/V-5" controls the solenoid valves within the lubricator tank. When the switch button titled "Gas/Oil" is depressed,

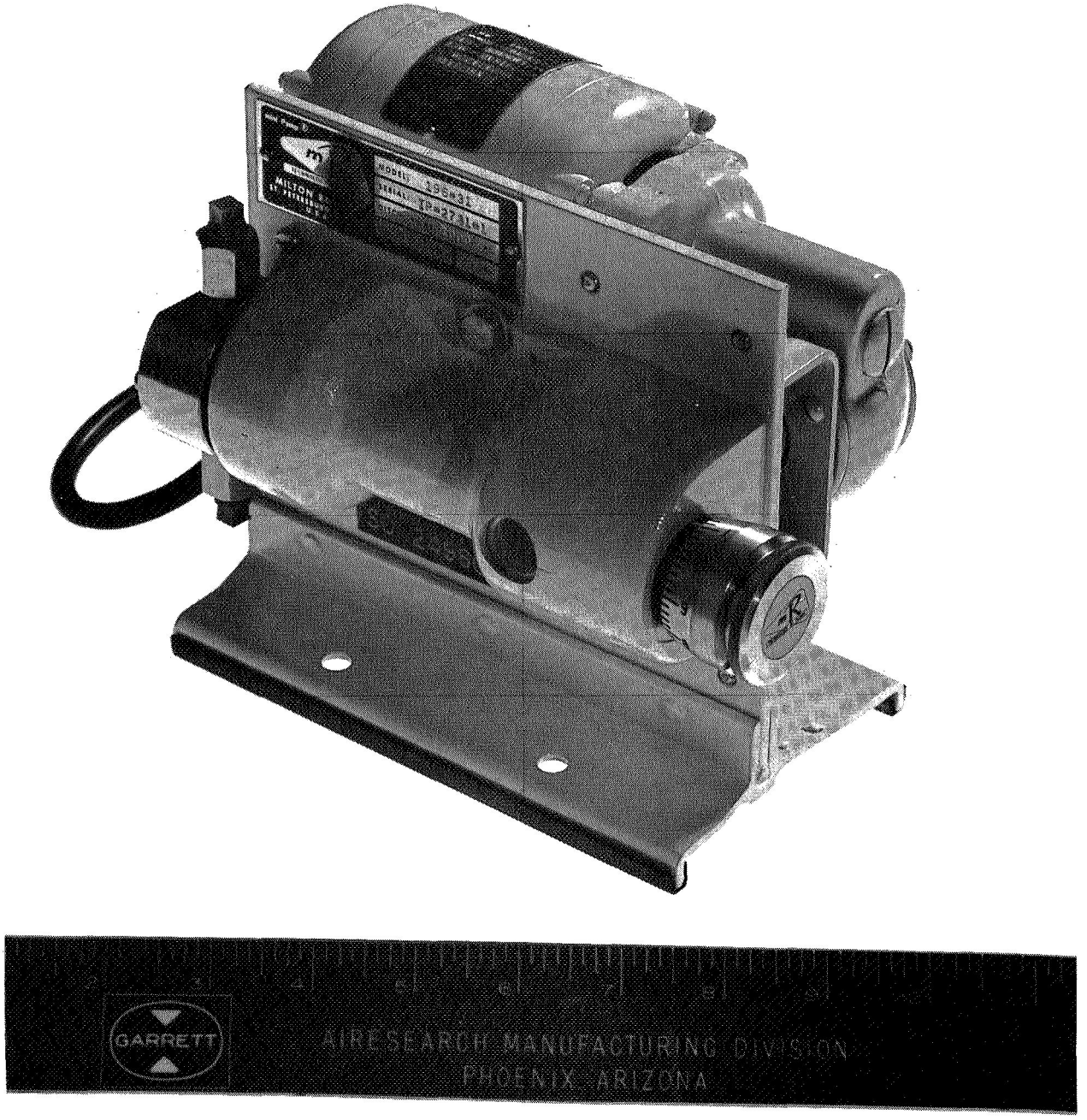

MILTON ROY MODEL 196-31 MINIPUMP

FIGURE 26

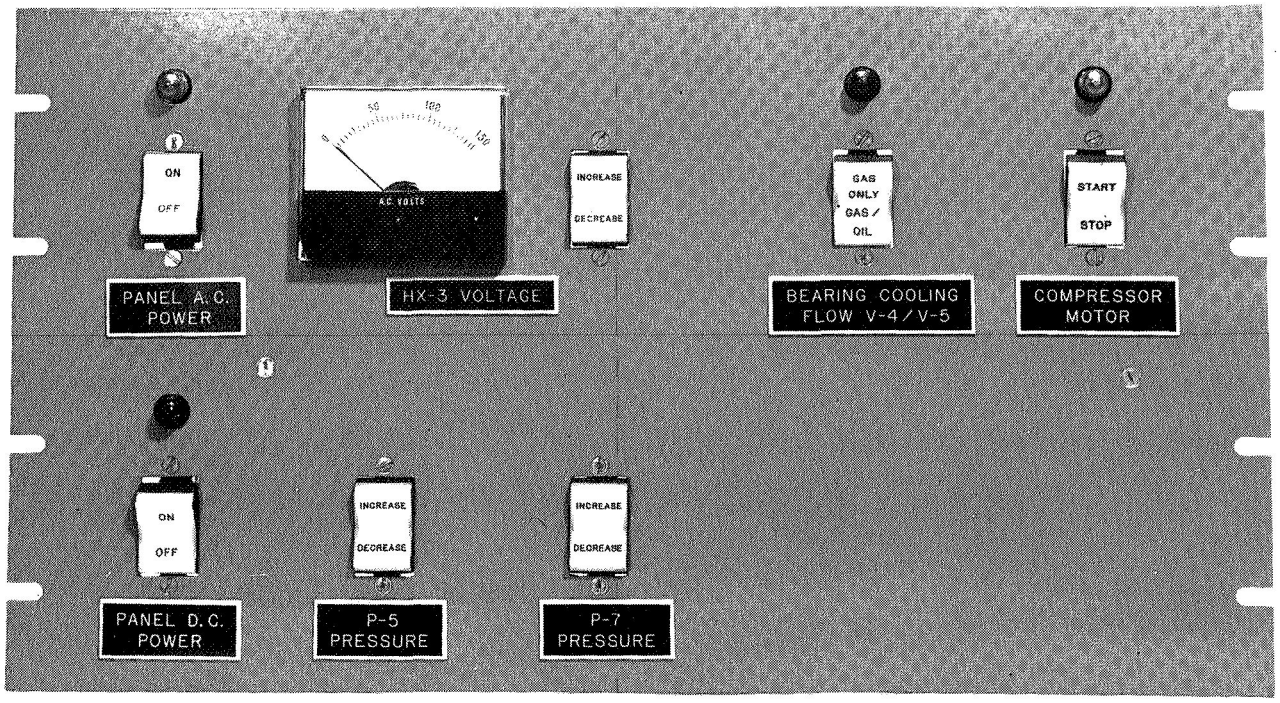

GAS-FLOW CONTROL PANEL

FIGURE 27

the valve V-4 is opened and the valve V-5 is closed; the helium-xenon gas flows through the oil-mist injector section. This is the normal run position. When the switch button, "Gas Only", is depressed, the red light above the switch will be illuminated, and the helium-xenon gas will bypass the oil-mist injector section; the valve V-4 will be closed and the valve V-5 will be opened. The gas-flow control panel also contains three switches labeled "Increase-Decrease" that control the electrically-heated heat-exchanger (HX-3) and pressures P-5 and P-7. A voltmeter is located adjacent to the control switch for the HX-3 heat-exchanger. The P-5 and P-7 switches control the position of the Reg-1 and Reg-2 motorized regulators, respectively.

The oil injection into the cooling gas flow can be regulated with the lubricator control panel (Figure 28). The oil level in the reservoir with the lubricator tank is indicated on the digital voltmeter. The lubricator panel contains a light to indicate when the pump is injecting oil into the gas stream; this light will blink at a rate of approximately 30 times a minute and has a "Press-to-Test" button.

Figure 29 illustrates three instrumentation panels. The right hand panel contains the pressure transducer indicators for the loop pressures P-5, P-6, P-9, and P-10. P-5 is the pressure downstream from the lubricator pump; P-6 is the pressure within the compressor tank; P-9 is the pressure of the purge gas supply to the alternator cavity; P-10 is the pressure within the lubricator tank. The middle panel contains the pressure transducer indicators for the loop pressures P-3, P-4, P-7, and P-8. P-3 is the pressure within the alternator purge cavity; P-4 is that at the turbine hub; P-7 is the pressure of the discharge of helium-xenon as it leaves the compressor tank; P-8 is the loop pressure downstream from the F-1 filters. The left

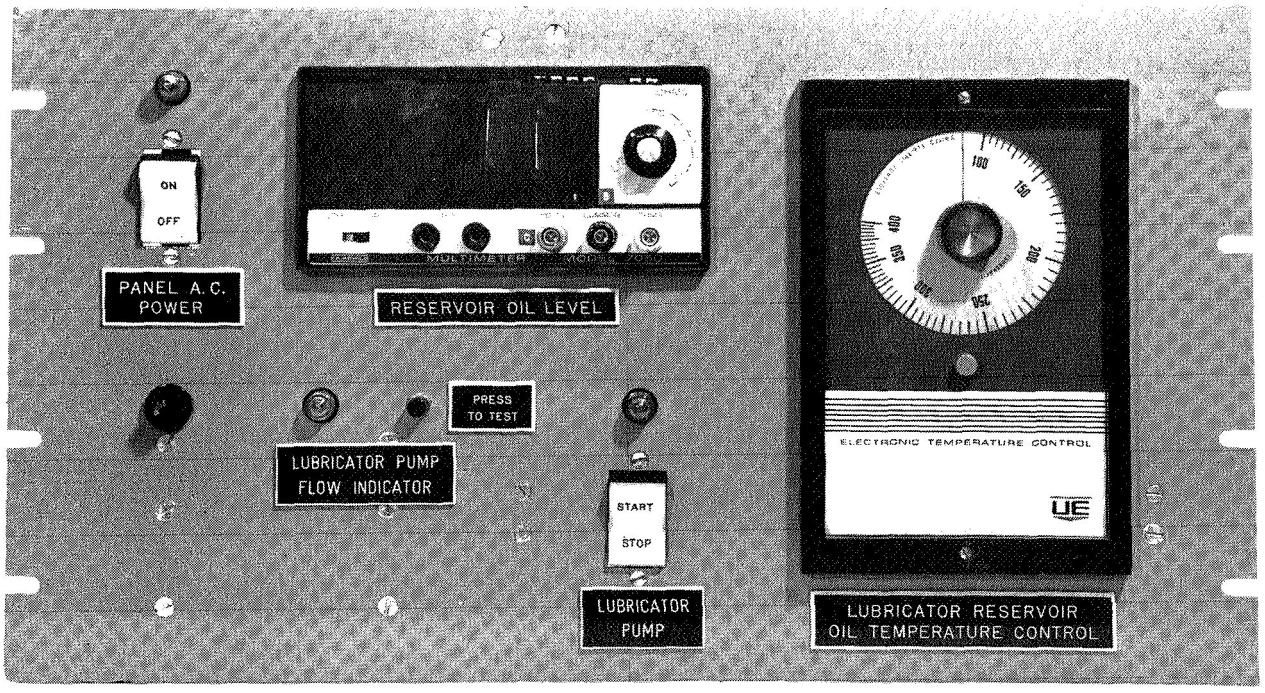

LUBRICATOR CONTROL PANEL

FIGURE 28

MP-24759

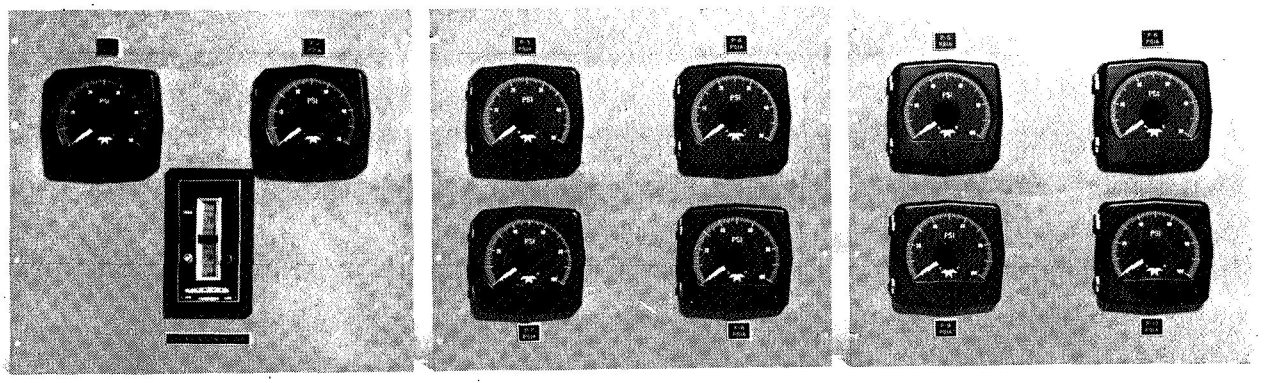

INSTRUMENTATION PANELS BRU-R COOLING LOOP

FIGURE 29

hand panel contains the deviation controller and the pressure transducer indicators for the compressor hub (P-1) and the bearing cavity (P-2).

A complete lubrication and cooling system schematic is in Appendix D, Drawing 699220.

5. BEARING DESIGN AND TEST EVALUATION

The bearings in the BRU-R were designed to support the axial and radial loads of the turbine wheel, compressor impeller, and alternator rotor. The two 30-mm ball bearings are mounted in resilient four-lobe flex mounts. The resilient mount adjacent to the compressor is spring-loaded to provide an axial preload on both bearings. Each bearing is individually cooled and lubricated with a helium-xenon gas mixture with oil-mist.

5.1 Shaft Dynamics

As with many designs of rotating equipment, the BRU-R shaft dynamic characteristics dictated the selection of bearing size and span. Figure 30 shows the elastic and mass model of the BRU-R assembly used to establish the rotor dynamics. The bearing span was placed at 8.650 in. in conjunction with a 30-mm bearing bore size. This configuration resulted in a rotor fundamental (free-free) bending mode critical speed of 53,600 rpm, which is 24 percent above the designed 120-percent overspeed requirement of 43,200 rpm. Figure 31 shows the first two critical speeds as a function of bearing stiffness. The analysis revealed that with solid-bearing mounting (implying a stiffness in the order of 250,000 lb/in.), the first two critical speeds would be very near the operating speed of 36,000 rpm. Consequently, resilient bearing mounts were incorporated to reduce the first and second critical speeds. Using a resilient mount stiffness of 30,000 to 40,000 lb/in., the first and second critical speeds are reduced to 10,000 to 15,000 rpm and well below the normal operating speed. These critical vibration ranges were verified during coastdown tests, as discussed in 10.2.2.1. Figure 32 shows the configuration of the resilient mount designed for the BRU-R.

STIFFNESS MODEL

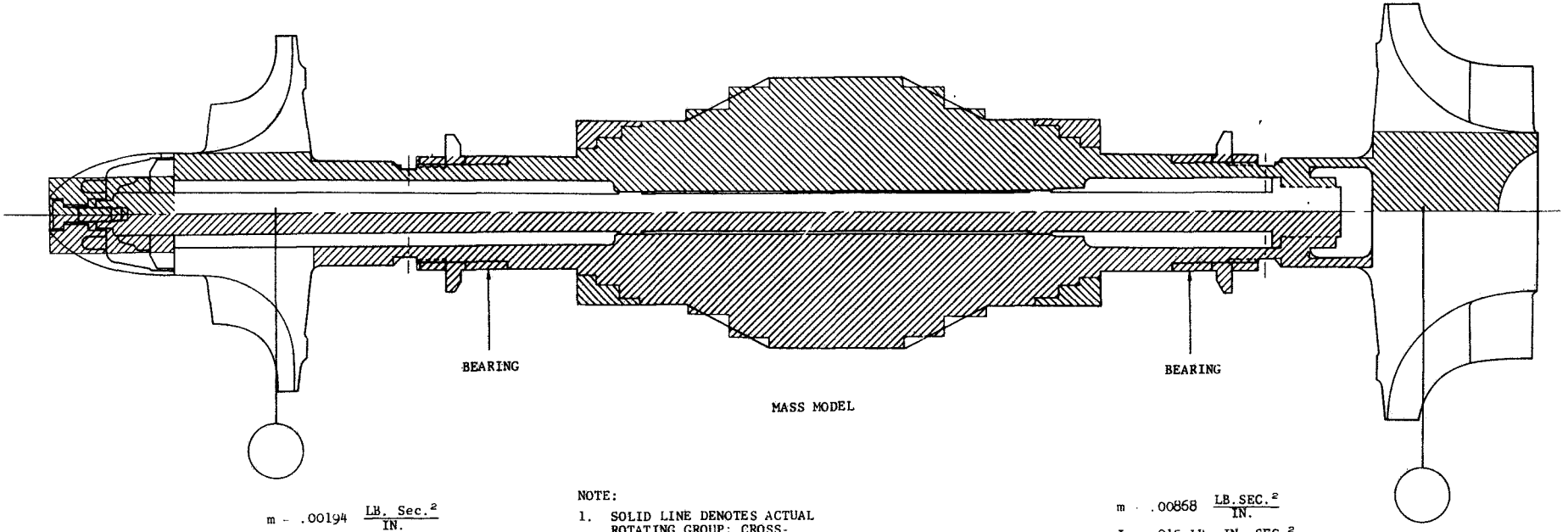

MASS MODEL

$m = .00194 \ \frac{LB.\ Sec.^2}{IN.}$

$I_p = .00205$ LB. IN. SEC.^{2}

$I_d = .00197$ LB. IN. SEC.^{2}

NOTE:

1. SOLID LINE DENOTES ACTUAL ROTATING GROUP; CROSS-HATCHING DENOTES MASS AND STIFFNESS MODELS.

$m = .00868 \ \frac{LB.SEC.^2}{IN.}$

$I_p = .015$ LB. IN. SEC.^{2}

$I_d = .0089$ LB. IN. SEC.^{2}

1 INCH

PREPARED	DRC	8 67	BRU-R CRITICAL SPEED MASS AND STIFFNESS MODELS
WRITTEN			A9020
APPROVED			AiResearch Manufacturing Company of Arizona

FIGURE 30

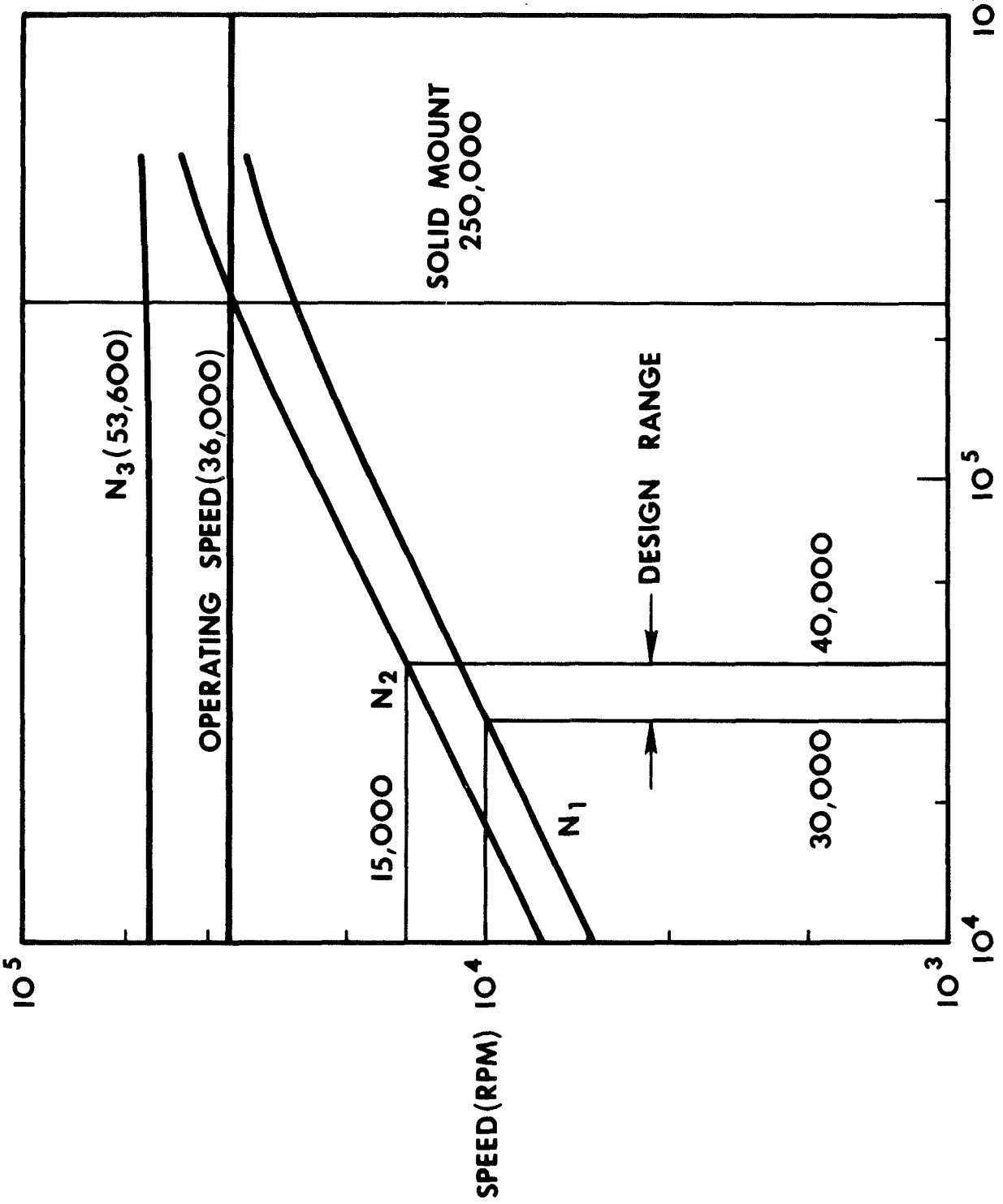

BRU-R CRITICAL SPEEDS AS A FUNCTION OF BEARING STIFFNESSES

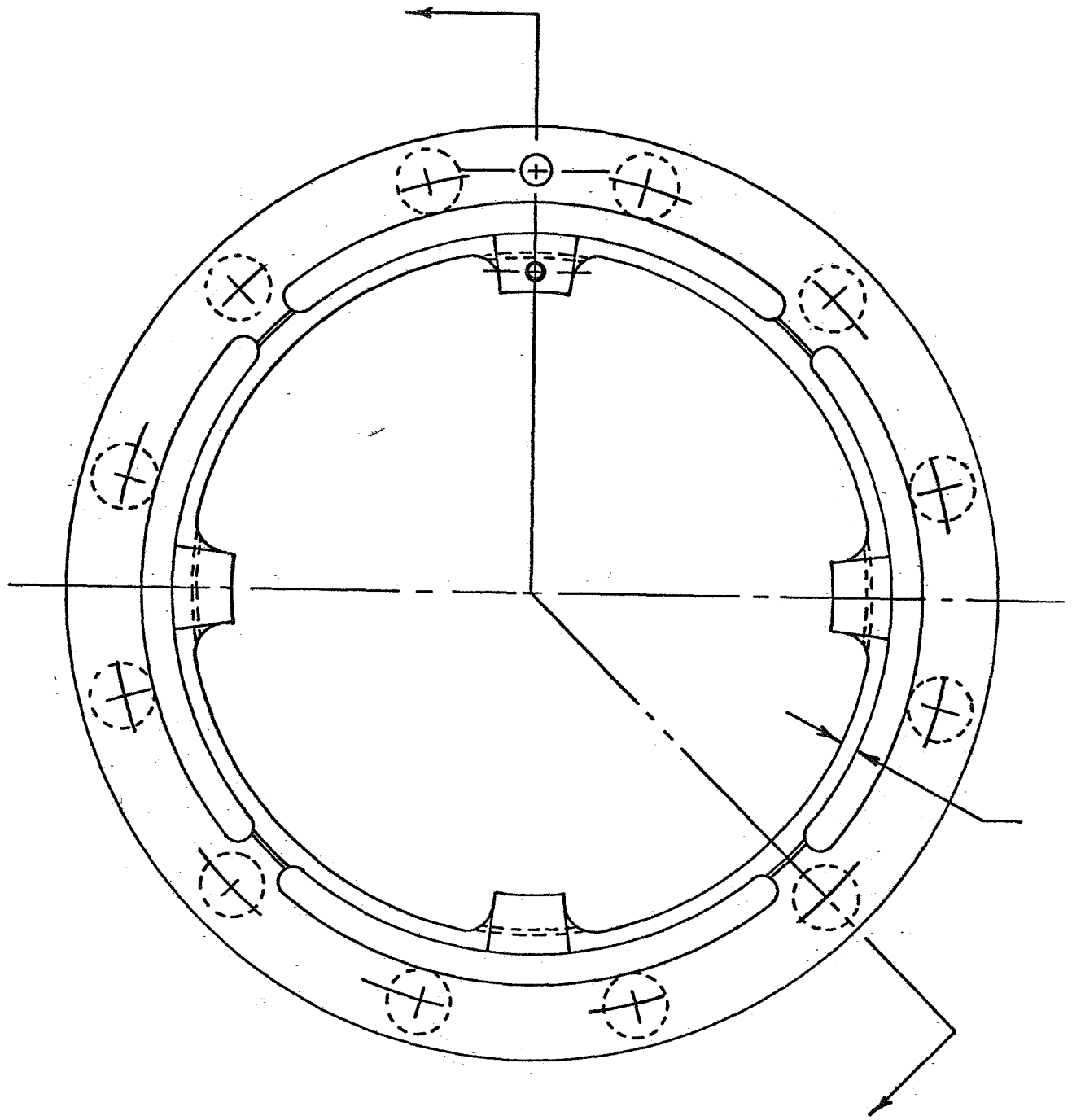

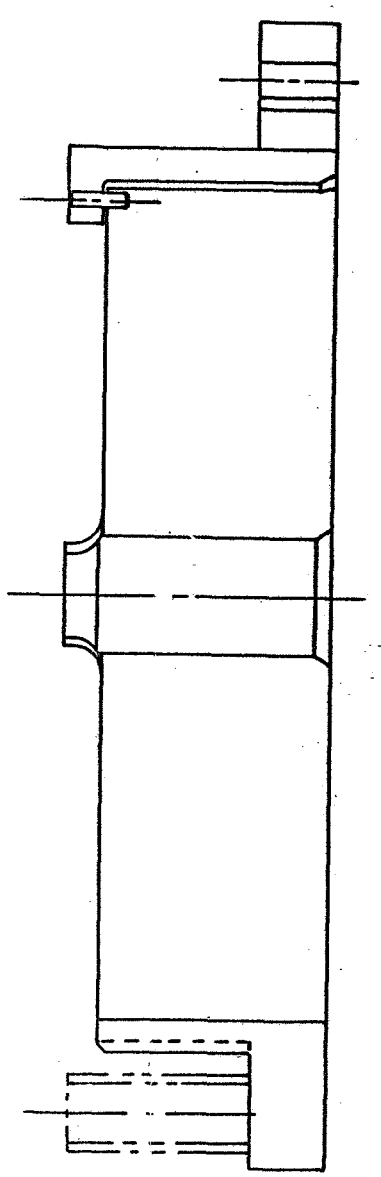

PREPARED	DRC	10/67	BRU-R RESILIENT BEARING MOUNT	A34129
WRITTEN				
APPROVED			AiResearch Manufacturing Company of Arizona	

FORM P793A-1

FIGURE 32

The dynamic operating loads on the resiliently mounted bearings for a rotor cg eccentricity of 0.0002-in. are shown in Figure 33. The loads remain low even at the overspeed of 43,200 rpm.

5.2 Bearing Design

The rolling-element bearings were optimized for the BRU-R to fulfill the system requirements of minimum power loss and wear, light weight, and high reliability (time between overhaul, 500 hr) and yet to stay within present bearing design and manufacturing technology to ensure their availability. This is normal design practice for high-speed turbomachinery bearings.

The design selected as a result of the bearing optimization program is shown in Figure 34. The major characteristics are:

Bore diameter	30 mm
Outside diameter	55 mm
Width	13 mm
Ball diameter	9/32 in.
Inner-race curvature	56% of ball diameter
Outer-race curvature	54% of ball diameter
Contact angle	22 deg
Ring and ball material	Consumable-electrode vacuum-melted M-50 tool steel
Separator material	4340 Steel, silver-plated

The calculated maximum bearing power losses with oil-mist lubrication are 191 w at the turbine end and 190 at the compressor end. The B_{10} life of the turbine-end bearing is 25,260 hr and of the compressor-end bearing is 25,623 hr. This results in a minimum system life of 13,770 hr and gives a 3100-hr time between overhaul (TBO).

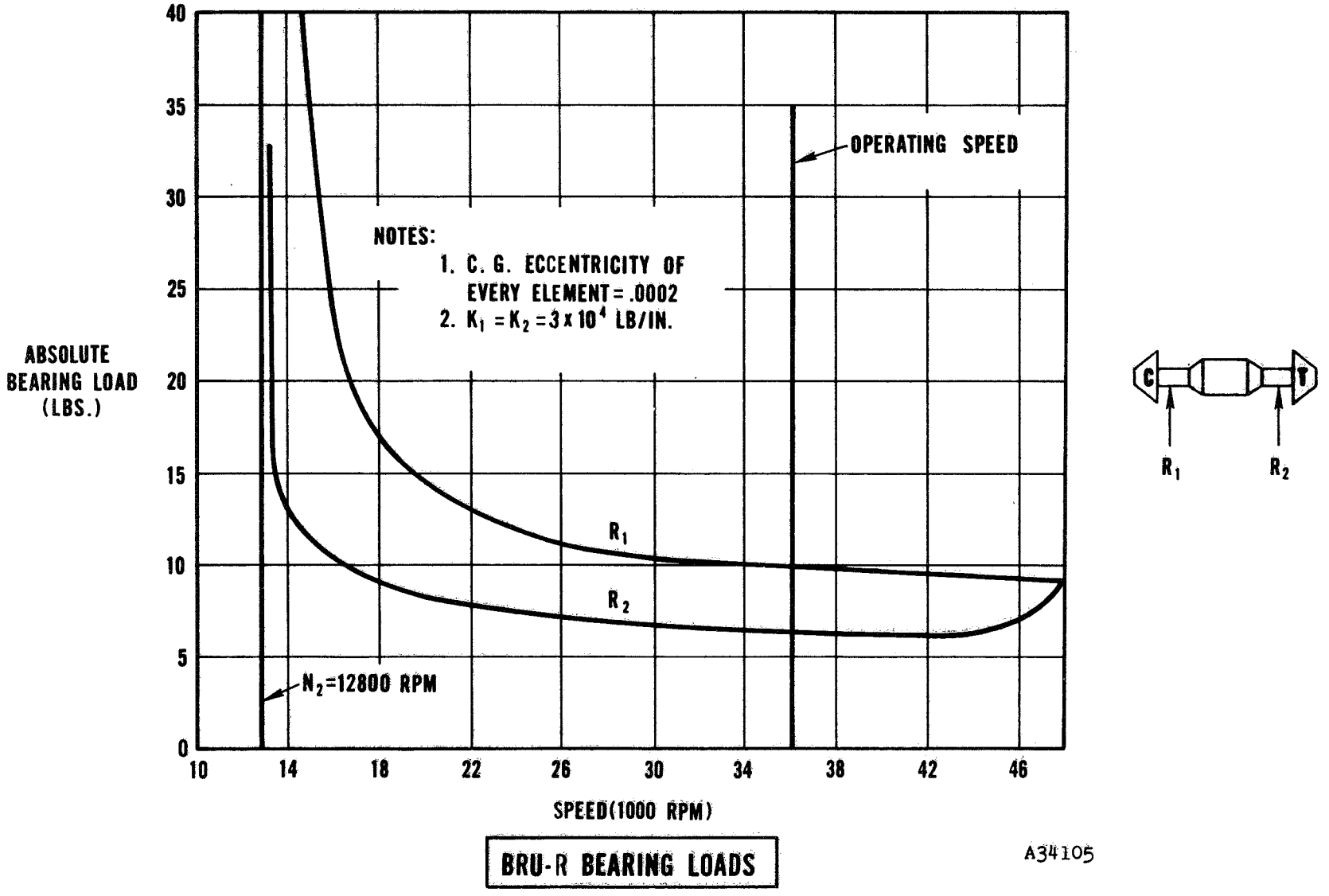

BRU-R BEARING LOADS

A34105

FIGURE 33

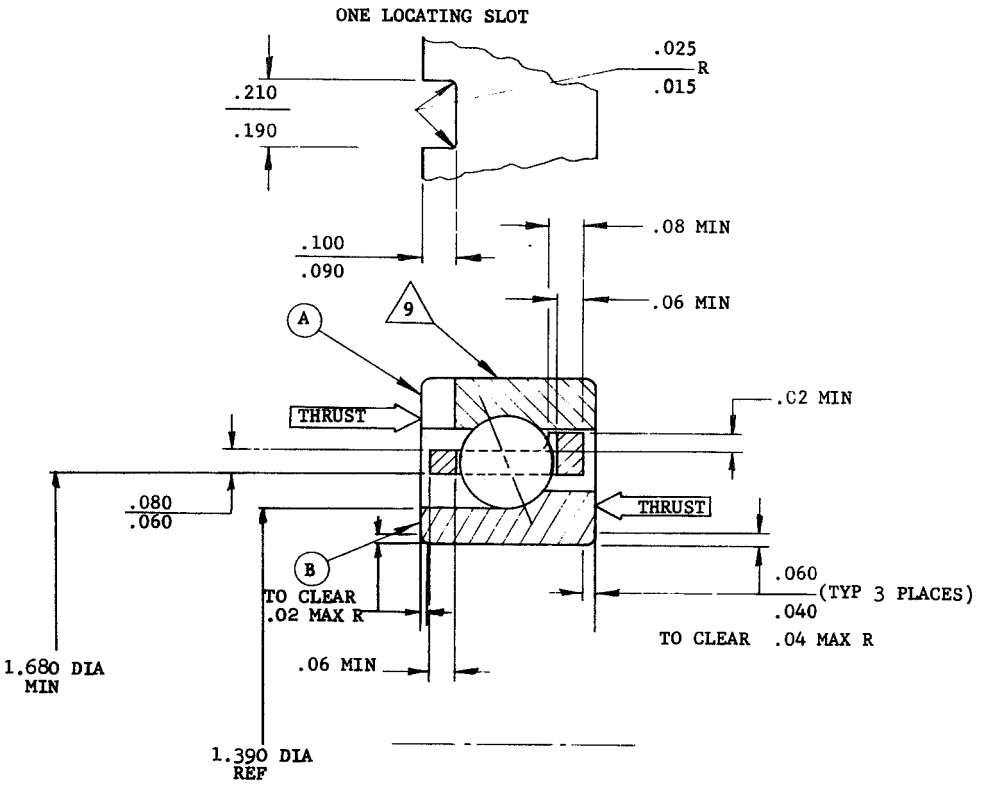

BEARING DESCRIPTION	SINGLE ROW, ANGULAR CONTACT, 7106	GRADE	AIRESEARCH 5

INNER RING	OUTER RING	SPECIAL FEATURES
MATERIAL: CEVM M-50 STEEL PER AMS 6490	MATERIAL: CEVM M-50 STEEL PER AMS 6490	1. CONTACT ANGLE TO BE 20° - 24° UNDER 5 POUND THRUST LOAD.
BORE: (M) 1.1809 - 1.1811 (30 MM)	OD: (M) 2.1651 - 2.1654 (55 MM)	2. SEPARATOR HARDNESS TO BE R_c 28-38
WIDTH: (M) .5018 - .5118 (13 MM)	WIDTH: .5018 - .5118 (13 MM)	3. SEPARATOR TO BE SILVER PLATED PER AMS 2410, .001 - .002 THICK
RACE DEPTH: 15 MIN % BALL/ROLLER DIA.	RACE DEPTH: 10 MIN % BALL/ROLLER DIA.	4. PARTS SHALL NOT CHANGE IN DIMENSION IN EXCESS OF .000050 IN/IN WHEN EXPOSED TO 750°F FOR 10 HOURS.
RACE CURVATURE: 55.5 - 56.5 % BALL/ROLLER DIA.	RACE CURVATURE: 53.5-54.5 % BALL/ROLLER DIA.	
SEPARATOR PILOT LAND TO GROOVE RUNOUT: TIR	SEPARATOR PILOT LAND TO GROOVE RUNOUT: .0005 TIR	5. HEAT TREATMENT OF CEVM M-50 TO BE PER HT-55.
SEPARATOR	**ROLLING ELEMENTS**	6. SEPARATOR BALL POCKET CLEARANCE TO BE .017 - .027.
MATERIALS: SAE 4340 STEEL PER AMS 6415	MATERIAL: CEVM M-50 STEEL PER AMS 6490	7. FACES "A & B" TO BE FLUSH WITHIN ±.0001 WITH 5 LB. THRUST LOAD APPLIED IN DIRECTION SHOWN. (M)
	ELEMENTS PER ROW: 14	8. BEARING MUST NOT DISASSEMBLE UNDER NORMAL HANDLING.
CONSTRUCTION: MACHINED	ELEMENT DIA.: 9/32 INCH	9. HARDNESS OF RINGS AND BALLS TO BE Rc 60 MIN.
ASSEMBLY: ONE PIECE	ELEMENT LENGTH:	
PILOTING SURFACE: OUTER RING LAND	**CLOSURES**	
PILOT CLEARANCE: .008 - .018	NUMBER: NONE	
ASSEMBLED BEARING CHARACTERISTICS	TYPE: (SHIELDS, SEALS)	
TOTAL (DIAMETRAL, AXIAL) CLEARANCE OF	MATERIAL:	
UNDER LBS GAGE LOAD	CONSTRUCTION:	

PACKAGING PER AIRESEARCH SPEC CP - 14	PRODUCTION BULK PACK	COMMERCIAL SPARES PACK	MILITARY SPARES PACK
PRESERVATIVE:	MIL-L-6085	MIL-L-6085	MIL-B-197
AIRESEARCH PART NUMBER:	358546 - 1	358546 - 1	358546 - 4

PROCUREMENT PER ASL 358546

FIGURE 34

A34130

The design of rolling-element bearings for reliable operation at high speeds in turbomachinery is complicated by conditions that do not exist or do not affect bearing performance at low speeds. Some of these conditions are:

(a) Centrifugal loading of the outer race and rolling elements

(b) Skidding at the rolling-element-to-race contacts

(c) Localized heating at the contacts

Analysis of these effects is complex and requires the use of digital computer techniques. The method used in the analysis of this application was developed by Mr. A. B. Jones, Jr., whose theory has been published by McGraw-Hill Book Company in Section 3 of the "Mechanical Design and Systems Handbook."

In conjunction with Figure 33, the radial loads due to eccentricity in this analysis were 10 lb at the compressor bearing and 6 at the turbine bearing. A total of 16.75 lb of static radial load accounted for shaft and wheel weights. An axial component of 31 lb due to aerodynamic imbalance was also assumed.

5.2.1 Bearing Power Loss

Power loss from bearing friction has two possible causes: one, effects due to bearing speed and lubricant viscosity, and the other, due to the effect of load. The effect of lubricant viscosity on bearing friction is predominant at increasing speeds but is almost independent of bearing geometry and small at low speeds. For the operating conditions of this application, the bearing power loss due to lubricant viscosity is approximately 55 percent of the total, with oil-mist lubrication. This would increase to 84 percent if oil-jet lubrication

were used, and the calculated bearing power losses would increase to 532 w at the turbine end and to 531 at the compressor end.

Minimum bearing power loss is of paramount importance in this application because the complete cooling system must be sized in proportion to the bearing losses. Due to the low specific heat (Cp = 0.059) of the He-Xe cooling gas, approximately 0.9 lb/min gas flow is required to adequately remove each 100 w of heat generated in the bearing. For example, a nonoptimized bearing of conventional design operating under the BRU-R conditions with oil-mist lubrication and a calculated power loss of 276 w would require a gas cooling system 45 percent larger than required for the optimized BRU-R bearing.

In the analysis of bearing system life, the B_{10} life for each bearing was determined. The individual bearing lives were then combined statistically to obtain the expected B_{10} life of the system (L_{10})--the life for which 90 percent of the bearings in the system can be expected to survive without a fatigue failure.

To obtain the system TBO, the B_{10} life (L_{10}) was modified to obtain the B_1 life (L_1)--the life for which 99 percent of the bearings can be expected to survive without a fatigue failure.

Figure 35 shows the relationship between B_{10} life (L_{10}) and bearing life (L_x) for probabilities of survival from 90.00 percent to 99.99 percent. It can be seen that the B_1 life (L_1) is 0.225 times the B_{10} life (L_{10}).

5.2.2 Race Curvature

The curvature of the inner and outer races influences both bearing power loss and fatigue life. Generally, tight curvatures give long fatigue life but cause high power loss, while with loose curvatures the reverse is true.

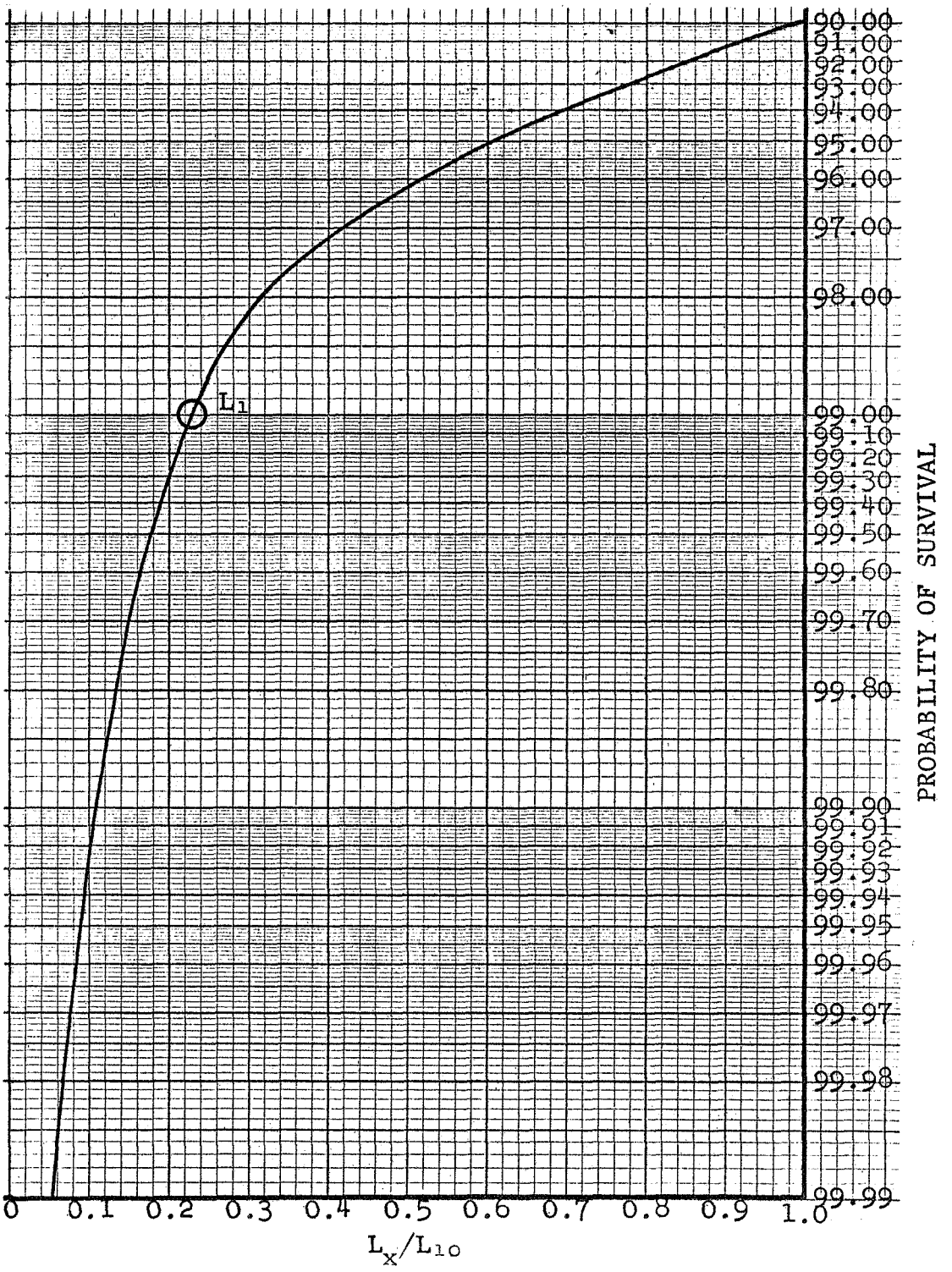

BEARING LIFE VERSUS RELIABILITY A33229

FIGURE 35

In order to optimize for this specific application, race curvatures ranging from 52 to 56 percent of the ball diameter were considered.

Figures 36 and 37 show the effects of race curvature on bearing power loss and life. An outer-race curvature of 54 percent and an inner of 56 percent of the ball diameter were chosen. From the curves, the slight power loss and life decrease is evident for the curvatures greater than 56 percent. In order to achieve minimum power loss, a 56-percent inner-race curvature was selected. Outer-race curvature, however, has less influence on torque than on bearing system life. Thus, a 54-percent outer-race curvature was selected to achieve a long life.

5.2.3 Contact Angle

The angle of contact between the races and balls affects the thrust-carrying ability of the bearing and its performance under combined radial and axial loads.

Analysis indicated that the optimum contact angle would lie in the range between 20 and 30 deg. Since the life of the bearing with this contact angle is adequate (Figure 38) and the contact-angle variation due to load and speed is not excessive, the 22-deg contact angle was selected. From Figure 39 it can be seen that minimum power loss would be obtained with this angle.

5.2.4 Preload

The effect of preload is to decrease fatigue life and increase power loss (Figures 40 and 41). Thus, it would seem that a very low preload should be used. However, Figure 42 shows that the preload also influences the ball spin/roll ratio, which is a measure of the skidding

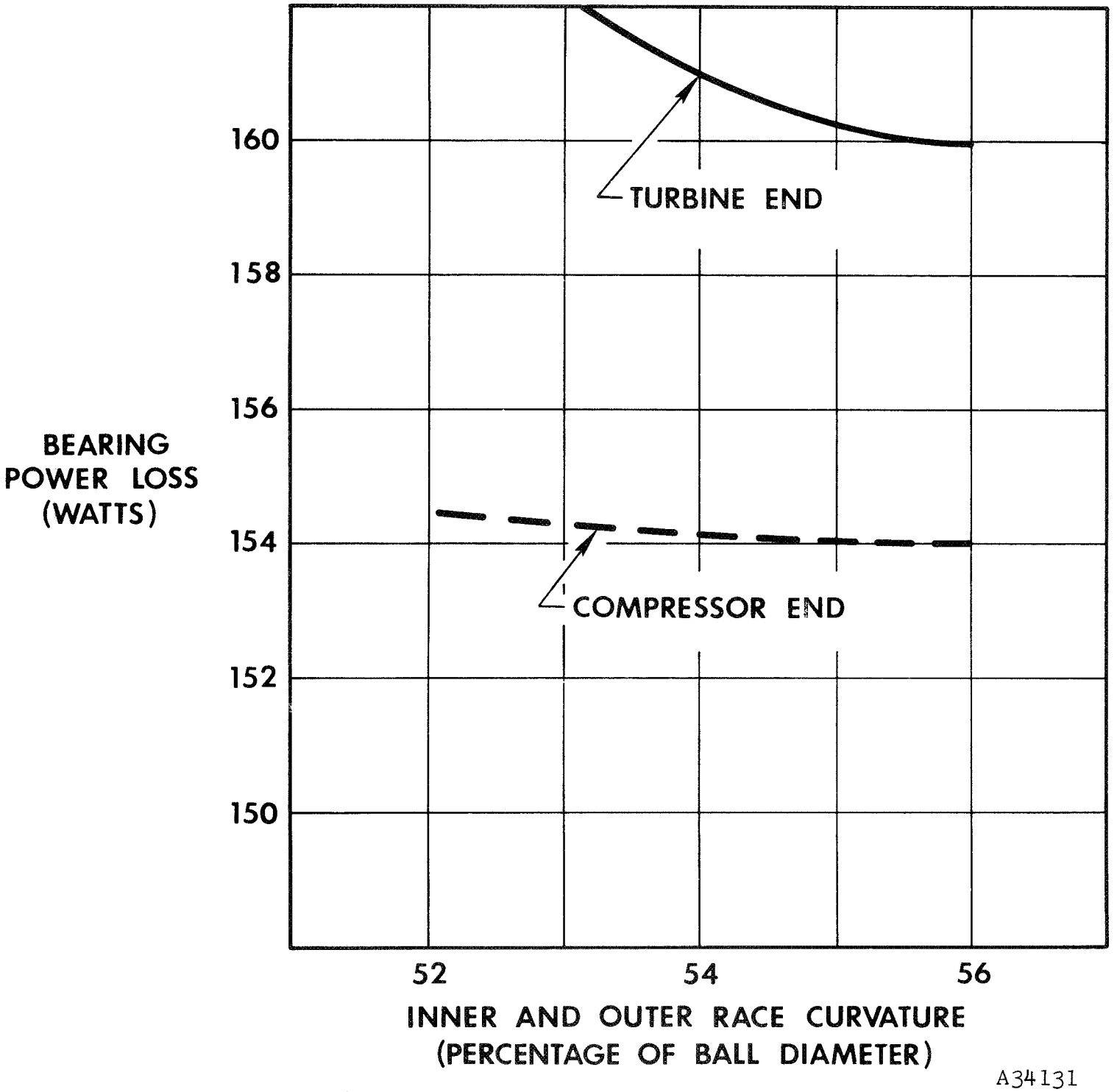

EFFECT OF COMBINED RACE CURVATURES ON BEARING POWER LOSS

FIGURE 36

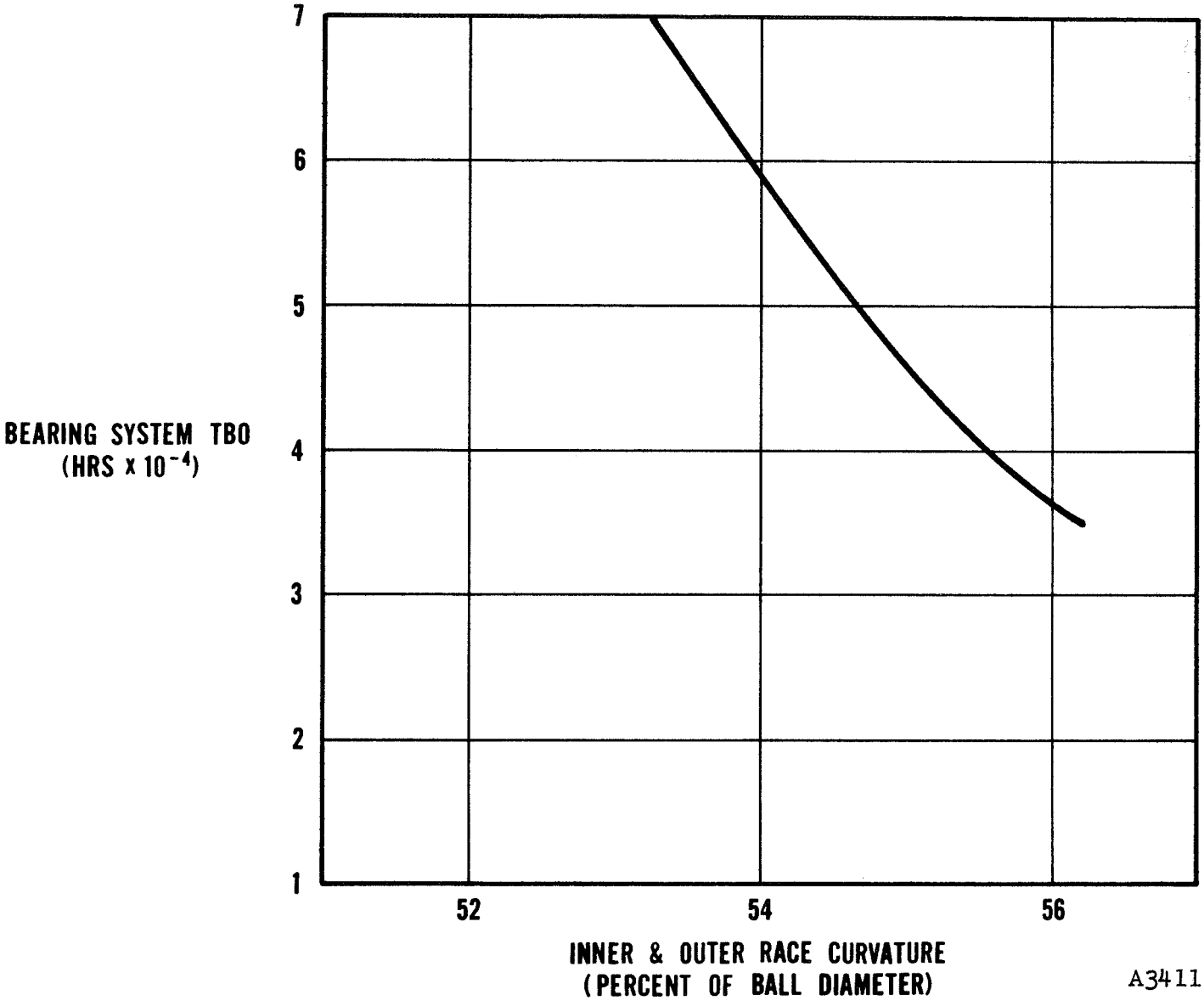

EFFECT OF COMBINED RACE CURVATURES ON BEARING SYSTEM FATIGUE LIFE

FIGURE 37

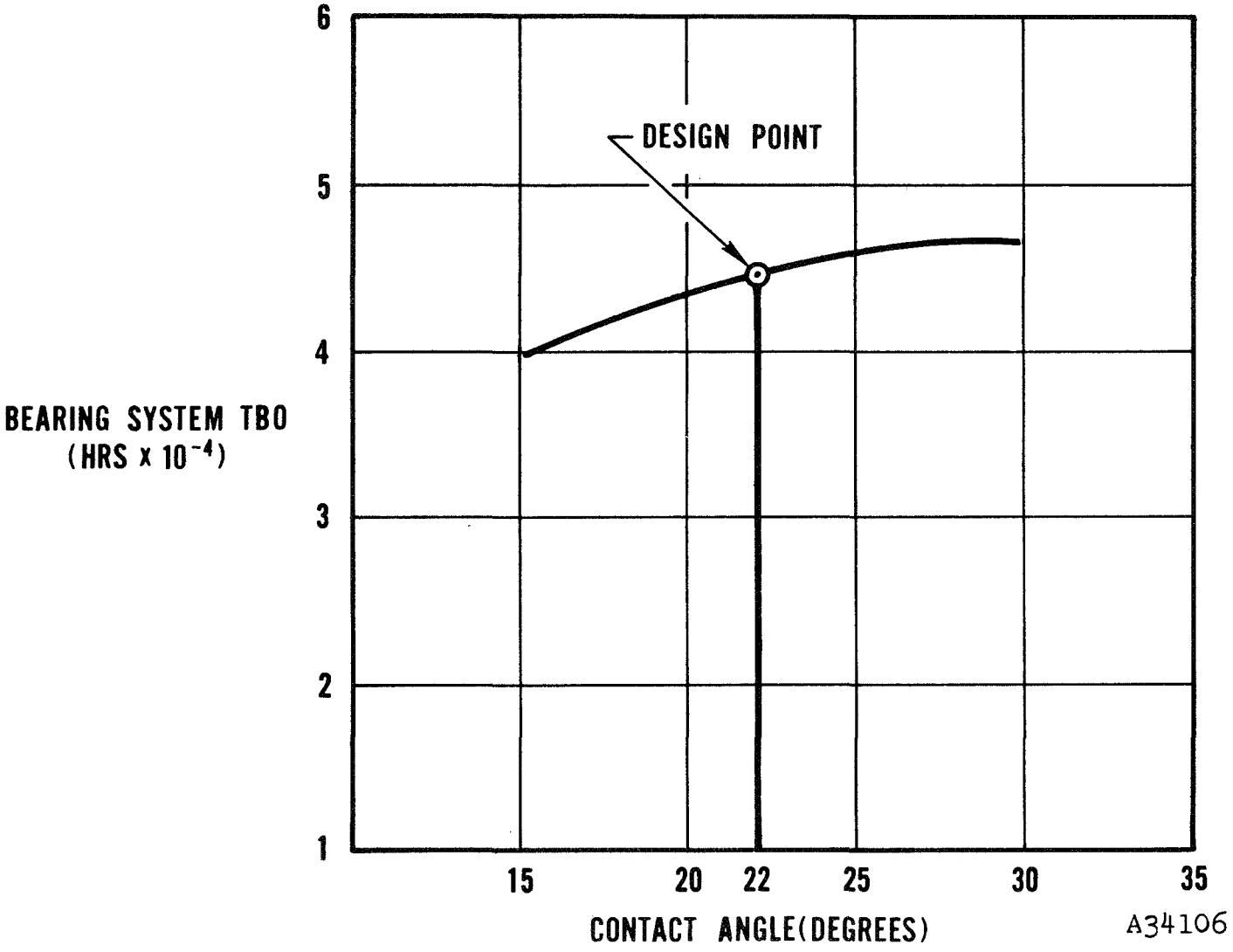

EFFECT OF CONTACT ANGLE ON BEARING SYSTEM FATIGUE LIFE

FIGURE 38

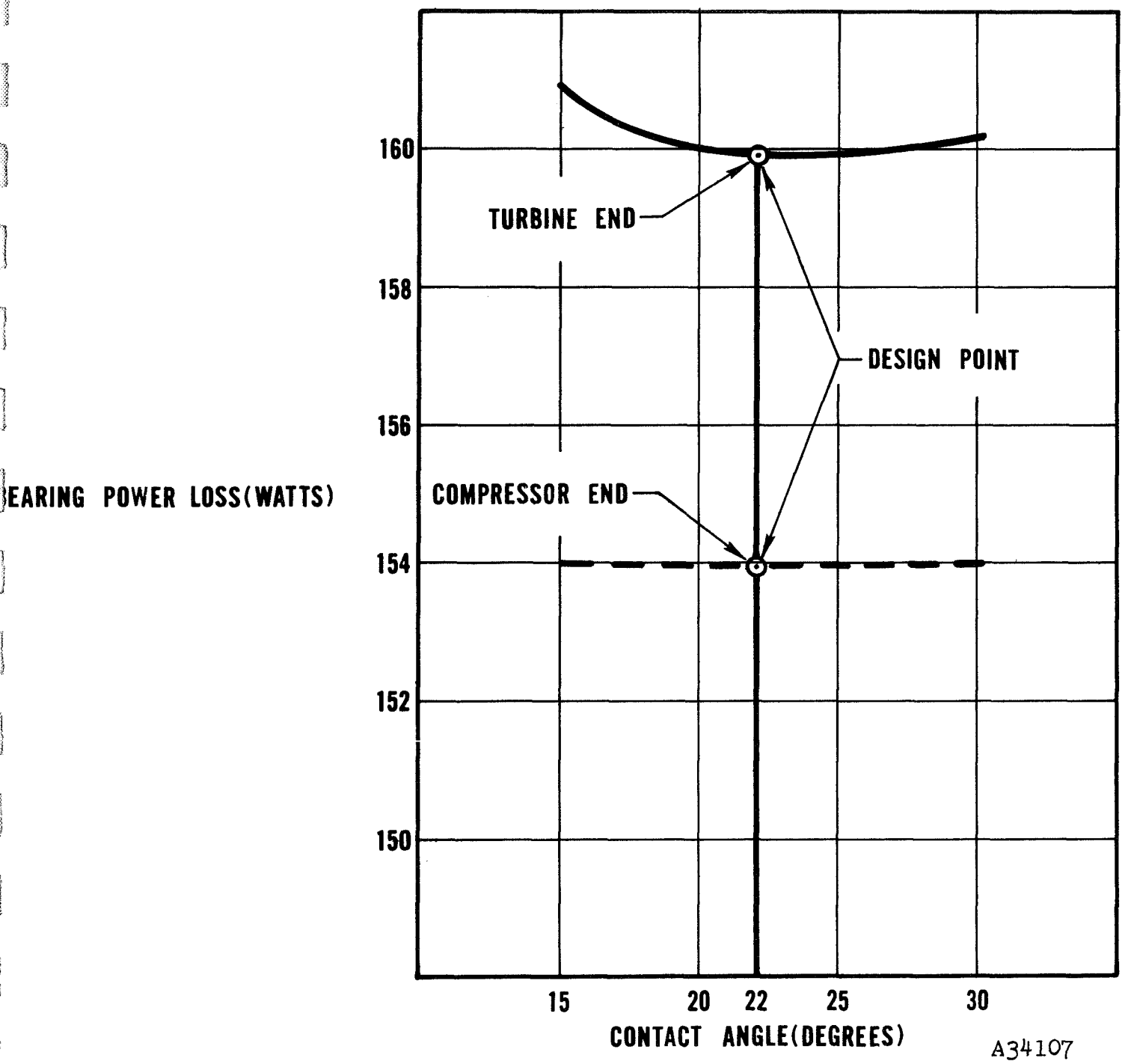

EFFECT OF CONTACT ANGLE ON BEARING POWER LOSS

FIGURE 39

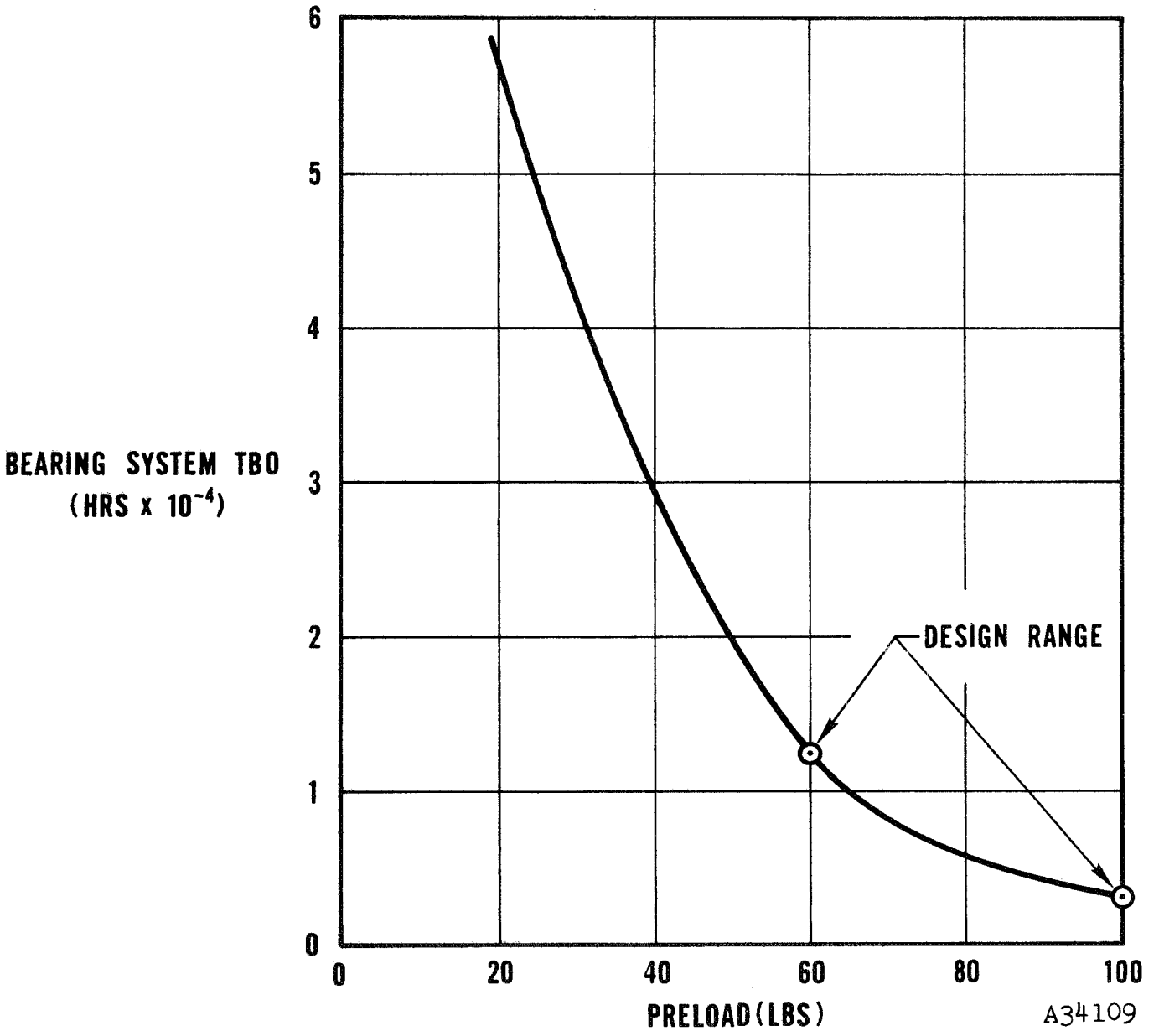

EFFECT OF PRELOAD ON BEARING SYSTEM FATIGUE LIFE

FIGURE 40

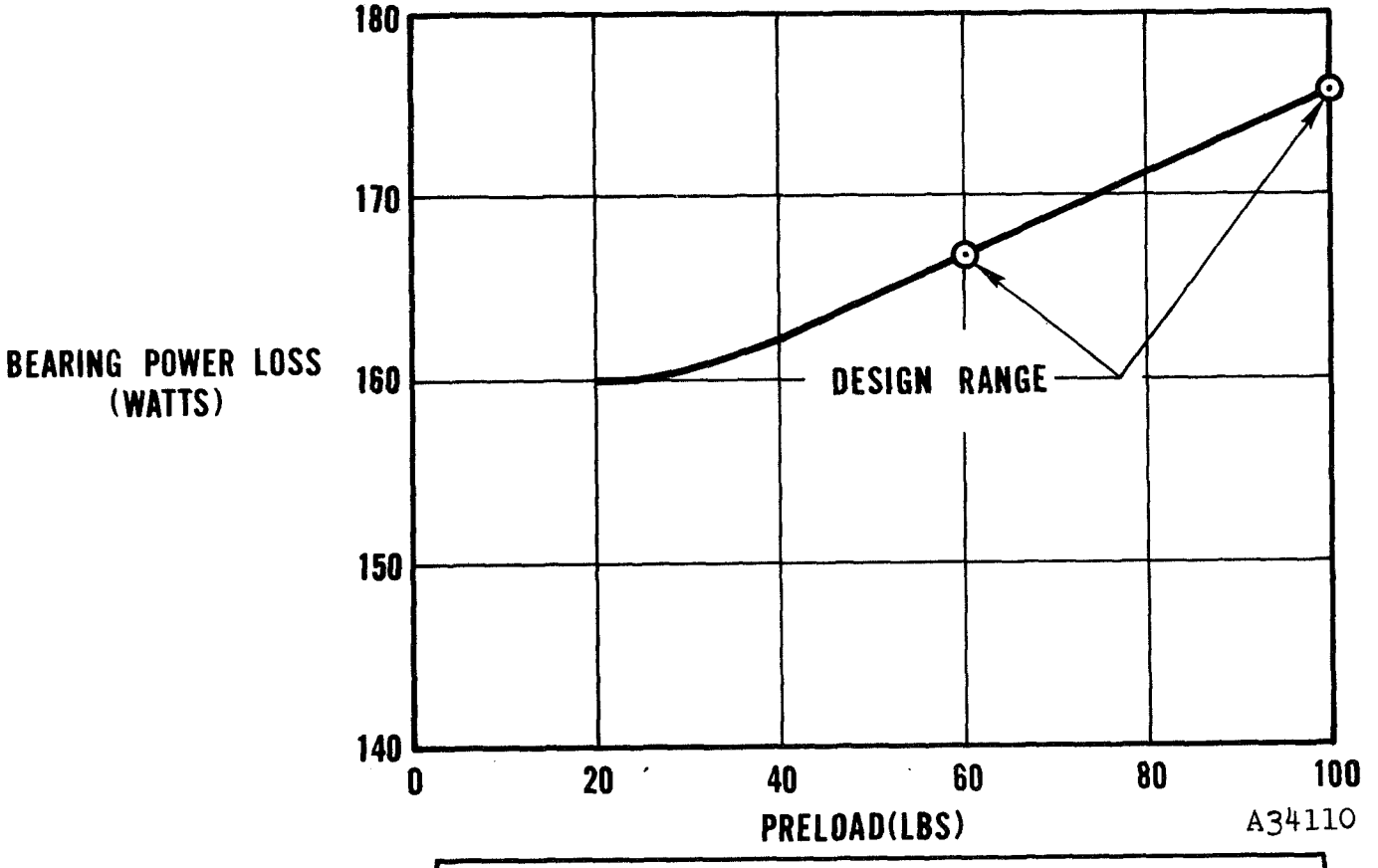

EFFECT OF PRELOAD ON BEARING POWER LOSS

FIGURE 41

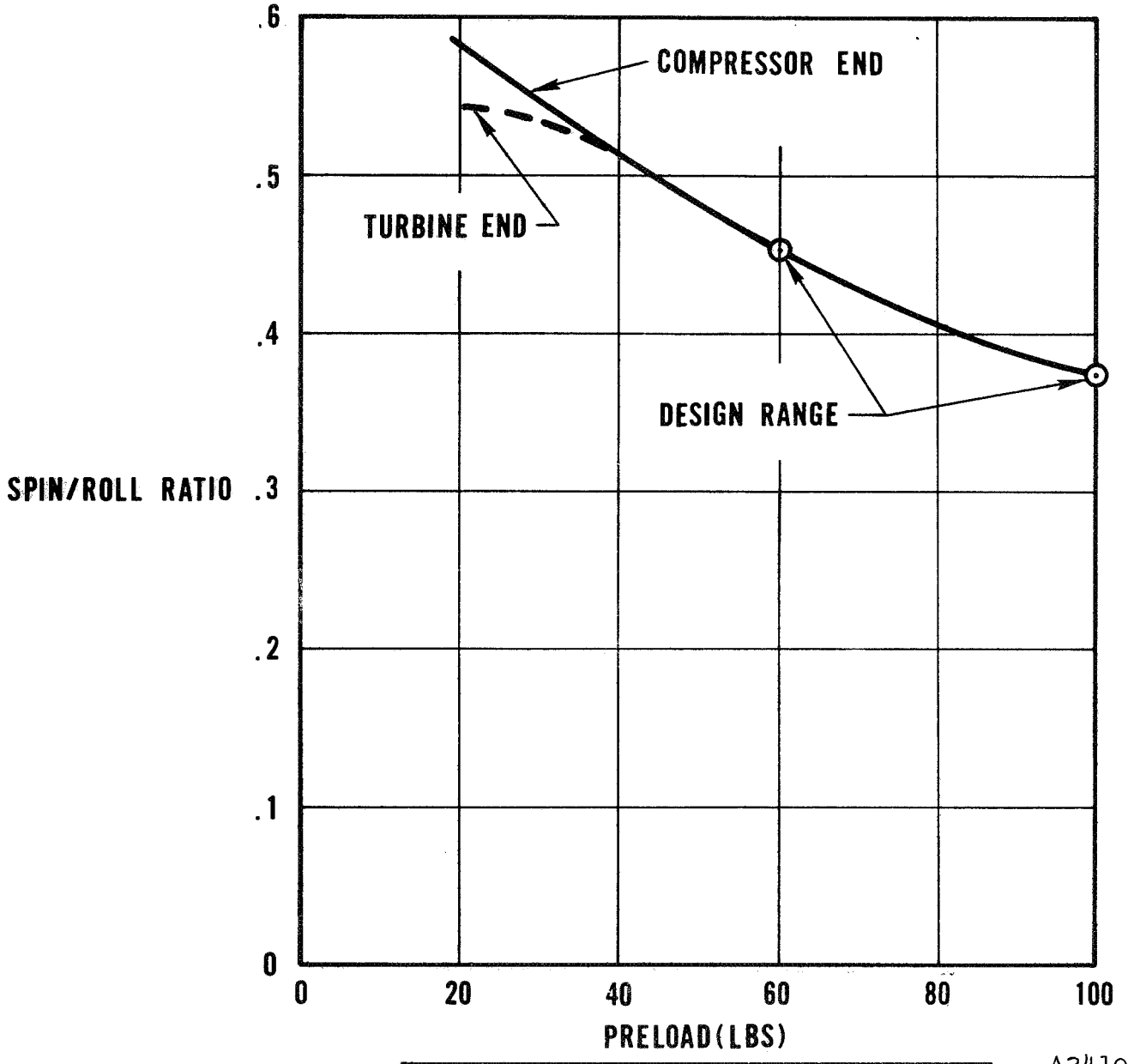

EFFECT OF PRELOAD ON BALL SPIN

FIGURE 42

and wear that will occur between the ball and the race. In order to minimize the spin/roll ratio, it is desirable to use the highest practical preload--in this case 60 to 100 lb.

5.2.5 Materials

Consumable-electrode vacuum-melted (CEVM) M-50 tool steel was selected for bearing rings and balls because of its high temperature resistance and excellent fatigue-life characteristics. Bearings having CEVM M-50 rings and rolling elements have fatigue lives up to 10.7 times those attainable with the use of conventional SAE 52100 bearing steel.

The separator material is silver-plated SAE 4340 Steel. Steel was selected rather than bronze since the bearing temperatures are expected to be as high as 350°F. At this temperature, bronze has poor mechanical properties, while SAE 4340 Steel maintains good mechanical properties. Thus, this steel is the better material for this application.

5.2.6 Separator Design

The separator is designed as a thin-section, outer-ring land-guided, one-piece machined-type to minimize drag and has several advantages over an inner-ring land-guided design:

(a) It allows maximum flow of lubricant to the hot inner race and through the bearing.

(b) The rotating inner-ring forces the lubricant to the separator/guiding land contact which minimizes friction and wear.

(c) The heat generated by separator rubbing is absorbed by the outer-ring, which is normally the cooler of the two and has the least severe loading.

5.2.7 Design Comparison

The optimum bearing design for this application is nonstandard. Figure 43 is a comparison between the optimum and the more conventional bearing design.

The tighter race curvatures of the conventional design would logically be expected to result in longer fatigue life than that of the optimized design, which has wide race curvatures. However, bearings with tight race curvatures require relatively high thrust preloads to maintain contact between the inner race and the balls in the radially unloaded portion of the race circumference. This prevents excessive pounding of the separator pockets which can ultimately cause premature bearing failure. Thus, the minimum required preload for the optimum design is only 60 lb, while that for the conventional design is 120 lb. This accounts for the greater fatigue life and lower power loss calculated for the optimum design.

5.3 Bearing Test Evaluation

The test evaluation of the bearings was performed in conjunction with the seal testing described in Section 6.3 and were performed in the bearing and seal test rig shown in Figure 44. The evaluation consisted of oil-mist lubrication and bearing endurance tests. For expediency, the oil-mist lubrication tests were performed with 20-mm ball bearings. The bearing and seal test rig was later modified, and endurance testing was performed with 30-mm ball bearings of the BRU-R design configuration.

	OPTIMIZED BEARING (PART 358546)	CONVENTIONAL DESIGN
INNER-RACE CURVATURE (PERCENT OF BALL DIAMETER)	55.5 TO 56.5	52 TO 53
OUTER-RACE CURVATURE (PERCENT OF BALL DIAMETER)	53.5 TO 54.5	52 TO 53
CONTACT ANGLE (DEGREES)	22	22
MINIMUM PRELOAD REQUIRED (LBS)	60	120
MAXIMUM PRELOAD (LBS)	100	150
BEARING SYSTEM B_1 LIFE (L_1), UNDER MAXIMUM PRELOAD (HOURS)	3,100	2,600
BEARING POWER LOSS (WATTS)		
TURBINE END	191	276
COMPRESSOR END	190	276

BEARING DESIGN COMPARISON

FIGURE 43

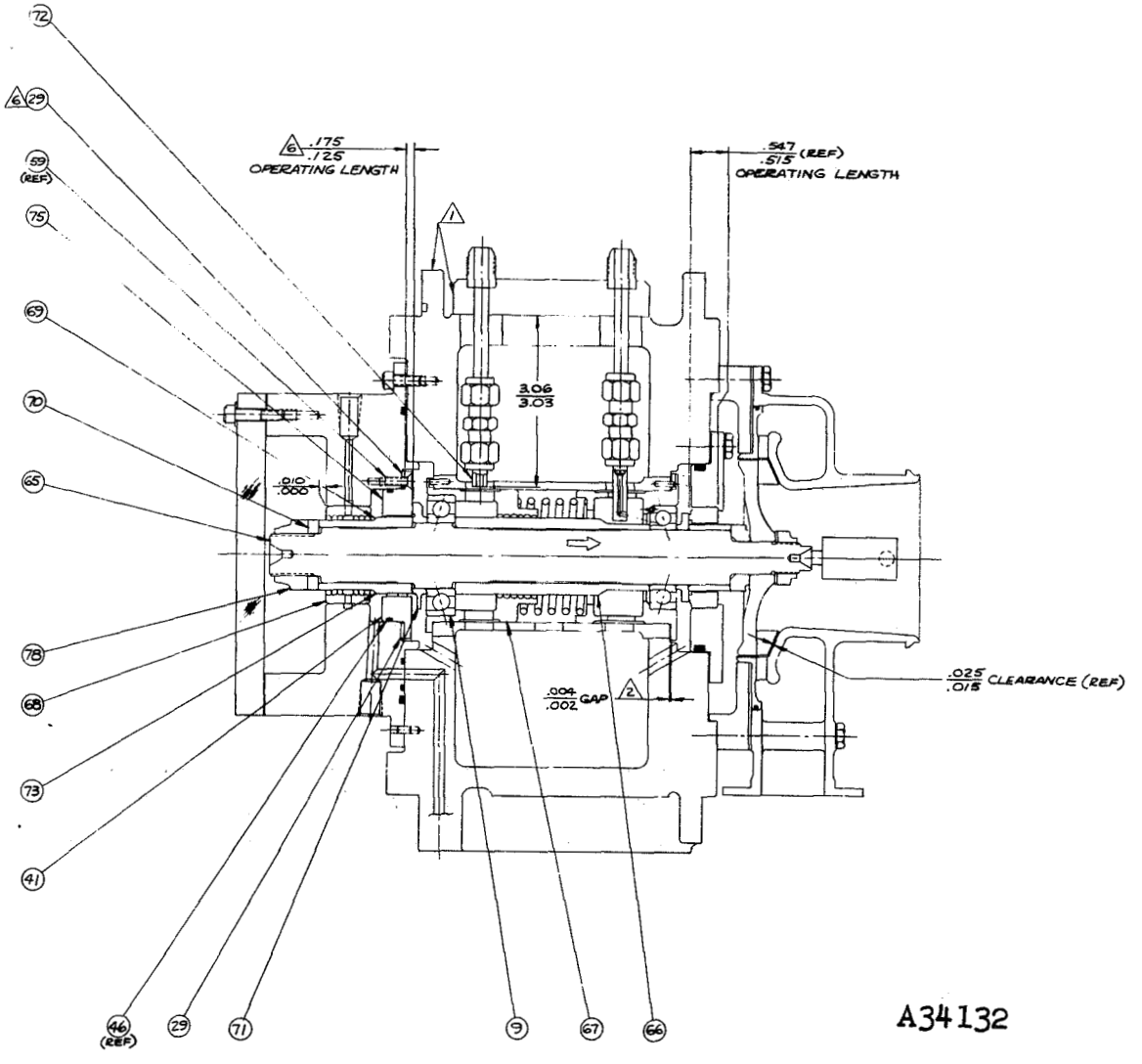

BEARING AND SEAL TEST RIG SCHEMATIC

FIGURE 44

5.3.1 Oil-Mist Lubrication Tests

Exploratory tests of gas-cooled oil-mist lubricated ball bearings were conducted with 20-mm ball bearings. The initial tests were performed over speed ranges between 20,000 and 65,000 rpm. Approximately 20 hr of testing was accumulated. The air/oil-mist ratios (by weight) investigated were as follows:

Mixture Ratio Air/Oil by Weight	Airflow Rate, lb/min	Oil Flow Rate (7808), gm/min
50:1	0.2687	2.440
200:1	0.2687	0.610
400:1	0.2687	0.305
800:1	0.2687	0.152

Severe bearing wear was encountered after 4 hr of running at 65,000 rpm with an air/oil mixture of 800:1.

Bearing temperatures were primarily a function of the cooling air mass flow and virtually independent of the air/oil mixture ratios tested.

Industrial air/oil-mist lubricated systems normally operate with air/oil ratios of 250:1 to 400:1. These systems are very conservative and tend to supply an excess of oil for lubrication.

Based on industrial practice and the desire to minimize the oil control required in the BRU-R system, an air/oil-mist ratio of 400:1 was selected for test. A 250-hr endurance test was run on the 20-mm bearing, operating at 50,000 rpm (DN = 1,000,000) with an air/oil-mist ratio of 400:1. The cooling airflow was maintained at 0.25 lb/min. Based on the satisfactory completion of this endurance test, the rig

was subsequently modified to permit testing the 30-mm bearing size selected for the BRU-R. Tests were conducted on a commercially available 30-mm bearing, operating at 36,000 rpm (DN = 1,080,000) to determine the optimum cooling airflow. Airflows were varied between 0.30 and 0.50 lb/min while the oil flow was held constant at approximately 0.0011 lb/min (air/oil ratio, 400:1 at 0.50 lb/min airflow).

Bearing temperatures were measured by four equally spaced thermocouples welded to the outer race of the bearing. The bearing temperatures associated with a cooling airflow of 0.30 lb/min averaged 147°F as compared to an average of 137°F observed for an airflow of 0.50 lb/min. The temperatures resulting from the lower airflow were unstable and spanned a range of 35°F, whereas the temperatures associated with the higher airflow were stable and spanned a range of only 20°F.

Using the 250-hr endurance test on the 20-mm bearing operating at a DN value of 1,000,000 as reference for satisfactory cooling airflow, the equivalent airflow for the 30-mm bearing operating at the same DN value (36,000 rpm) was calculated as approximately 0.46 lb/min.

5.3.2 Bearing Endurance Tests

Endurance testing of the 30-mm bearing of the BRU-R design configuration was initiated in conjunction with tests of various seals. The cooling airflows were maintained at 0.45 to 0.50 lb/min and the oil regulated to 0.0011 (i.e., air/oil ratio of 400:1).

Five bearings were tested in the bearing and seal test rig for a total of 1864 hr--endurance test times of 132, 562, 78, 34, and 1058 hr. The first bearing, with a test time of 132 hr, was replaced because of roughness and a worn separator caused by an assembly error. During a seal test, a scheduled disassembly for seal inspection was performed, and upon reassembly, the bearing was installed so that the axial preload was applied in the wrong direction. After 16 hr of operation

following this assembly error, roughness became apparent. The bearing was replaced, and this second one was successfully operated for 562 hr, before it was intentionally replaced.

The third and fourth bearings were tested for 78 and 34 hours, respectively. These bearings were removed because of problems that appeared in the test rig. After 78 hours of operation on the third bearing, a greatly increased flow of cooling gas to the test rig was observed. Upon disassembly, the broken nozzle supplying the cooling air and oil-mist lodged in the bearing carrier (Figure 45). The nozzle is normally located as shown in Figure 46. Further investigation revealed that the bearing carrier had rotated in a direction opposite to that of the bearing and shaft rotation with sufficient force to shear a 0.094-in.-dia antirotation pin and break the 0.25-in. dia tube of the cooling nozzle. However, both the BRU-R test bearing (30 mm) and the bearing of the test rig (25 mm) were free-turning and had not seized. Inspection of the BRU-R bearing revealed that the silver plate on the 4340 separator had been extruded and worn by the balls. Figure 47 shows a typical separator ball pocket with the silver plate deformation. Detailed inspection of the bearing proved the bearing balls and races were in excellent condition, although the silver plate on the separator was excessively thick. The bearing was sent to the vendor for an analysis. The test rig was repaired and a new bearing (the fourth) was installed. On the theory that the high-velocity cooling air jet from the nozzle was loading the balls and separator, a new nozzle with greatly reduced air velocity relative to the bearing was fabricated and installed. After 34 hr of testing, the rig was disassembled and inspected. The bearing carrier had again rotated in a direction reverse to shaft rotation but had not sheared the antirotation pin. The bearing-separator ball pockets showed similar wear of the silver plate. Considerable fretting of the bearing carrier in the test rig was noticed on both tests where separator wear had been experienced. The conclusion of the vendor was that the bearing had

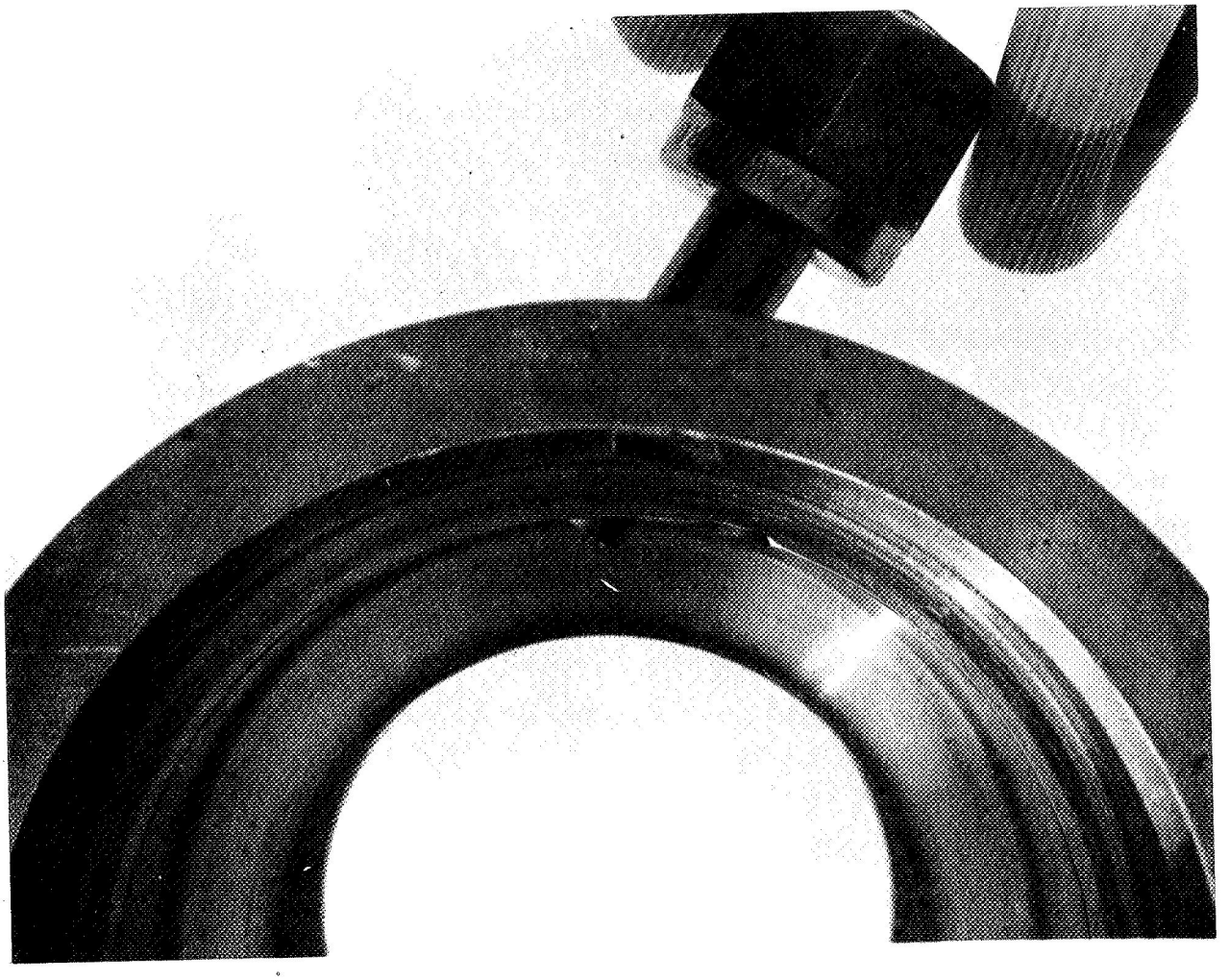

BEARING CARRIER AND DISPLACED
COOLING NOZZLE

FIGURE 45

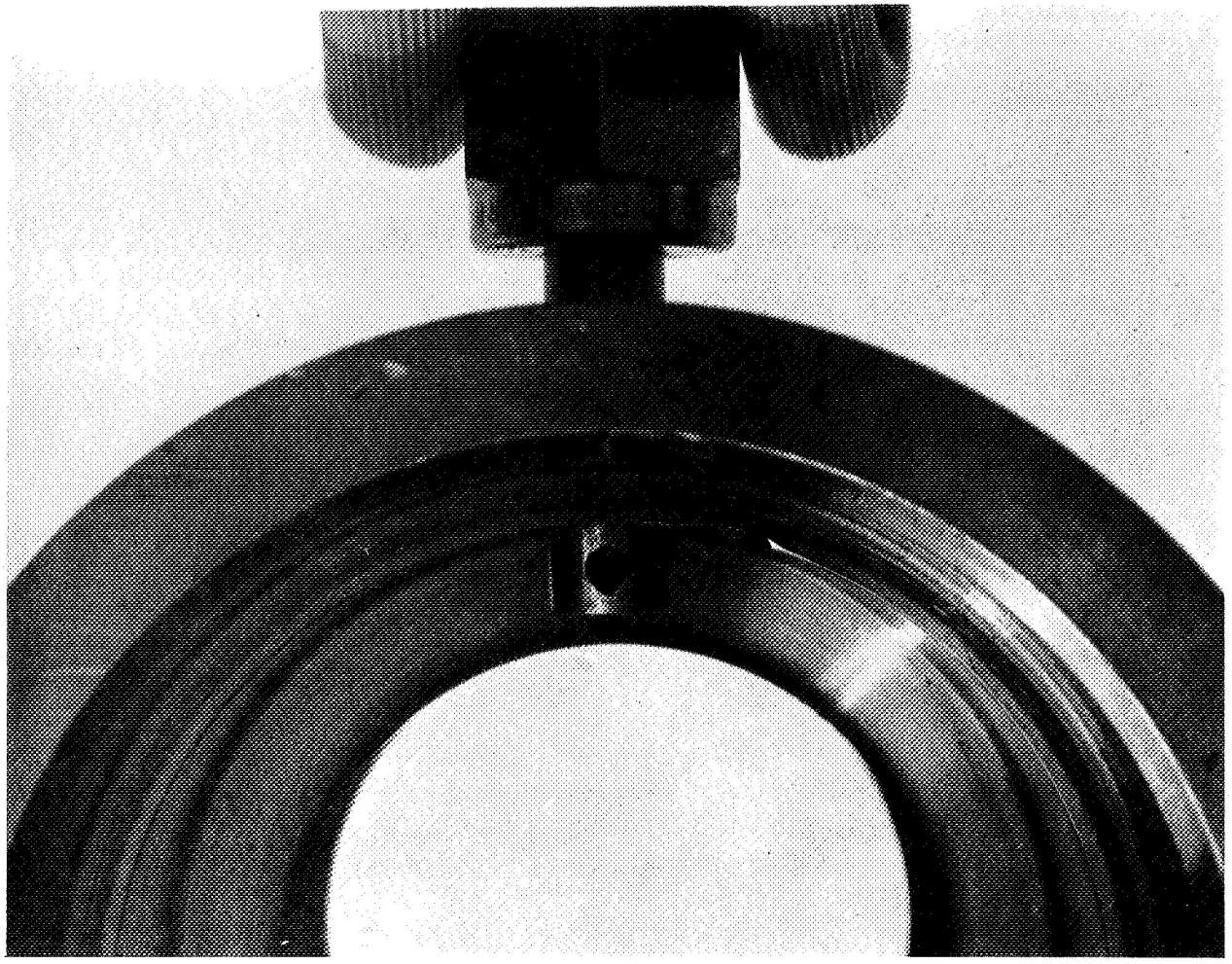

BEARING CARRIER AND COOLING NOZZLE

FIGURE 46

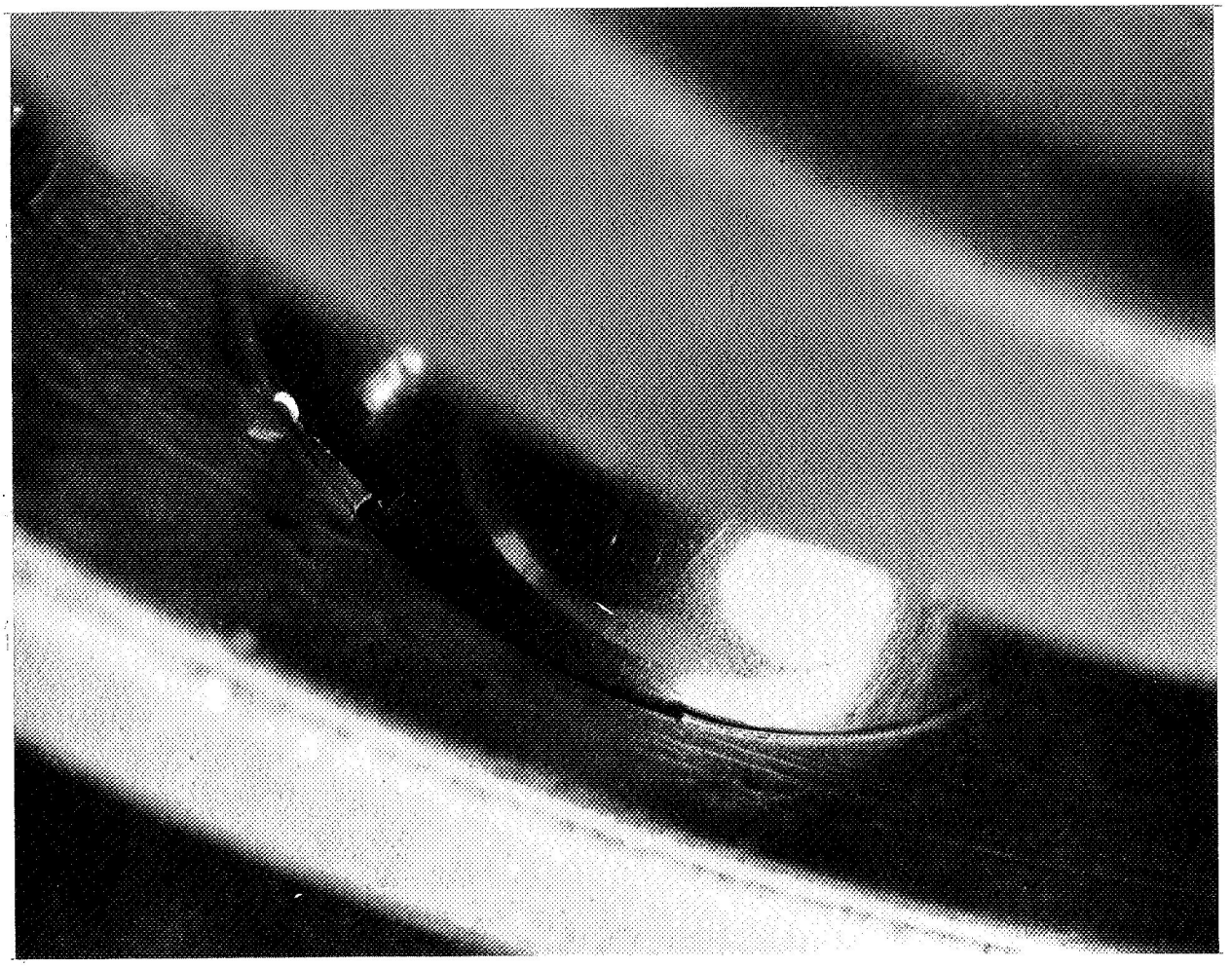

BALL AND SEPARATOR

FIGURE 47

been subjected to high radial loads. The vendor's report emphasized that the bearing was in excellent condition despite the silver plate smearing on the separator. The high radial loads were undoubtedly caused by a loose fit of the bearing carrier. The bearing carrier and housing had experienced considerable fretting. At the time the endurance testing was terminated, the average clearance between parts was over 0.003 in. The bearing carrier and housing were reworked to a clearance of 0.0003 in.

The fifth bearing was successfully tested for a duration of 1058 hr. This bearing was tested in conjunction with the comparative and endurance tests of the hydrodynamic face seals. The endurance test was voluntarily terminated in order to permit assembly and setup of the BRU-R and lubrication and cooling system. At the completion of this test, the bearing was in excellent condition.

6. SEAL DESIGN AND TEST EVALUATION

The seals in the BRU-R were designed to minimize the contamination of the cycle working fluid with the lubricant to cool the bearings. Two seals were designed to surround each bearing cavity. A hydrodynamic face-seal was designed to prevent oil from entering the cycle working fluid at either the turbine wheel hub or the compressor impeller hub. A radial labyrinth seal was provided to prevent oil from migrating into the alternator cavity. The seals were designed in conjunction with the BRU-R Lubrication and Cooling System to provide a differential pressure--a directional flow of helium-xenon--across each seal to continually purge and scavenge the oil-mist away from the seals, through the bearing cavity, out and down through the duct at the bottom of the BRU-R. The effectiveness and the life of the designs were demonstrated in a test evaluation program with a seal test rig.

6.1 Seal System Requirements

The seal system was designed with the objective of obtaining the lowest possible leakage of the lubricant into the cycle working fluid. The total accumulated leakage of MIL-L-7808 oil into the cycle working fluid was not to exceed 0.07 lb of oil maximum for the 500 hr of operating-life of the bearings and seals.

To achieve the seal objective, controlled leakage seals were positioned on each side of the individual bearing cavity. The function of each was to permit a limited amount of helium-xenon working fluid to flow into each bearing cavity with a minimum of seal power loss. The direction of flow was established by maintaining a favorable pressure differential across each seal. This was determined by analyzing the pressures back of the compressor impeller and turbine wheels as a function of power level and speed. The pressures at a radius of 0.63 in. on both the turbine wheel and compressor impeller correspond to

those imposed on the inside of the seal surface. Since transient conditions imposed on the seals during startup and shutdown are of short duration, the pressures corresponding to steady-state operation at 36,000 rpm were selected for use in seal design and are listed as follows:

Power Level kw_e	Pressure-Compressor at Radius = 0.63 in., psia	Pressure-Turbine at Radius = 0.63 in., psia
2.25	10.2	10.5
6.00	19.1	19.8
10.5	32.0	32.9

In order to minimize the pressure differentials across the seals and thereby leakage, the cooling system bearing cavity pressures were assigned as follows:

		Seal Pressure Differential	
Power Level, kw_e	Bearing Cavity Pressure, psia	Compressor Seal psi	Turbine Seal psi
2.25	10	0.2	0.5
6.00	18.9	0.2	0.9
10.50	31.5	0.5	1.4

The power loss was minimized by providing the seal with a gas thrust bearing of sufficient self-acting load capability that the mating seal surfaces and rotor are separated by a gas film at operating speed. The nonrotating seal surface is supported by an elastic bellows and is, therfore, free to displace axially. The leakage flow rate across the seal is thus established by matching the bellows flexibility and preload with the self-acting load capability generated in the gas film.

6.2 Hydrodynamic Face Seal Design

A cross-sectional view of the hydrodynamic face-type seal is shown in Figure 48. The seal design incorporates a conventional damped bellows holding a carbon nose but is unique in providing a Rayleigh stepped-sector gas bearing as well as a sealing land in the face of the carbon. The gas bearing feature permits the seal to operate with a thin film of gas between the seal nose and rotor, while providing an excellent sealing surface. The geometry for the initial gas bearing seal nose is shown in Figure 49. Eighteen stepped-sectors with a depth of 0.0002 in. are incorporated on the outer edge of the seal nose to provide the hydrodynamic film. The sealing land is located at the inner edge of the nose. Carbon material was selected for the seal nose to provide conventional sealing properties until the gas bearing becomes hydrodynamic and can support the preload.

The seal design ultimately used in the BRU-R is a variation of this design that interchanges the relative locations of the sealing land and the stepped-sector gas bearing. In this final design, the gas-bearing geometry is located on the inside diameter and the sealing land is located on the outside diameter.

The seal is installed so that the bellows will provide a face preload of between 3 and 4 lb. This preload assures stability of the gas bearing portion of the seal during BRU-R operation and also provides static sealing. The seal design is overbalanced so that the BRU-R loop may be evacuated to low pressures for start-up and purging without separating the seal surfaces and causing oil contamination of the main loop.

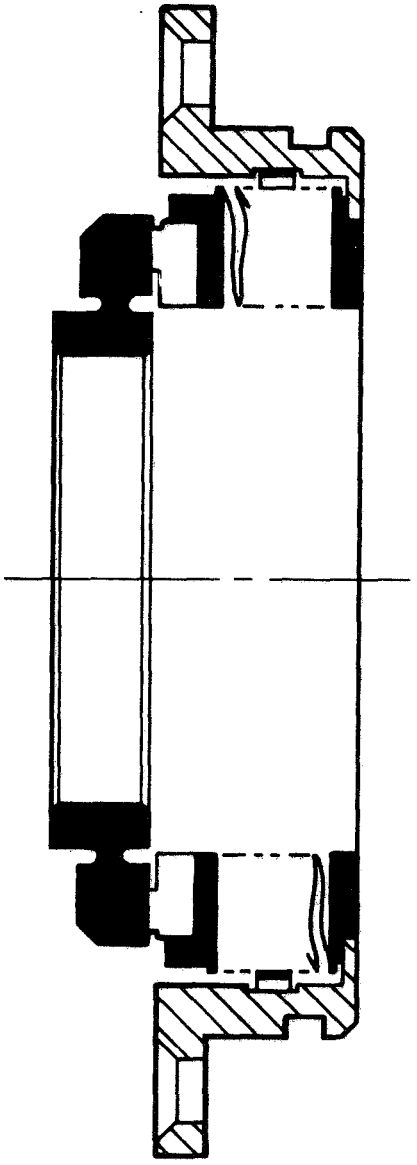

A34112

CARBON FACE SEAL

FIGURE 48

NOTES:

1. SEAL REGION DIMENSIONS:
   INSIDE RADIUS = 0.7675 IN.
   OUTSIDE RADIUS = 0.8175 IN.
2. BEARING REGION DIMENSIONS:
   INSIDE RADIUS = 0.8375 IN.
   OUTSIDE RADIUS = 0.9575 IN.

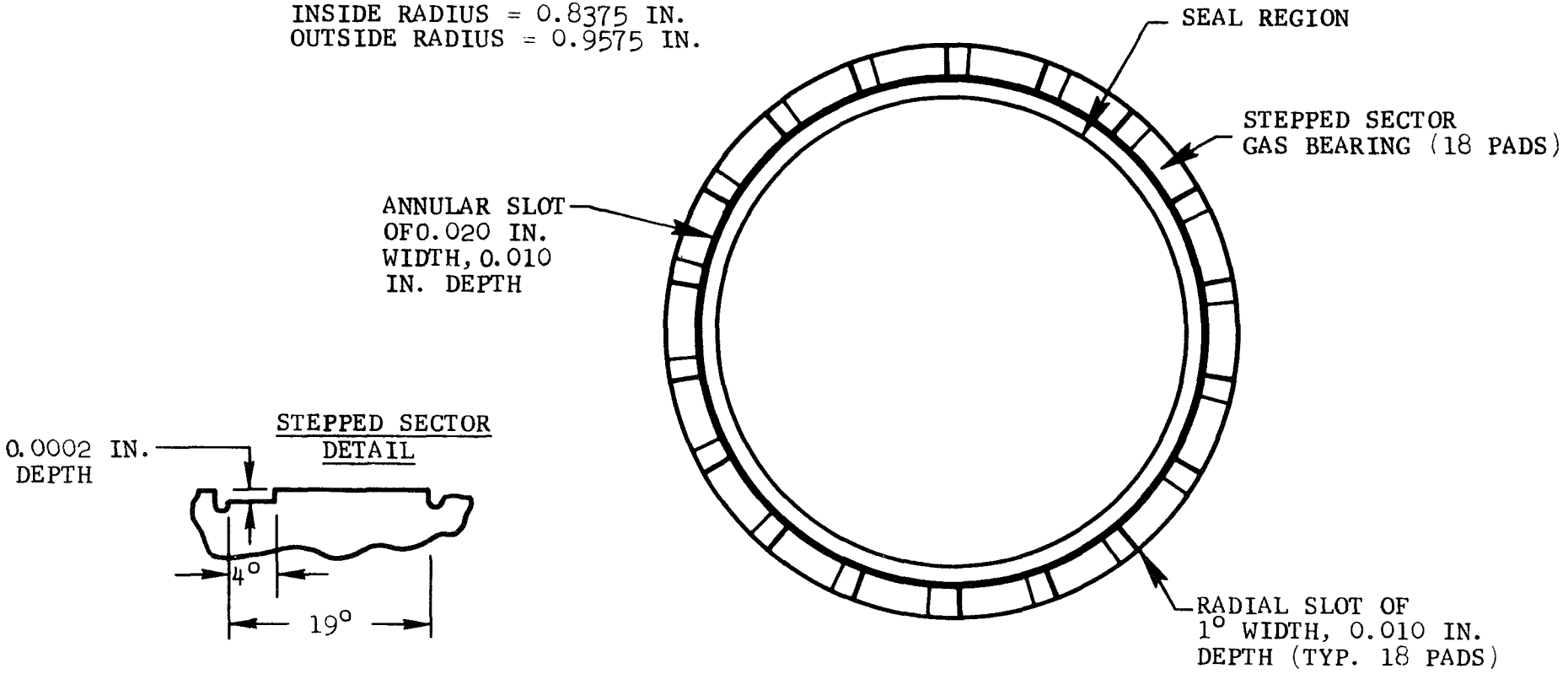

HYDRODYNAMIC SEAL,
BRU-R

A34128

FIGURE 49

During a start-up of the BRU and under the specified preload of 3 to 4 lb, the seal will have rubbing contact until the BRU-R reaches a shaft speed of 5000 to 8000 rpm. At this speed, the gas bearing will become hydrodynamic and generate a gas film-thickness of 0.000050 in. The curve on the right of Figure 50 shows this seal performance; the power loss is shown on the left side. Losses range between 28 and 35 w as a function of seal preload and ambient pressures corresponding to 2.25- and 10.5-kw_e alternator power levels.

With the seal preload corresponding to the load capacity of the stepped-section gas bearing, Figure 51 shows that the seal will operate with a gap or film-thickness of 0.00014 to 0.00018 in., again a function of preload and ambient pressures. The power loss shown pertains to the gas bearing portion of the seal only. The hydrodynamic face seal leakages resulting from the various pressure levels and differentials associated with the BRU-R power levels of 2.25 and 10.5 kw_e are shown in Figures 52 and 53, respectively. Assuming a nominal seal gas film-thickness of 0.00015 in., each face seal will permit a maximum leakage of 0.0000025 lb/min at the 2.25-kw_e power level and 0.00002 lb/min at the 10.5 kw_e power level.

6.3 Seal Test Evaluation

The seal test program evaluated three different face-type seals and a radial seal. The face-type seals all are bellows-mounted with a carbon-nose. Two of the seals are hydrodynamic with a gas-bearing geometry incorporated in the carbon-nose and are the "primary" designs for the BRU-R. One seal has the gas bearing geometry on the outside diameter and the other on the inside diameter. The third face-type seal is a contacting carbon-nose face seal and was tested as a "back-up" seal. Testing the back-up design was initiated first because of the manufacturing times involved. The radial seal was a noncontacting labyrinth with "Kapton" polyimide lands.

1. r_i = .8175
2. 18 STEPPED SECTOR PADS
3. 4° PER STEP, .0001 IN. DEPTH
4. VISCOSITY = 5 x 10^{-9} REYNS

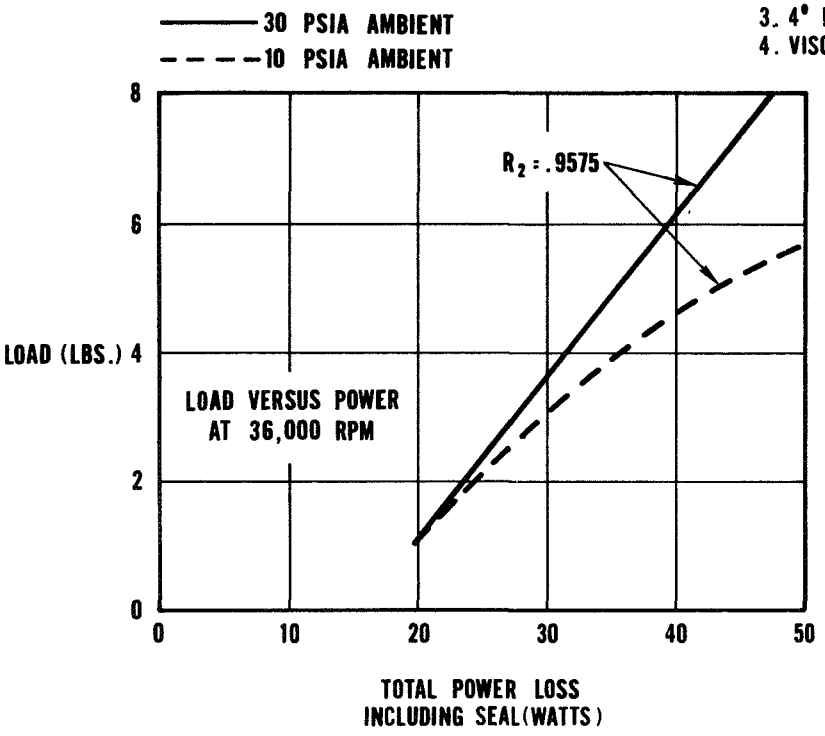

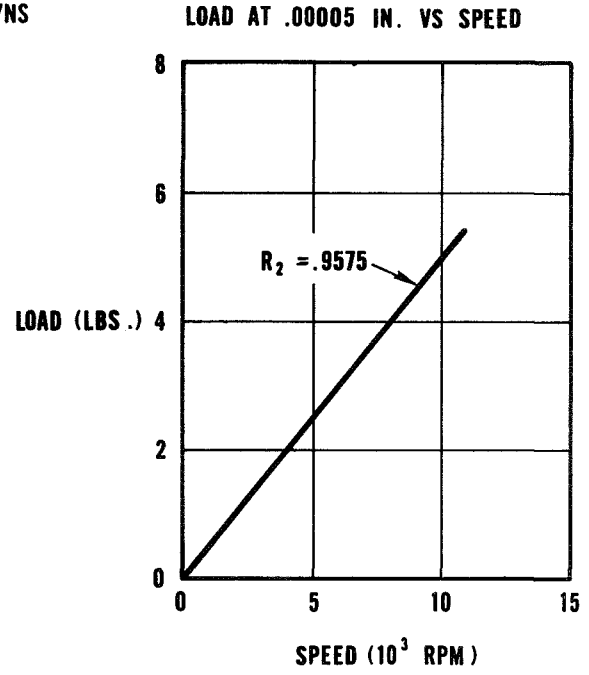

SEAL PERFORMANCE

A34113

FIGURE 50

AIRESEARCH MANUFACTURING COMPANY OF ARIZONA
A DIVISION OF THE GARRETT CORPORATION
PHOENIX, ARIZONA

NOTES:
1. BEARING OUTER PAD: .9575 IN.
2. BEARING INNER PAD: .8375 IN.
3. 18" PADS, 4° ARC PER STEP, .0002 IN. STEP DEPTH
4. LUBRICANT VISCOSITY: 5×10^{-9} REYNS

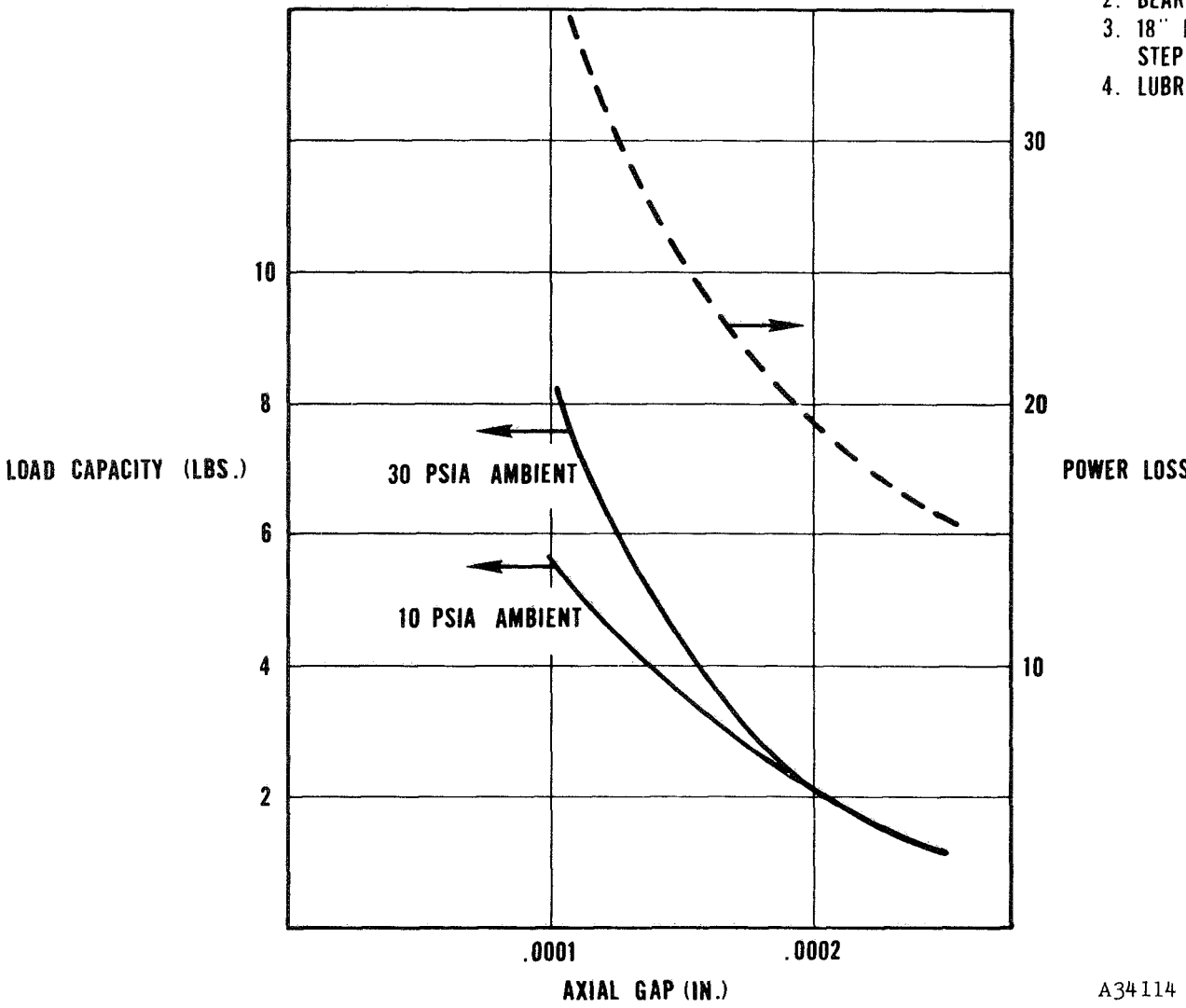

STEPPED SECTOR HYDRODYNAMIC PERFORMANCE 36,000 RPM R_o = .9575 IN.

FIGURE 51

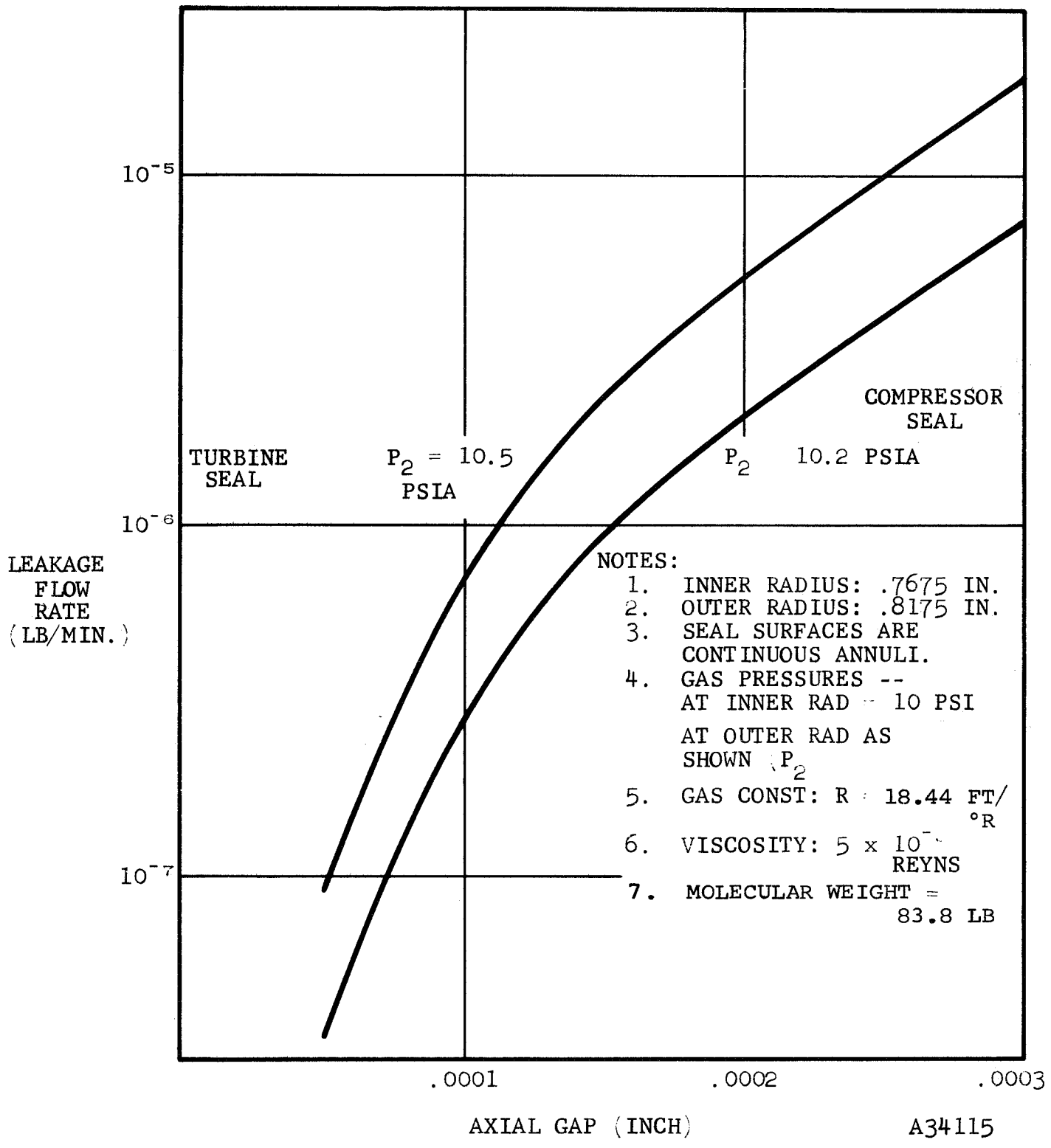

HYDRODYNAMIC SEAL PERFORMANCE, HELIUM-XENON MIXTURE, 330°F

FIGURE 52

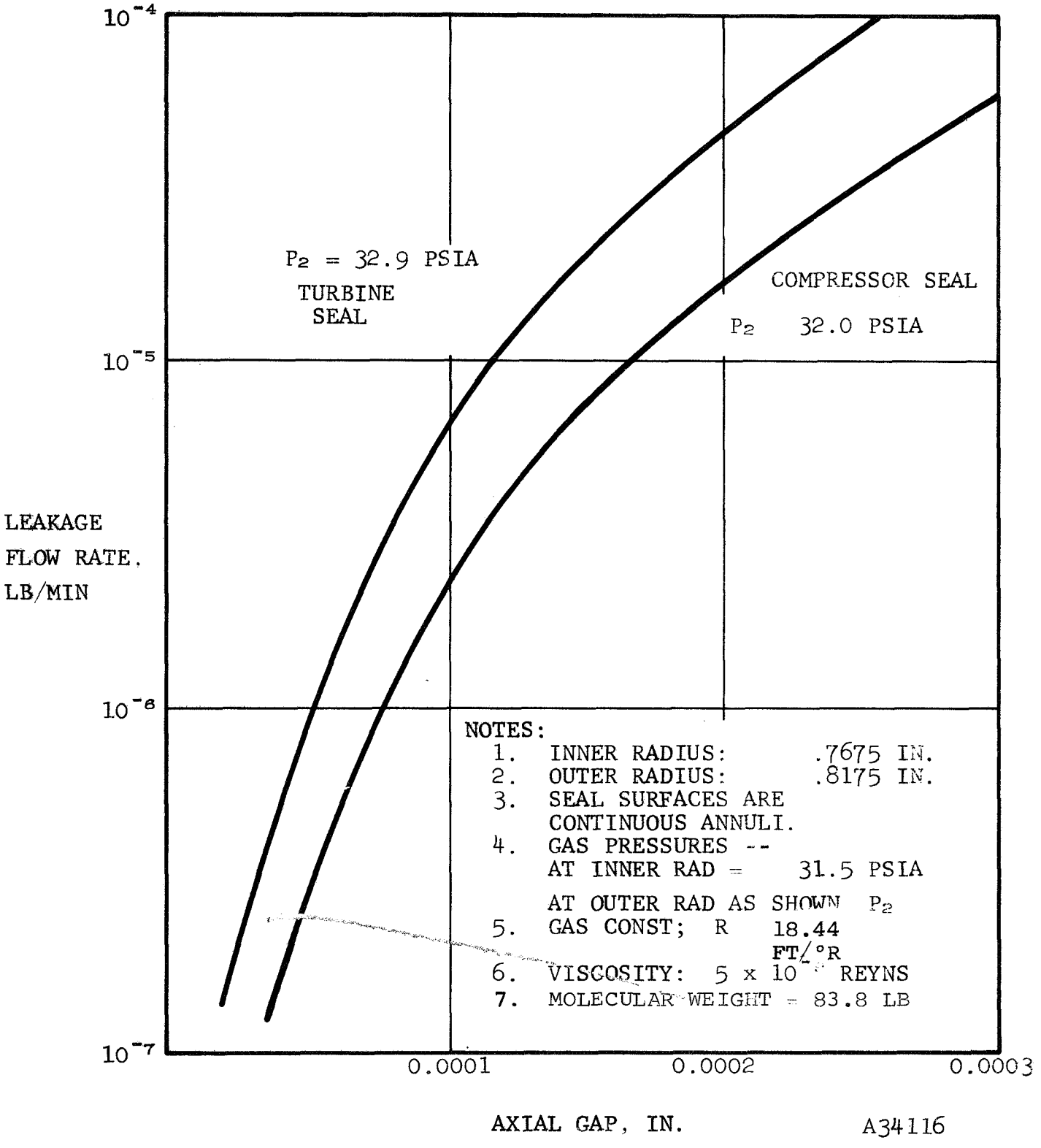

HYDRODYNAMIC SEAL PERFORMANCE, HELIUM-XENON MIXTURE, 330° F

FIGURE 53

All seal designs were dynamically and statically leak-checked, as discussed in the following paragraphs. Of the two seal designs with the gas bearing geometry, that with the geometry on the inside radius demonstrated superior performance. The carbon-nose contacting seal proved adequate for a back-up design.

6.3.1 Contacting Carbon-Nose Seal Testing

The contacting carbon-nose seal is bellows-mounted and intended as a "back-up" for the hydrodynamic seal designs. The contacting carbon-nose seal, P/N 699190, is shown in Appendix D. The initial testing of the carbon-nose seal consisted of a 30-hr test in the same test rig as in the bearing tests (Figure 44). The seal was operated at 36,000 rpm with 0.5-lb/min flow of air-oil-mist being supplied as lubrication and cooling to the 30-mm ball bearing and seal. The air/oil ratio was maintained at 400:1 for this test. The seal and rotor were inspected at 10-, 20-, and 30-hr intervals, and the sealing effectiveness remained constant. Figure 54 shows the debris generated by the seal during the first 10 hr of the test. The initial wear rate of the carbon face was 0.0001 in./hr of operation. The carbon wear rate decreased to approximately 0.00001 in./hr during the balance of the 30-hr test. The seal rotor sustained no measurable wear, although some scratches were visible at an area corresponding to the outside diameter of the carbon face. Based on the established wear rate, this seal design has an established life of 500 to 1000 hr and has been installed with a face load of 4 lb. Additional tests were performed with a reduced face load on the carbon.

Testing of the carbon-face seal, P/N 699190-1, continued with a 3-lb load. The test conditions were the same, and a total of 509 hr of endurance testing was accumulated on one seal. The seal rotor after the 509-hr test is shown in Figure 55 and the carbon-nose face-seal is shown in Figure 56. A second seal was tested approximately

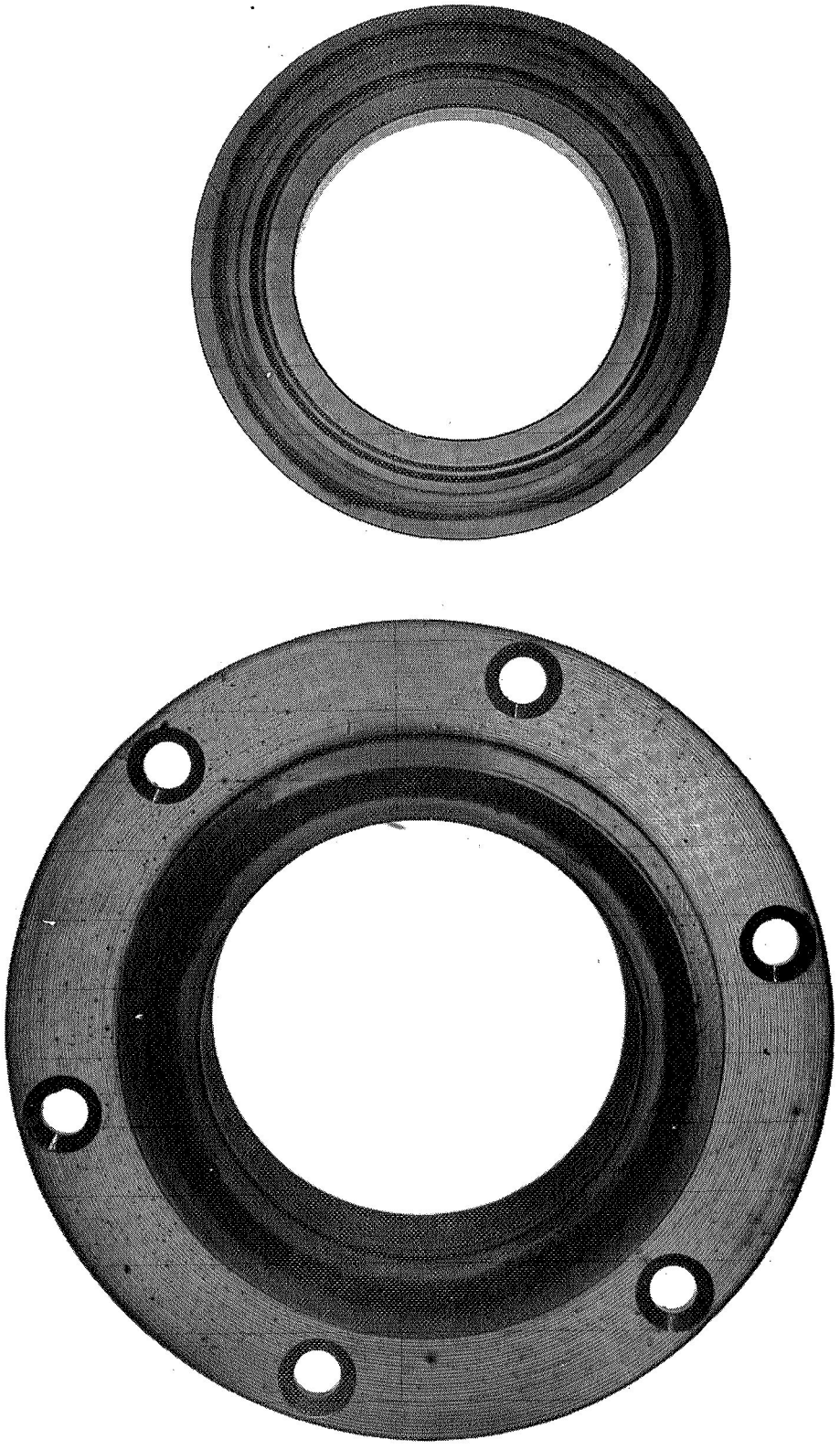

CARBON-NOSE SEAL AFTER 10 HOURS

FIGURE 54

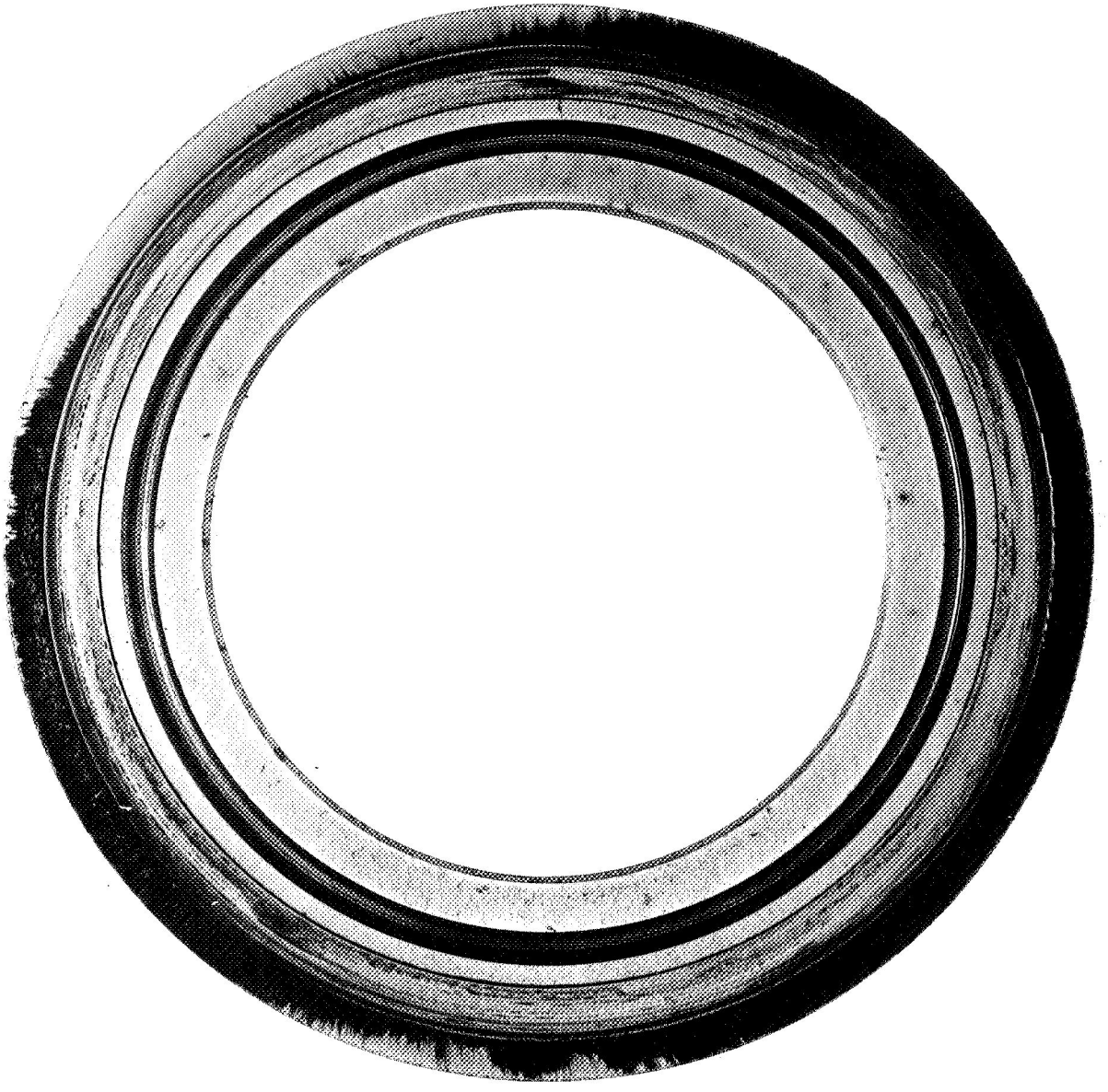

ROTOR AFTER 509-HOUR ENDURANCE TEST

FIGURE 55

MP-19576

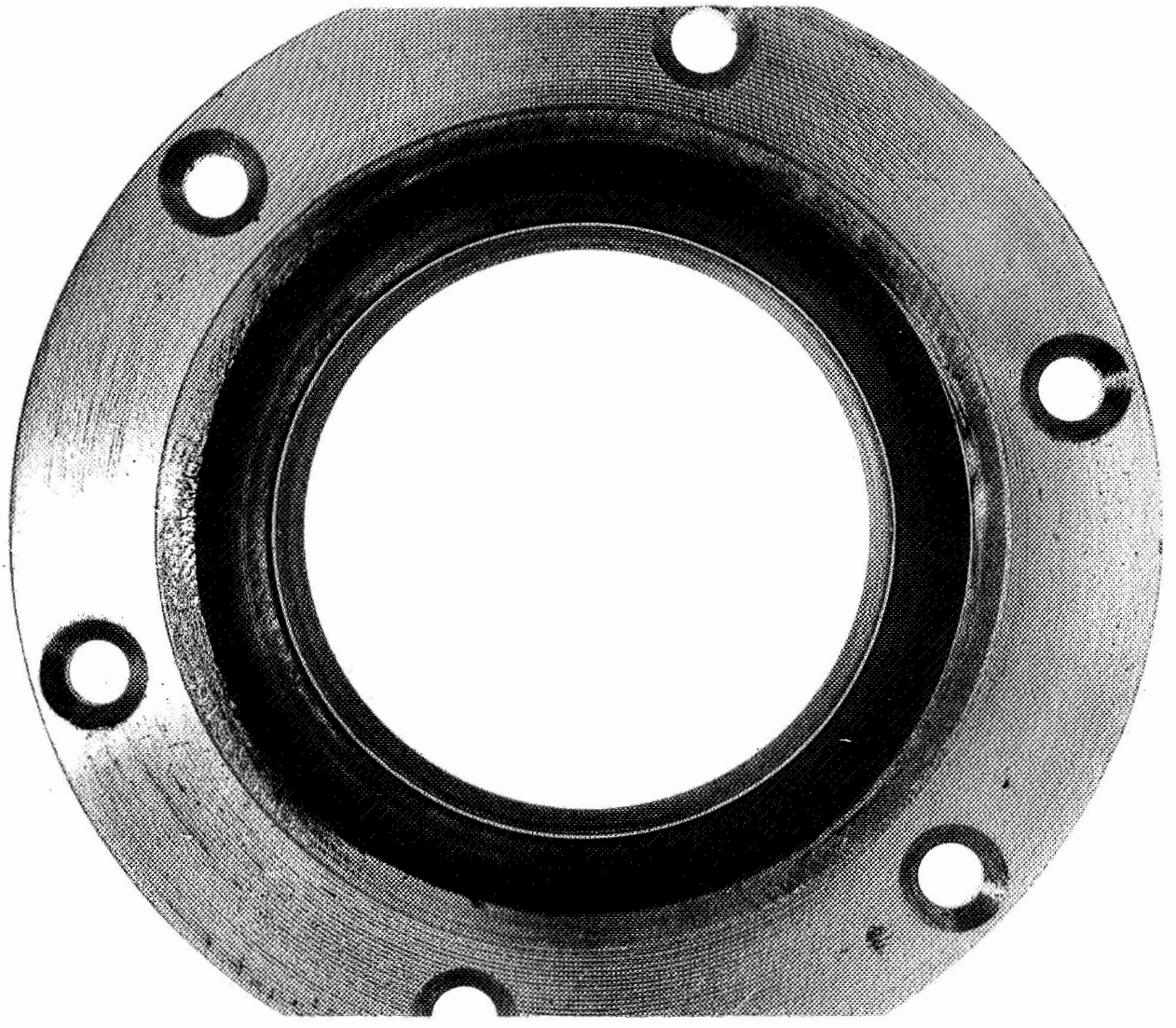

CARBON-NOSE FACE SEAL
AFTER 509-HOUR ENDURANCE TEST

FIGURE 56

MP-19577

56 hr. The leakage rate of the endurance seal after 509 hr of operation at 36,000 rpm and under a differential pressure of 2 psi was 0.000027 lb air/min. Seal leakage under static conditions was essentially the same. The equivalent seal leakage for operation in a helium-xenon environment corresponding to the 10.5 kw_e BRU-R power level is 0.000071 lb/min. The original calculated leakage for this type of seal was 0.0531 lb/min. The measured wear of the carbon nose after 509 hr of operation was 0.0015 in. Based upon this wear rate and a usable carbon nose height of 0.015 in., the estimated seal nose life is 5000 hr.

6.3.2 Hydrodynamic Face Seal Testing

Two designs of the hydrodynamic seals were evaluated in the bearing and seal test rig. Each design has a gas-bearing geometry incorporated in the carbon nose of the seal. The difference between the two designs is that one has the gas-bearing on the inside diameter with a solid land on the outside diameter, and the other seal uses the gas-bearing on the outside diameter and a solid land on the inside diameter. As with the contacting carbon-nose seal testing, the evaluation of the hydrodynamic face seal was performed in the seal test rig shown in Figure 44.

The initial testing of the hydrodynamic seal was performed with the gas-bearing on the outside diameter. These tests revealed that the inner sealing land was contacting the rotor while the gas bearing portion of the seal was not. The seal and rotor wear patterns after 12 hr of operation are shown on Figure 57. The gas bearing portion of the seal was functioning but the inner sealing land surface was worn 0.0002 in. below that of the original coplaner gas bearing surfaces. Subsequent analysis indicated that the wear was caused by thermal distortion of the rotor. In normal operation, the seal surfaces are separated 0.00015 in. by the hydrodynamic thrust of the bearing. However,

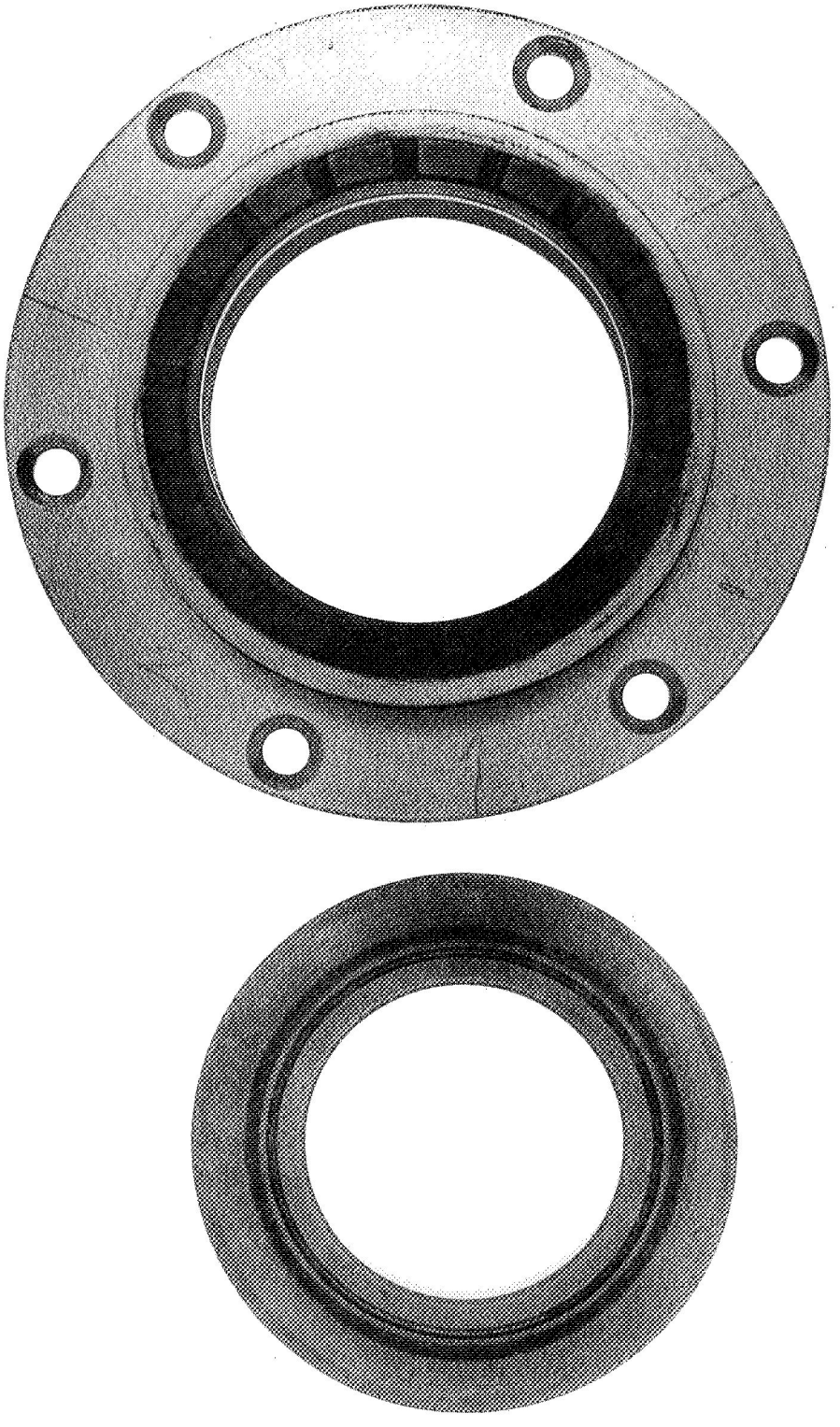

HYDRODYNAMIC SEAL & ROTOR

FIGURE 57

during start-up, the seal rubs against the rotor with consequent large frictional heating. The major portion of this heat is removed by the bearing coolant, which impinges on the back side of the rotor. Thus, a fairly large axial temperature gradient exists in the rotor which causes the outer radius to bend away from the thrust surface. The arrangement of the thrust bearing, seal land, and the deflected position of the rotor are sketched below.

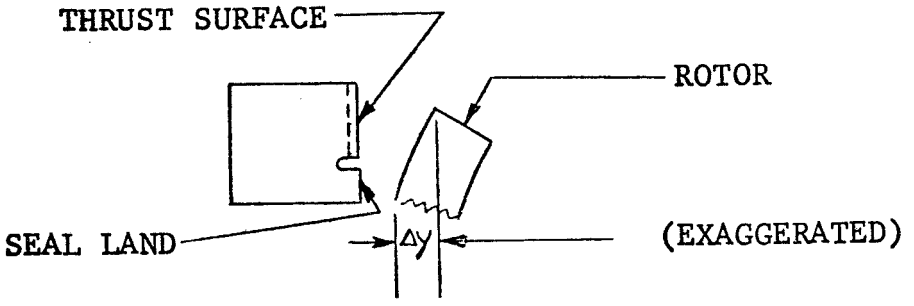

The frictional heating present under steady-state conditions, with undistorted surfaces, will cause a deflection (Δy) of the order of 6.5×10^{-5} in. However, as the rotor bearing surface distorts, the power loss will increase due to the decreased gas film-thickness; consequently, a further distortion is induced. The minimum film-thickness can, in fact, diminish to zero before thermal equilibrium is established. If rubbing were to occur, the distortion of the rotor surface would be further accelerated.

In order to reduce the effect of rotor thermal distortion, rotors made from tungsten carbide were substituted for the originally designed 440C stainless steel rotors.

The next test was performed with a hydrodynamic seal having the gas-bearing geometry on the inside diameter. The seal in this test was not flat and had high points in three areas; also, there had been distortion during the installation of the eloxed carbon nose in the seal holder. Subsequently, the manufacturing techniques were revised

to permit the Elox machining of the seal nose after installation in the seal holder and this problem did not reappear. The seal used in this test had a distorted seal face of 0.0001 in. A test of 100 hr, including 16 starts and stops, was performed using the distorted seal and a 440C Stainless Steel rotor. The hydrodynamic seal at the end of 40 hr is shown in Figure 58 and at the end of 100 hr in Figure 59. The gas bearing surface was lightly rubbed at three separate high points on the seal face. Due to the distortion of the seal surface during assembly, the seal leakage was statically measured at 160 x 10^{-6} lb/min under a differential pressure of 2.0 psi. The seal leakage at 36,000 rpm under the same differential pressure was 440 x 10^{-6} lb/min. The leakage rates were measured after 40 and 100 hr of testing and were identical. While the leakage is relatively high due to the distorted seal face, it is still two orders of magnitude less than originally predicted. The test indicated that the gas bearing was functioning properly. This conclusion is based on measurements of the seal test rig drive torque and on inspections during the disassembly of the test rig. When the seal was operating hydrodynamically, there was a measurable decrease in the test-rig drive torque. Inspections during disassembly revealed the absence of carbon dust and no measurable wear of the seal face.

Comparative tests of the two hydrodynamic seal designs were performed with a tungsten carbide rotor. The first part was a static test to determine the differential pressure required to cause seal lift-off and leakage. With the seal design having gas bearing geometry on the inside diameter, seal leakage occurred under a differential pressure of 19 psi; on the outside diameter, leakage was under a differential pressure of 8.6 psi. The difference in differential pressure at lift-off of the two seals was due to the location of the gas bearing geometry and the corresponding pressure balance. The static test results reveal that either design is acceptable in the BRU-R, as the normal

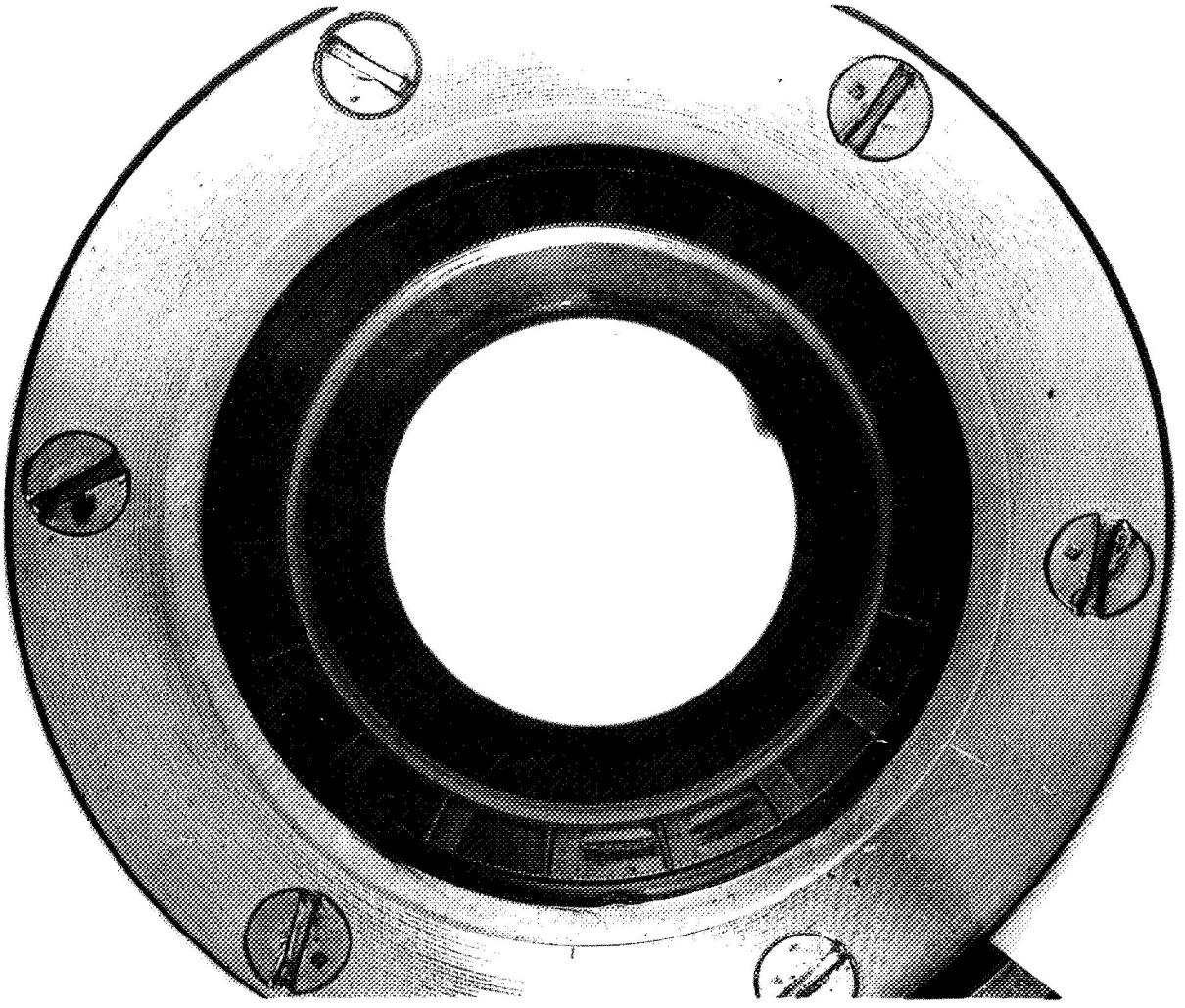

HYDRODYNAMIC FACE SEAL AFTER
40-HOUR TEST

FIGURE 58

MP-19901

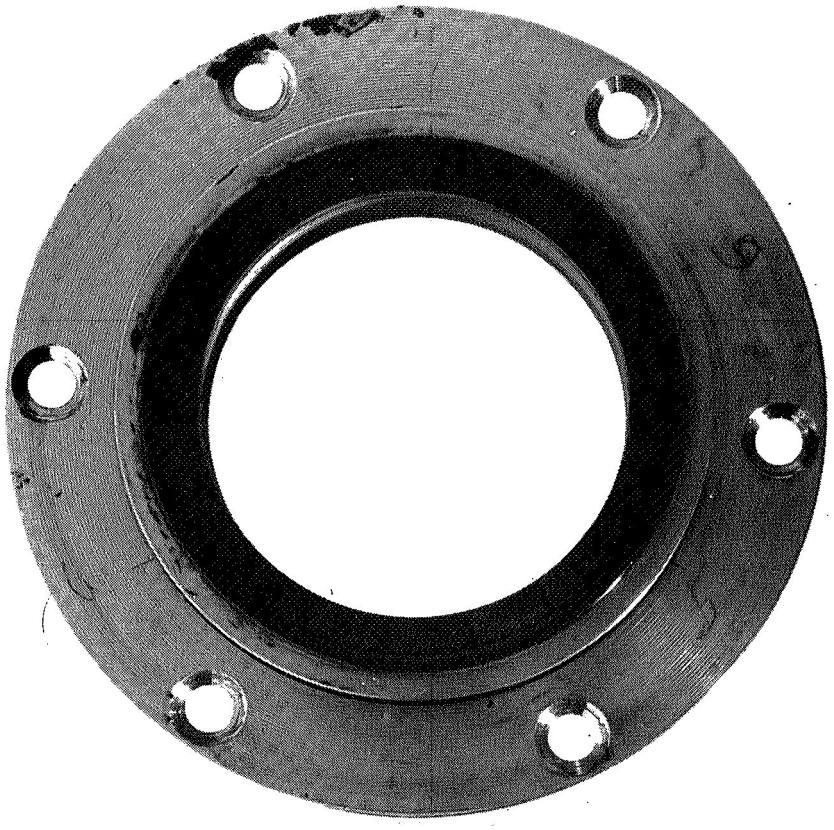

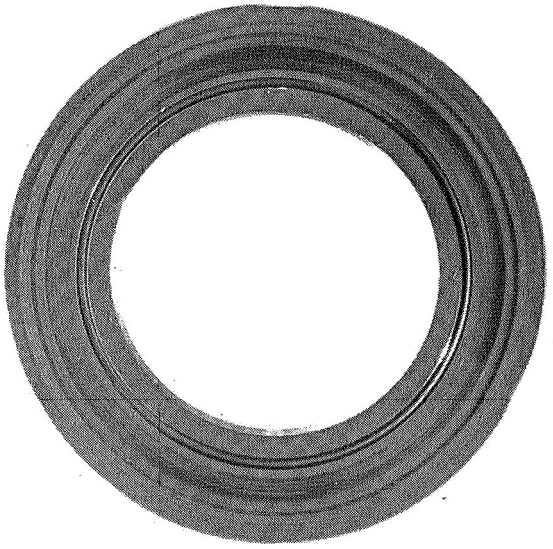

HYDRODYNAMIC FACE SEAL AND 440C ROTOR
INSIDE GAS BEARING GEOMETRY - 100 HOURS

FIGURE 59

operating differential pressure will be approximately 0.7 psi. Special care in purging the Brayton Cycle Loop and Lubrication and Cooling System would be required if the seal with the gas bearing geometry on the outside radius were used.

The second part was a dynamic test. The hydrodynamic test with the gas-bearing geometry on the inside diameter was tested for 107 hr under simulated BRU-R conditions with 20 starts and stops. The seal (Figure 60) was in excellent condition with only light rub marks, resulting from the unlubricated starts and stops. The second seal design with the gas-bearing geometry on the outside diameter was operated for 10 hr and inspected. Each gas-bearing pad of the seal was coated with a thin film of carbonized oil. The seal is shown in Figure 61. In this seal design, the MIL-L-7808 oil-mist is drawn into the gas bearing geometry and is subsequently raised to high enough temperatures to coke the oil. As the oil cokes, particles build on the gas bearing and destroy the load capacity of the bearing with subsequent rubbing and higher temperatures. This test was repeated with a new seal with the same coking buildup (Figure 62).

Accurate measurement of the seal nose operating temperatures proved impractical. However, temperatures measured on the steel backing of the carbon-nose ranged from a steady 250°F for the design with the gas bearing on the inside to a highly variable 350° to 450°F for the design with the gas bearing on the outside. The variable temperatures coincide with the build-up of coke on the seal nose and the subsequent dislocation of the particles.

The conclusions of these comparative tests were that the tungsten carbide rotors have eliminated the problems caused by thermal distortion of the rotor and that the hydrodynamic seal with the gas-bearing geometry on the inside diameter be utilized.

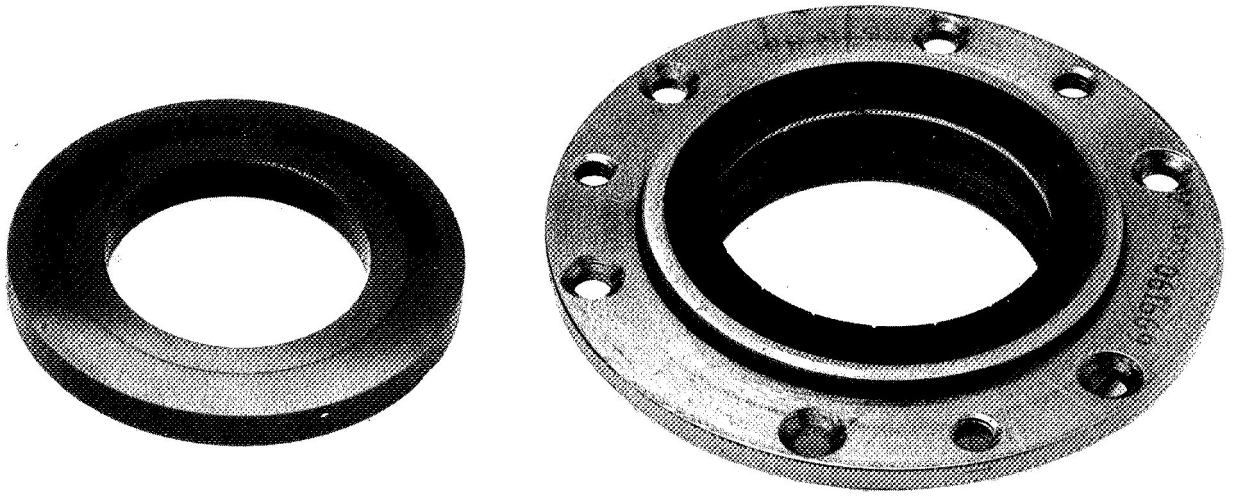

ONE HUNDRED SEVEN-HOURS ON HYDRODYNAMIC
FACE SEAL WITH INSIDE GAS-BEARING
GEOMETRY AND T-CARBIDE ROTOR

FIGURE 60

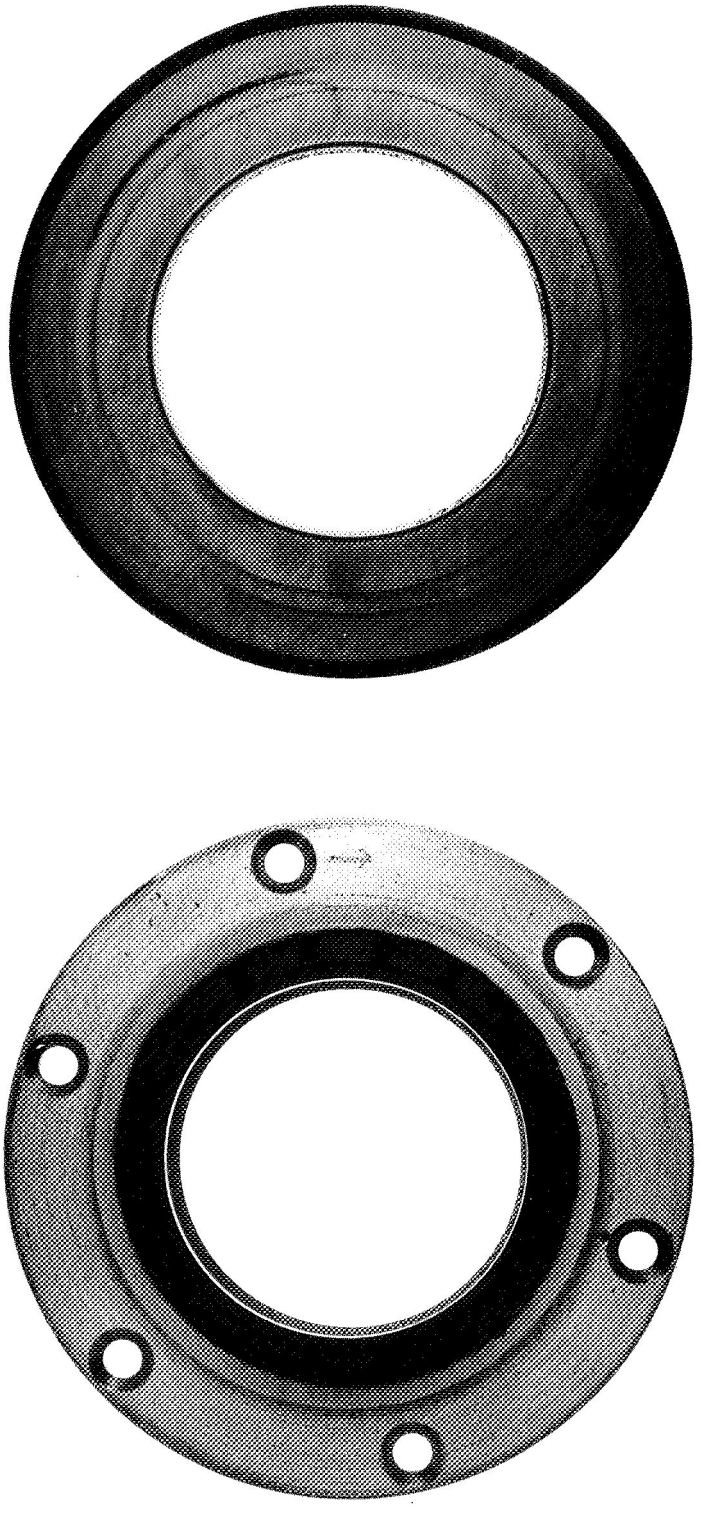

TEN-HOURS ON HYDRODYNAMIC FACE SEAL WITH
OUTSIDE GAS-BEARING GEOMETRY AND T-CARBIDE ROTOR

MP-21108

FIGURE 61

RETEST OF HYDRODYNAMIC FACE SEAL WITH
OUTSIDE GAS-BEARING GEOMETRY AND CARBIDE ROTOR

FIGURE 62

MP-21266

It would appear that either design of the seal would be satisfactory in a completely dry and unlubricated application. However, if oil-mist is used for lubrication, the gas bearing geometry should be on the unlubricated side of the seal. Otherwise, severe coking will be encountered which will rapidly lead to a loss of sealing effectiveness.

The final test of the hydrodynamic face seal evaluation was an endurance test of the design with the gas-bearing geometry on the inside diameter. The seal was operated for 1000 hr and included 79 starts and stops (Figure 63). Inspection did not reveal any measurable wear during the endurance test, and seal leakage remained unchanged. Thermocouples attached to the carbon nose steel backing revealed that the seal temperature remained constant at 175°F throughout the test.

6.3.3 Radial Seal Testing

The radial seal is located between the bearing and the alternator cavities. This seal consists of "Kapton" polyimide lands (Figure 64) and permits nondestructive rubbing with the shaft during critical-speed displacements and close leakage control.

The labyrinth seal was fabricated to provide a 0.0035-diametral clearance with the shaft. This clearance was chosen to provide a pressure drop of approximately 1.30 psi with an airflow of 0.055 lb/min. These flow conditions for air correspond to those predicted for the helium-xenon gas mixture to be used in the BRU-R Lubrication and Cooling System. The radial labyrinth seal was subjected to a 100-hr dynamic test in the seal test rig. No wear was experienced and the seal performed as expected. A close-up view of the Kapton lands after 100 hr is shown in Figure 65.

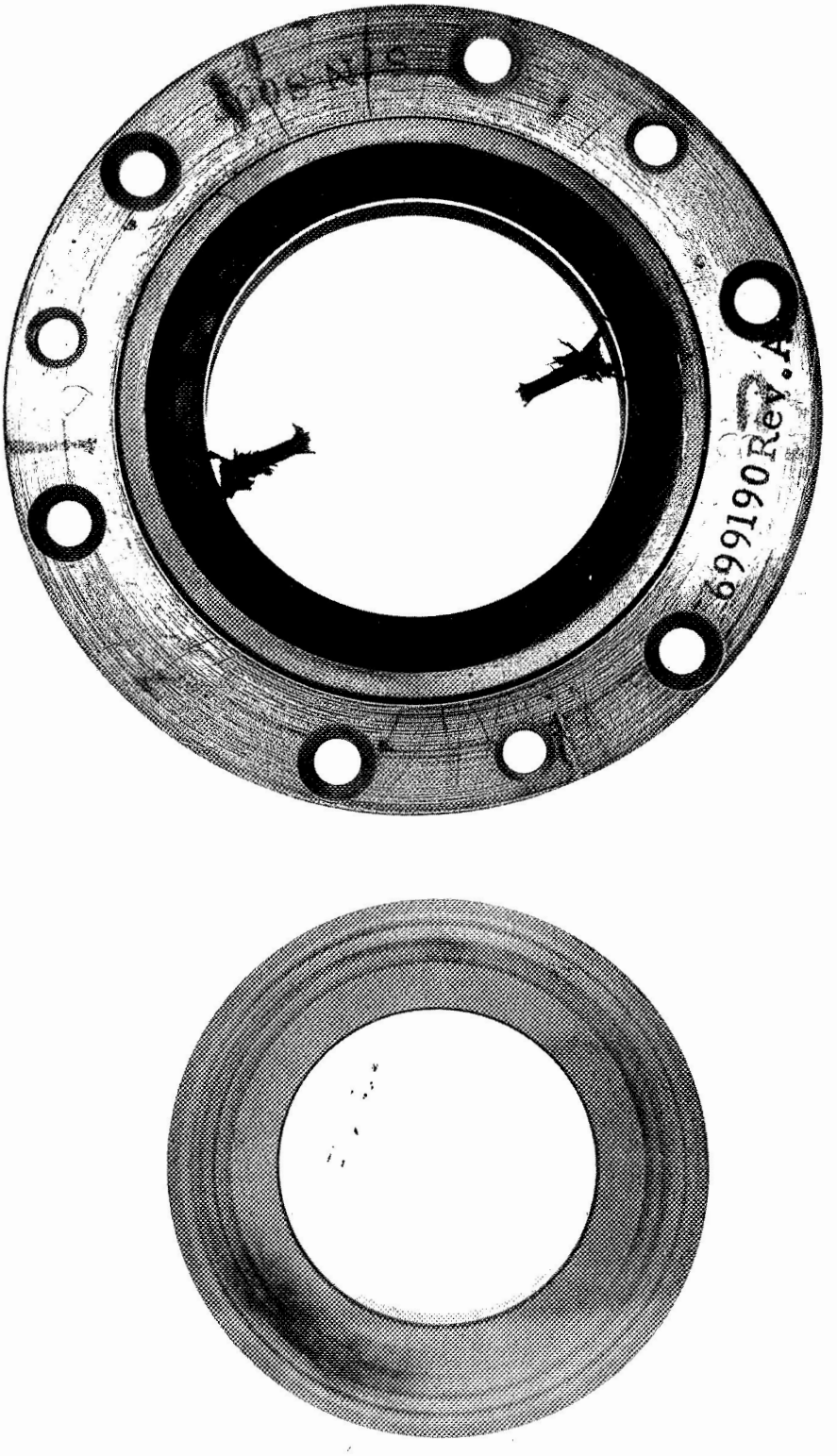

HYDRODYNAMIC FACE SEAL WITH INSIDE GAS-BEARING GEOMETRY - 1000 HOURS

FIGURE 63

MP-21834

RADIAL LABYRINTH SEAL

FIGURE 64

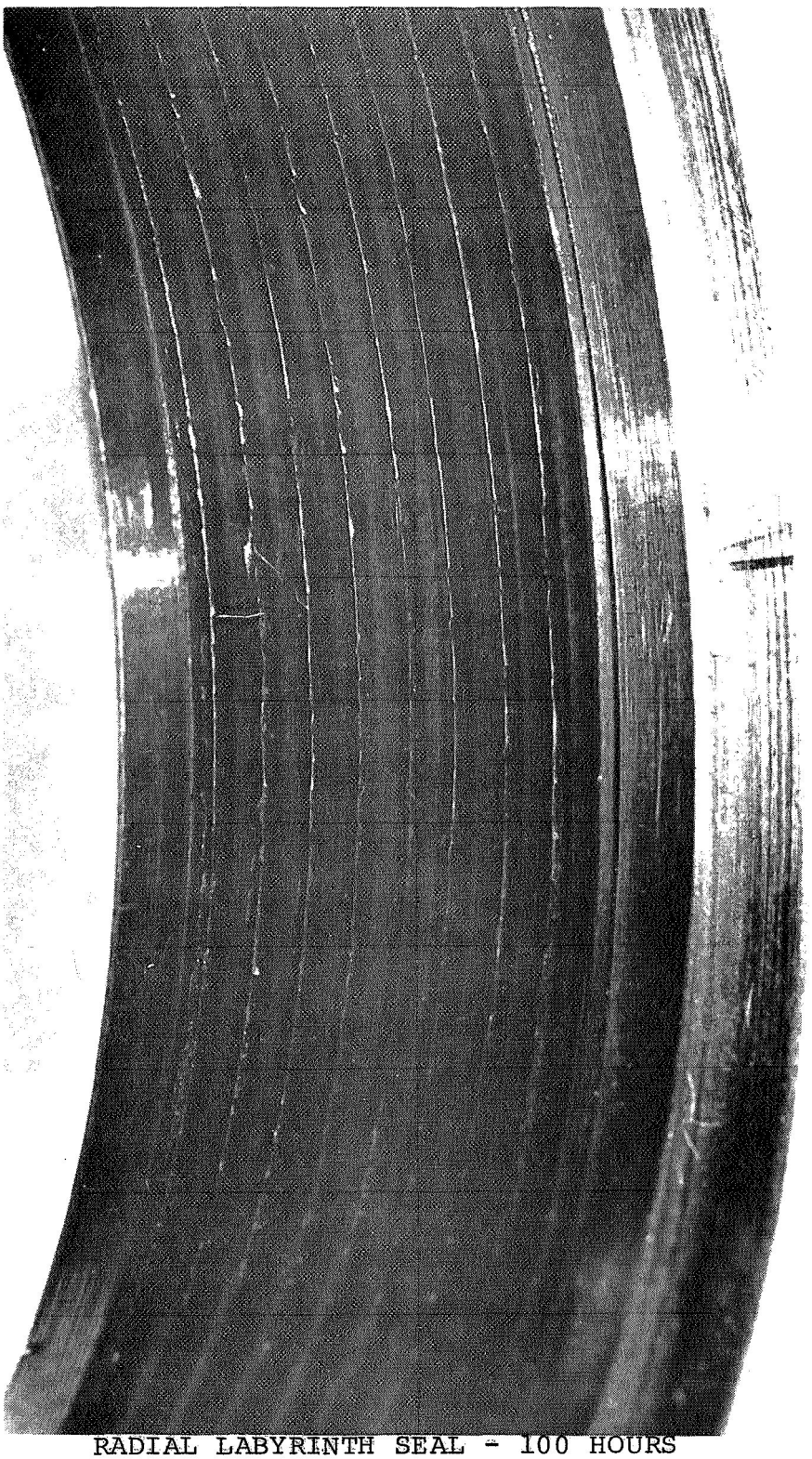

RADIAL LABYRINTH SEAL - 100 HOURS

FIGURE 65

7. THERMAL ANALYSIS

A thermal analysis was made for the BRU-R at steady-state conditions of 2.25, 6.0, and 10.5 kw power levels. The thermal analysis of the BRU-R was similar to the analysis (performed under Contract NAS3-9427) for the BRU in that the two units are identical in many areas. However, the changes made in the BRU-R to accommodate the ball bearings and seals caused a substantial increase in the complexity of the thermal analysis and quite a different distribution of temperatures and heat-flow from the existing BRU.

7.1 Thermal Comparison of BRU-R and BRU

The basic differences between the BRU-R and the BRU from a heat-transfer standpoint are (1) the addition of three heat-sinks, (2) the deletion of the gas leakage flow through labyrinth seals at each wheel, and (3) the addition of a significant heat source at each bearing and each seal. The heat-sinks added are the two gas-flows carrying lubricant through each bearing and the auxiliary liquid cooler with spiral passages near the turbine wheel. The latter, with Dow Corning 200 fluid as the coolant, absorbs the turbine waste-heat more effectively than does the combination of the gas leakage flow through the labyrinth seal and the copper shield, which carries heat to the alternator cooler in the BRU.

The three gas bearings (two journal and one thrust) of the BRU are replaced in the BRU-R by two ball bearings of 30-mm-bore diameter. These bearings require a complete closed-cycle subsystem to provide cooling and lubrication. In addition to the bearings, this also provides a significant heat-sink to localized sections of the BRU-R. An additional source of heat exists in the hydrodynamic face seals, installed between the bearings and the wheels. The bearing cavity pressure is maintained low enough that cycle gas leaks into the bearing cavities and oil cannot leak into the cycle. The seal rotors also

serve as oil slingers. Radial-labyrinth seals between the bearings and the alternator are also added in this area, and the alternator cavity is pressurized with cycle gas to prevent oil leakage. The labyrinth seal of the BRU has been replaced by a massive solid ring, which carries heat from the shaft and the back shroud to a liquid cooler. Another heat-sink has been incorporated in the BRU-R near the turbine wheel to absorb the turbine waste-heat. Spiral passages have been added to the turbine seal carrier assembly for circulating Dow Corning 200 Coolant. This prevents the turbine heat from flowing into the ball-bearing area and creating high temperatures. Because of the turbine heat-sink, the bearing lubrication requirement, and the pressure tap passages for the seal differential pressure control, the mass of the alternator end-bells has been increased to accommodate these passages. Other significant differences between the BRU-R and the BRU are that the BRU-R shaft is smaller in diameter and has only two curvic couplings instead of three. No copper shunts are required in the BRU-R shaft. The BRU-R turbine wheel shaft is smaller and is made in two parts. The BRU-R compressor impeller is titanium rather than the stainless steel of the BRU.

7.2 BRU-R Thermal Analysis

The thermal analysis of the BRU-R was performed using helium-xenon as the gas for both the thermodynamic cycle working fluid and the Lubrication and Cooling System. The analysis was performed on the assumption that the compressor and turbine scrolls were insulated.

Since no published data was found on the performance of a ball bearing as a heat-exchanger, tests were run on the bearing and seal test rig to determine the effectiveness of this "heat-exchanger". Air was forced through a ball bearing turning at 36,000 rpm. The heat-exchanger effectiveness is defined as the ratio of the gas temperature rise across the bearing to the inlet temperature difference between the gas and bearing. The data were converted to apply to helium-xenon gas by considering the bearing as a single-pass heat-exchanger at constant hot-side temperature. The resulting effectiveness value was 0.68.

For a steady-state condition of 2.25, 6.0, and 10.5 kw, the heat-flow distribution data for the BRU-R are shown in Figures 66, 68, and 70, and the corresponding temperature distributions are shown in Figures 67, 69, and 71, respectively.

Due to the addition of the liquid-cooled heat-sink adjacent to the turbine heat shield, the flow requirements of the Dow Corning 200 cooling fluid increase from 1.0 gal/min for the BRU to 1.5 for the BRU-R.

A brief study was made of the major effects of changing the BRU-R cycle gas from helium-xenon (molecular weight = 83.8) to Krypton. A similar study of these effects has been made on the BRU. The condition investigated for the BRU-R was the 10.5-kw_e power level, at which the maximum temperatures occur.

The changes resulting from the substitution of Krypton for helium-xenon were (a) reducing the cooling effectiveness of the gas jets on the ball bearings and (b) reducing the thermal conductance across the alternator flux gaps, turbine shaft gap, etc. The only important difference between the two gases is that the thermal conductivity of Krypton is about 41 percent of the conductivity of helium-xenon. The results tabulated below are conservative at the turbine end because no allowances for the differences in gas thermal conductivities were made in the wheels.

LOSS DISTRIBUTION DATA:

POWER LEVEL	2.25 KW, 0.85 PF
ALTERNATOR ELECTROMAGNETIC LOSSES	298 WATTS
ROTATING GROUP WINDAGE LOSSES (EXCLUDING WHEELS)	312 WATTS
BALL BEARING LOSSES	380 WATTS
ALTERNATOR SEAL LOSSES	80 WATTS
HYDRODYNAMIC SEAL LOSSES	80 WATTS

HEAT SINK DATA:

ALTERNATOR AND TURBINE COOLANT	DOW CORNING 200
COOLANT INLET TEMPERATURE	70°F
ALTERNATOR COOLER FLOW RATE	0.12 LBM/SEC.
DISCHARGE TEMPERATURE	87.5°F
TURBINE COOLER FLOW RATE	0.06 LBM/SEC.
DISCHARGE TEMPERATURE	85°F
He-Xe GAS FLOW TO BEARINGS	3.69 LBM/MIN AT 100°F
COMP. BEARING DISCHARGE TEMP.	210°F
TURB. BEARING DISCHARGE TEMP.	218°F

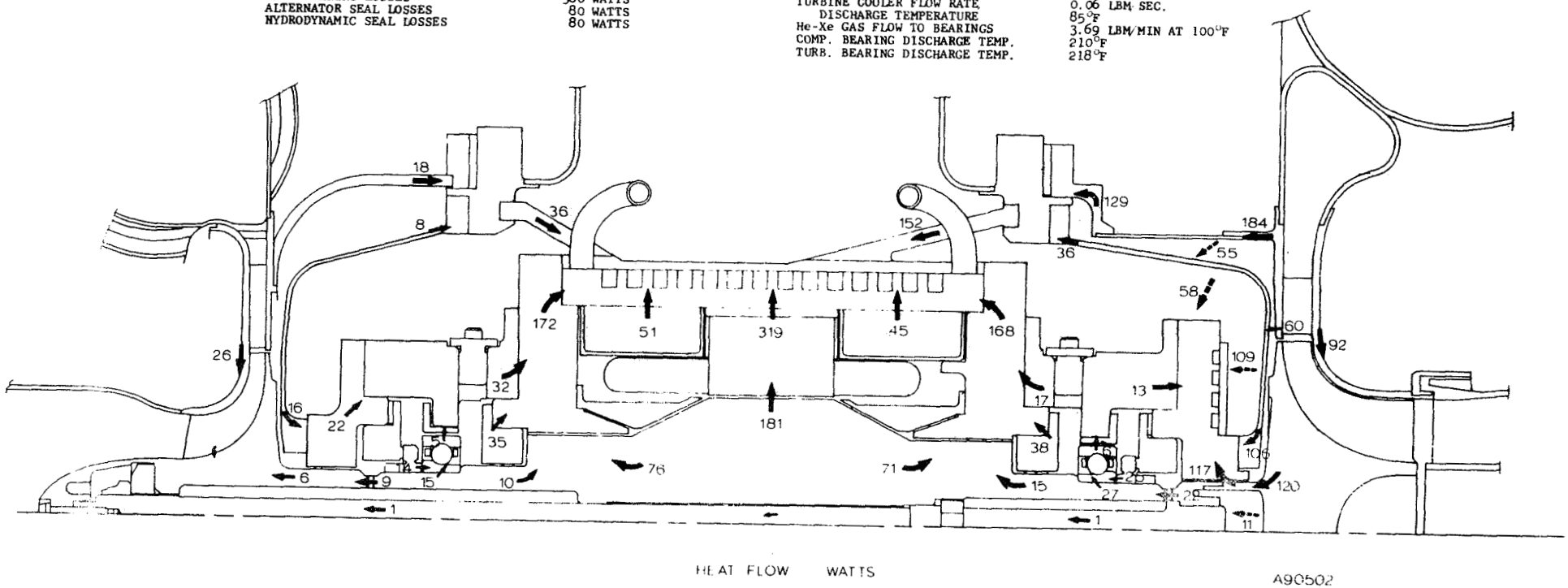

HEAT FLOW AT 2.25 KW

FIGURE 66

LOSS DISTRIBUTION DATA:

POWER LEVEL	2.25 KW, 0.85 PF
ALTERNATOR ELECTROMAGNETIC LOSSES	298 WATTS
ROTATING GROUP WINDAGE LOSSES (EXCLUDING WHEELS)	312 WATTS
BALL BEARING LOSSES	380 WATTS
ALTERNATOR SEAL LOSSES	80 WATTS
HYDRODYNAMIC SEAL LOSSES	80 WATTS

HEAT SINK DATA:

ALTERNATOR AND TURBINE COOLANT	DOW CORNING 200
COOLANT INLET TEMPERATURE	70°F
ALTERNATOR COOLER FLOW RATE/ DISCHARGE TEMPERATURE	0.12 LBM/SEC. 87.5°F
TURBINE COOLER FLOW RATE/ DISCHARGE TEMPERATURE	0.06 LBM/SEC. 85°F
He-Xe GAS FLOW TO BEARINGS	3.69 LBM/MIN AT 100°F
COMP. BEARING DISCHARGE TEMP.	210°F
TURB. BEARING DISCHARGE TEMP.	218°F

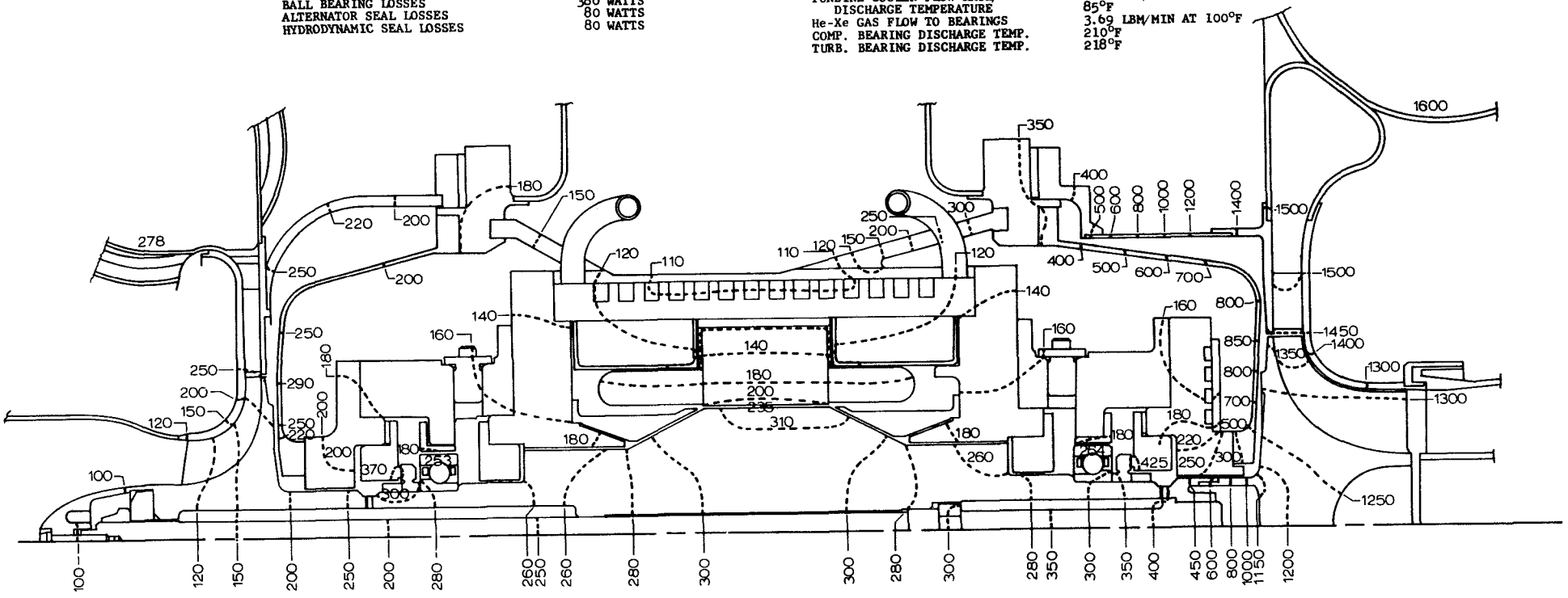

TEMPERATURE DISTRIBUTION: 2.25 KW

FIGURE 67

LOSS DISTRIBUTION DATA:

POWER LEVEL	6.0 KW, 0.85 PF
ALTERNATOR ELECTROMAGNETIC LOSSES	411 WATTS
ROTATING GROUP WINDAGE LOSSES (EXCLUDING WHEELS)	403 WATTS
BALL BEARING LOSSES	380 WATTS
ALTERNATOR SEAL LOSSES	80 WATTS
HYDRODYNAMIC SEAL LOSSES	80 WATTS

HEAT SINK DATA:

ALTERNATOR AND TURBINE COOLANT	DOW CORNING 200
COOLANT INLET TEMPERATURE	70°F
ALTERNATOR COOLER FLOW RATE/ DISCHARGE TEMPERATURE	0.12 LBM/SEC. 91 °F
TURBINE COOLER FLOW RATE/ DISCHARGE TEMPERATURE	0.06 LBM/SEC. 88.5°F
He-Xe GAS FLOW TO BEARINGS	3.69 LBM/MIN AT 100°F
COMP. BEARING DISCHARGE TEMP.	213°F
TURB. BEARING DISCHARGE TEMP.	220°F

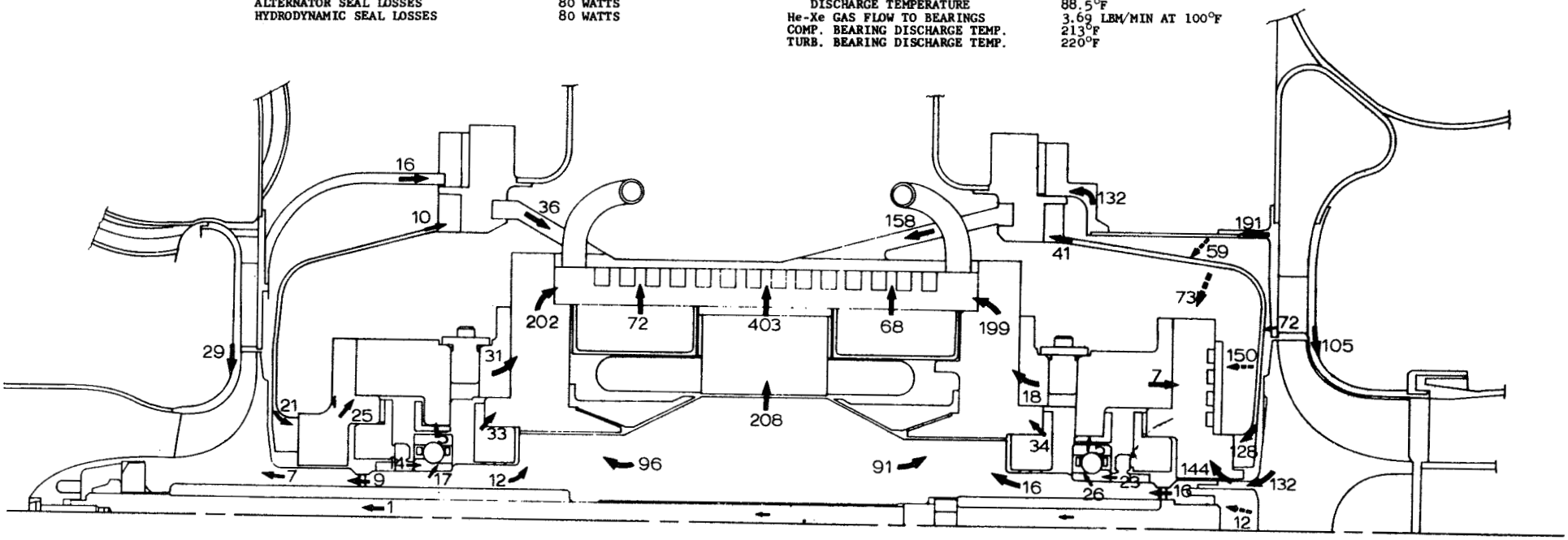

HEAT FLOW – WATTS

A90503

HEAT FLOW AT 6.0 KW

FIGURE 68

AIRESEARCH MANUFACTURING COMPANY OF ARIZONA
A DIVISION OF THE GARRETT CORPORATION
PHOENIX, ARIZONA

LOSS DISTRIBUTION DATA:

POWER LEVEL	6.0 KW, 0.85 PF
ALTERNATOR ELECTROMAGNETIC LOSSES	411 WATTS
ROTATING GROUP WINDAGE LOSSES (EXCLUDING WHEELS)	403 WATTS
BALL BEARING LOSSES	380 WATTS
ALTERNATOR SEAL LOSSES	80 WATTS
HYDRODYNAMIC SEAL LOSSES	80 WATTS

HEAT SINK DATA:

ALTERNATOR AND TURBINE COOLANT	DOW CORNING 200
COOLANT INLET TEMPERATURE	70°F
ALTERNATOR COOLER FLOW RATE,	0.12 LBM/SEC.
DISCHARGE TEMPERATURE	91°F
TURBINE COOLER FLOW RATE;	0.06 LBM/SEC.
DISCHARGE TEMPERATURE	88.5°F
He-Xe GAS FLOW TO BEARINGS	3.69 LBM/MIN AT 100°F
COMP. BEARING DISCHARGE TEMP.	213°F
TURB. BEARING DISCHARGE TEMP.	220°F

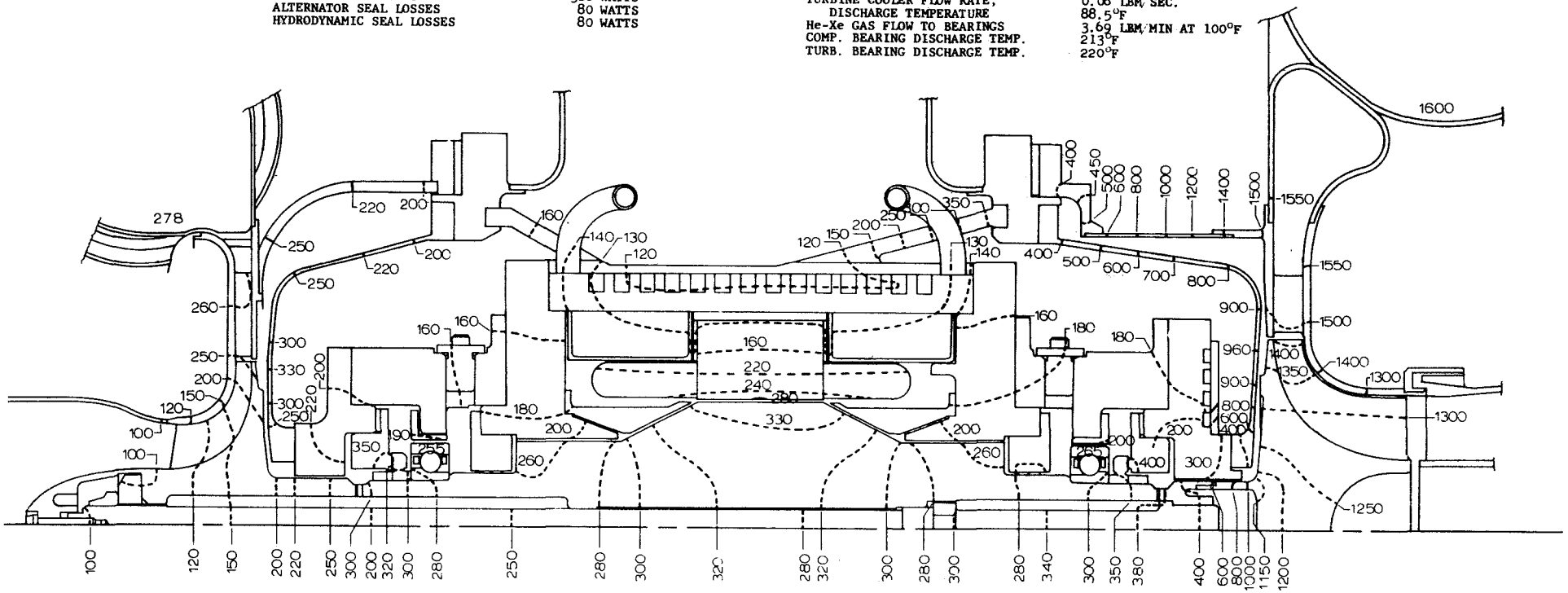

TEMPERATURE DISTRIBUTION: 6.0 KW

FIGURE 69

AIRESEARCH MANUFACTURING COMPANY OF ARIZONA
A DIVISION OF THE GARRETT CORPORATION
PHOENIX, ARIZONA

LOSS DISTRIBUTION DATA:

POWER LEVEL	10.5 KW, 0.85 PF
ALTERNATOR ELECTROMAGNETIC LOSSES	682 WATTS
ROTATING GROUP WINDAGE LOSSES (EXCLUDING WHEELS)	540 WATTS
BALL BEARING LOSSES	380 WATTS
ALTERNATOR SEAL LOSSES	80 WATTS
HYDRODYNAMIC SEAL LOSSES	80 WATTS

HEAT SINK DATA:

ALTERNATOR AND TURBINE COOLANT	DOW CORNING 200
COOLANT INLET TEMPERATURE	70°F
ALTERNATOR COOLER FLOW RATE/ DISCHARGE TEMPERATURE	0.12 LBM SEC. 98°F
TURBINE COOLER FLOW RATE/ DISCHARGE TEMPERATURE	0.06 LBM SEC. 92°F
He-Xe GAS FLOW TO BEARINGS	3.69 LBM MIN AT 100°F
COMP. BEARING DISCHARGE TEMP.	220°F
TURB. BEARING DISCHARGE TEMP.	224°F

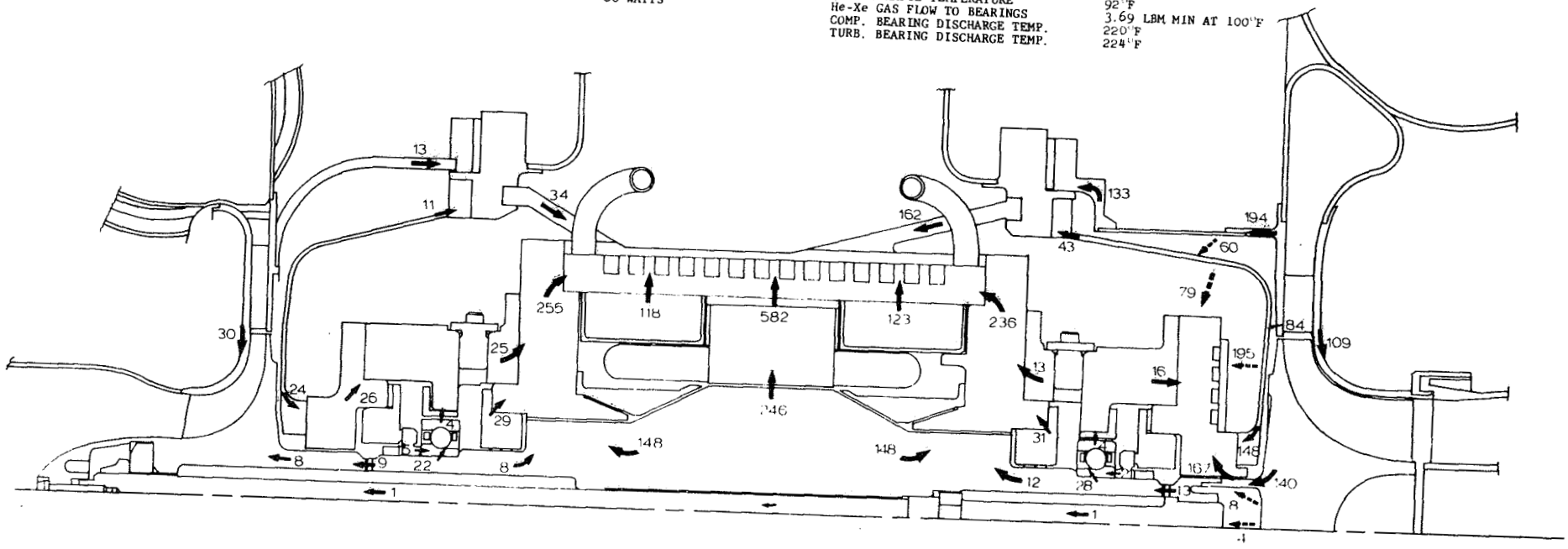

HEAT FLOW - WATTS

A90504

HEAT FLOW AT 10.5 KW

FIGURE 70

AIRESEARCH MANUFACTURING COMPANY OF ARIZONA
A DIVISION OF THE GARRETT CORPORATION
PHOENIX, ARIZONA

LOSS DISTRIBUTION DATA:

POWER LEVEL	10.5 KW, 0.85 PF
ALTERNATOR ELECTROMAGNETIC LOSSES	682 WATTS
ROTATING GROUP WINDAGE LOSSES (EXCLUDING WHEELS)	540 WATTS
BALL BEARING LOSSES	380 WATTS
ALTERNATOR SEAL LOSSES	80 WATTS
HYDRODYNAMIC SEAL LOSSES	80 WATTS

HEAT SINK DATA:

ALTERNATOR AND TURBINE COOLANT	DOW CORNING 200
COOLANT INLET TEMPERATURE	70°F
ALTERNATOR COOLER FLOW RATE/ DISCHARGE TEMPERATURE	0.12 LBM/SEC. 98°F
TURBINE COOLER FLOW RATE/ DISCHARGE TEMPERATURE	0.06 LBM/SEC. 92°F
He-Xe GAS FLOW TO BEARINGS	3.69 LBM/MIN AT 100°F
COMP. BEARING DISCHARGE TEMP.	220°F
TURB. BEARING DISCHARGE TEMP.	224°F

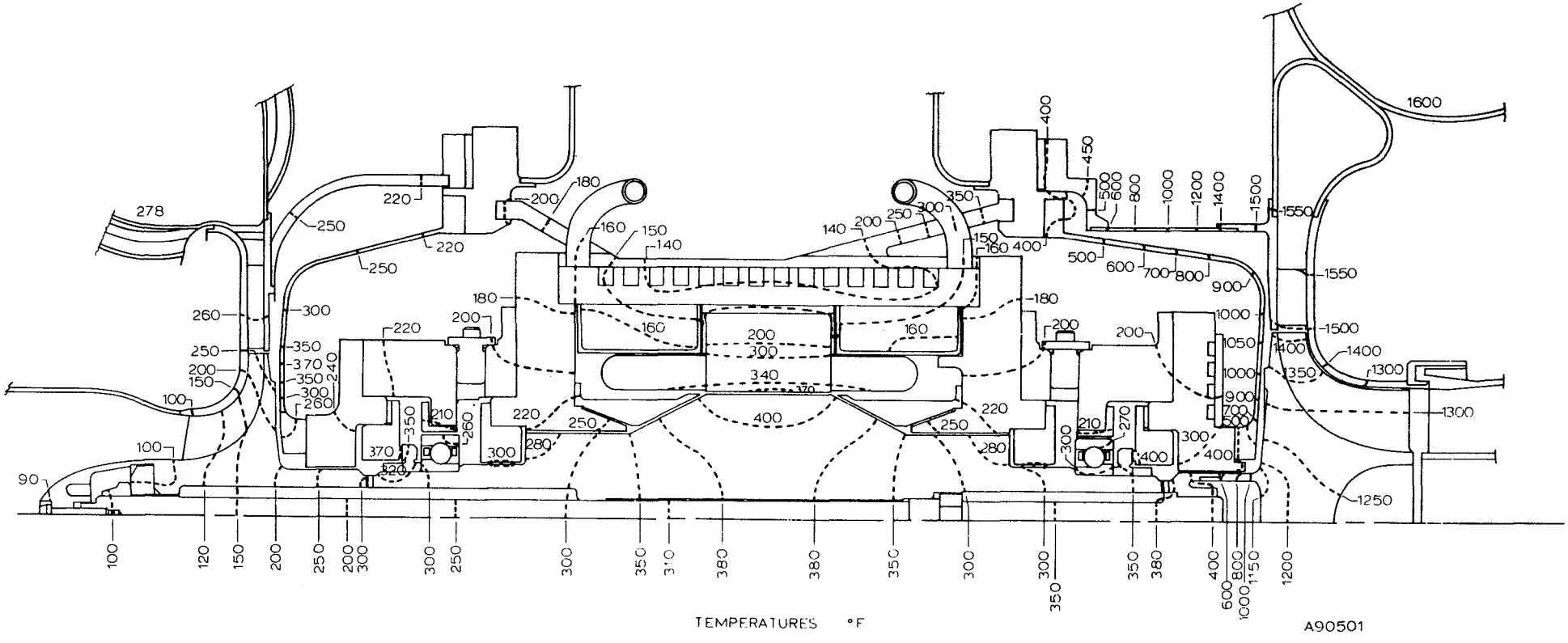

TEMPERATURE DISTRIBUTION: 10.5 KW

FIGURE 71

Location	Temperature With He-Xe, °F	Temperature With Krypton, °F
Turbine-end ball bearing at the inner race	300	388
Axial-face seal rotor (or oil-slinger)	368	404
Alternator rotor at OD	407	428
Turbine back-shroud at wheel tip	1054	1005

The thermal penalties associated with a change to Krypton gas are not severe but should be considered.

7.3 Thermal Expansion

Thermal expansion calculations were performed on the BRU-R under four steady-state conditions. Three of these are the 2.25-, 6.0-, and 10.5-kw power levels with helium-xenon cycle gas, and the fourth is the 10.5-kw power level with Krypton.

Values for relative thermal expansion were computed for the following locations:

(a) Shaft and rotor vs tie-bolt--Positive expansion increases tie-bolt tension.

(b) Compressor bearing vs carrier housing--Positive expansion increases the mount-to-housing gap width and decreases the preload force.

(c) Turbine wheel-to-scroll gap--Positive expansion increases the axial-gap width.

(d) Compressor wheel-to-scroll gap--Sign convention same as (c).

(e) Turbine-end hydrodynamic seal--Positive expansion increases the bellows working height, which decreases the seal load.

(f) Compressor-end hydrodynamic seal--Sign convention same as (e).

(g) Overall unit--Positive expansion increases the compressor inlet-to-turbine exhaust-flange length.

These values of expansion are given in inches in the table below:

		Helium-Xenon			Krypton
	Location	2.25 kw	6.0 kw	10.5 kw	10.5 kw
(a)	Tie-bolt	-0.00195	-0.0015	-0.00075	-0.0013
(b)	Bearing	+0.0089	+0.0089	+0.0104	+0.0117
(c)	Turbine gap	+0.0135	+0.0148	+0.0153	+0.0148
(d)	Compressor gap	-0.0077	-0.0076	-0.0095	-0.0108
(e)	Turbine seal	-0.0006	-0.0005	-0.00055	-0.0006
(f)	Compressor seal	-0.0093	-0.0092	-0.0108	-0.0121
(h)	Overall unit	0.0491	0.0509	0.0528	0.0528

The above values show that the maximum change in shaft-to-tie-bolt relative expansion occurs at the 2.25-kw power level. This represents a relaxation in the tie-bolt tension of about 750 lb. This relaxation is insignificant as the tie-bolt is installed to a load of 8000 to 10,000 lb during assembly.

The thermal expansion calculations at the compressor bearing reveals that if the BRU-R is operated "hot", the bearing preload will

decrease. As the bearing preload decreases, the ball spin/roll ratio increases which means that there is more tendency for skidding and wear. This is not a problem for the BRU-R, as discussed in Paragraph 3.4. The bearing analysis recommended a minimum preload of 60 lb. Assembly procedures were established to achieve a preload of 80 to 100 lb, thereby compensating in part for the preload decrease. Thus, the thermal expansion will not materially affect bearing life. These calculations also reveal that the clearance between the turbine wheel and the turbine scroll will increase if the BRU-R is operated to these power conditions. For example, the turbine scroll is installed to achieve a clearance of 0.009 ±0.001. If the BRU-R is operated with helium-xenon to the 2.25-kw power level with a turbine inlet temperature of 2060°R, the gap between the turbine wheel and scroll will increase by 0.0135 in.; the gap will be 0.0225 if the initial clearance is the nominal value. Likewise, the thermal expansion will cause the gap between the compressor impeller and the compressor scroll to decrease. The compressor scroll is installed to a clearance of 0.018 ±0.001. "Hot" operation at a power level of 2.25 kw will result in a gap of 0.0103 if the clearance is initially set to the nominal value during assembly. Overall, thermal expansion does not appear to present a significant clearance problem.

8. CURVIC COUPLING DEVELOPMENT

The turbine wheel and the compressor impeller are attached to the alternator rotor through a 1.062-in.-dia curvic coupling and secured with a tie-bolt. This curvic coupling design is rather unique in that its small diameter initiated curvic coupling tests that were performed on laboratory setups to determine optimum tie-bolt loads, stability, and deflection. The tests consisted of axial and bending deflection. On the basis of these tests, a tie-bolt load of 10,000 lb was established as optimum for the BRU-R.

8.1 Axial Deflection Tests

The axial deflection tests were performed by loading special test pieces with a hydraulic press as shown in Figure 72. The test parts were machined with provisions for measuring the deflection of one side with respect to the other at four places, 90 deg apart. This was necessary since the individual measurements varied considerably according to load alignment and individual tooth configuration, but the average reading appeared stable. Two tooth designs were tested, one with concave and one with convex teeth. Deflections were measured with dial gauges having 0.0001-in. scale divisions. The gauges were vibrated with electromechanical buzzers to overcome internal friction.

For both the concave and convex tooth designs, the load was varied from 0 to 10,000 lb in increments of 1000. At each load setting, the deflection was measured at four places. This test sequence was repeated to verify the initial measurements. The axial deflection measurements of both the concave and the convex tooth designs are shown in Figure 73. The concave tooth design was stiffer than the convex and had a slightly smoother load-deflection curve. This indicated that the better mating of a concave with a convex tooth, instead of convex to convex, resulted in a better coupling with less binding and catching of

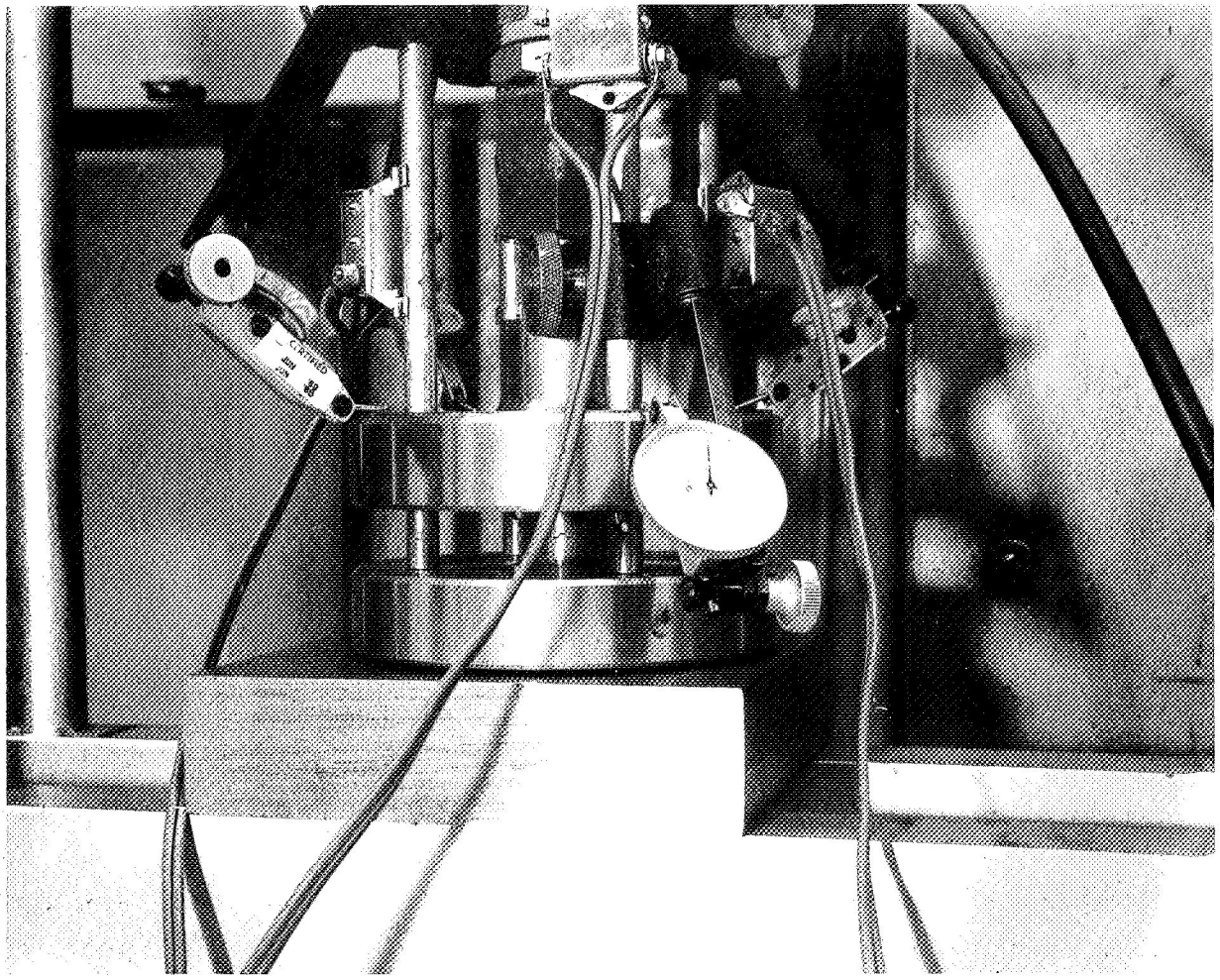

AXIAL DEFLECTION TEST
1.062 -IN.-DIAMETER
CURVIC COUPLING

FIGURE 72

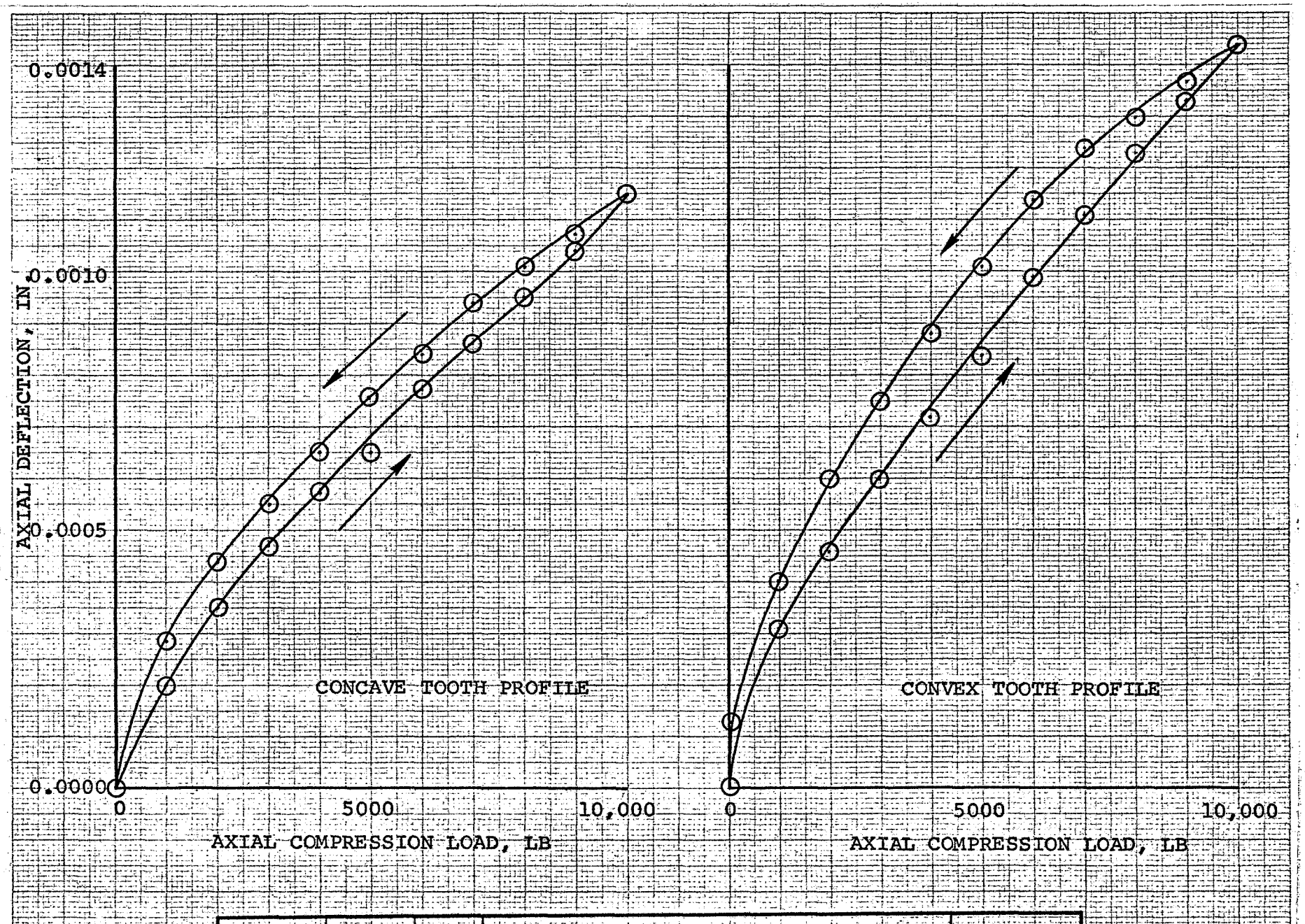

CALCULATED BY			AXIAL DEFLECTION TEST OF CURVIC TOOTH COUPLING (1.062-IN. SHAFT DIAMETER)
TRACED BY	JED	10/69	FIGURE 73
CHECKED BY			
APPROVED BY			AiResearch Manufacturing Company of Arizona
UNIT NO.			

P5105

the teeth as they were pressed together. Average deflection of the concave tooth coupling was 0.00115 in. at 10,000 lb, and the average deflection of the convex design was 0.00144 in. at 10,000 lb load. Stiffness of the couplings increased as the teeth were jammed tighter together at higher loads.

8.2 Bending Deflection Tests

The bending deflection test was conducted on the same hydraulic press as shown in Figure 74. A shaft was machined that was mechanically similar to the intended main rotor. It contained two curvic couplings that were located on either side of the load application point, between it and the support points. Tie-bolt loads were measured with four strain gauges arranged in a bridge circuit to measure tensile or compressive strains only, excluding bending. The tie-bolt was then calibrated by applying known loads and noting resulting strain. No increase in tie-bolt load was noted during the tests, probably due to the insensitivity of the measuring system to the bending mode. The shaft was held in V-blocks, and the load applied through a 1-in.-dia steel ball at the middle of the shaft. Deflections were measured at the center of the shaft directly underneath the point of load, and underneath the 1 1/2-in.-thick ground stock supporting the V-blocks.

Deflections under the supports were averaged and then subtracted from those at the center of the shaft to obtain the corrected deflection. No attempt was made to measure distortion of the shaft cross section. The wall thickness was at least 0.360 in. at the supports and 0.465 in. at the load application point, and it was felt that there would be no significant deflections in view of overall dimensions and load values.

At a tie-bolt load of 10,000 lb, the shaft with two curvic couplings and 1.062-in. outside diameter had a corrected permanent offset

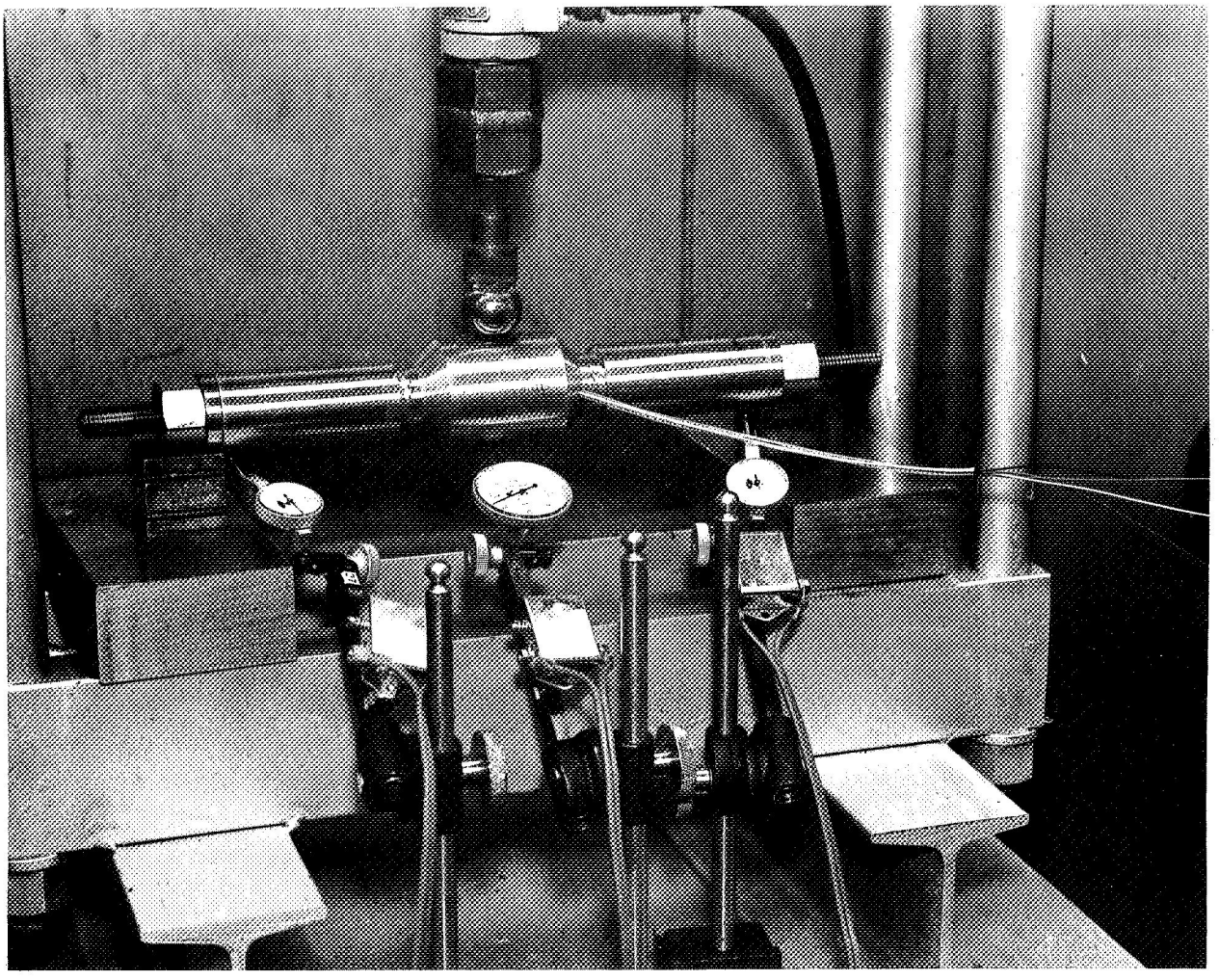

BENDING DEFLECTION TEST
FOR 1.062 -IN.-DIAMETER
CURVIC COUPLING

FIGURE 74

of 0.00035 in. for an applied side load of 1700 lb. The load-deflection curve (Figure 75) departed from a linear relationship at a side load of about 900 lb. At lower tie-bolt loads of 9000 and 8000 lb, the permanent offsets were greater (Figure 76), 0.00050 and 0.00095 in., respectively, and the load-deflection curve departed from a linear relationship earlier, about a 700-lb side load for a 9000-lb tie-bolt load and 500 lb for an 8000-lb load.

On the first load-cycle after assembly of the shaft, the frictional forces holding the teeth were overcome at a side load, depending on tie-bolt load. The shaft then deflected in a nonlinear manner until some of the slippage was reversed, and the final offset was less than at full-load. A comparison of three successive loading cycles at 8000-lb tie-bolt load showed that the offset was on the order of 0.001-in. at 1400-lb side load and 0.0006 in. at zero side load. At about 1100-lb side load, a mechanical lock-up of the teeth occurred, and the curve for all three cycles was identical from there to the ultimate load of 1400 lb. After the first cycle, when the permanent offset occurred, the shaft load-deflection curve exhibited no further drastic changes with additional loading cycles.

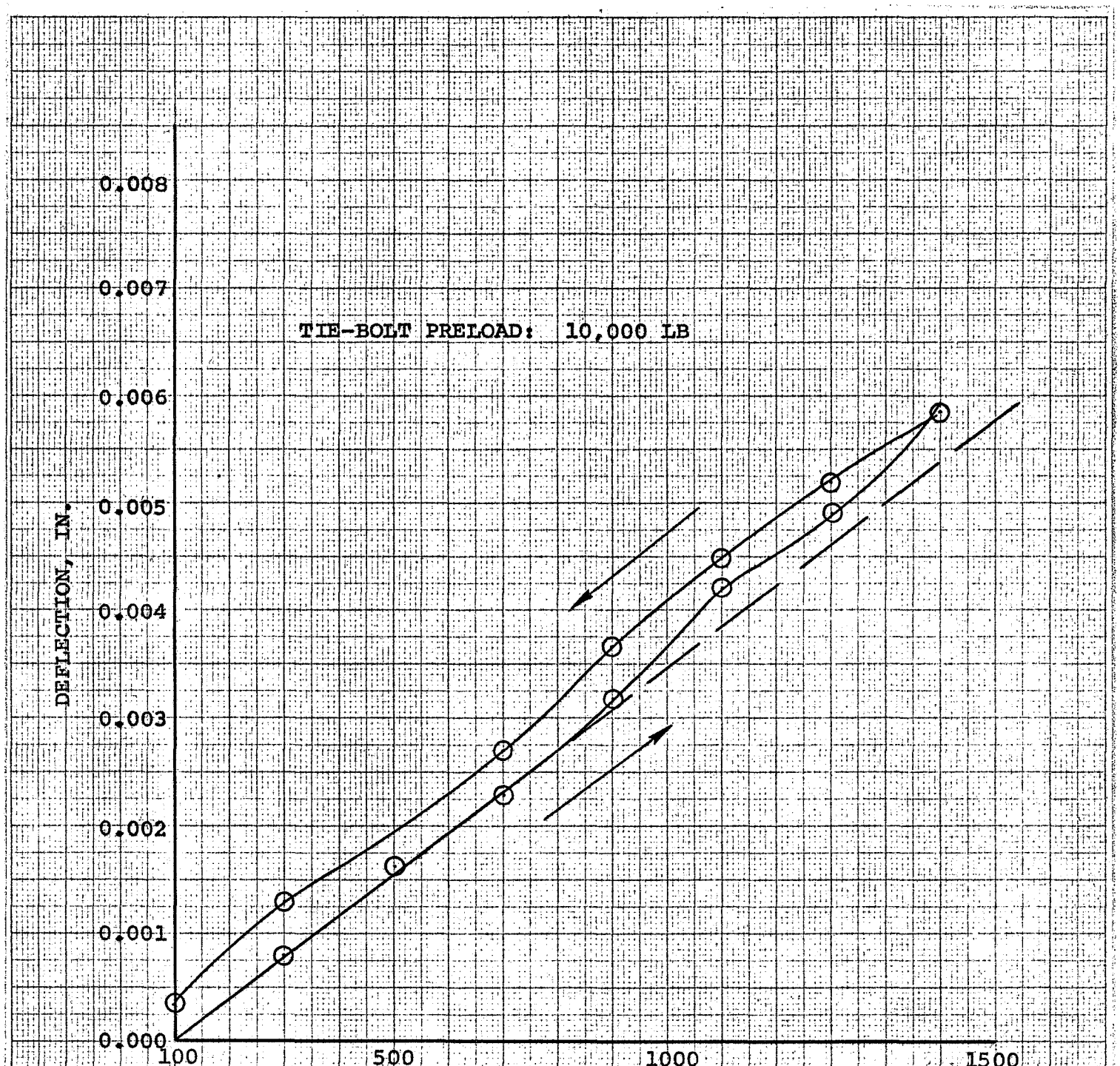

CALCULATED BY		BENDING DEFLECTION TEST OF 1.062-IN.-DIA CURVIC COUPLING	FIGURE 75
TRACED BY			
CHECKED BY			
APPROVED BY		AIRESEARCH MANUFACTURING COMPANY	
UNIT NO.			

P 5106

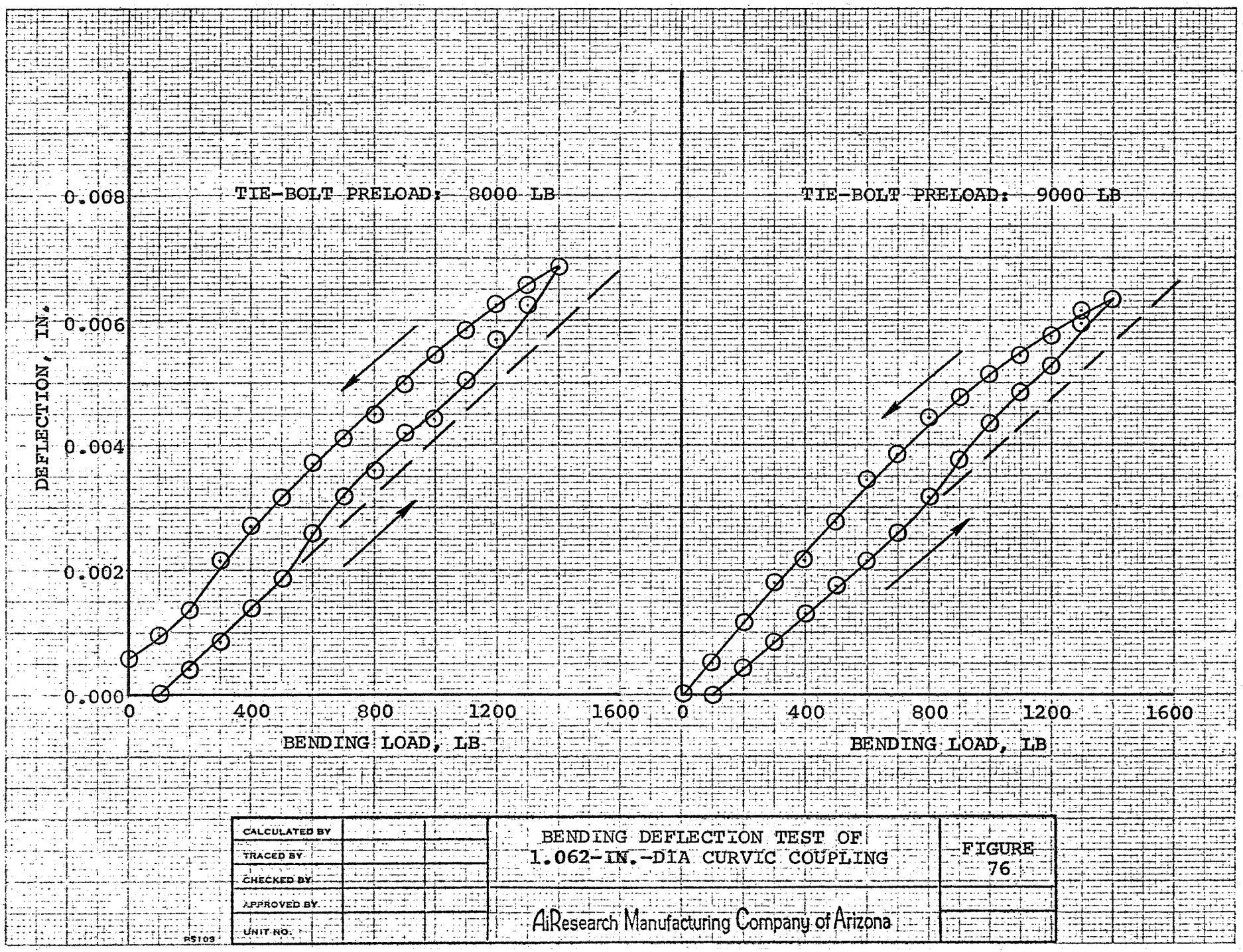

CALCULATED BY			BENDING DEFLECTION TEST OF 1.062-IN.-DIA CURVIC COUPLING
TRACED BY			FIGURE 76
CHECKED BY			
APPROVED BY			AiResearch Manufacturing Company of Arizona
UNIT NO.			

RS109

9. SHAFT MOBILITY TEST

A shaft mobility test was performed on the BRU-R rotating components to establish the free-free bending frequency. The purpose of the test was to determine if the requirement for 120-percent overspeed could be safely achieved. The rotating components of the BRU-R were assembled and subjected to two tests; one was performed with a barium-titanate gauge and an oscilloscope, and the other with a shaker and an accelerometer in a mobility test rig. The conclusion of these tests was that the actual third critical frequency was approximately 48,000 rpm. This is very close to the 43,200 rpm speed of the 120-percent overspeed requirement but is within acceptable limits.

9.1 Barium-Titanate Gauge Test

The BRU-R rotating components shown in Figure 77 were assembled as shown in Figure 78. A barium-titanate gauge was bonded to the center of the BRU-R shaft as shown in Figure 79. The gauge was connected to one channel of a dual beam oscilloscope while a variable frequency oscillator was connected to the other scope channel. The shaft was suspended on a wire and struck with a mallet. By varying the oscillator as the shaft was struck, a Lissajous figure could be formed and the natural bending frequency of the shaft established, 713 Hz. The bearings, seal rotors, and nuts were removed and the test repeated with the resulting natural frequency of 678 Hz. The bearings, seal rotors, and nuts apparently stiffen the shaft and raise the natural frequency 35 Hz.

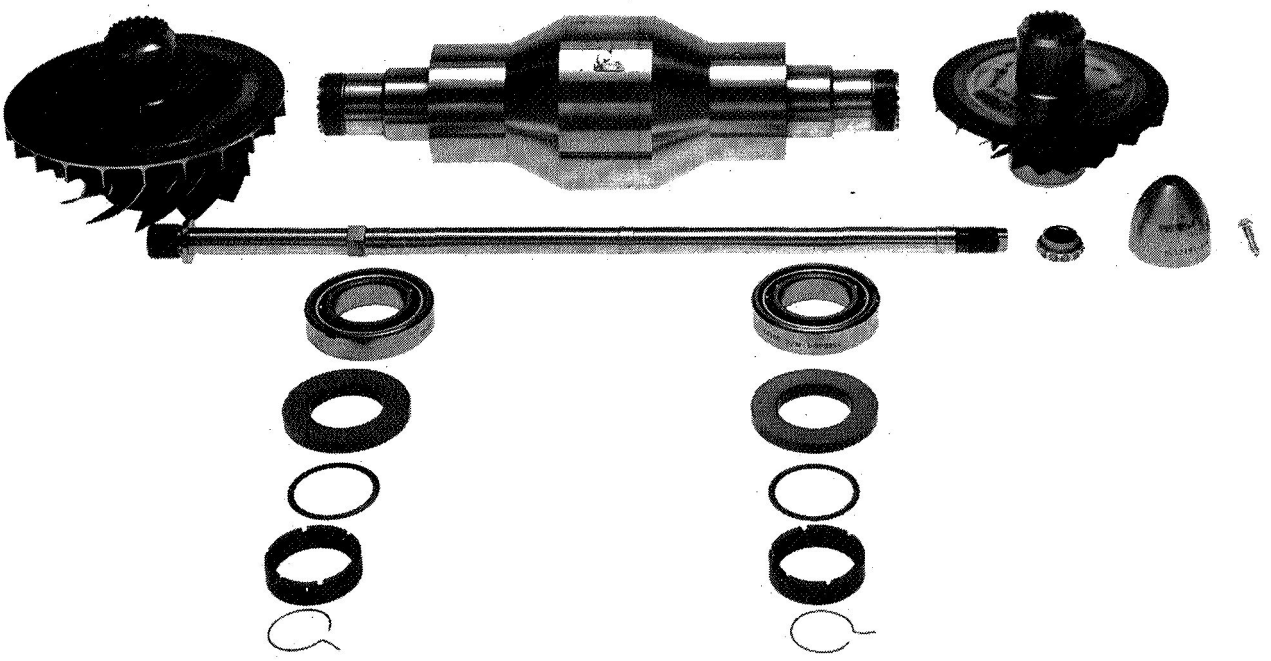

BRU-R ROTATING COMPONENTS

FIGURE 77

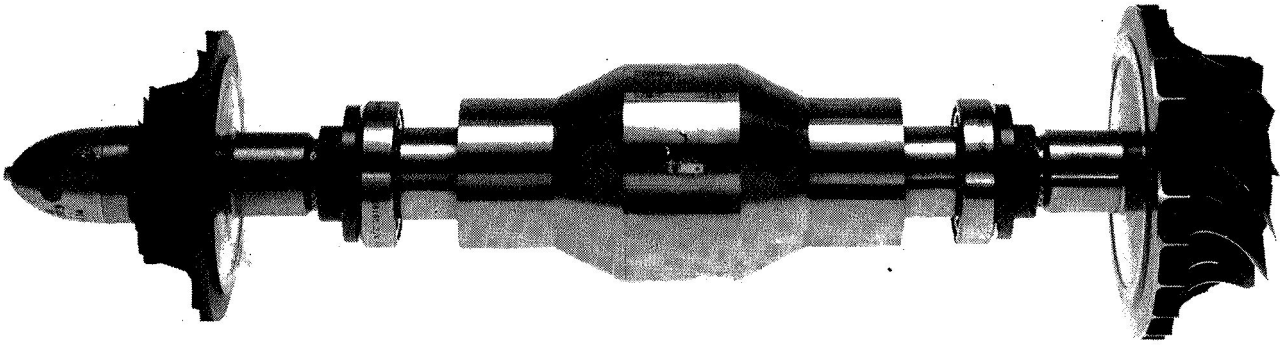

ASSEMBLED BRU-R
ROTATING COMPONENTS

FIGURE 78

BARIUM-TITANATE GAUGE
BONDED TO CENTER OF BRU-R SHAFT

FIGURE 79

9.2 Mobility Test Rig

The assembled shaft, including bearings, seal rotors, and nuts was suspended by the bearing races, on rubber shock cords (Figure 80). An electric shaker driven by a variable oscillator was attached to the center of the shaft and suspended on a shock cord. The shaker added 11 gm to the mass of the BRU-R shaft. The basic equipment used in this test consisted of an automatic sweep oscillator that drives the shaker at frequencies between 70 and 1000 Hz. An accelerometer on the shaker was connected to one leg of an X-Y plotter, and the oscillator frequency signal was connected to the other leg. The oscillator was started and a graphical plot of the shaft acceleration versus frequency was made. A typical plot is shown in Figure 81. The peak acceleration, i.e., natural frequency of the shaft, occurred at 708 Hz. The lower natural frequency obtained in this test was attributed to the increased mass added by the shaker.

The nodal points of the shaft, while at natural resonance, were determined by a hand-held accelerometer (Figures 82 and 83). The node at the compressor end was located inboard of the bearing, and that at the turbine end was outboard.

Computer calculations indicate that the compressor and turbine wheels will provide enough gyroscopic stiffening to raise the natural free-free bending frequency of the BRU-R rotating shaft by approximately 90 Hz. This would result in an acutal third-critical frequency of approximately 800 Hz, i.e., 48,000 rpm. While this is near the 120-percent design speed requirement of 43,200 rpm, it falls within acceptable bounds. The actual verification of the third critical occurring at 48,000 rpm is discussed under Section 10.2.2.1.

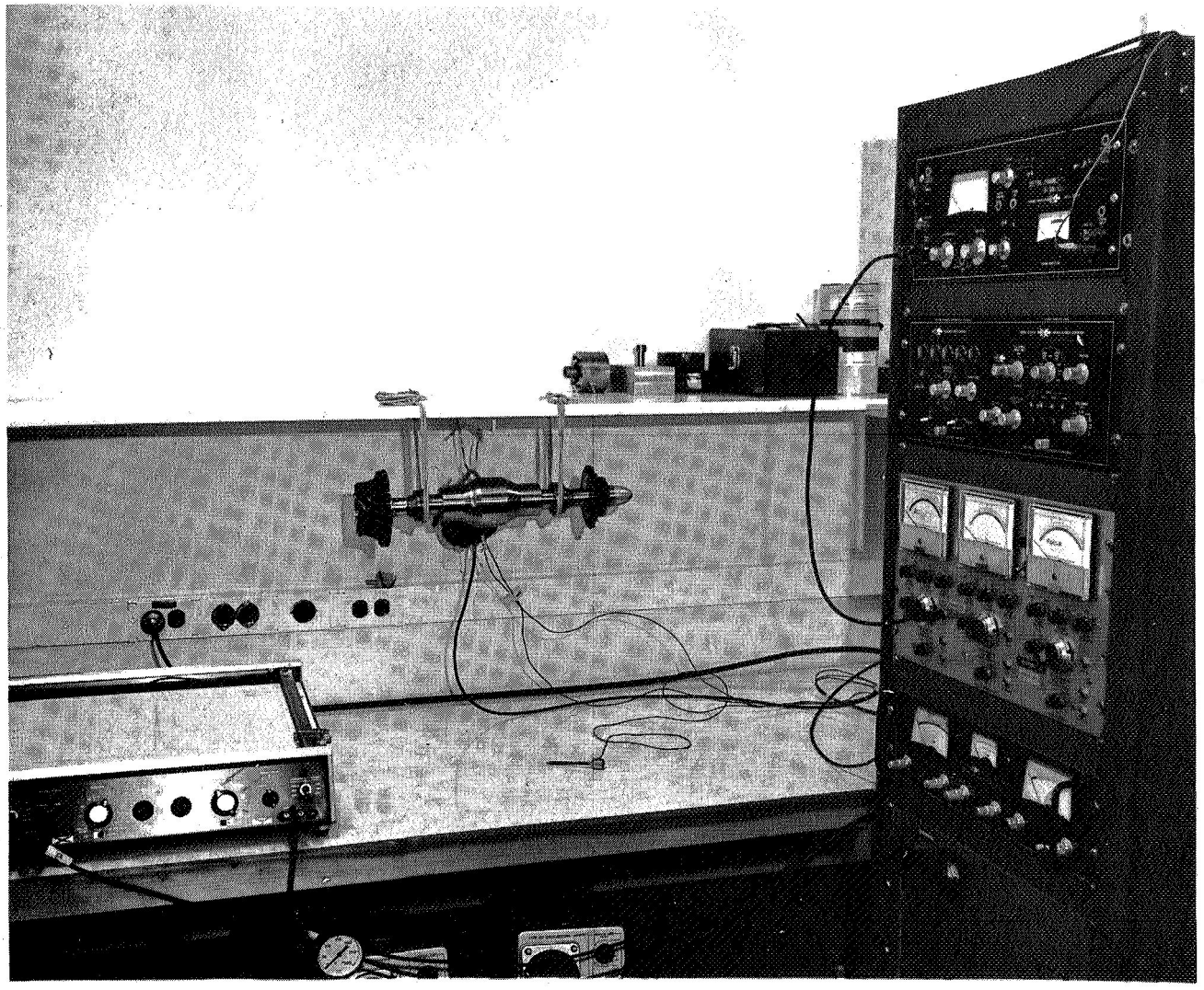

ASSEMBLED BRU-R SHAFT
SUSPENDED ON RUBBER SHOCK CORDS

FIGURE 80

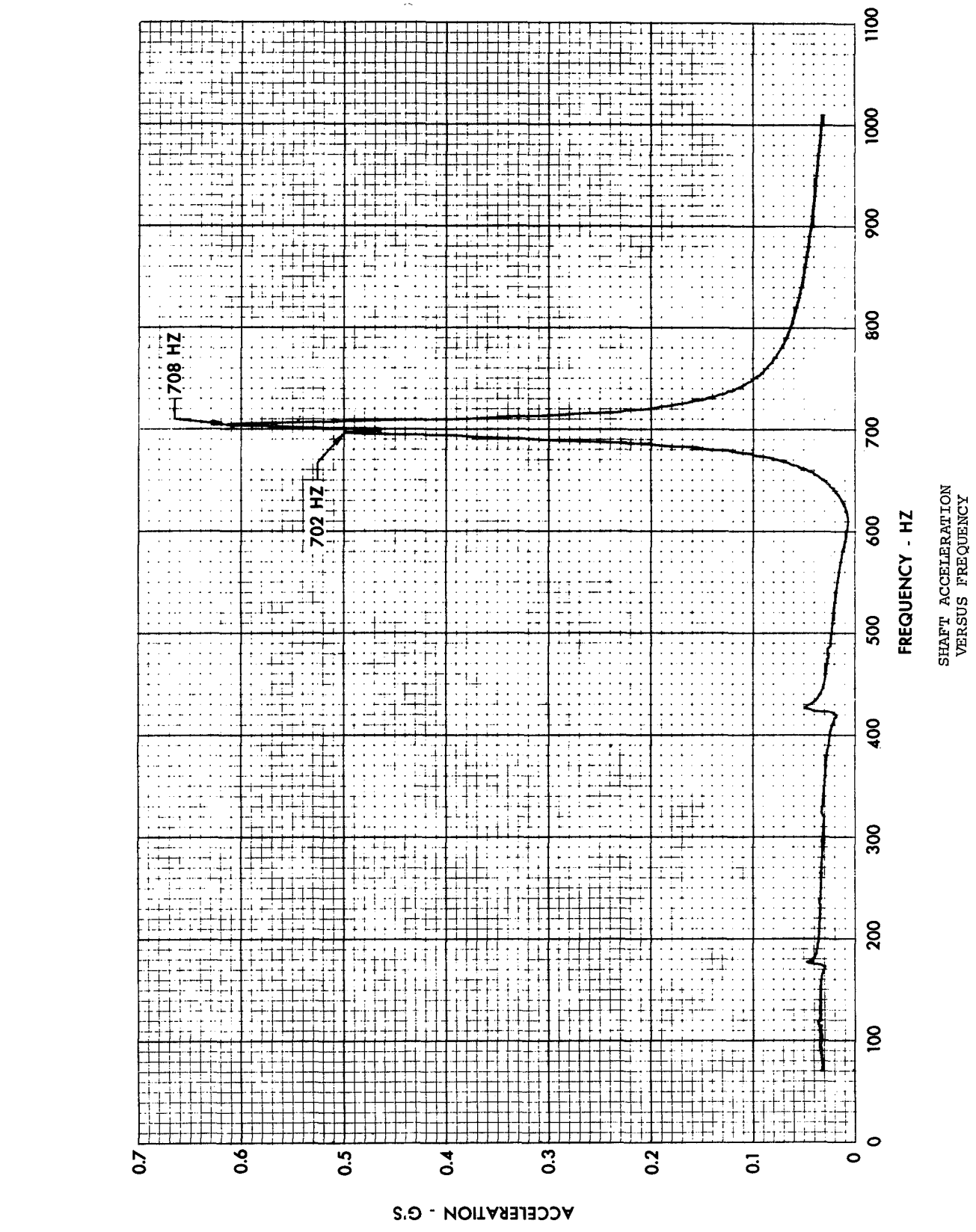
15 JAN 69
BRU-R
DRIVE 0.5 LBS
DRIVE ACC
708 HZ
702 HZ
ACCELERATION - G'S
0.7
0.6
0.5
0.4
0.3
0.2
0.1
0
0
100
200
300
400
500
600
700
800
900
1000
1100
FREQUENCY - HZ
SHAFT ACCELERATION
VERSUS FREQUENCY

FIGURE 81

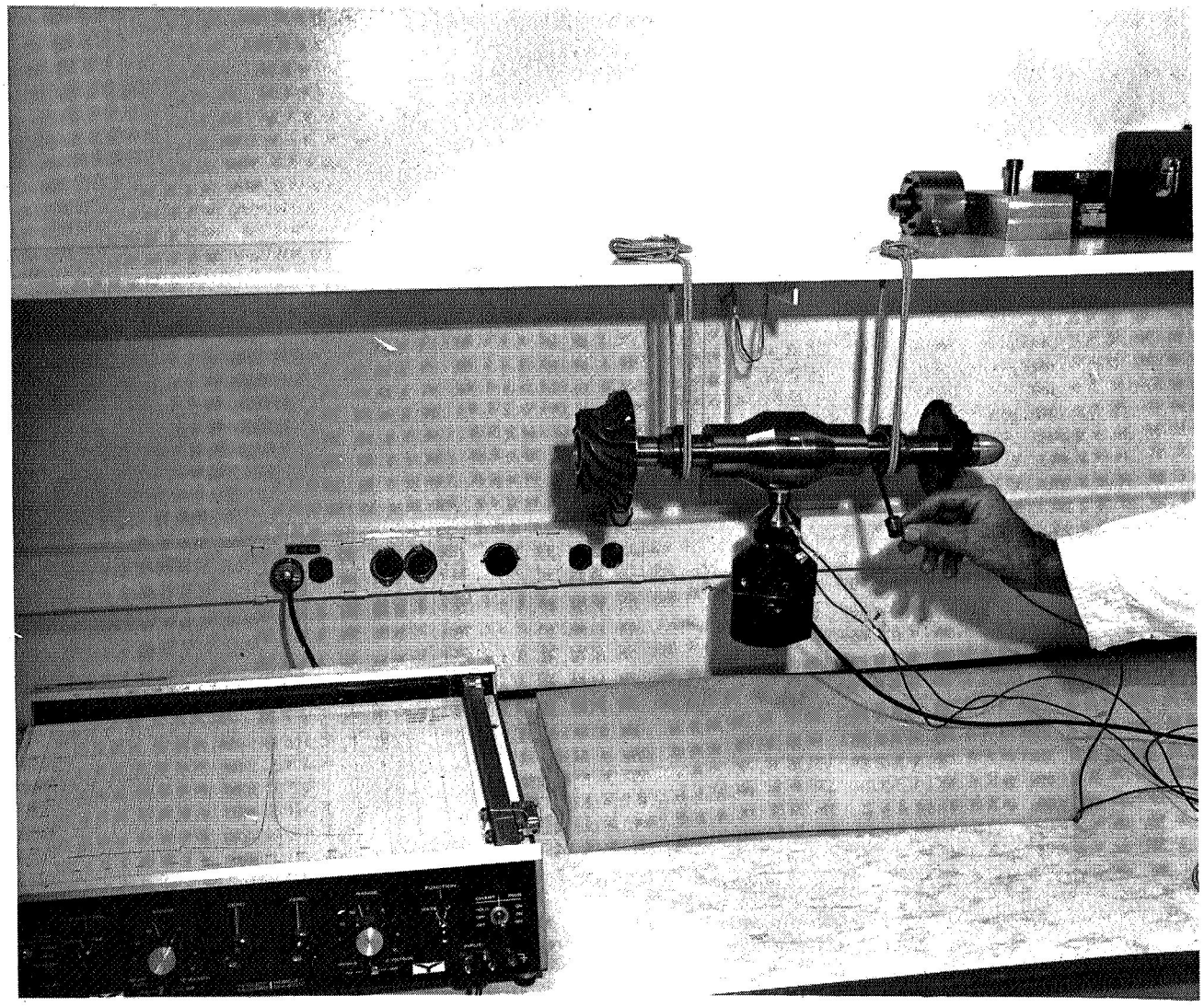

DETERMINING NODAL POINTS
OF BRU-R SHAFT

FIGURE 82

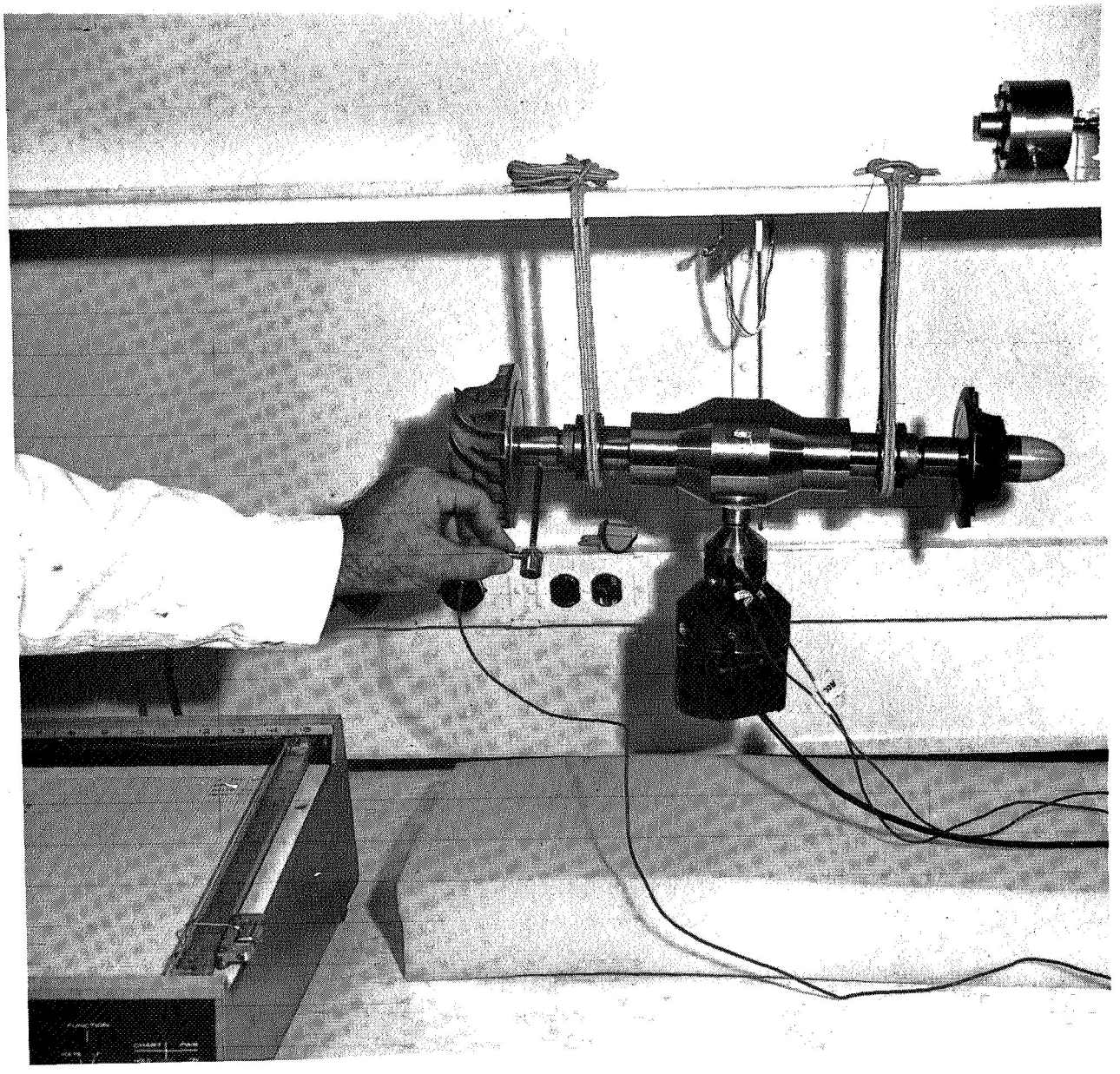

DETERMINING NODAL POINTS
OF BRU-R SHAFT

FIGURE 83

10. INSPECTION AND ACCEPTANCE TEST

The BRU-R inspection and acceptance test activity consisted of three separate tests: 500-, 50-, and 5-hr. The 500-hr was performed with an electrical heater attached to the turbine end to simulate the thermal input equivalent to the 6.0-kw_e power level. The BRU-R was operated with dummy inertial masses replacing the aerodynamic components; an air turbine was used to drive the BRU-R. Seal leakage rates were measured from a leak-proof pressure vessel (can) on the turbine end. At the completion of the test, the BRU-R was operated at 120-percent speed for 10 min.

The 50-hr test was performed with new bearings and seals and with the same test procedure as in the 500-hr test but without the electrical heater on the turbine end. The purpose of the 50-hr test was to verify the oil leakage rates for the first 50 hr of the 500-hr test.

The 5-hr test was performed with the turbine wheel and compressor impeller installed; the BRU-R was driven with compressed air. At the completion of the test, the BRU-R was operated at 120-percent design speed for 10 min.

10.1 500-Hour Test

The purpose of this test was to demonstrate the performance of the seals in conforming to the oil leakage requirement of 0.07 lb of oil for a 500-hr operational period. An additional requirement was that the test be performed with a heat-input to the turbine end that simulates operation at a 6.0-kw_e power level.

10.1.1 Description of Test Setup

The BRU-R was assembled with dummy inertial masses in place of the aerodynamic components (Figure 84). An air turbine motor was installed at the compressor end to drive the BRU-R (Figure 85), and an electrical heater was installed at the turbine end (Figure 86).

The instrumentation of the BRU-R consisted of 36 chromel-alumel thermocouples and three capacitance probe speed pickups. The location of 32 of the thermocouples is shown in Figure 12. Four additional thermocouples were attached to the inside of the turbine shroud assembly at diameters of approximately 5.0 and 7.0 in. The thermal analysis at the 6.0-kw_e power level predicted that the temperatures of these two locations on the turbine shroud assembly should be approximately 930° and 620°F, respectively. A leak-proof vessel (can) was installed over the dummy turbine wheel, and the vessel was fitted with a length of tubing and a valve with which to draw gas samples from the turbine cavity.

The BRU-R was installed in the Lubrication and Cooling System (Figure 87); the control room is shown in Figure 88. The flow schematic of the test setup is in Appendix D as Drawing 699220 and was described in detail in Section 4. The test loop included two tanks (Figures 89 and 90) sized to duplicate the estimated volumes of the connecting piping in the NASA Plum Brook SPF BRU-R installation. The oil-mist lubricator in the 500-hr test was a modified Norgren L02-200-OE HAU lubricator head; the lubricator is shown installed in the lubricator tank in Figure 91. This lubricator was unreliable in maintaining oil-flow rates without frequent readjustment of the oil-mist lubricator and was replaced with the venturi mixing section and positive displacement pump described in Section 4 after the completion of the test.

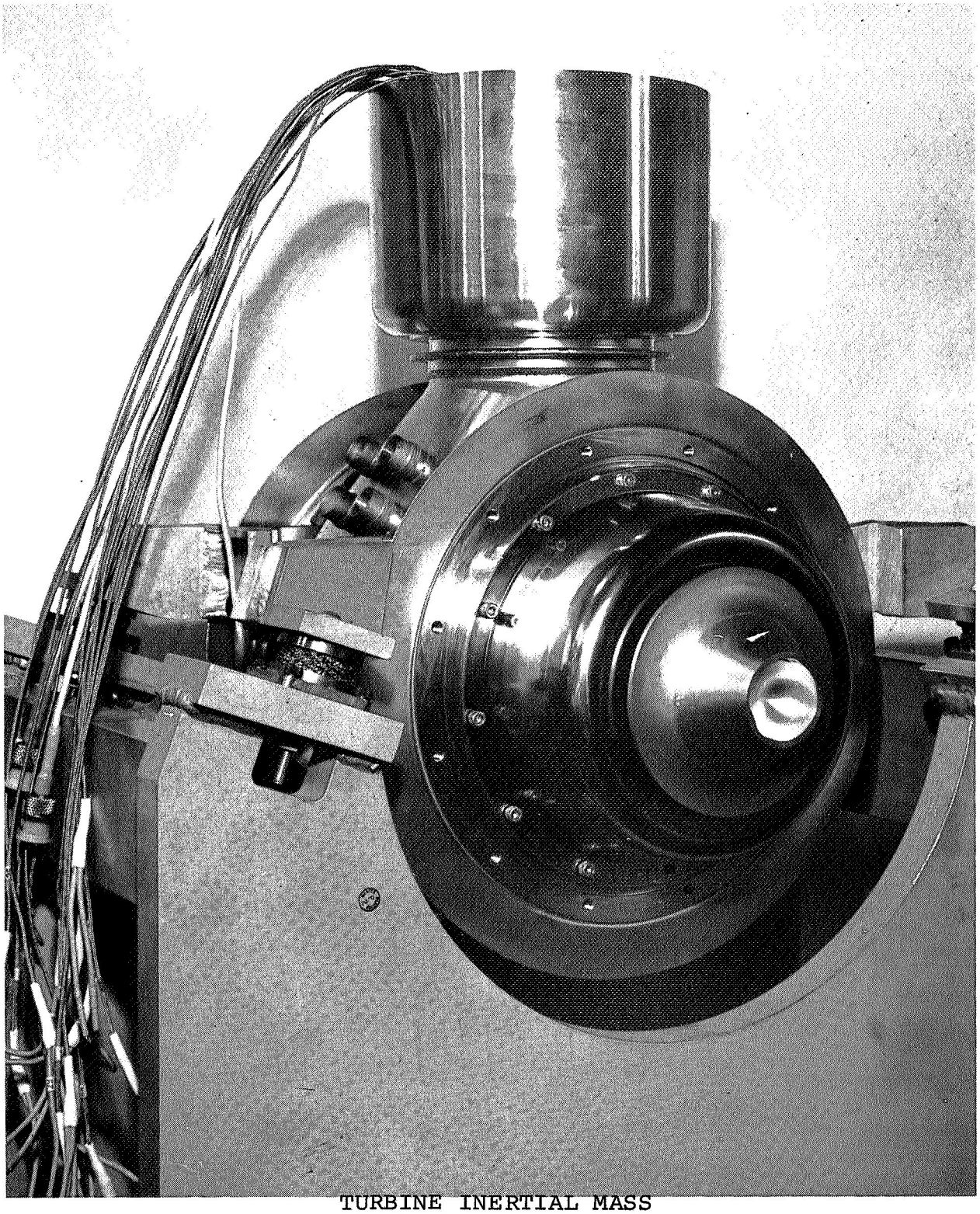

TURBINE INERTIAL MASS

FIGURE 84

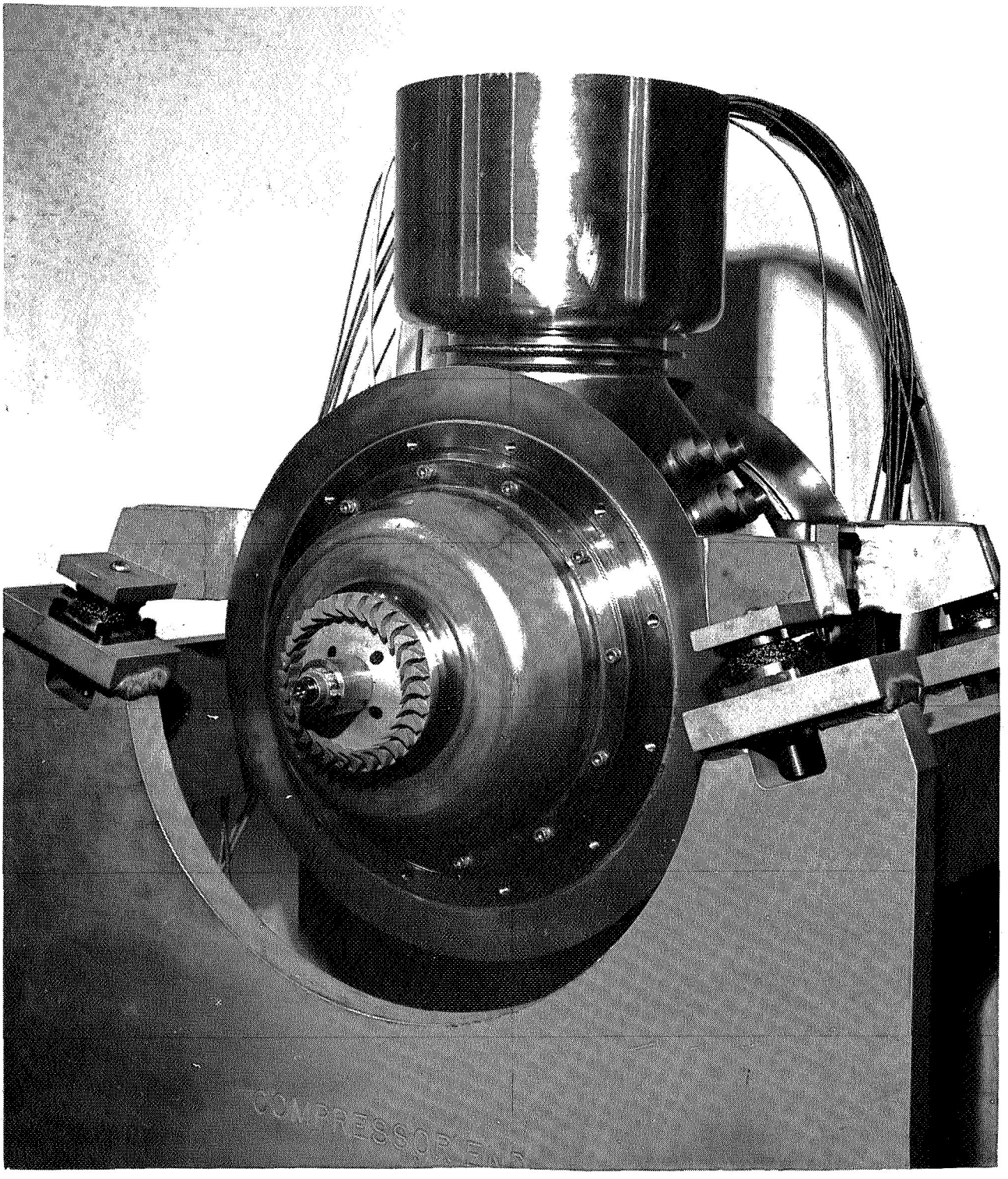

AIR TURBINE MOTOR INSTALLATION

FIGURE 85

MP-22779

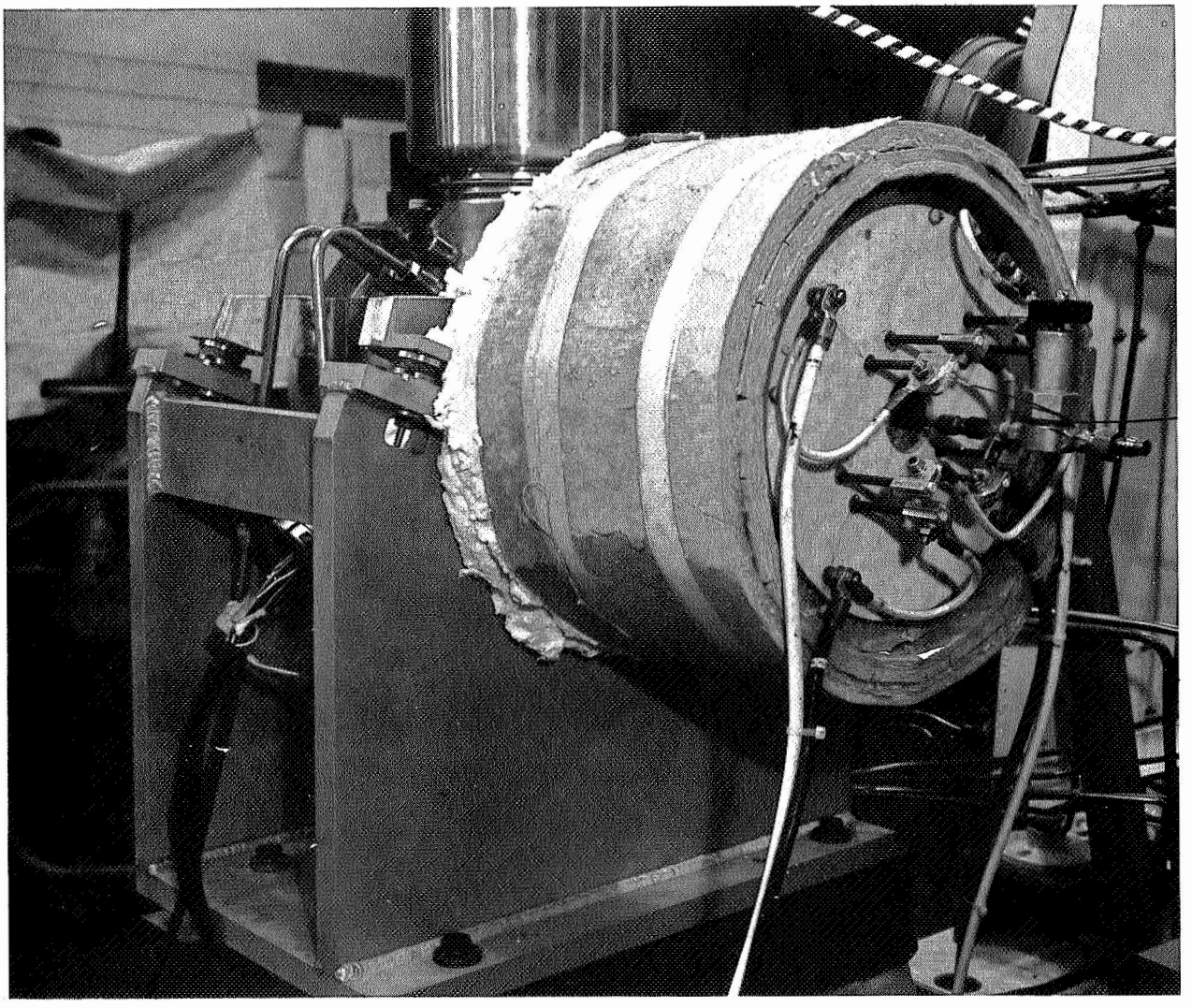

TURBINE HEATER

FIGURE 86

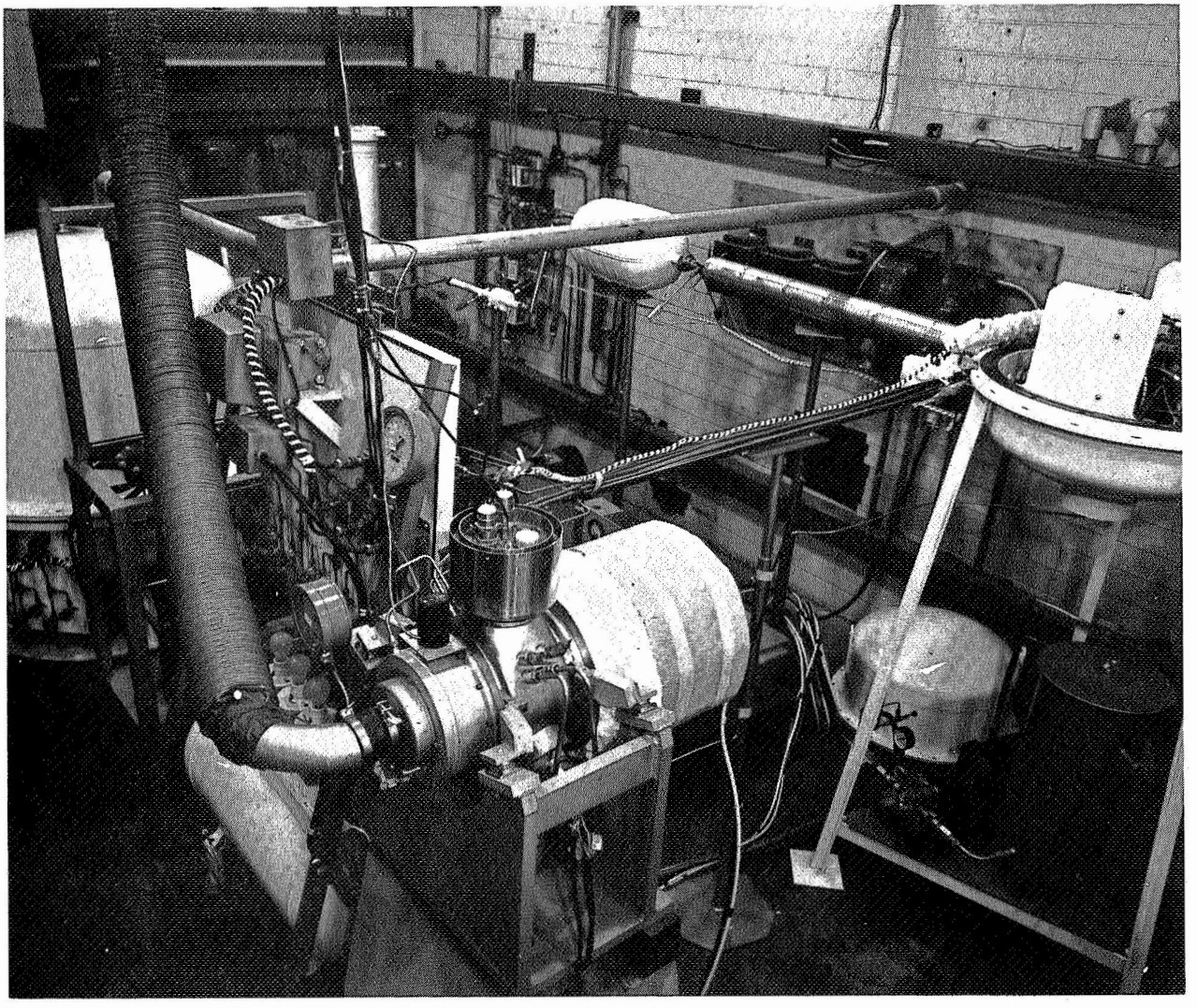

BRU-R LUBRICATION AND COOLING LOOP

FIGURE 87

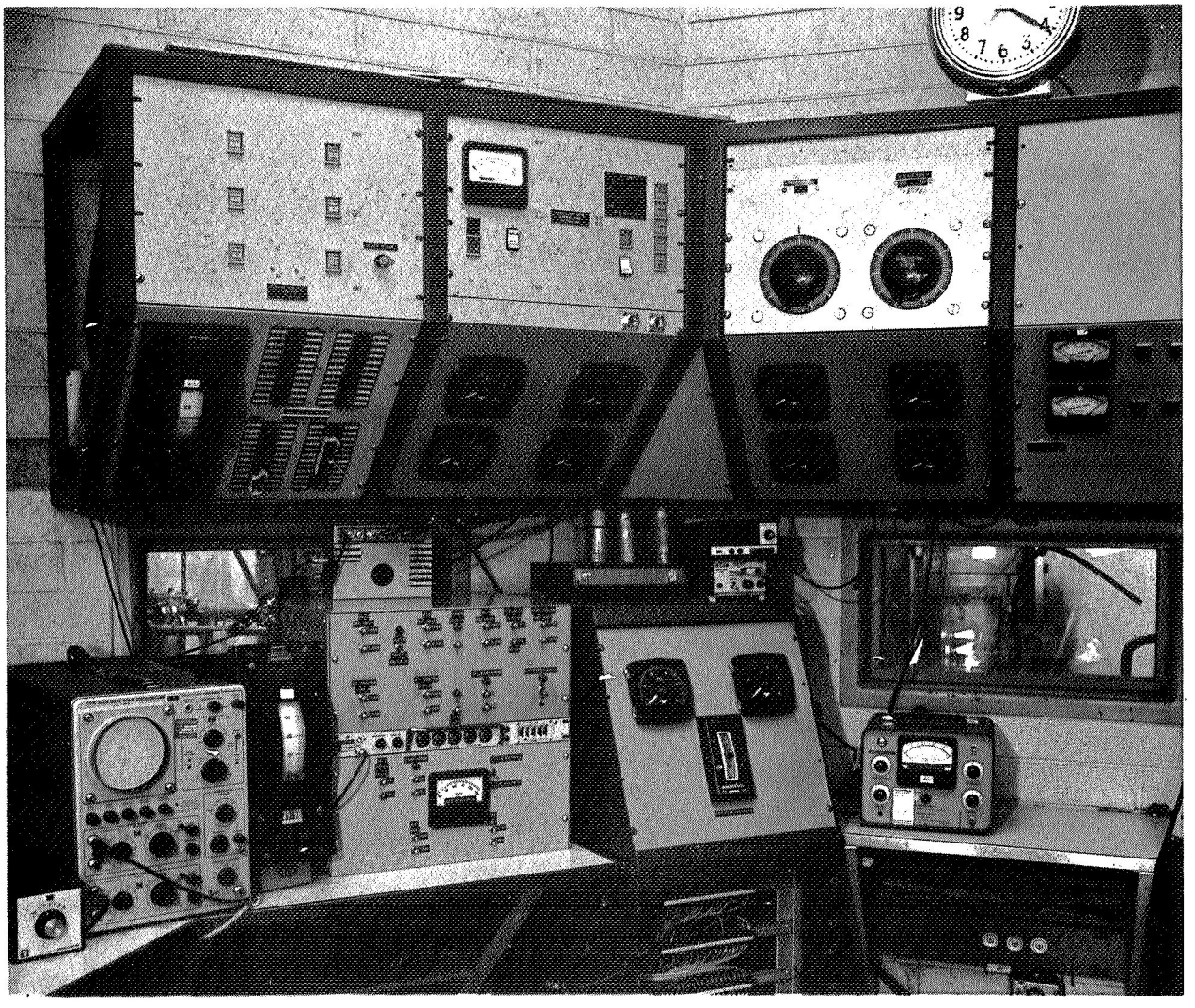

BRU-R CONTROL ROOM

FIGURE 88

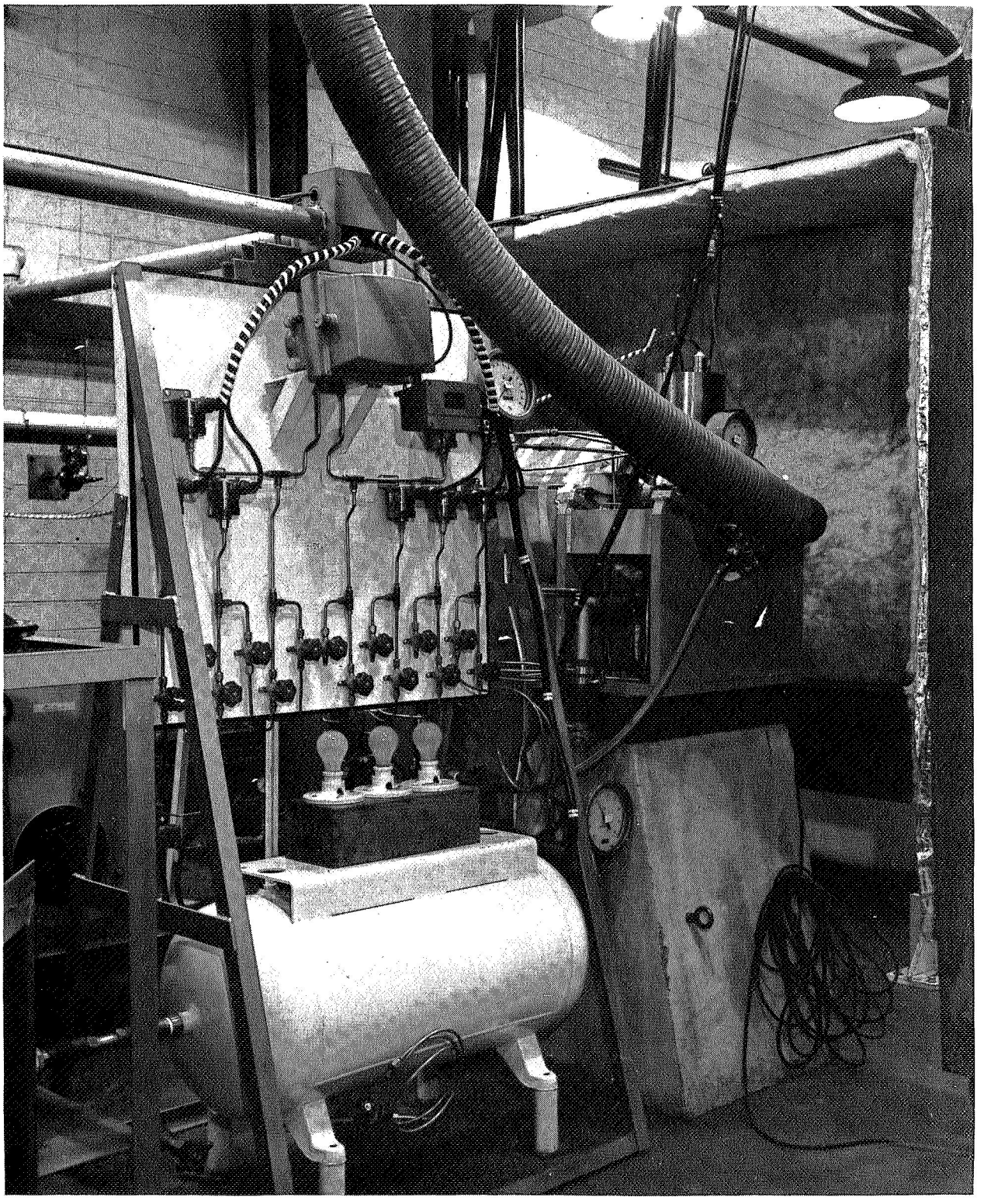

RETURN LINE VOLUME
SIMULATION TANK

FIGURE 89

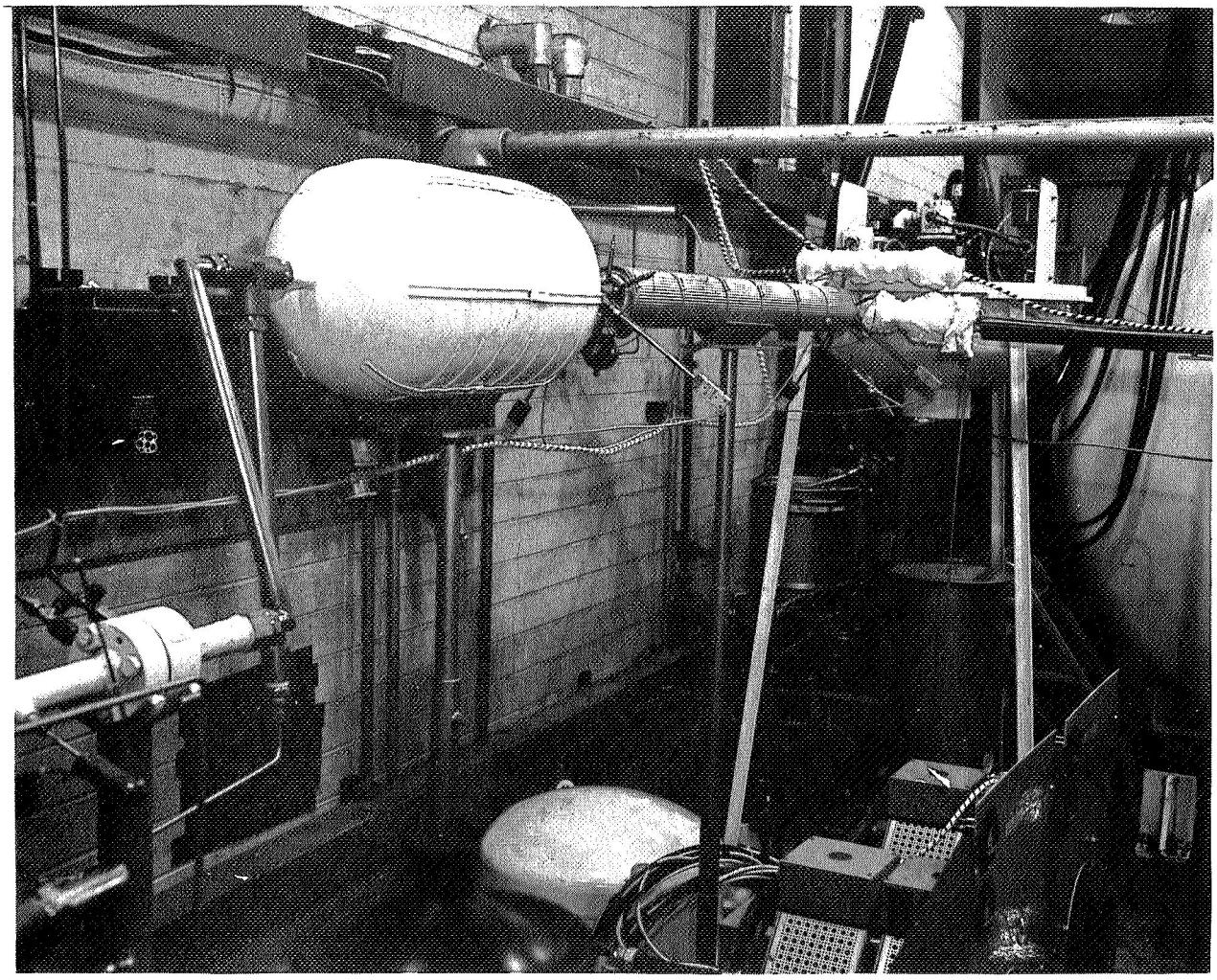

HIGH-PRESSURE LINE VOLUME
SIMULATION TANK

FIGURE 90

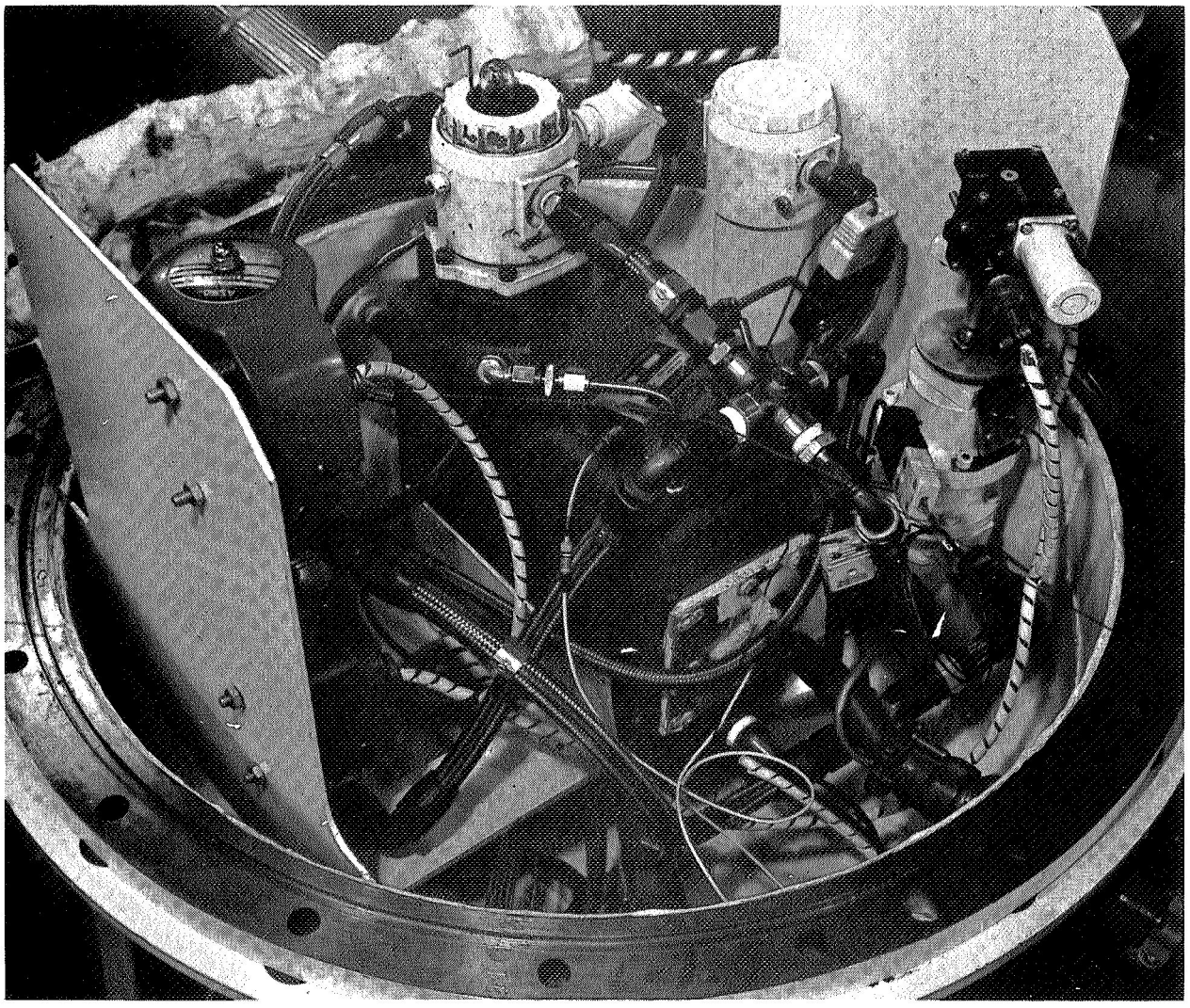

LUBRICATOR TANK

FIGURE 91

10.1.2 Test Performance

The 500-hr test was initiated on March 19 and completed on April 21, 1969. The unit was operated for a total of 502.5 hr at the design speed of 36,000 rpm. The electrical heater mounted on the turbine end of the BRU-R produced temperatures of 900° to 955°F on the turbine shroud assembly at diameters of approximately 5.0 and 7.0 in., respectively. This corresponds to a heat input equivalent to operation at a 6.0-kw_e power level. Sixty-eight starts of the BRU-R were made during the test. At the conclusion, the unit was operated at 120 percent of design speed for 10 min without change in the vibration level. The temperatures measured in the BRU-R and its Lubrication and Cooling System are summarized in Tables II and III, respectively. Also, Lubrication and System operational pressures and flow rates are shown in Tables IV and V.

10.1.2.1 BRU-R Vibration

The vibration level of the BRU-R ranged from 0.005 to 0.017 mil double-amplitude displacement for the entire 502.5 hr of operation. The vibration level remained unchanged during the 120-percent overspeed test.

10.1.2.2 Bearing Lubrication

A total of 64.52 lb of MIL-L-7808 oil was supplied to the BRU-R bearings during the 502.5 hr of operation. The average oil flow rate to each bearing was 0.00107 lb/min; the design flow rate was 0.0011 lb/min.

TABLE II

TYPICAL TEMPERATURES IN BRU-R

Thermocouple Number	Thermocouple Location	Test Temperature Range, °F		
		500-hr*	50-hr	5-hr
1	Alternator exciter-compressor end	97 - 110	94 - 102	90 - 97
2	Alternator field windings	106 - 128	97 - 113	100 - 108
3	Alternator field windings	121 - 152	95 - 123	109 - 117
4	Alternator laminations	**	100 - 130	118 - 127
5	Alternator laminations	113 - 140	92 - 113	100 - 108
6	Alternator laminations	127 - 150	102 - 130	115 - 127
7	Alternator laminations	137 - 155	96 - 120	105 - 115
8	Alternator field windings	127 - 145	99 - 123	110 - 118
9	Alternator field windings	125 - 145	96 - 120	107 - 117
10	Alternator exciter-turbine end	100 - 115	85 - 100	87 - 93
11	Cooling jacket-alternator	90 - 101	85 - 95	84 - 90
12	Main housing flange	305 - 350	95 - 131	92 - 98
13	Resilient-mount bearing, turbine end	132 - 150	106 - 120	104 - 110
14	Resilient-mount bearing, turbine end	147 - 160	115 - 130	111 - 117
15	Bearing cavity, turbine end	142 - 158	97 - 110	95 - 101
16	Bearing cavity, turbine end	151 - 170	**	**
17	Cooling jacket-turbine	108 - 123	86 - 95	85 - 90
18	Cooling jacket-turbine	115 - 130	85 - 96	84 - 90
19	Main housing flange	315 - 357	93 - 133	91 - 99
20	Cooling flow-bearing, turbine end	225 - 247	102 - 130	97 - 104
21	Cooling flow-bearing, turbine end	200 - 218	105 - 125	102 - 108
22	Cooling jacket-alternator	90 - 103	**	**
23	Cooling flow scavenge	95 - 117	82 - 96	77 - 90
24	Cooling flow scavenge	137 - 155	93 - 115	85 - 95
25	Cooling flow-bearing, compressor end	132 - 150	**	**
26	Cooling flow-bearing, compressor end	140 - 158	125 - 147	130 - 140
27	Bearing cavity, compressor end	**	**	**
28	Bearing cavity, compressor end	130 - 147	117 - 143	128 - 139
29	Resilient-mount bearing, compressor end	140 - 155	130 - 152	137 - 145
30	Resilient-mount bearing, compressor end	138 - 157	127 - 155	140 - 150
31	Outer race bearing, compressor end	190 - 208	200 - 215	188 - 197
32	Outer race bearing, turbine end	197 - 218	179 - 190	**

*Heater installed on turbine end - turbine shroud temperature of 900° to 955°F and turbine shroud leg temperature of 562° to 685°F.

**Thermocouple inoperative during test (faulty electrical plug).

TABLE III

TYPICAL TEMPERATURES IN LUBRICATION AND COOLING SYSTEM

Thermocouple Number	Thermocouple Location	Test Temperature Range, °F		
		500-hr*	50-hr**	5-hr†
37	REG-1 Discharge	70 - 108	80 - 90	83 - 85
38	Lubricator discharge	70 - 100	80 - 90	83 - 86
39	Lubricator discharge	70 - 100	80 - 90	82 - 88
40	Top of lubricator reservoir	70 - 95	††	††
41	Bottom of lubricator reservoir	67 - 95	††	††
42	Lubricator tank	70 - 94	††	††
45	HX-3 outlet	110 - 117	80 - 91	85 - 88
46	HX-3 outlet	110 - 112	80 - 91	84 - 88
47	HX-3 inlet	82 - 95	83 - 91	84 - 88
48	HX-3 inlet	82 - 95	83 - 92	84 - 85
100	Compressor gas inlet	86 - 104	87 - 100	92 - 98
101	Compressor gas inlet	86 - 104	87 - 100	92 - 98
102	Compressor cooling water inlet	65 - 88	75 - 78	76 - 77
103	Compressor cooling water outlet	77 - 103	75 - 78	76 - 77
104	Compressor housing, top	87 - 112	98 - 103	99 - 102
105	Compressor housing, bottom	102 - 115	92 - 116	104 - 114
106	Compressor oil sump	101 - 113	85 - 114	100 - 112
107	Compressor oil sump	103 - 116	85 - 115	100 - 113
108	HX-1 gas outlet	75 - 86	79 - 88	82 - 86
109	HX-1 gas outlet	76 - 86	79 - 88	82 - 86
110	Motor hub	110 - 124	92 - 126	108 - 122
116	Motor cooling fin	94 - 116	84 - 114	100 - 113
117	Motor cooling fin	89 - 108	85 - 107	93 - 101
118	HX-4 surface outlet	70 - 85	77 - 88	81 - 84
119	HX-4 surface inlet	70 - 85	77 - 88	82 - 86
120	HX-2 gas inlet	196 - 218	204 - 211	208 - 210
121	HX-2 gas outlet	99 - 115	108 - 111	109 - 111
125	Gas out of F-1 filter	73 - 95	83 - 96	87 - 93
126	Gas out of F-1 filter	73 - 94	83 - 95	86 - 90

*Cell ambient temperature of 70° - 94°F

**Cell ambient temperature of 80° - 89°F

†Cell ambient temperature of 80° - 85°F

††Thermocouple not attached

B14927

TABLE IV

TYPICAL LUBRICATION AND COOLING SYSTEM PRESSURES

Pressure Transducer Number	Transducer Location	Test Pressure Range, psia		
		500-hr*	50-hr	5-hr
P1	Compressor Hub	15.8-16.4	15.9-16.0	17.6-17.8
P2	Sump	15.6-16.2	15.8-15.9	17.5-17.7
P3	Alternator Housing	17.8-18.2	17.2-17.4	18.8-19.0
P4	Turbine Hub	15.8-16.5	16.2-16.8	18.2-18.4
P5	Lubricator Discharge	63.4-65.1	63.8-65.0	63.9-64.2
P6	LCS Compressor Tank	10.7-11.5	11.0-12.2	11.0-11.3
P7	R-1 Chamber	81.0-84.5	80.0-83.0	80.8-81.5
P8	F-1 Filter Line Discharge	80.5-83.5	79.9-83.0	80.8-81.5
P9	Regulator -1 Discharge	72.0-75.8	70.8-73.1	70.8-72.5

TABLE V

LUBRICATION AND COOLING SYSTEM FLUID-FLOW RATES

Flow Number	Flowmetering Location	Flow Range, gpm		
		500-hr*	50-hr**	5-hr**
W1	Heat Exchanger 1 Compressor In	0.725-1.71	- - -	- - -
W2	Heat Exchanger 2 Compressor Out	1.00 -2.93	2.16 -2.41	2.37-2.54
W3	Heat Exchanger 4 Motor	0.80 -2.20	0.42 -0.67	0.73-0.77
W4	Compressor Coolant	2.32 -2.46	2.20 -2.25	2.23-2.25
W5	Alternator Coolant	0.72 -0.95	0.70 -0.73	0.70-0.74
W6	Turbine Coolant	0.50 -0.80	0.245-0.250	0.25-0.25

*Heater installed on turbine end-turbine shroud temperature of 900°F to 955°F and turbine shroud leg temperature of 562° to 685°F.
**HX1 inoperative

B14928

10.1.2.3 Bearing Temperatures

The BRU-R bearing outer-race temperatures remained unchanged throughout the test when compared under identical cooling-gas and oil-flow conditions. Generally, the bearing at the turbine end of the shaft ran approximately 10°F hotter than the compressor bearing, due to the thermal input of the electrical heater at the turbine. Compressor bearing temperatures ranged from 197° to 210°F, while the turbine end bearing operated between 205° to 215°F.

10.1.2.4 Hydrodynamic Face Seal Leakage

One of the primary objectives of the test was to evaluate the hydrodynamic face seals that prevent oil contamination of the BRU-R loop gas. Due to the use of the air turbine drive on the BRU-R dummy compressor and subsequent venting of one side of the compressor seal to an argon buffered but unsealed compressor cavity, only the seal at the turbine end could be exposed to a sealed turbine cavity into which oil leakage could be measured.

10.1.2.4.1 Gas Leakage

The Lubrication and Cooling System was designed to provide a constant differential pressure across the hydrodynamic face seals so that any gas flow through the seals would be from the Brayton cycle loop into the cooling and lubrication loop. This direction of flow would aid in reducing oil vapor contamination of the cycle working fluid. The total design argon gas leakage through both seals for the set differential pressure of 0.4 psi was approximately 4×10^{-6} lb/min. At that leakage rate, 0.012 lb of argon would have entered the cooling and lubrication loop during the 502 hr of test. No measureable increase in cooling loop pressure was observed, thus indicating that the seal leakage was within the limits of the instrumentation used.

10.1.2.4.2 Oil Leakage - Turbine Wheel Cavity

Gas samples were periodically drawn from the sealed turbine wheel cavity and subjected to infrared spectrophotometer analysis with a 10-meter gas cell. Gas samples were drawn at approximately 125, 242, 307, 386, 436, and 500 hr of operation. Gas sample 1, taken after 125 hr of operation, contained 282 ppm of hydrocarbons, including traces of acetone. The acetone was introduced into the gas sample via the sample bottle when cleaned. Subsequent bottles were cleaned with carbon tetrachloride and presented no further problems. After 242 hr of operation, substantial oil contamination was experienced in gas Sample 2. The excessive contamination was caused by an open valve in the gas sample circuit. With the valve open to atmosphere, the differential pressure across the hydrodynamic seal was reversed, and oil-mist entered the cavity. As the oil-mist was drawn into the hot turbine cavity, the oil was decomposed or "cracked" into other gases and, as was later discovered in the disassembly inspection (Section 10.1.3), a carbonaceous deposit resulted on the shroud and the dummy turbine wheel. As a result of this unfortunate mishap, gas Sample 2 contained 7000 ppm of CO_2, 31,000 ppm of CO, and traces of methane and ethylene. In all subsequent samples, the sample bottle was rinsed with benzene to determine if any oil had "condensed" on the walls. This solution was evaporated, and in each case, the resultant residue weight was less than 0.001 gm. After the valve condition was corrected, no further excessive contamination was noted. The gas sample results are summarized below:

Operation, hr	Contamination, ppm		
	CxHy	CO_2	CO
125	282	0	0
242	-	7000	31,000
307	40	350	0
386	98	0	0
436	192	0	753
500	97	320	650

The presence of carbon dioxide in the sample can be traced to contamination of the cooling gas itself--a trend discussed in Section 10.1.2.6.

These gas sample measurements demonstrate that the seal hydrocarbon leakage rates of the BRU-R are less than the specified requirement of 0.070 lb for a 500-hr test. For example, consider the contamination experienced in gas Sample 1, which contained 282 ppm of hydrocarbons after 125 hr. In order to determine the actual seal leakage, this proportion must be related to the turbine cavity volume with a volume of approximately 550 cm^3. A contamination of 282 ppm or 0.0282 percent in this cavity means that there are 0.155 cm^3 of gaseous hydrocarbons present. It was assumed that the molecular weight of the hydrocarbons could be approximated by using the molecular weight of normal hexane (C_6H_{14}) which is 86. The exact composition of the hydrocarbons in the gas sample is unknown, but normal hexane is likely to be present and to be one of the heaviest volatile hydrocarbons in the sample. Since 1 gm molecular weight occupies 22.4 liters, this contamination of 282 ppm of hydrocarbons will weigh 5.95×10^{-4} gm. At this rate for two seals over a 500-hr period, the total contamination would be 4.76×10^{-3} gm or 1.048×10^{-5} lb. This is only 0.015 percent of the one leakage requirement of 0.070 lb for a 500-hr period.

10.1.2.5 Lubricator

The Norgren oil-mist lubricator used in this test was unreliable in maintaining oil-flow rates without frequent re-adjustment of the controls. In addition, the loop had to be shut down for approximately 1 min every 8 hr in order to balance pressures within the lubricator and prevent a complete stoppage of oil flow. Attempts to modify a spare lubricator to prevent the malfunction met with limited success. A positive displacement, motor-driven lubricator was incorporated on the subsequent tests of the BRU-R.

10.1.2.6 Lubrication and Cooling System Contamination

The oil contamination of the Lubrication and Cooling System gas was checked by analyzing a gas sample drawn from the loop at a point immediately downstream from the dual F-1 filters. Infrared spectrophotometer analysis was made at 380, 430, and 500 hr of operation. The results are tabulated below:

	Contamination, ppm	
Operation, hr	C_xH_y	CO_2
380	20	150
430	30	325
500	40	155

The general increase in hydrocarbon contamination at the end of the test indicates a decrease in the effectiveness of the F-1 filter elements. Also, it is believed that the presence of CO_2 and CO in the BRU-R turbine cavity gas sample can be explained by the LCS gas contamination rather than assuming seepage from the bearing cavity to the LCS gas. A change of filter elements every 250 hr of operation should minimize the oil contamination. It should be noted that all lines downstream from F-1 were clean and dry at the completion of the 500-hr test.

10.1.2.7 Lubrication and Cooling System Filter Performance

After completion of 500 hr of operation, the various filters in the Lubrication and Cooling System were inspected, and entrapped oil weighed. The bulk of the lubricating oil introduced during the system was found in the large tank, simulating the volume of the SPF return line to the reciprocating compressor (Figure 89). The results are:

Location	Oil Weight, lb
Return Line Volume Tank	63.230
F-1	0.050
F-2	0.360
F-3 (automatic dump)	0.006
F-4 (automatic dump)	0.000
Compressor Tank Sump	0.870
TOTAL	64.52

It should be noted that oil piping between F-1 filters and the lubricator were dry, with no visible trace of oil.

10.1.2.8 Automated Controller

The Taylor automated control system, used to maintain the differential pressure between P_1 and P_2, performed without fault. The controller was able to hold the set differential pressure of 0.4 psi within ±0.02 throughout the test.

10.1.2.9 HX-3 Heater

The heater (HX-3) was operated during the last 24 hr of the test to maintain cooling-gas temperature at 100°F. Manual control was easy and stable.

10.1.3 Disassembly Inspection

The BRU-R was disassembled, following completion of the 500-hr test.

10.1.3.1 Turbine Wheel Cavity

Upon removal of the electrical heater assembly from the BRU-R, carbon was observed on the face of the turbine shroud, the gold-plated surfaces of the turbine wheel, and (to a lesser extent) on the inside of the heater shroud (Figures 92 and 93). Approximately 0.1 gm of carbon was scraped from the components.

10.1.3.2 Dummy Turbine Wheel

Further disassembly revealed the back of the turbine wheel was lightly spotted with carbon (Figure 94). The reason for oil condensing only in spots is unknown.

10.1.3.3 Turbine Shroud

The carbon formations on the inside of the shroud are shown in Figure 95. These spots were caused by radial jets of cooling-gas and oil-mist passing through thermocouple lead holes in the turbine bearing carrier and impinging upon the high-temperature shroud. The next assembly was made with the holes plugged to prevent recurrence of this carbon formation.

10.1.3.4 Hydrodynamic Face Seals

The hydrodynamic face seals and stators showed no evidence of wear after 500 hr of operation and 68 starts. The seal at the turbine end of the shaft had the carbon face coated with fresh oil, but there was

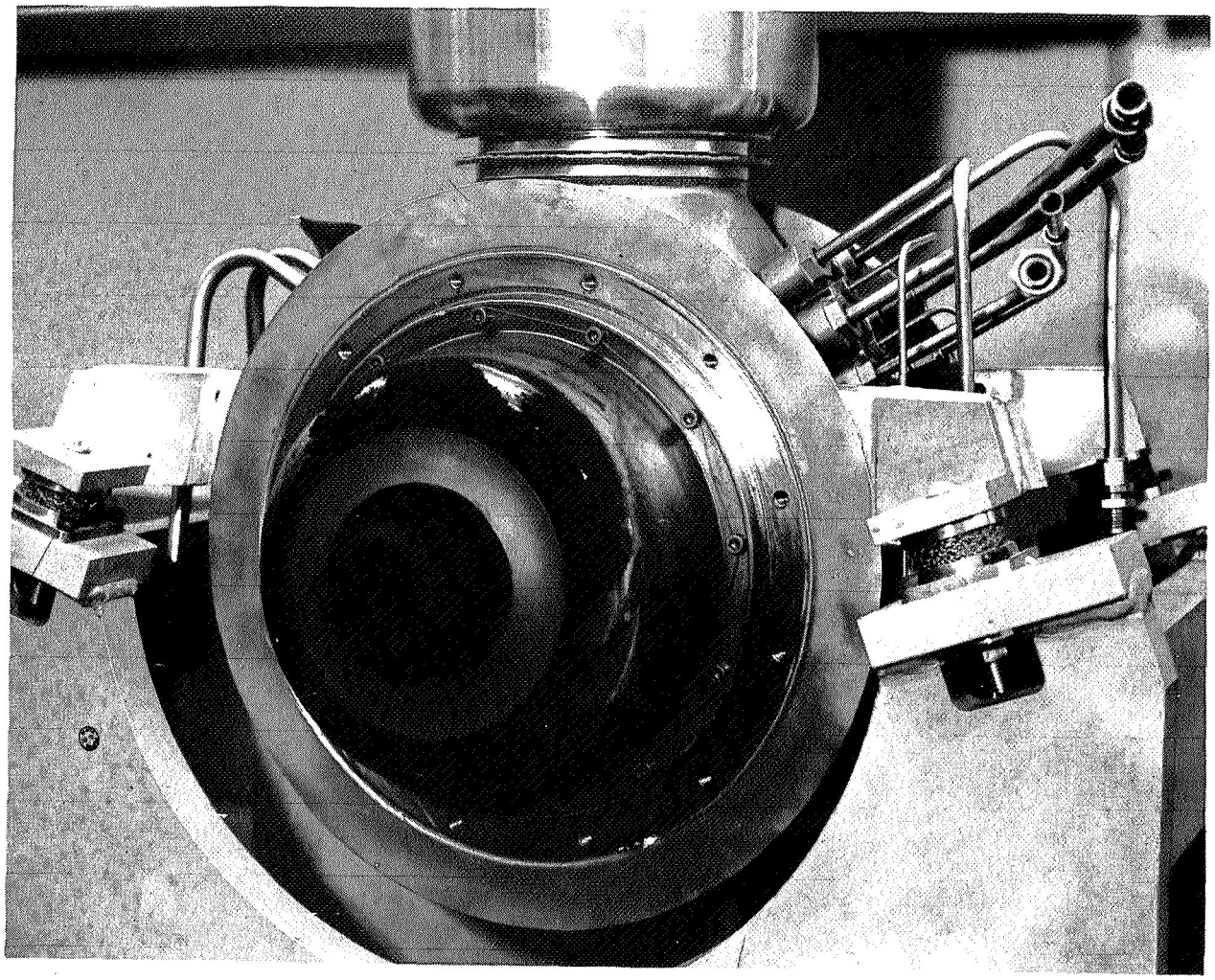

TURBINE SHROUD AND
DUMMY TURBINE WHEEL

FIGURE 92

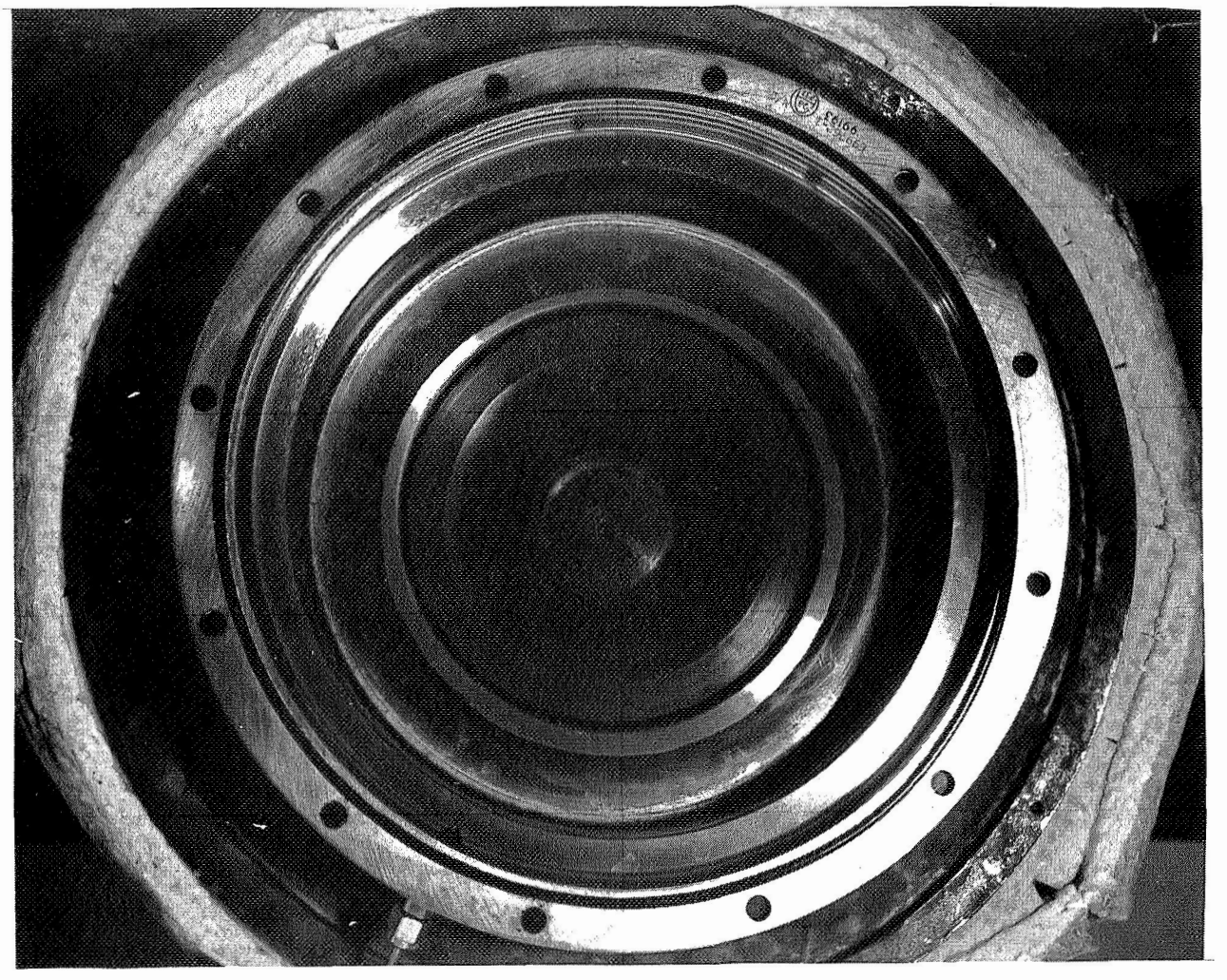

HEATER SHROUD

FIGURE 93

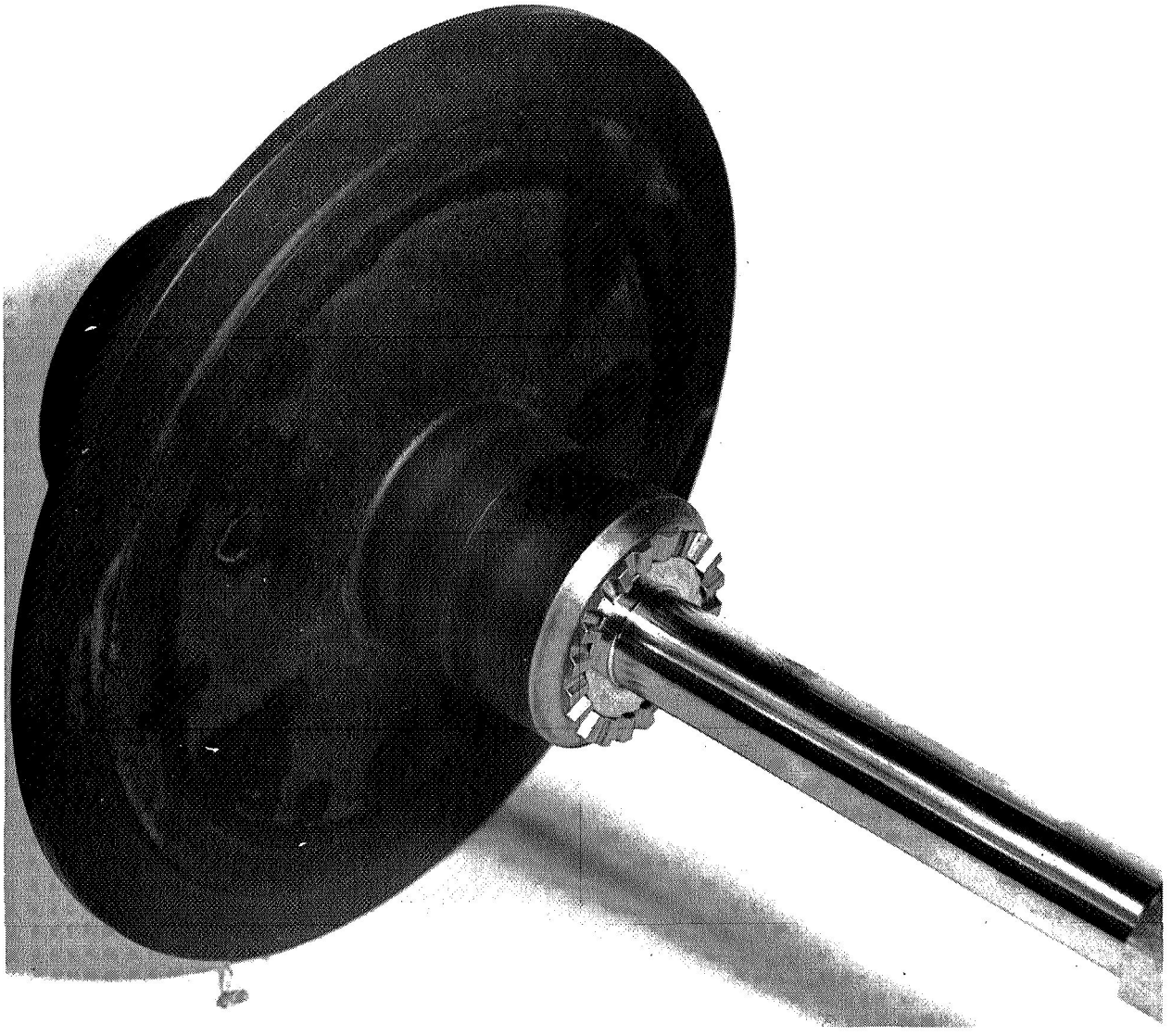

DUMMY TURBINE WHEEL

FIGURE 94

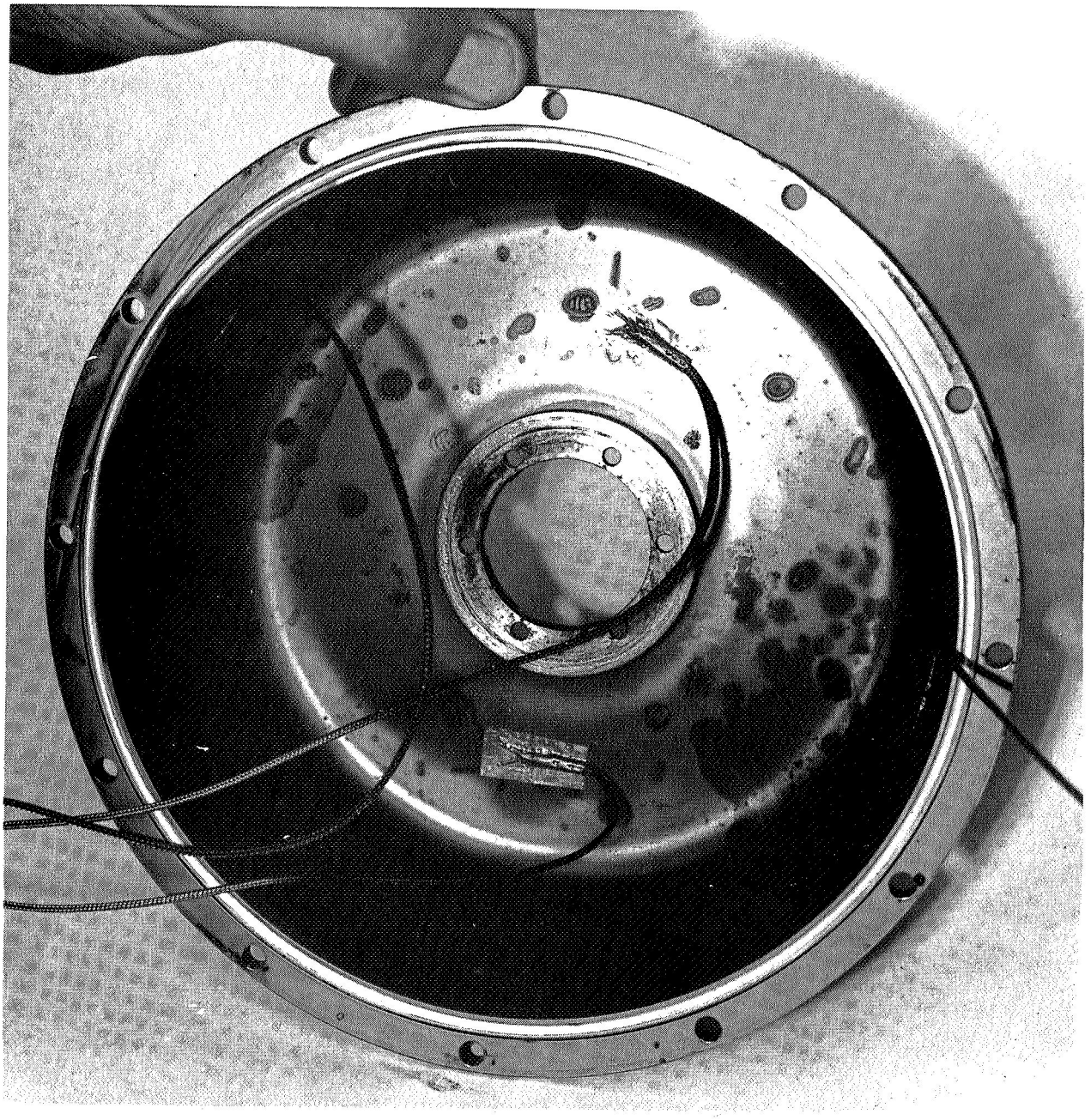

TURBINE SHROUD

FIGURE 95

no evidence of any significant carbon buildup on the hydrodynamic gas bearing geometry. The seal is shown in Figure 96.

The total quantity of oil leaking through the turbine end seal could not be measured except by weight of the carbon deposits on shrouds, seal carrier, and turbine wheel. The carbon removed from these components weighed approximately 0.2 gm. Since the carbon in MIL-L-7808 oil constitutes 69 percent of the weight, it can be assumed that at least 0.29 gm of oil passed through the seal. The amount of oil leaking through the seal during the 75 hr of operation when the cavity valve was open is impossible to determine.

The hydrodynamic face seal at the compressor end of the shaft was dry. The compressor cavity outside the face seal contained 3 gm of oil. Assuming that the compressor end-seal permitted the entire 3 gm of oil leakage in the compressor cavity, the total hydrodynamic seal leakage would be comprised of the following elements:

	Weight of Oil, lb
Compressor end (3 gm)	0.0066200
Turbine end (weight of oil equivalent to 0.2 gm of carbon)	0.0006400
Spectrophotometer extrapolation (Page 10-16)	0.0000105
Total seal leakage for 500 hr	0.0072705
Total seal leakage permitted by contract	0.070

The total leakage is 10.3 percent of that permitted by contract; however, the compressed air used to drive the motoring turbine contained traces of oil that could have condensed in the same cavity. Also, the amount of oil leaking through the turbine end seal, when the turbine cavity valve was inadvertently left open, was impossible to determine. Therefore, it is believed that a more representative seal leakage rate is obtained by extrapolating the infrared spectrophotometer measurements (Paragraph 10.1.2.4.2). In fact, these show that a negligible quantity of oil was "leaking" past the seals.

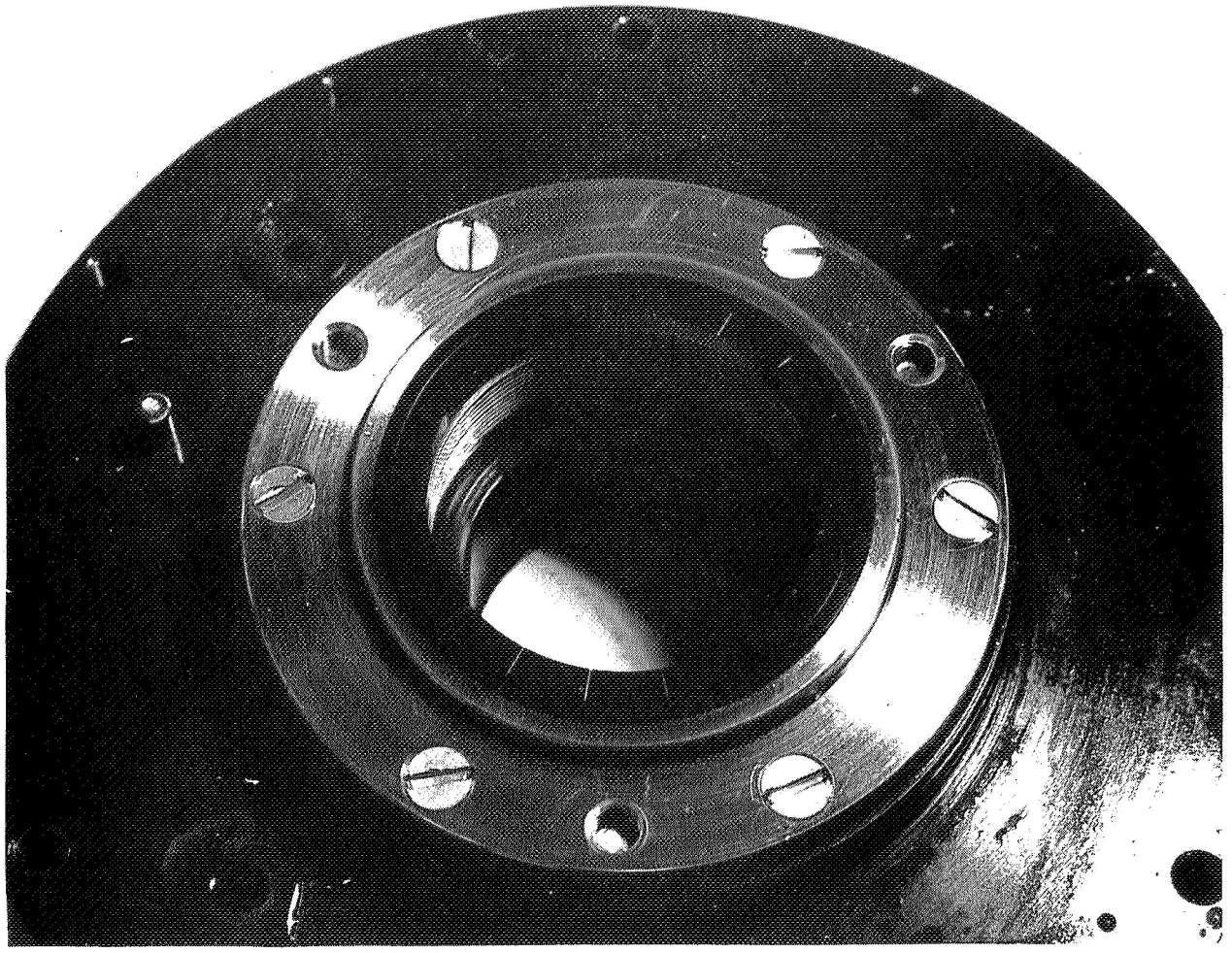

HYDRODYNAMIC FACE SEAL:
TURBINE END

FIGURE 96

MP-23659

10.1.3.5 Alternator Cavity

The alternator cavity, which was supplied with 0.2 lb/min of cooling argon, was dry and free from all traces of oil.

10.1.3.6 Bearings

The P/N 358546 bearings were in excellent condition without any trace of oil-coking or discoloration. Separators, races, and balls appeared to be as originally installed.

10.1.3.7 General Condition

All components of the BRU-R, including labyrinth seals, resilient bearing mounts, shaft, and housings, completed the 500-hr test without any evidence of malfunction or failure.

10.2 Fifty-Hour Test

The purpose of the 50-hr test was to verify the oil leakage rates that were experienced during the first 50 hr of the 500-hr test. This was Part 1 of the acceptance test and was to be performed with dummy inertial masses in place of the aerodynamic components.

10.2.1 Description of Test Setup

Following the detailed inspection after the 500-hr test, the BRU-R was assembled with new bearings and new seals. An air turbine motor was used to drive the BRU-R as in the previous test; the electrical heater was not used. The Norgren lubricator head was replaced with the positive displacement metering pump and venturi section described in Paragraph 4.4 and shown in Figure 25. The remainder of the test equipment was the same as in the 500-hr test.

10.2.2 Test Performance

The 50-hr test was initiated on July 9 and successfully completed July 11, 1969. The BRU-R was operated for a total of 50 hr 25 min at the design speed of 36,000 rpm. (See tables on Pages 10-12 through -14.)

10.2.2.1 BRU-R Vibration

The vibration level of the BRU-R remained between 0.015 to 0.020 mil double-amplitude displacement for the entire 50.4 hr of operation. During coast-down, vibration levels were recorded as a function of shaft speed. These verified earlier predictions (Sections 5 and 9) of critical speed ranges. Those vibrations and their corresponding speeds are summarized below:

Shaft Speed, rpm	Double-Amplitude Vibration, mil
36,000	0.020
31,500	0.100
23,700	0.105
21,000	0.100
16,200	0.130
6,000	0.120

The 0.13-mil level at 16,200 rpm, while not excessive, appears to define the lower critical while the 0.12-mil reading at 6000 defines the transition region for the hydrodynamic seals.

Also, the unit was inadvertently overspeeded which verified the bending mode critical speed predicted at the conclusion of Section 9.2. At a shaft speed of approximately 48,000 rpm, vibration showed marked increase, as predicted; however, this is well above the 120-percent design overspeed of 43,200 rpm.

10.2.2.2 Bearing Lubrication

A total of 7.36 lb of MIL-L-7808 oil was supplied to the BRU-R bearings during the 50.4 hr of operation. The average oil-flow rate to each bearing was 0.00122 lb/min; the design flow rate was 0.0011 lb/min.

10.2.2.3 Bearing Temperatures

The BRU-R bearing outer-race temperatures remained unchanged throughout the test. Generally, the bearing and the resilient mount at the compressor end of the shaft ran approximately 20°F hotter than the turbine end bearing and resilient mount. This is the reverse of the 500-hr test where the turbine end bearing and mount ran 10°F hotter than the compressor end bearing and mount. However, the 500-hr test had an electrical heater mounted on the turbine end, whereas the heater was not used during the 50-hr. Also, since these two tests were performed in April and July, respectively, the temperature difference in the compressed air to drive the air turbine motor could account for some of the temperature differential. The compressor bearing temperatures ranged from 200° to 215°F and the resilient mount from 127° to 155°F. The turbine bearing temperatures ranged from 183° to 190°F and the resilient mount temperature from 106° to 130°F.

10.2.2.4 Hydrodynamic Face Seal Leakage

As in the 500-hr test, the oil leakage past the hydrodynamic face seal was determined by drawing a gas sample from the sealed turbine cavity. The gas sample was analyzed in an infrared spectrophotometer with a 10-m gas cell. There were no measurable quantities of hydrocarbons present in the gas sample. The sample bottle was rinsed with benzene, the solution evaporated, and the weight of the residue was less than 0.001 gm.

10.2.2.5 Lubrication and Cooling System Oil Contamination

A gas sample was drawn from the Lubrication and Cooling System after the 50-hr test. This sample was analyzed on the infrared spectrophotometer, and no measurable quantities of hydrocarbon were found. The sample bottle was rinsed with benzene, the solution evaporated, and the residue weight was less than 0.001 gm.

10.2.3 Disassembly Inspection

After completion of the 50-hr test, the BRU-R was disassembled to the dummy inertial wheels for visual examination of the turbine cavity and the compressor housing. There was no evidence of oil in either. There was a trace of oil on the diameter of the compressor seal carrier where the capacitance probes protrude. This trace was recognized as a glossy sheen and was evident by touch but was not enough to be measured. The oil could have been from the compressed air for the drive turbine or from a "wicking" effect along the capacitance probes. It is doubtful that the oil came past the compressor seal, as the seal bellows appeared dry.

10.3 5-Hr Test

The purpose of the 5-hr test was a demonstration of the BRU-R before shipment. This test was Part 2 of the acceptance test and was performed with the aerodynamic components. The test was witnessed by Mr. Lloyd W. Ream of NASA Lewis Research Center.

10.3.1 Description of Test Setup

Following inspection after the 50-hr test, the dummy inertial masses were removed and replaced with the compressor impeller and the turbine wheel, which were installed in the BRU-R. A spacer for the

compressor scroll was machined to obtain a clearance of 0.017 to 0.019 in. between the compressor impeller and the scroll. A spacer for the turbine wheel was machined to a clearance from 0.019 to 0.020 in. between the turbine wheel and the scroll. It should be noted that this spacer was intentionally made thicker than specified (0.008 to 0.010 in.) to prevent damage from occurring while operating on cold gas during the 5-hr test. A second spacer for the turbine wheel was machined to obtain a clearance of 0.008 to 0.010 in. and was installed before shipment. The scrolls were installed on the BRU-R and a compressed air line was ducted to the turbine scroll inlet. This test setup is shown in Figure 97.

10.3.2 Test Performance

The 5-hr test was successfully completed on July 17, 1969. The test consisted of operating the BRU-R for 5 hr at the design speed of 36,000 rpm and at 120 percent of design speed for 10 min. (See tables on Pages 10-12 through 10-14.)

10.3.2.1 BRU-R Vibration

The vibration level of the BRU-R during the 5-hr test remained between 0.015 and 0.022 mil double-amplitude displacement. During the 120-percent overspeed test, the vibration ranged from 0.05 to 0.076 mil.

10.3.2.2 Bearing Temperatures

The compressor bearing outer-race temperature during the 5-hr test ranged from 188° to 197°F. This is approximately 12°F cooler than experienced during the 50-hr test. The compressor bearing resilient-mount temperature ranged from 137° to 150°F, which is approximately

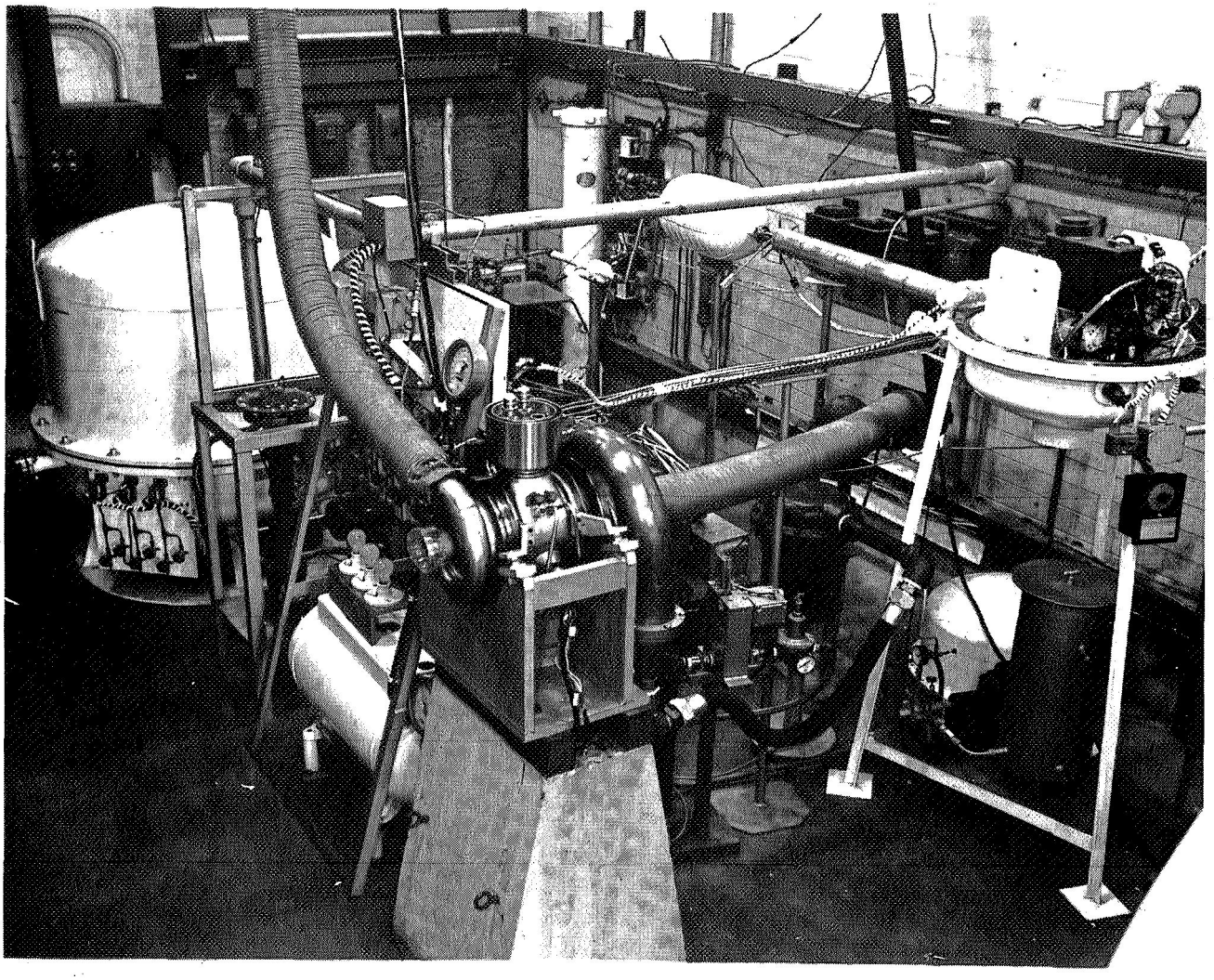

BRU-R AND COOLING LOOP
FOR 5-HR TEST

FIGURE 97

the same as the 50-hr test. Because of facility instrumentation difficulty, no temperature measurements of the turbine bearing outer race could be made. The turbine bearing resilient-mount temperature ranged from 104° to 117°F; the resilient-mount temperature stabilized 13°F cooler than that of the 50-hr test. During the 120-percent overspeed test, the compressor bearing outer race was 217°F.

11. CONCLUSIONS

A prototype Brayton Rotating Unit operating on gas-cooled oil-mist lubricated rolling-element bearings (BRU-R) has been designed, fabricated, and tested. A closed cycle Lubrication and Cooling System provides the BRU-R with gas cooling and oil-mist lubrication but also incorporates a unique hydrodynamic face-seal to preclude contaminating the Brayton cycle working fluid with bearing oil. The bearings and seals were evaluated in component development tests and in separate 500- and 50-hr endurance tests of the BRU-R. The seal leakage rates were well below the level specified by Contract. As a final acceptance test, the BRU-R was operated with the aerodynamic components for 5 hr at design speed and for 10 min at 120-percent overspeed.

The requirement that the total oil leakage into the cycle working fluid should not exceed 0.07 lb of oil for 500 hr of operation was easily achieved. In fact, seal leakage measurements revealed that a negligible quantity of oil (1.048×10^{-5} lb in 500 hr) was "leaking" into the cycle working fluid. Primarily responsible for this low leakage rate were the hydrodynamic face seal of the BRU-R and the seal differential pressure control of the BRU-R Lubrication and Cooling System.

The testing performed with the hydrodynamic face seal demonstrated that the seal does become hydrodynamic as the shaft speed increases, that there is no contact between the carbon nose and the seal rotor at the design speed, and that the seal is capable of making repeated start-stop cycles without imparing the sealing effectiveness. In addition, the seal has static sealing capability. No estimate can be made on the seal-life because no measureable wear was observed during the test runs of 1000 hr on the seal test rig and 500 hr on the BRU-R. Development test experience with the hydrodynamic face-seal revealed

that the gas bearing geometry should be on the inside diameter of the carbon nose if the oil-mist environment is on the outside diameter.

The seal differential pressure control of the BRU-R Lubrication and Cooling System made a significant contribution to achieving a low oil leakage past the seals. The seal differential pressure control consists of a differential pressure transmitter, a deviation indicating controller (an analog computer), an electropneumatic transducer, and two control valves. This control was able to automatically maintain the bearing cavity pressure lower than the pressure at the compressor impeller hub and thereby provide continual purging across the hydrodynamic face seal.

Development testing with various air/oil-mist ratios in the bearing and seal test rig revealed that bearing temperatures are primarily a function of cooling air mass-flow and virtually independent of the air/oil mixture ratio. Endurance testing on the BRU-R bearing and seal test rig demonstrated that angular contact ball bearings can be successfully operated with gas/oil mixture ratios of 400:1.

Preliminary rolling element design and subsequent testing revealed that for this application, 30-mm bore bearings with 9/32-in.-diam balls, 22-deg contact angles, 56-deg inner- and 54-deg outer-race curvatures were optimum.

APPENDIX A

LIST OF FIGURES

DRAWING

TABLE

APPENDIX A

RADIAL-FLOW TURBOCOMPRESSOR

The contract initially specified a radial-flow, oil-lubricated turbocompressor operating with argon as the cycle working fluid. Before the contract was redirected to the BRU-R configuration, the mechanical layout of the radial-flow turbocompressor had been performed and an analysis of the bearings had been completed.

I. SYSTEM REQUIREMENTS

The system requirements for the radial-flow turbocompressor are contained in Table A-1. The turbocompressor has a design speed of 38,500 rpm and employs argon as the cycle working fluid with a turbine inlet temperature of 1950°R. The turbocompressor was to operate as part of a Brayton cycle space power system while employing low-loss, oil-lubricated, rolling element bearings. The bearings and seals were to be selected to operate within the objectives of low-power loss and low-leakage rates for a minimum of 500 hr before replacement is required.

II. PRELIMINARY MECHANICAL DESIGNS

The initial layout (No. 1) of the turbocompressor is shown in Figure A-1. The rotating group is supported by two 25-mm angular contact ball bearings. The shaft is an integral part of the turbine wheel. A buffered labyrinth seal and a contacting face-seal separates each bearing from the adjacent aerodynamic component. A labyrinth seal is situated between each bearing to keep the bearing cooling-flows separated. The results of the dynamic analysis of this arrangement are

TABLE A-1

SYSTEM REQUIREMENTS
RADIAL-FLOW TURBOCOMPRESSOR

	Condition A	Condition B[3]
Cycle working fluid	Argon	Argon
Mass flow rate, lb/sec	0.27	0.611
Turbine inlet temperature, °R	1950	1950
Turbine pressure ratio		1.56
Turbine inlet pressure, psia	5.87	13.2
Compressor inlet temperature, °R	536	536
Compressor pressure ratio		2.30
Compressor inlet pressure, psia	2.66	6.0
Design operating life, hr	10,000	
Test operating life (TBO), hr (bearings and seals)	500[2]	
Speed capability, % design	0 to 120[1]	
Speed at design, rpm		38,500
Bearing lubricant and coolant	MIL-0-7808 or equivalent	
Argon coolant supply, °R	560	
pressure	compressor delivery	
flow, % max		1.0
Bearing lubricant objectives,		
flow lb/hr max	To be determined by contractor	
Exit temperature, °R max	836	
Internal leakage, lb/yr max	0.06	

Environmental Specifications - *NASA P0055-1 and NASA P0055-2

*Detailed evaluation to the limit of the Specification P0055-1 may be limited to Section 2.2.1 with the wave shape of Section 2.1.1.3. Required and reasonable mountings to keep the other requirements of the specifications within acceptable limits shall also be established by analysis.

NOTES:
1. Sustain 20% overspeed for 5 min at end of 500 hr of test operation (a design objective).
2. Refers only to minimum bearing and seal life before replacement is required (a design objective).
3. The turbine and compressor will be designed for optimum performance under Condition B system.

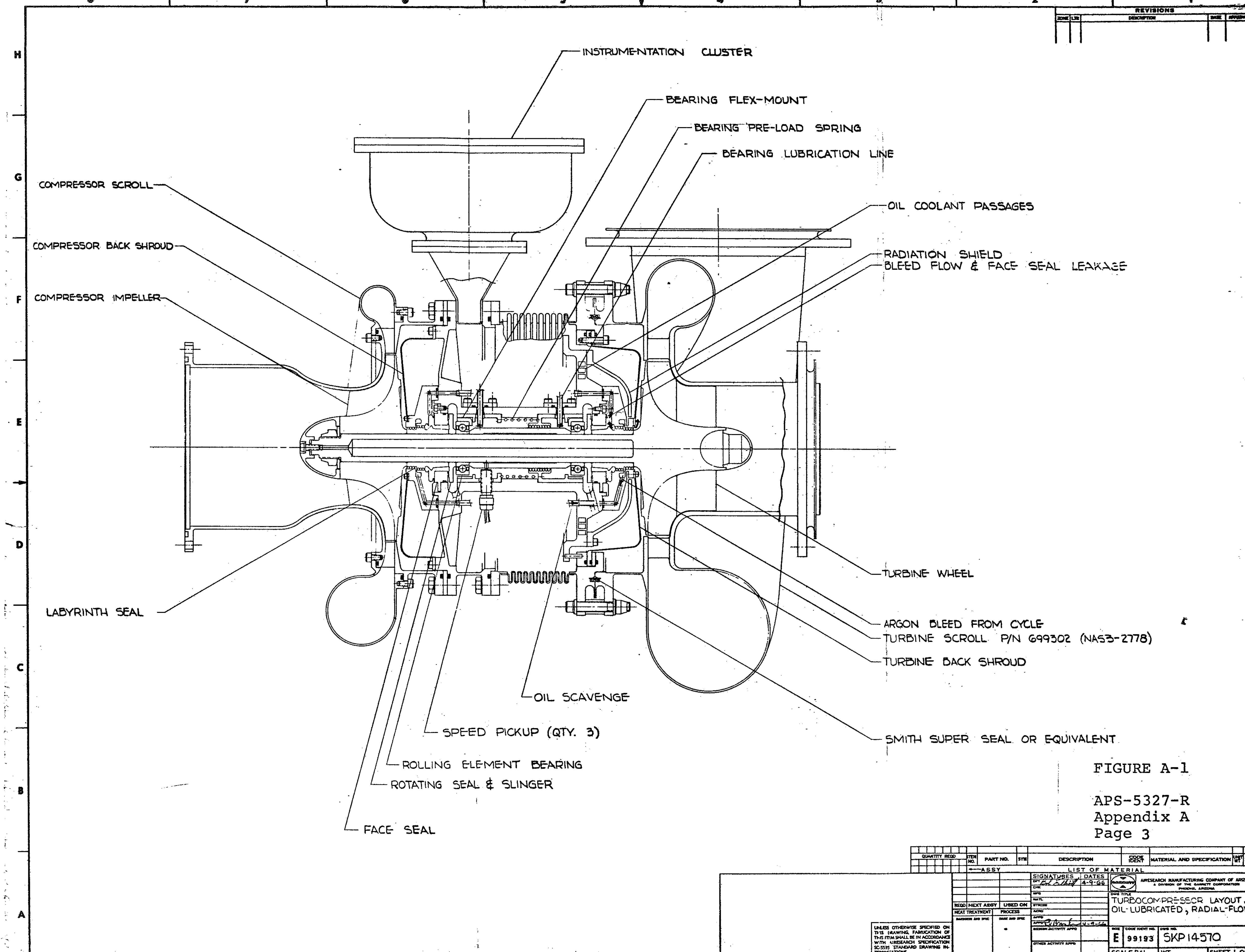

FIGURE A-1

APS-5327-R
Appendix A
Page 3

shown in Figure A-2. The fundamental bending mode critical is approximately 85,000 rpm. The rotating group geometry and resilient-mount spring-rate used for the dynamic analysis appear in Figure A-3.

Since the free-free bending mode critical of layout No. 1 was more than adequately high, consideration was given to reducing the bearing bore size to 20 mm. This reduced bearing bore size is beneficial in that it reduces labyrinth seal and nose-piece diameters in the face contact seals. Figure A-4 is the layout for the 20-mm bearing arrangement. The turbine wheel is integral with the shaft as in the first 25-mm bore size bearing layout. The results of the dynamic analysis of layout No. 2 are presented in Figure A-5. The fundamental bending mode critical is approximately 77,200 rpm. The rotating group geometry and resilient-mount spring-rate used for the dynamic analysis are shown in Figure A-6.

Inspection of the two layouts reveals a rather detrimental assembly problem. The integral shaft turbine-wheel assembly would require that all seals and bearings be installed from the compressor end of the shaft. While such an assembly procedure is possible, it would be cumbersome. If, for instance, the turbine face contact seal needed to be replaced, the entire rotating assembly would have to be disassembled, with attendant loss of all bearings and the compressor face contact seal. In addition, the good heat-transfer path down the integral shaft would aggravate an already serious problem of cooling the turbine bearing inner race.

To eliminate these assembly problems, arrangements using curvic couplings were evaluated. Figure A-7 shows one of the arrangements that were studied. This design uses 25-mm ball bearings. A tie-bolt, running through the shaft and secured by a self-locking nut at the compressor end, holds the rotating group together. A similar design using 20-mm ball bearings was discarded because of the size limitations imposed on the tie-bolt. In order to keep adequate inertial properties

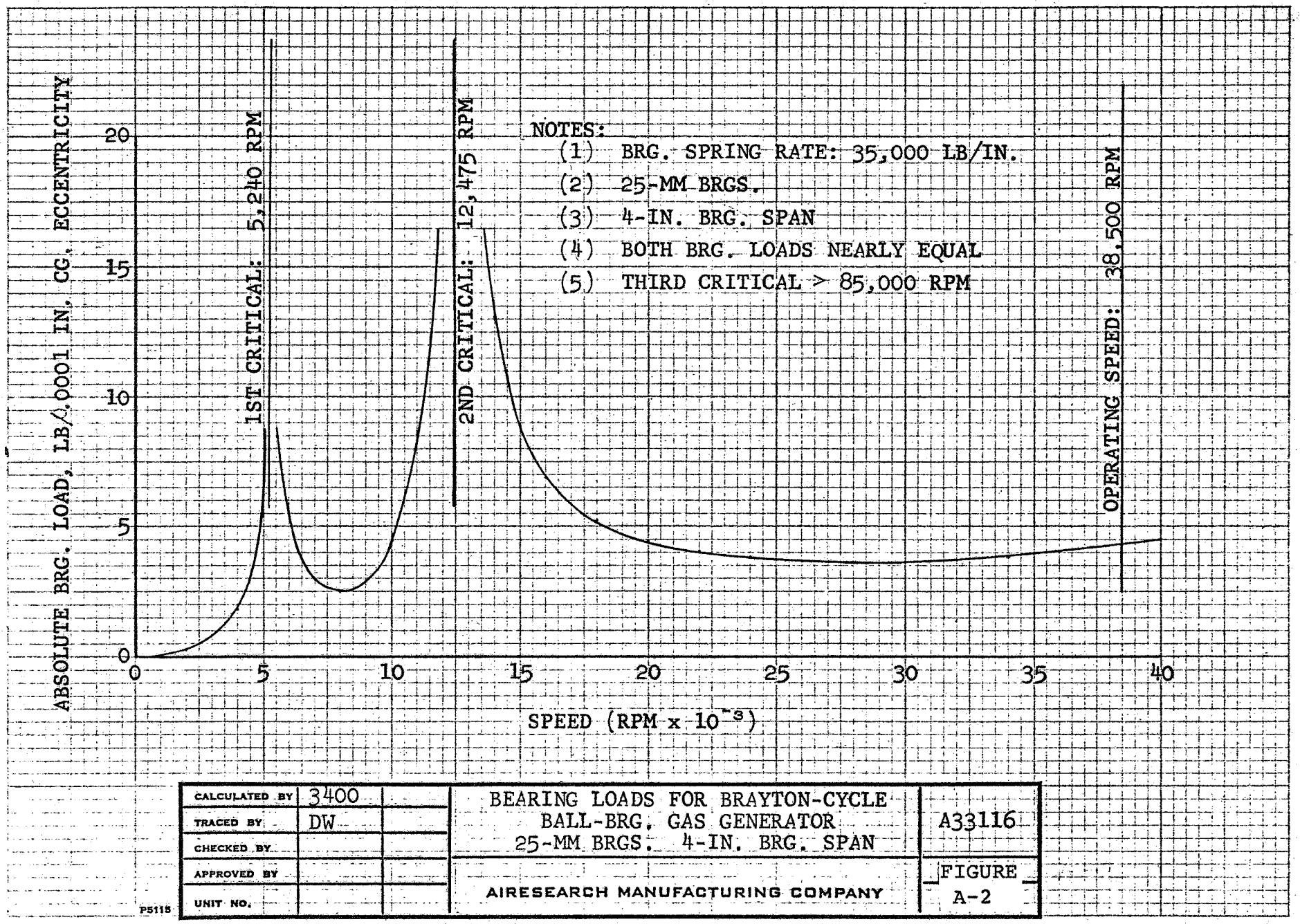

CALCULATED BY	3400	BEARING LOADS FOR BRAYTON-CYCLE BALL-BRG. GAS GENERATOR 25-MM BRGS. 4-IN. BRG. SPAN	A33116
TRACED BY	DW		
CHECKED BY			
APPROVED BY		AIRESEARCH MANUFACTURING COMPANY	FIGURE A-2
UNIT NO.			

P5115

NOTES:

1. SHADED AREA INDICATES MATERIAL USED IN SHAFT STIFFNESS CALCULATION
2. FLEX-MOUNTED 20 mm BALL BEARINGS
3. 4.0 IN. BEARING SPAN
4. MAXIMUM SPEED: 46,000 RPM

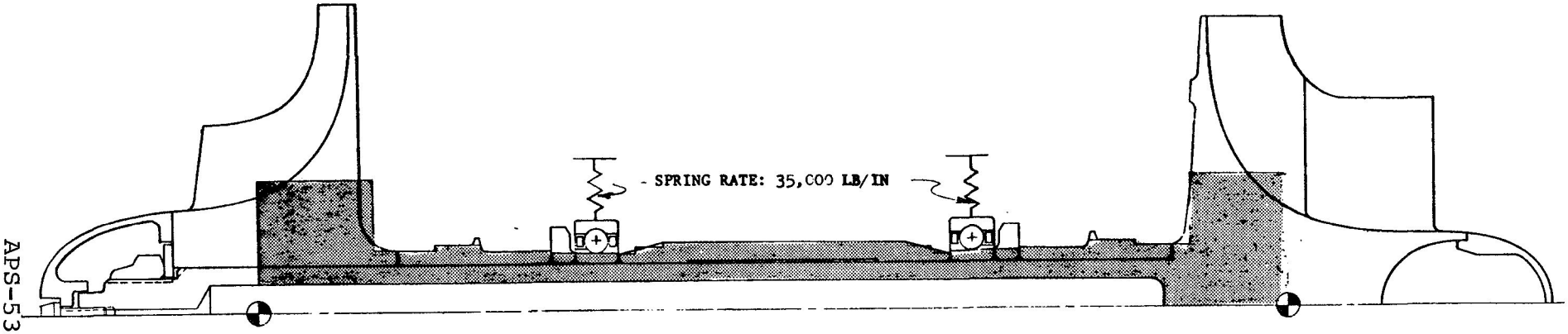

$M = 0.0119$ LB $SEC^2/IN.$

$I_P = 0.0172$ LB IN. SEC^2

$I_D = 0.010$ LB IN. SEC^2

$M = 0.015$ LB SEC^2/IN

$I_P = 0.033$ LB IN. SEC^2

$I_D = 0.021$ LB IN. SEC^2

BRAYTON-CYCLE ROLLING ELEMENT
BEARING TURBOCOMPRESSOR

FIGURE A-3

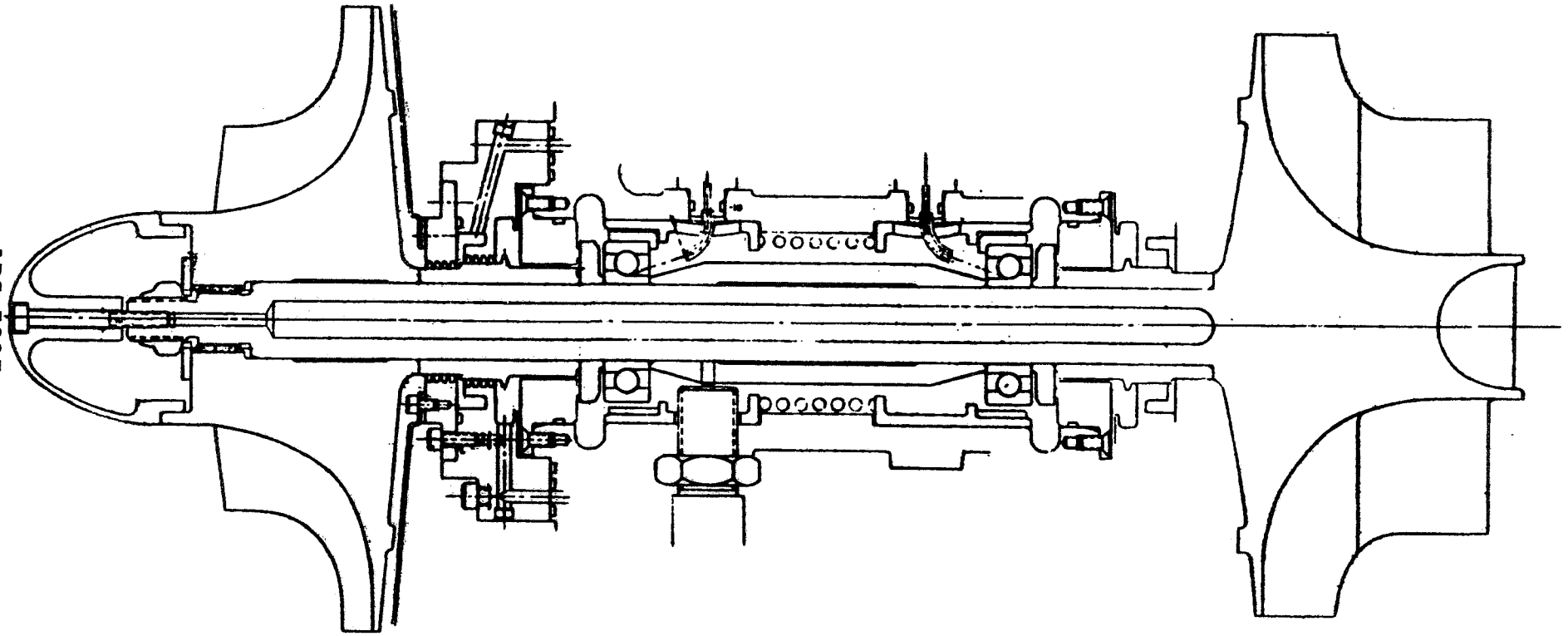

LAYOUT NO. 2
RADIAL TURBOCOMPRESSOR
20 mm BEARINGS
SHAFT INTEGRAL WITH TURBINE WHEEL

FIGURE A-4

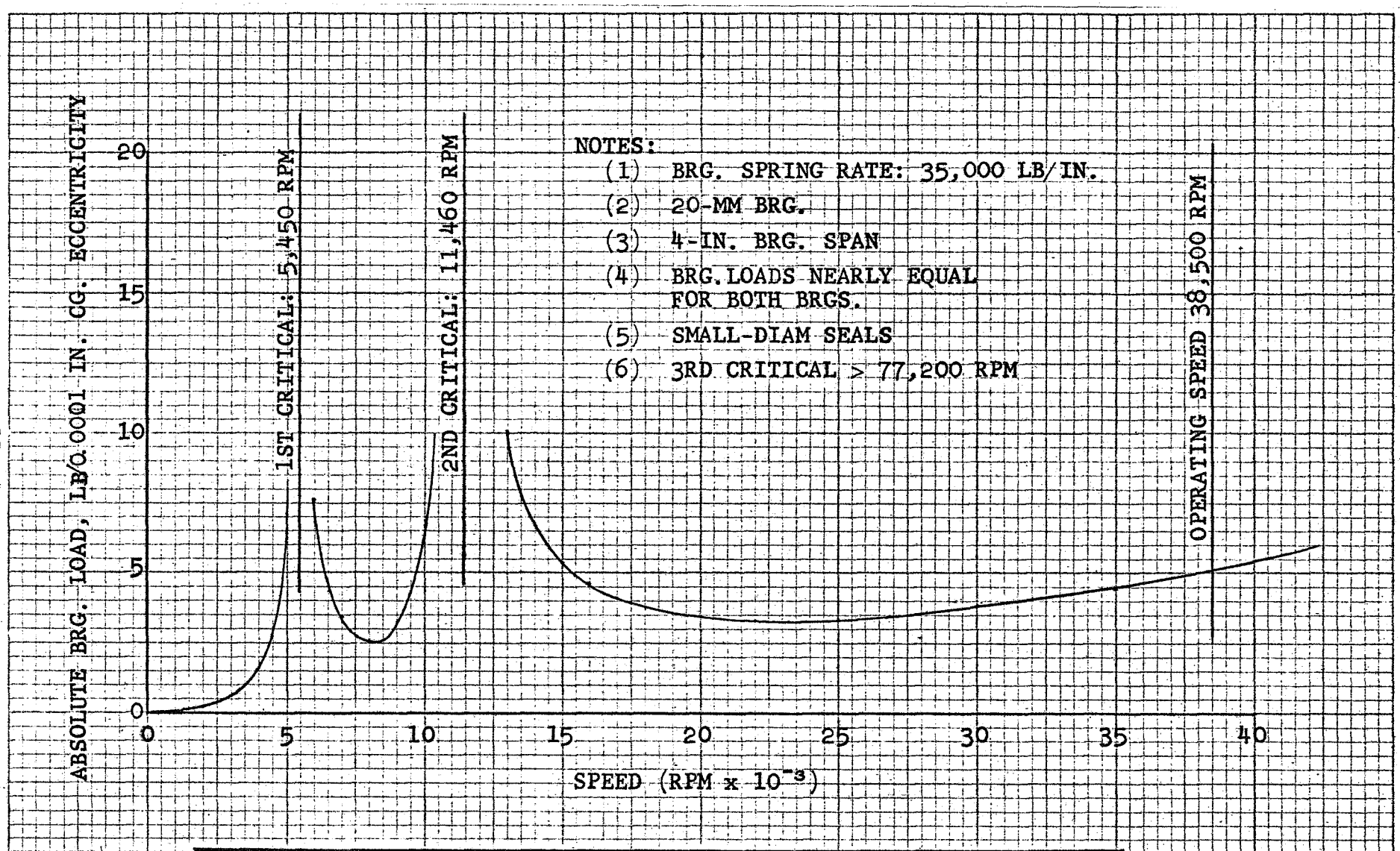

CALCULATED BY	3400	BEARING LOADS FOR BRAYTON-CYCLE BALL-BRG. GAS GENERATOR 20-MM BRGS. 4-IN. BRG. SPAN
TRACED BY	DW	A33112
CHECKED BY		
APPROVED BY		FIGURE A-5
UNIT NO.		AIRESEARCH MANUFACTURING COMPANY

P5115

NOTES:

1. SHADED AREA INDICATES MATERIAL USED IN SHAFT STIFFNESS CALCULATION
2. FLEX-MOUNTED 20 mm BALL BEARINGS
3. 4.0 IN. BEARING SPAN
4. MAXIMUM SPEED: 46,000 RPM

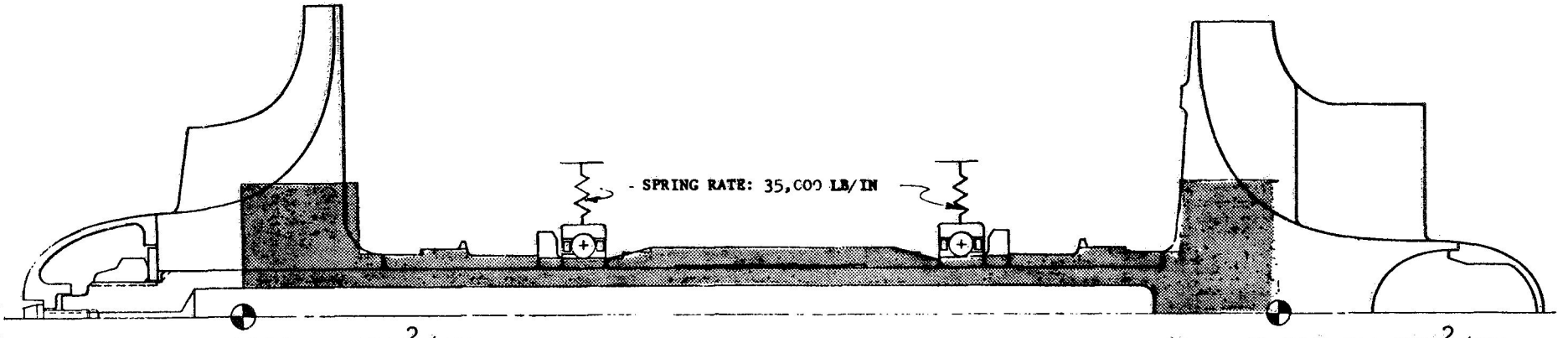

$M = 0.0119$ LB $SEC^2/IN.$
$I_P = 0.0172$ LB IN. SEC^2
$I_D = 0.010$ LB IN. SEC^2

$M = 0.015$ LB $SEC^2/IN.$
$I_P = 0.033$ LB IN. SEC^2
$I_D = 0.021$ LB IN. SEC^2

BRAYTON-CYCLE BALL-BEARING
GAS GENERATOR

FIGURE A-6

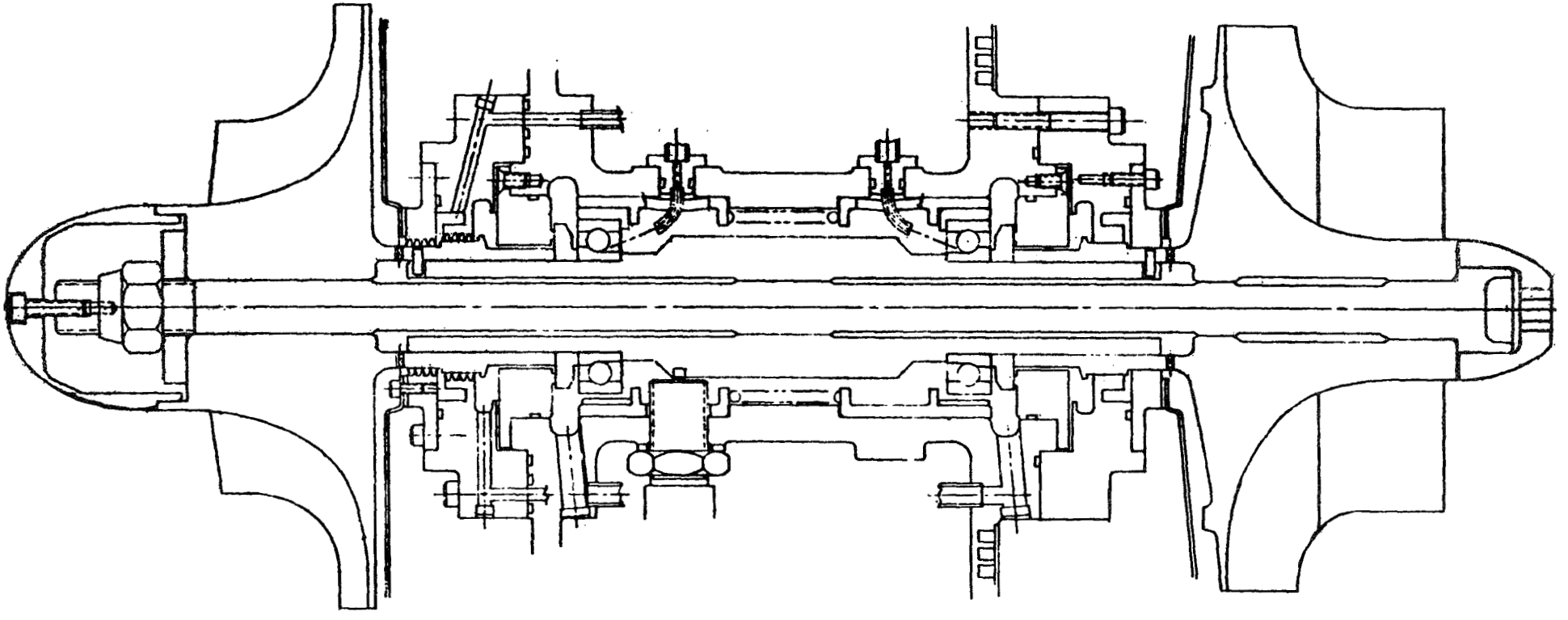

LAYOUT NO. 4
25 mm BALL BEARING
CURVIC COUPLINGS USED AT
BOTH TURBINE AND COMPRESSOR

FIGURE A-7

in such a shaft design (from a critical-speed consideration), the tie-bolt should not exceed the shaft central hole dimensions. The tie-bolt of the 20-mm bearing design did not appear adequate to lock-up the curvic couplings and take the added stresses, due to the anticipated differential growth between the rotating group elements and the tie-bolt itself. A critical speed analysis was performed and the fundamental bending mode speed was in excess of 60,000 rpm. The curvic coupling design approach was abandoned because it was believed that the integral shaft and turbine wheel was a simpler and equally effective approach for the turbocompressor.

III. FINAL TURBOCOMPRESSOR DESIGN

The final turbocompressor design before the contract redirection is shown in Figure A-8. This design uses an integral turbine wheel and shaft construction. The cast Inconel 713 turbine wheel is to be electron-beam-welded to an SAE 4340 Steel shaft. The compressor impeller has an interference fit with the shaft and utilizes an internal spline for positive drive. The bearing bore size is 25 mm.

The critical speed analysis was performed using the mass and stiffness model (Figure A-9). Figure A-10 shows the critical speeds as a function of bearing resilient-mount spring-rate. It can be seen from Figure A-10 that there is no need for bearing resilient mounts, as the first and second system critical speeds are well below the design operating speed of 38,500 rpm. The bearing loads for rigidly mounted bearings are shown in Figures A-11 and A-12. The bearing spring rate for the rigid mounting configuration was chosen as 250,000 lb/in. The bearing loads were computed with a 0.0002-in. eccentricity assumed for each mass. Figure A-11 represents the bearing loads for a mass eccentricity distribution that produces maximum excitation of the second (cylindrical mode) critical speed. Figure A-12 shows the results for an eccentricity distribution that yields maximum excitation of the third (beam) critical. The maximum bearing load for the operating speed of 38,500 rpm is 29 lb.

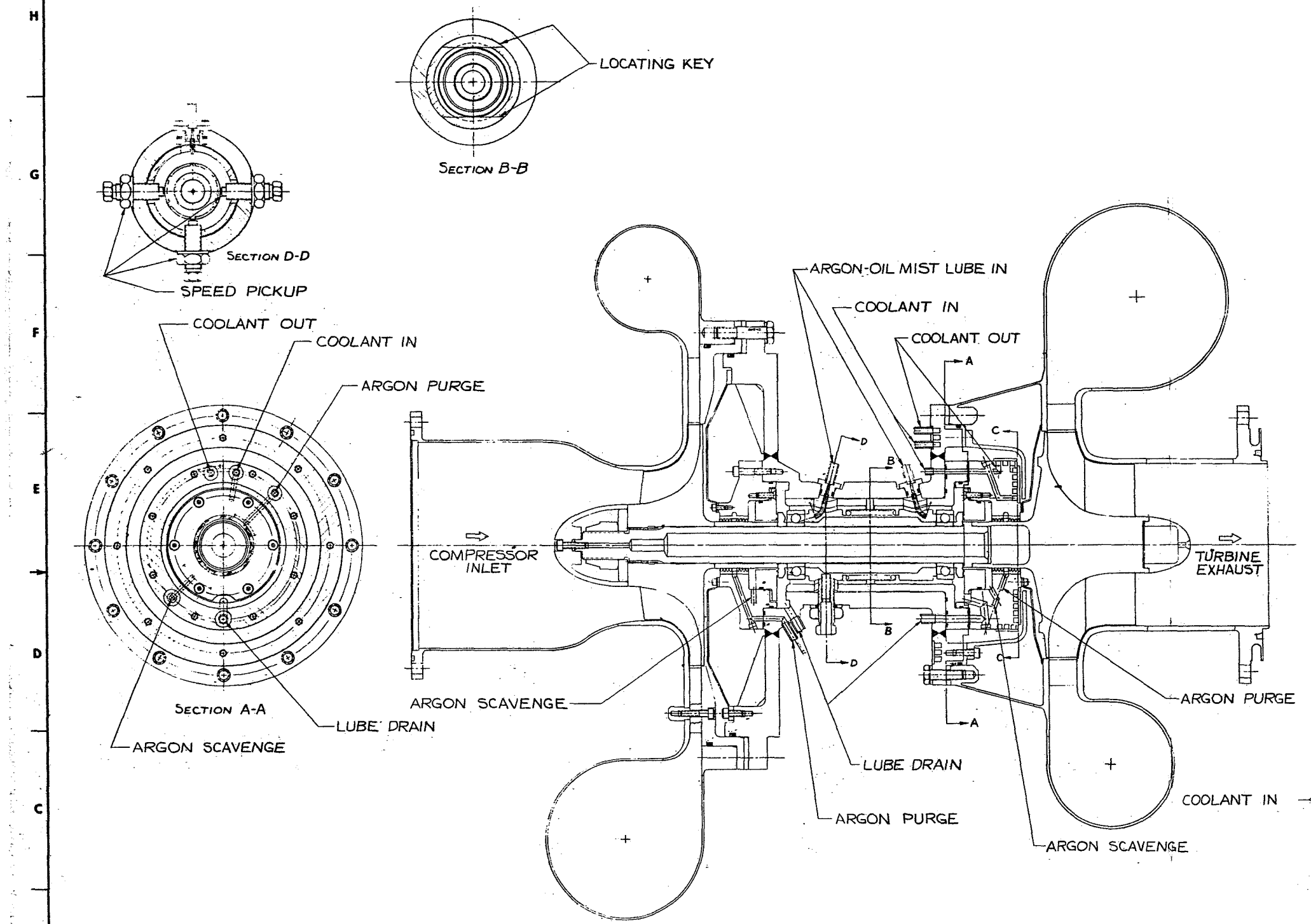

FIGURE A-8

APS-5327-R
Appendix A
Page 12

AIRESEARCH MANUFACTURING COMPANY
A DIVISION OF THE GARRETT CORPORATION
PHOENIX, ARIZONA

TURBOCOMPRESSOR LAYOUT, BALL BEARING

SIZE E | CODE IDENT NO. 99193 | DWG NO. L308053 | SCALE 1/2 | WT | SHEET OF

L308053

MASS MOMENTS OF INERTIA - IN. LB SEC^2

	TURBINE	COMPRESSOR
POLAR (I_p)	0.033	0.017
DIAMETRAL (I_D)	0.021	0.011

MODULUS OF ELASTICITY - PSI

- $2.5(10)^7$
- $2.7(10)^7$
- $2.9(10)^7$
- $1.6(10)^7$

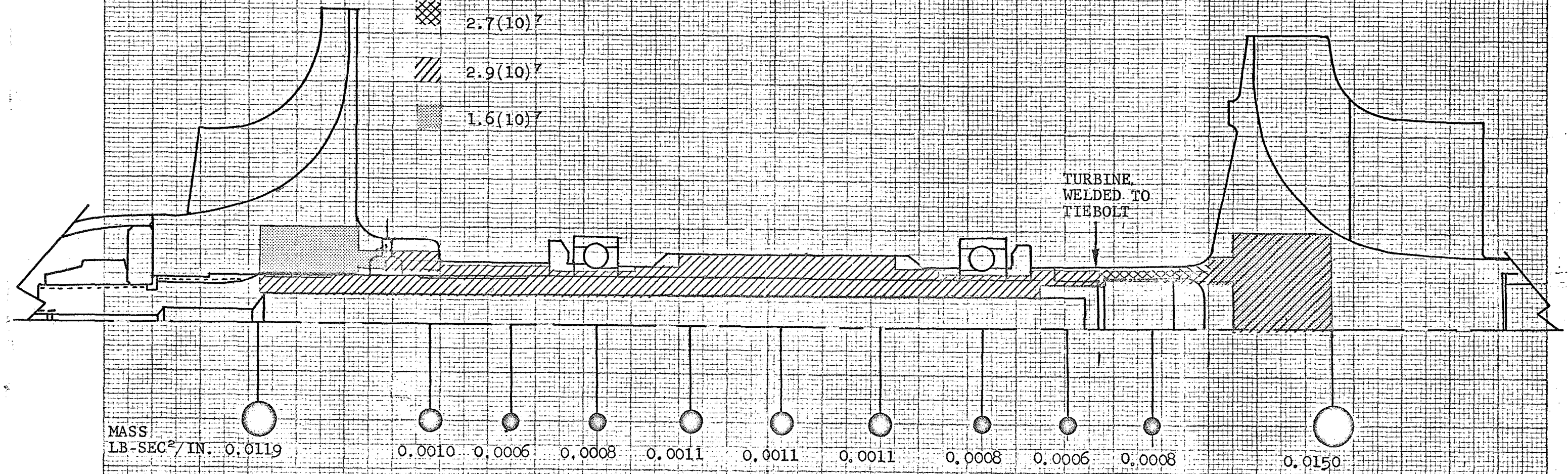

FIGURE 2

CALCULATED BY			PRIMARY DESIGN FOR BRAYTON TURBOCOMPRESSOR ON BALL BEARINGS	A33244
TRACED BY	WD	10-66		
CHECKED BY	FS	10-66		
APPROVED BY			AiResearch Manufacturing Company of Arizona	FIGURE A-9
UNIT NO.				

PS113

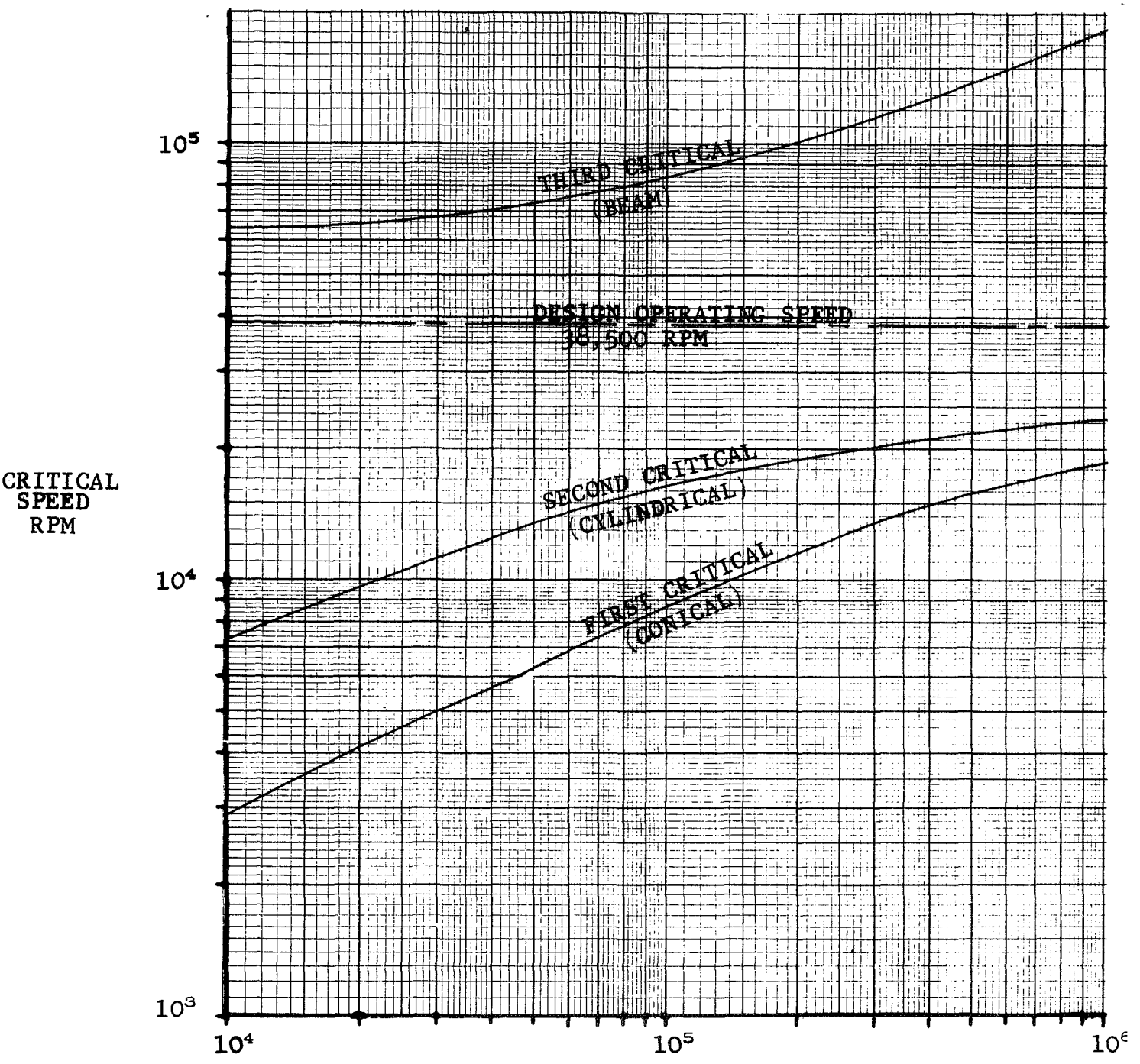

PREPARED	WD	10-66	CRITICAL SPEED VS BEARING SPRING RATE BRAYTON TURBOCOMPRESSOR ON 25MM BALL BEARINGS	A33245
	FS	10-66		
WRITTEN				FIGURE A-10
APPROVED			AiResearch Manufacturing Company of Arizona	

FORM P793A-1

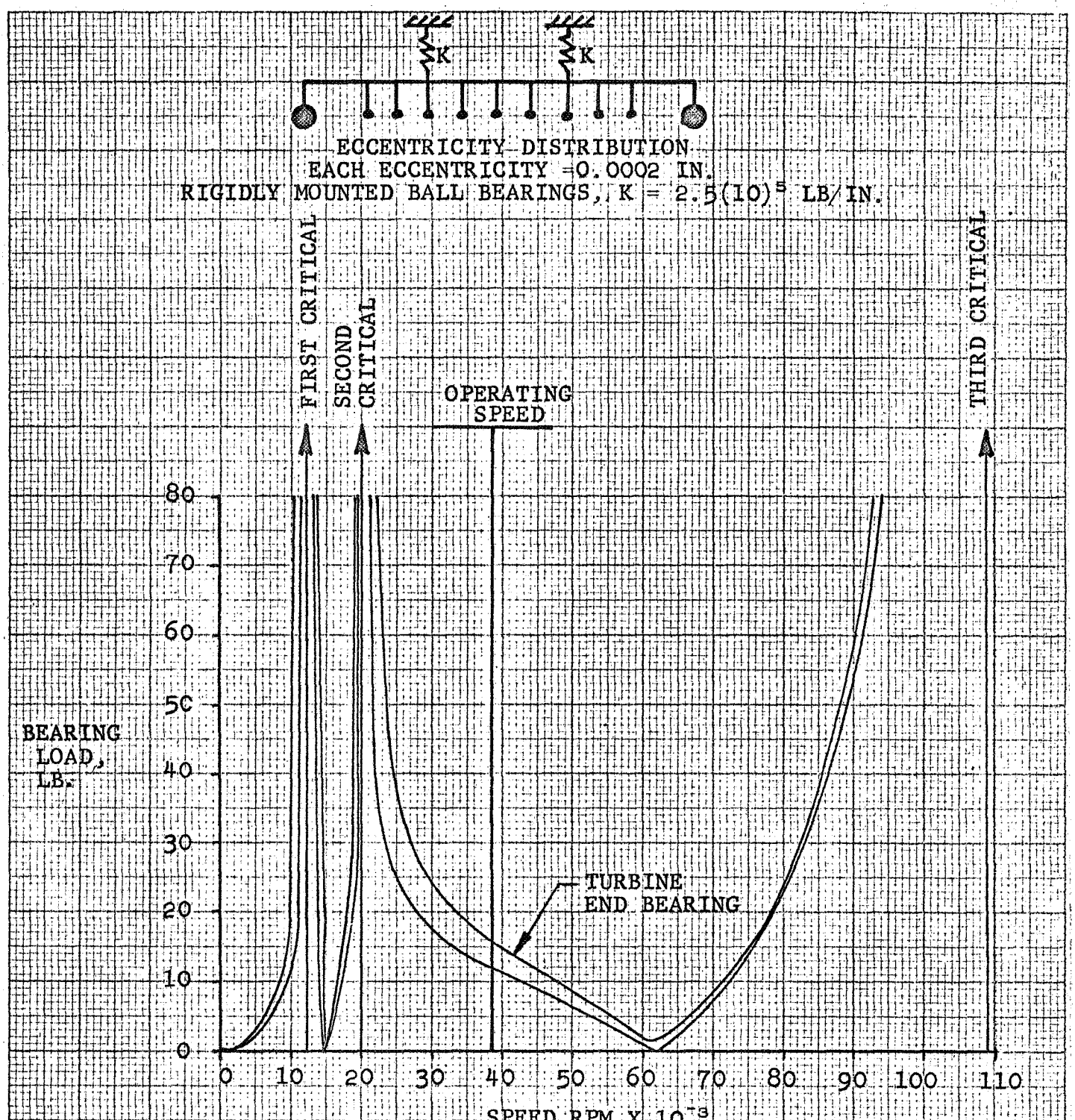

CALCULATED BY	CDC	3400
TRACED BY	WD	10-66
CHECKED BY	FS	10-66
APPROVED BY		
UNIT NO.		

BEARING LOADS FOR BRAYTON TURBOCOMPRESSOR ON 25MM BALL BEARINGS

A33246

FIGURE A-11

AiResearch Manufacturing Company of Arizona

PB110

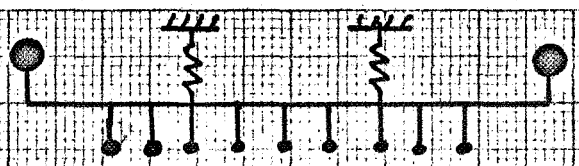

ECCENTRICITY DISTRIBUTION
EACH ECCENTRICITY = 0.0002 IN.
RIGIDLY MOUNTED BALL BEARINGS, K = $2.5(10)^5$ LB/IN.

FIRST CRITICAL
SECOND CRITICAL
OPERATING SPEED
THIRD CRITICAL

BEARING LOAD LB

0 10 20 30 40 50 60 70 80

COMPRESSOR END BEARING

0 10 20 30 40 50 60 70 80 90 100 110

SPEED RPM X 10^{-3}

CALCULATED BY	CDC	3400	BEARING LOADS FOR BRAYTON TURBOCOMPRESSOR ON 25MM ID BALL BEARINGS
TRACED BY	WD	10-66	A33247
CHECKED BY	FS	10-66	FIGURE
APPROVED BY			A-12
UNIT NO.			AiResearch Manufacturing Company of Arizona

PB110

IV. TURBOCOMPRESSOR BEARING DESIGN

The rolling element bearing design was performed on the turbocompressor using the analysis developed by Mr. A.B. Jones whose theory has been published by McGraw-Hill Book Company in Section 3 of the "Mechanical Design and Systems Handbook". The design approach was to consider the effect of varying race curvature, contact angle, and preload on bearing friction and life, and from the results to select the best combination. This approach is the same as was previously described in Section 5.

The bearing design selected as a result of the bearing optimization program is shown on Drawing 358492. The major characteristics of the bearing are:

Bore diameter	25 mm
Outside diameter	47 mm
Width	12 mm
Number of balls	13
Ball diameter	1/4 in.
Inner-race curvature	56% of ball diameter
Outer-race curvature	54% of ball diameter
Contact angle	20 deg
Ring and ball material	Consumable-electrode vacuum-melted M-50 tool steel
Separator material	Iron-silicon-bronze, silver-plated

The calculated bearing power losses with use of oil-mist lubrication are: 134 w at the turbine end and 133 w at the compressor end. The B_{10}-life of the turbine-end bearing is 43,200 hr, and the B_{10}-life of the compressor-end bearing is 35,700 hr. This results in a bearing system B_{10}-life of 18,800 hr, giving a 3,700-hr system TBO.

REVISIONS			
LTR	DESCRIPTION	DATE	APPROVED
A	SEE ENGINEERING ORDER	11/8/66	[signature]

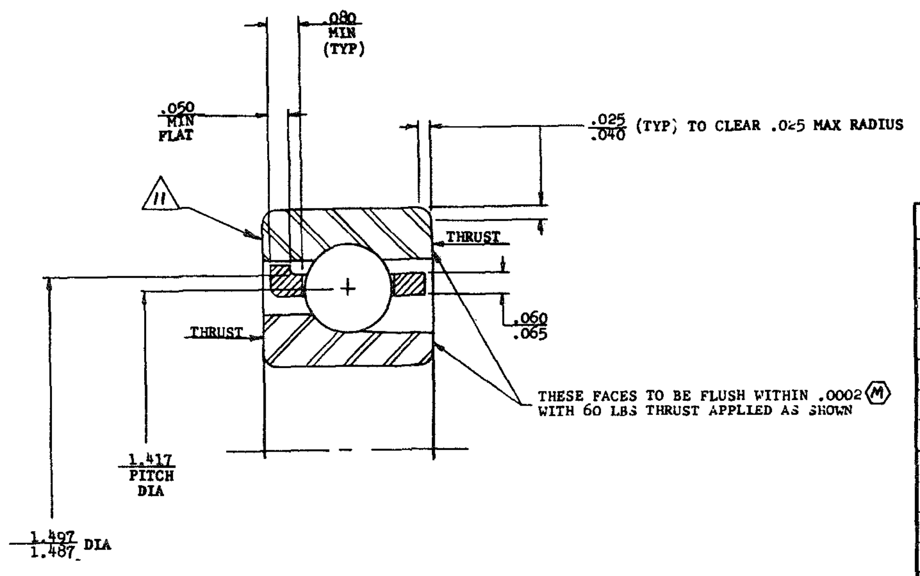

BEARING DESCRIPTION BALL, ANGULAR CONTACT, (7105 SIZE)		GRADE AIRESEARCH 5
INNER RING	OUTER RING	ASSEMBLED BEARING CHARACTERISTICS
MATERIAL: CEVM M-50 TOOL STEEL Rc 60-64	MATERIAL: CEVM M-50 TOOL STEEL Rc 60-64	TOTAL DIAMETRAL (DIAMETRAL, AXIAL) CLEARANCE OF
BORE: .9843-.9841 (25 MM) TAPER/FT: (M)	OD: 1.8504-1.8502 (47 MM) (M)	(M) .0028-.0034 UNDER 5 LBS GAGE LOAD
WIDTH: .4724-.4674 (12 MM) (M)	FLANGE OD:	SPECIAL FEATURES
RACE DEPTH: 20 MIN % BALL DIA	WIDTH: .4724-.4674 (12 MM) (M)	1. SEPARATOR TO BE SILVER PLATED PER AMS 2412 .001-.002 THICK.
RACE CURVATURE: (M) 55.6-56.4 % BALL DIA	FLANGE WIDTH: -	
SEPARATOR PILOT LAND TO GROOVE RUNOUT: - TIR	RACE DEPTH: 16 MIN % BALL DIA	2. RINGS AND BALLS NOT TO CHANGE DIMENSIONALLY IN EXCESS OF .000050 INCH-PER-INCH WHEN EXPOSED TO 750°F FOR 8 HOURS.
SEPARATOR	RACE CURVATURE: (M) 53.6-54.4 % BALL DIA	
MATERIALS: IRON-SILICON-BRONZE PER AMS 4616	SEPARATOR PILOT LAND TO GROOVE RUNOUT: .0005 TIR	3. BEARING SHALL BE NON-SEPARABLE DURING NORMAL HANDLING.
CONSTRUCTION: ONE-PIECE MACHINED	ROLLING ELEMENTS	4. SEPARATOR DIAMETRAL BALL-POCKET CLEARANCE TO BE .020-.026. (M)
ASSEMBLY:	MATERIAL: CEVM M-50 TOOL STEEL Rc 60-64	
PILOTING SURFACE: OUTER RING LAND	COMPLEMENT PER ROW: 13 x 1/4" DIA.	
PILOT CLEARANCE: .010-.016 (M)	CLOSURES	
OPERATIONAL LUBRICANT	NUMBER: NONE	
NAME: OIL, SYNTHETIC, GAS TURBINE LUBRICATING	TYPE: (SHIELDS, SEALS)	
MILITARY SPEC NO.: MIL-L-7808	MATERIAL:	
BEARING PRELUBRICATION: DIP AND DRAIN	CONSTRUCTION:	

PACKAGING PER AIR. SPEC CP-14	PRODUCTION BULK PACK	COMMERCIAL SPARES PACK	MILITARY SPARES PACK
PRESERVATIVE:	MIL-L-6085	MIL-L-6085	MIL-P-197
AIRESEARCH PART NUMBER:	358492-1	358492-1	358492-4
PROCUREMENT PER ASL 358492-1			

11. MARK PART NO. AND SERIAL NO. ON NOTED SURFACE PER AIRESEARCH SPEC MC-5014 CLASS III EXCEPT CHARACTERS ARE TO BE AS LARGE AS POSSIBLE.

10. (C) DESIGNATES CRITICAL CHARACTERISTIC
(M) DESIGNATES MAJOR CHARACTERISTIC

9. LOT CONTROL IS REQUIRED FOR THIS PART.
8. PARTS SHALL CONFORM TO AIRESEARCH SPEC SC-5354
7. PARTS PROCURED BY VENDOR PART NUMBER SHALL BE PROCURED IN ACCORDANCE WITH THIS AIRESEARCH SOURCE CONTROL DRAWING.
6. IDENTIFY PACKAGING WITH AIRESEARCH PART NUMBER.
5. ALL DESIGN AND PART NUMBER CHANGES SHALL RECEIVE PRIOR AIRESEARCH APPROVAL.
4. ONLY THE ITEMS LISTED ON THE ASL AND IDENTIFIED BY VENDOR'S NAMES, ADDRESSES AND PART NUMBERS HAVE BEEN TESTED AND APPROVED FOR USE IN THE END UNIT. A SUBSTITUTE ITEM SHALL NOT BE USED WITHOUT PRIOR TESTING AND APPROVAL BY AIRESEARCH.
3. MILITARY SPARES PACK BEARINGS ARE INTENDED TO FILL MILITARY SPARES ORDERS. BEFORE INSTALLATION, WASH OUT THE PRESERVATIVE AND REPLACE WITH OPERATING LUBRICANT. AFTER THIS OPERATION THE -4 IDENTIFICATION IS CHANGED TO -1 AND THE BEARINGS BECOME INTERCHANGEABLE WITH THE PRODUCTION BULK AND COMMERCIAL SPARES PACK BEARINGS. THEY SHOULD NOT BE USED IN FACTORY INSTALLATIONS BECAUSE OF THEIR RELATIVELY HIGH COST.
2. FOR ECONOMY, PRODUCTION BULK PACK BEARINGS ARE PREFERRED FOR ALL FACTORY INSTALLATIONS. COMMERCIAL SPARES PACK BEARINGS ARE INTENDED TO FILL COMMERCIAL SPARES ORDERS.
1. PRODUCTION BULK AND COMMERCIAL SPARES PACK BEARINGS ARE INTERCHANGEABLE.

UNLESS OTHERWISE SPECIFIED:

CRITICAL ITEM
SATISFACTORY PERFORMANCE OF THE END PRODUCT DEPENDS ON THE INTEGRITY AND RELIABILITY OF THIS SELECTED CRITICAL ITEM. THE GARRETT CORPORATION RECOMMENDS PROCUREMENT FROM THE ORIGINAL SUPPLIER AS SET FORTH IN ASPR 1-313.

SOURCE CONTROL DRAWING		
	SIGNATURES	DATES
DFT	[signature]	10/26/66
CHK	[signature]	11/-6/66
APPD	[signature]	10/27/66
APPD	[signature]	10/31/66
APPD		
DESIGN ACTIVITY APPD	[signature]	10/31/66
OTHER ACTIVITY APPD		

AIRESEARCH MANUFACTURING COMPANY
A DIVISION OF THE GARRETT CORPORATION
PHOENIX, ARIZONA

DWG TITLE
BEARING, BALL, ANNULAR

SIZE	CODE IDENT NO.	DWG NO.	
C	99193	358492	
SCALE NONE		WT	SHEET OF

DWG NO. 358492

P-8399A—BIMS K&E 1000-H

APPENDIX B

LIST OF FIGURES

DRAWINGS

APPENDIX B

LUBRICATION AND COOLING SYSTEM DESIGNS

The lubrication and cooling system described in Section 4 evolved from a buffered-sealing system to a closed-cycle system. This Appendix presents these designs and the historical development of the BRU-R Lubrication and Cooling System.

I. BUFFERED SEALING SYSTEM

When the program was redirected from a radial-flow turbocompressor to the BRU-R design, a buffered-sealing system was initially devised to provide oil-mist lubrication to the bearings. A schematic of this system is shown in Drawing SKP18091. In the buffered-sealing system, contacting seals are placed on both sides of each bearing to isolate the bearing from the alternator cavity and the adjacent aerodynamic component. The alternator cavity is purged with argon to prevent oil from entering the hot alternator. The bearing lubrication is provided by an oil-argon-mist system. The lubrication is dumped overboard after cooling the bearings. A buffered-labyrinth seal is situated between each aerodynamic component and the contacting face seal inclosing the bearing cavity. These labyrinth seals are buffered by a He-Xe gas mixture so that P-1 and P-2 are essentially equal (the same for P-4 and P-5), and P-3 and P-6 (purge gas exits) are maintained at a small pressure differential to P-1, P-2, P-4, and P-5.

Successful operation of this system is associated with the performance stability of the purge gas differential control valves designated on Drawing SKP18091 as valves V-1 and V-2. These special valves were to be designed and fabricated by the Contractor.

REVISIONS				
ZONE	LTR	DESCRIPTION	DATE	APPROVED
	A	REVISED	5/23/67	[illegible]

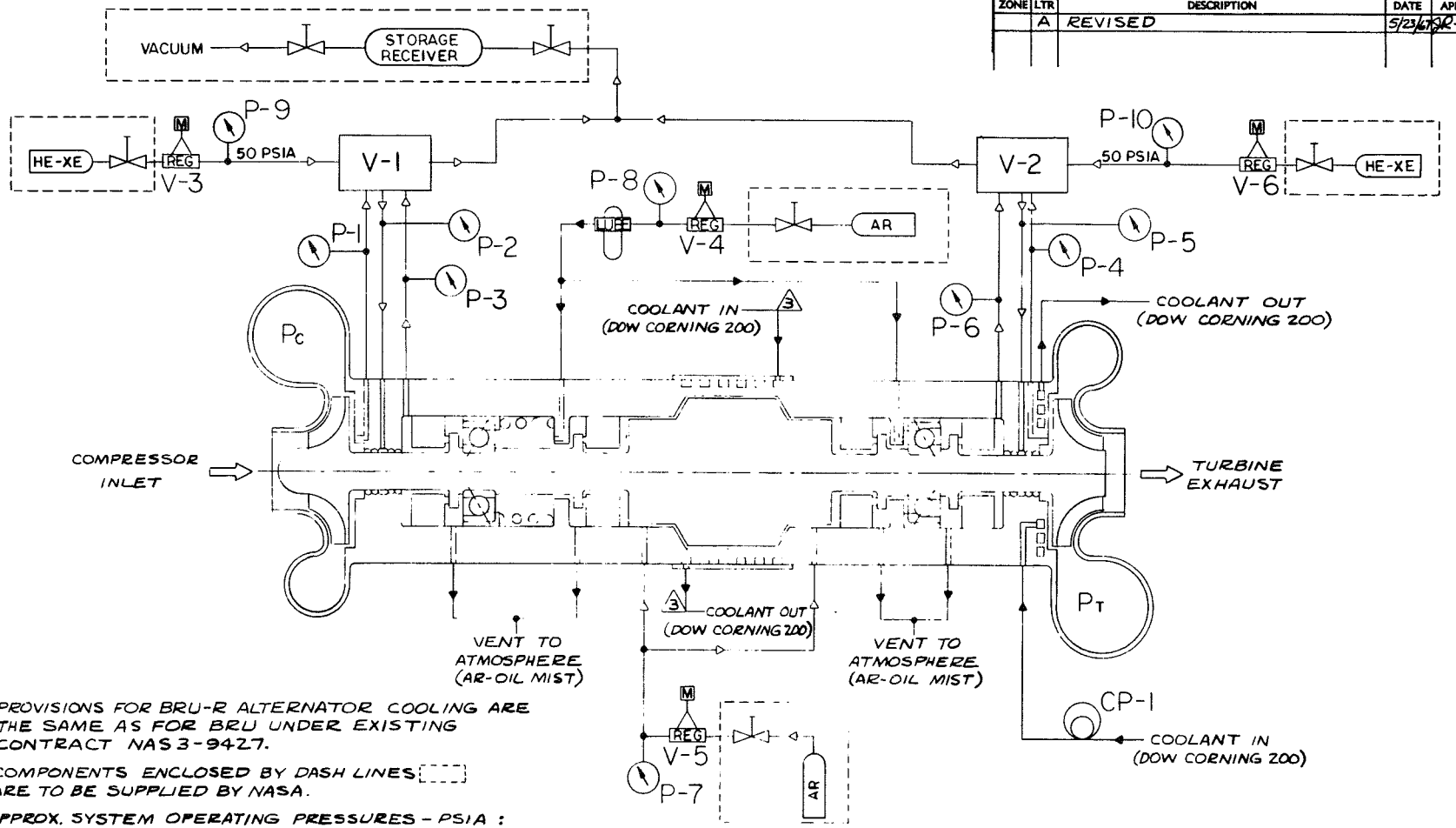

3 PROVISIONS FOR BRU-R ALTERNATOR COOLING ARE THE SAME AS FOR BRU UNDER EXISTING CONTRACT NAS3-9427.

2. COMPONENTS ENCLOSED BY DASH LINES [ ] ARE TO BE SUPPLIED BY NASA.

1. APPROX. SYSTEM OPERATING PRESSURES - PSIA :

KW	Pc	P-1	P-2	P-3	PT	P-4	P-5	P-6	P-7	P-8
2.25	14.3	8.6	8.6	8.3	13.7	8.2	8.2	7.9	15.0	30.0
6.0	27.0	16.2	16.2	15.9	25.8	15.5	15.5	15.2	25.1	30.0
10.5	45.0	27.0	27.0	26.7	43.2	25.9	25.9	25.6	42.6	30.0

QUANTITY REQD	ITEM NO.	PART NO.	SYM	DESCRIPTION	CODE IDENT	MATERIAL AND SPECIFICATION	ZONE
← ASSY				LIST OF MATERIAL			

	REQD	NEXT ASSY	USED ON
HEAT TREATMENT		PROCESS	
HARDNESS AND SPEC		NAME AND SPEC	—

SIGNATURES	DATES
DFT [illegible]	4-14-67
CHK	
MFG	
MATL	
STRESS	
AERO	
APPD [illegible]	4-28-67
APPD	
DESIGN ACTIVITY APPD [illegible]	10/5/67
OTHER ACTIVITY APPD	

UNLESS OTHERWISE SPECIFIED ON THIS DRAWING, FABRICATION OF THIS ITEM SHALL BE IN ACCORDANCE WITH AIRESEARCH SPECIFICATION SC-5535, STANDARD DRAWING INTERPRETATIONS.

AIRESEARCH MANUFACTURING COMPANY OF ARIZONA
A DIVISION OF THE GARRETT CORPORATION
PHOENIX, ARIZONA

DWG TITLE
SCHEMATIC
PROPOSED BRU-R OIL-MIST LUBRICATION AND BUFFERED SEALING SYSTEMS

SIZE	CODE IDENT NO.	DWG NO.
C	99193	SKP18091

SCALE NONE | WT - | SHEET 1 OF 1

REV A LTR | DWG NO. SKP18091 | B

Preliminary system studies indicated the following undesirable features of the proposed system (in regard to valves V-1 and V-2):

(a) P-2 would always have to be slightly higher than P-1 to present a control delta-pressure. This would continuously introduce a supply of He-Xe gas mixture into the BRU-R cycle process gas.

(b) The delta pressure between P-1 and P-3 should be kept very low (in the order of 0.2 to 0.5 in. H_2O) to preclude large He-Xe flows to the purge gas exit (P-3 or P-6).

(c) Due to possible face-seal leakage during transients or valve instabilities, the argon-oil gas mixture could be exhausted through the purge gas exit (P-3 and P-6) which would necessitate a formidable purge gas cleanup by NASA.

(d) Some He-Xe buffering gas could leak by the face-contact seals and exhausted to atmosphere with the argon-oil-mist lubrication.

The above difficulties stem from the very low pressure differential that can be developed across the labyrinth seals due to the desire to minimize the flow of the expensive He-Xe gas mixture. Breadboard testing of available contractor-designed components has shown that the design of valves V-1 and V-2 would be a difficult, if not impossible, task if control differential pressures in the order of 0.2 to 0.5 in. H_2O were to be maintained.

II. PRELIMINARY CLOSED-CYCLE COOLING SYSTEM DESIGN

Based on these difficulties, investigations were performed to explore other methods to lubricate the BRU-R and meet the stringent requirement of 0.07 lb of oil leakage into the cycle working fluid for 500 hr of operation. The system design objectives sought were:

(a) The system should be self-contained, with as few interfaces as possible.

(b) The gas in the oil-mist-lubrication system should be the same as the thermodynamic-cycle system gas to avoid mixing gases.

(c) The system should have stable operation during transient start-up and shutdown to prevent backflow of entrained oil into the BRU-R system process gas.

These investigations resulted in a closed-cycle lubrication and cooling system that is an extension of the Brayton cycle thermodynamic loop and is charged with the same gas mixture of helium and xenon. This lubrication and cooling system design is shown in Drawing SKP18117. The pressure in the bearing cavity (P_2) is maintained at a slightly lower pressure than either P_1 (at the shaft diameter of the compressor) or P_4 (at the shaft diameter of the turbine). This pressure differential will cause cycle gas to flow inward through the compressor and turbine face seals. The alternator cavity is pressurized from the compressor scroll discharge. System process gas will flow across the alternator radial seals due to the pressure drop (P_3 to P_2). The gas will be collected from the bearing cavity, cooled to approximately 100°F before entering a positive-displacement compressor, and then passed over a molecular sieve absorber. The scrubbed in-flow leakage gas is returned to the lowest pressure level in the closed Brayton cycle, the compressor inlet.

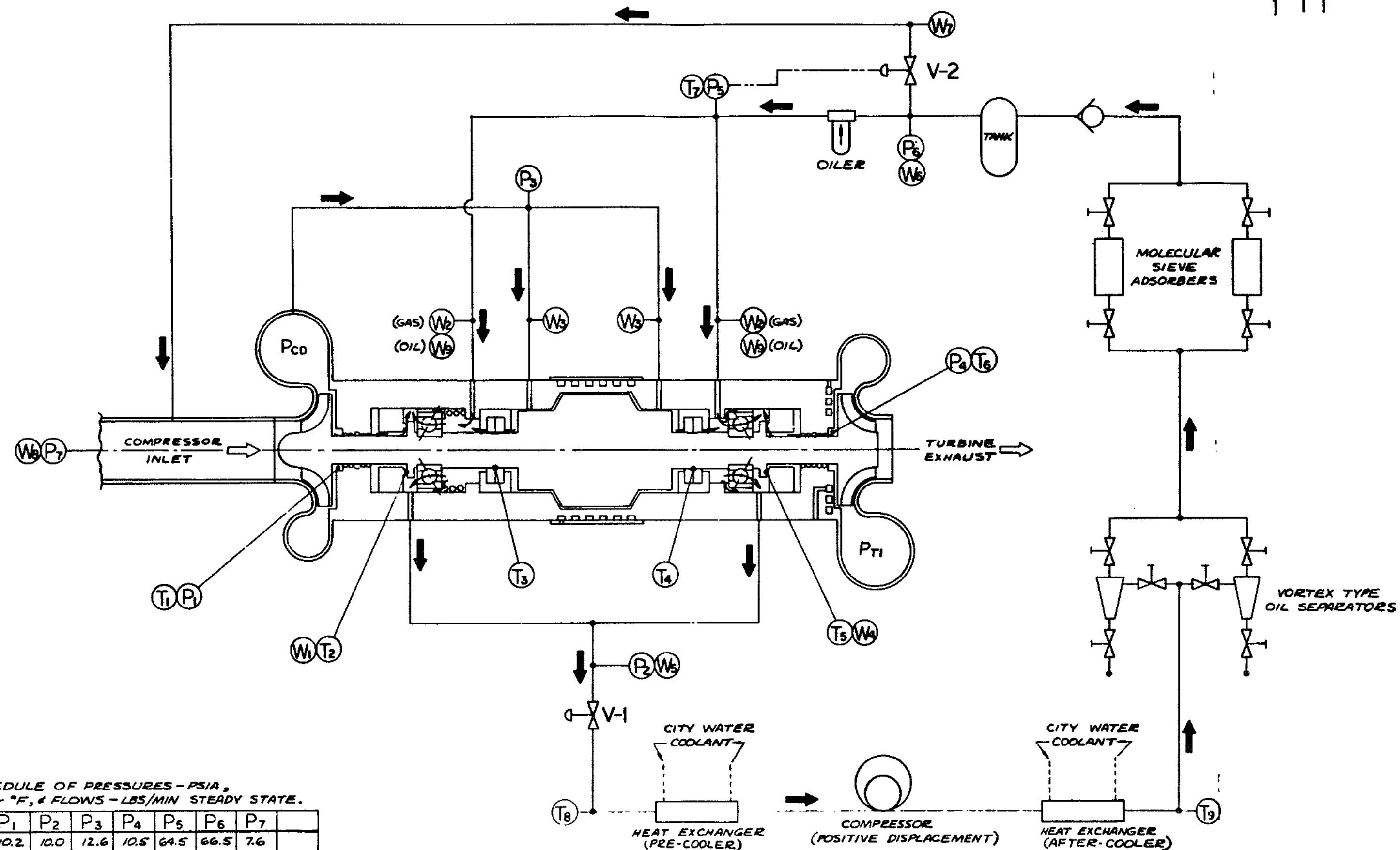

1. PROPOSED SCHEDULE OF PRESSURES – PSIA, TEMPERATURES – °F, & FLOWS – LBS/MIN STEADY STATE.

KW	P_{CD}	P_{T1}	P_1	P_2	P_3	P_4	P_5	P_6	P_7	
2.25	14.3	13.7	10.2	10.0	12.6	10.5	64.5	66.5	7.6	
6.0	27.1	25.8	19.1	18.9	25.1	19.8	64.5	66.5	14.3	
10.5	45.1	43.0	32.0	31.5	42.6	32.9	64.5	66.5	23.75	

KW	T_1	T_2	T_3	T_4	T_5	T_6	T_7	T_8	T_9	
2.25	230	300	300	320	500	1100	100	300	100	
6.0	240	300	300	320	500	1100	100	300	100	
10.5	240	350	350	350	500	1100	100	300	100	

KW	W_1	W_2	W_3	W_4	W_5	W_6	W_7	W_8	W_9	
2.25	.0127	1.845	.0907	.0177	3.902	3.69	.212	25.2	.0011	
6.0	.0145	1.845	.1455	.0327	4.028	3.69	.338	47.6	.0011	
10.5	.0341	1.845	.324	.0531	4.425	3.69	.735	79.2	.0011	

REVISIONS

ZONE	LTR	DESCRIPTION	DATE	APPROVED
	A	REVISED TO DATE		

UNLESS OTHERWISE SPECIFIED ON THIS DRAWING, FABRICATION OF THIS ITEM SHALL BE IN ACCORDANCE WITH AIRESEARCH SPECIFICATION SC-5535, STANDARD DRAWING INTERPRETATIONS.

LIST OF MATERIAL

AIRESEARCH MANUFACTURING COMPANY OF ARIZONA
A DIVISION OF THE GARRETT CORPORATION
PHOENIX, ARIZONA

DWG TITLE: SCHEMATIC, BRU-R

SIZE: D | CODE IDENT NO. 99193 | DWG NO. SKP18117

SKP18117

The flows across each of alternator seals are tabulated as W_3 in Drawing SKP18117 for the three power-level conditions. These flows were calculated by assuming a 0.001-in. radial gap at the seal lip diameter and, therefore, represent the maximum in-flow leakage to be expected. The total process gas in-flow to the BRU-R is represented by the sum of $W_1 + 2W_3 + W_4$. These are variables with respect to BRU-R speed (transient start and stop) and, of course, power-level operating conditions. The purposes of these gas in-flows are to preclude the possibility of oil finding its way into the process system gas and to keep the alternator cavity oil-free.

The main gas flow in the closed-cycle bearing lubrication/cooling system is the flow W_2 introduced at each bearing location. This is a gas-oil mist provided by the upstream oil fog device. The gas is introduced into each bearing cavity through a square-edged sonic orifice sized for the 10.5-kw_e power-level condition, so that the pressure ratio across the orifice $P_2/P_5 = 0.4881$. Thus, the upstream pressure $P_5 = 31.5/0.4881$ or 64.5 psia.

Lowering the value of P_2 for the other two power-operating conditions will not change the gas mass-flow across the sonic orifices. The value of W_2 is, thereby, a constant for each of the three power levels. This gas flow (for each bearing) is 1.845 lb/min. The total gas flow for bearing lubrication and cooling would then be $2W_2$, or 3.69 lb/min. The total oil-flow rate to be mixed with this gas-flow is $2W_9$, or 0.0022 lb/min. This gas-flow rate was based on air/oil-mist lubrication tests of 20- and 30-mm-bore-size bearings running at DN values of approximately 1,000,000. These tests described in Section 5 proved that bearings could operate very satisfactorily at DN values of 1,000,000 when supplied with an air/oil-mist ratio (by weight) of 400:1. For the 30-mm-bore-size bearings, 0.46 lb/min of a 400:1 air/oil mixture produced a bearing temperature rise of approximately 110°F. For the same approximate temperature rise of the

bearings--namely, 110°F--the following tabulated conditions would exist for two 30-mm-bore bearings (based on the Cp of the cooling gas used).

	Gas Specific Heat, Cp	Oil Flow Rate		Gas Flow Rate, ppm	Mixture Ratio, by weight
		gpm	ppm		
Air	0.241	1.02	0.0022	0.903	400:1
Argon	0.124	1.02	0.0022	1.755	780:1
He-Xe (Mol Wt 83.8)	0.059	1.02	0.0022	3.69	1640:1

It can be seen that the flow rate for the He-Xe gas is controlled by the value of the gas specific heat (Cp). The absolute values of oil flow are the same in each case, but the gas/oil-mixture ratio varies. Thus, the BRU-R will be essentially a gas-cooled machine, with just enough oil added to provide lubricity for the bearings.

The total collected gas outflow from the BRU-R bearing cavity (W_5) is equal to the sum of $W_1 + 2W_3 + W_4 + 2W_2$. These values, with the appropriate BRU-R bearing cavity pressures (P_2), are as follows:

Power Level, kw_e	P_2, psia	He-Xe Gas Flow, lb/min
2.25	10.0	3.902
6.0	18.9	4.028
10.5	31.5	4.425

III. INTERMEDIATE SYSTEM DESIGN

With the advent of the requirement to operate the BRU-R in the space chamber of the NASA Plum Brook SPF, the cooling and lubrication system underwent further study and analysis. Due to the severe environmental conditions of the space chamber, portions of the cooling system were remotely located from the BRU-R in a room at ambient environment.

The revised-cooling and lubrication system is shown in Figure B-1. The system schematic is very similar to that shown in Drawing SKP18117 and deviates basically in the relocation of valve V-1 and the tank to the compressor package. An additional glass wool filter has been incorporated in the compressor package. An automatic drain vortex oil separator is incorporated between the compressor after-cooler and the receiver. A heater and filter have been incorporated ahead of the oiler to control the temperature and contamination of the cooling gas after having been pumped through approximately 130 ft of pipe connecting the oiler and the molecular sieve absorbers.

AIRESEARCH MANUFACTURING COMPANY OF ARIZONA
A DIVISION OF THE GARRETT CORPORATION
PHOENIX, ARIZONA

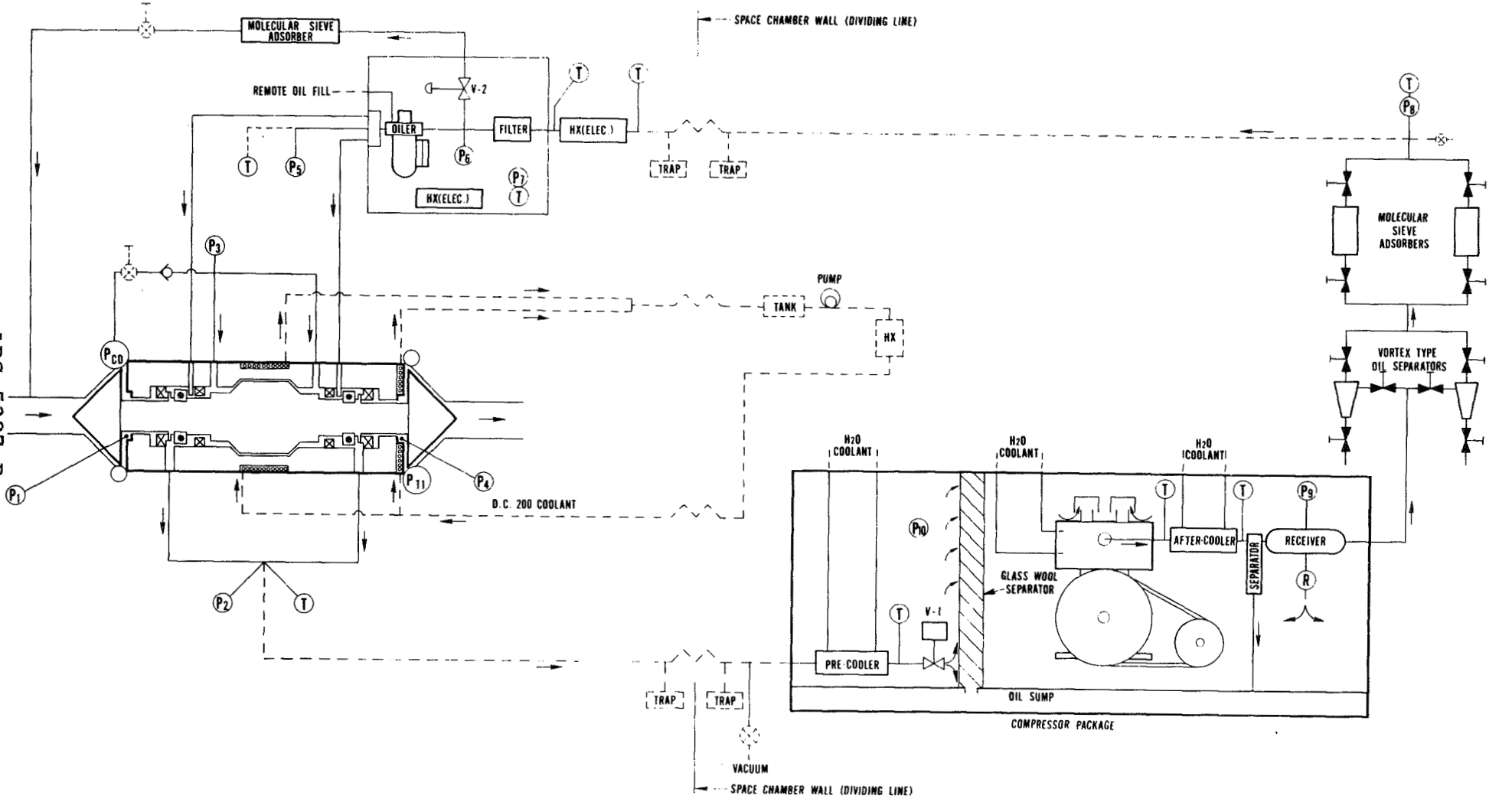

BRU-R LUBRICATION SCHEMATIC

FIGURE B-1

APPENDIX C

LIST OF FIGURES

LIST OF TABLES

DRAWINGS

APPENDIX C

RESEARCH COMPRESSOR COMPONENTS

The contract scope of work included the design, fabrication, and delivery of one set of research compressor parts to retrofit the Compressor Research Package (delivered under Contract NAS3-2778) with a backward-curved compressor impeller.

The 5.976-in. compressor impeller initially designed and provided for the Compressor Research Package was based on the second-stage radial impeller used in the Contractor Model 331 Engine, and a similar design is used in the Contractor T76 Turboprop Engine. Subsequently, the second stages of these engines were later redesigned with backward-curved exit blading. The 8.27-in. diameter impeller of the T76 Engine develops an efficiency of 85 percent at a pressure ratio of 2.10:1. Thus, it was the purpose of this task of the contract to apply the same design principles by scaling the T76 compressor to retrofit the Compressor Research Package.

I. BACKWARD-CURVED COMPRESSOR IMPELLER

The aerodynamic design of the backward-curved compressor impeller was performed by scaling the second-stage of the Contractor T76 Turboprop Engine using a 0.779 scale factor. The tip diameter of the scaled-down impeller is 6.442 in. in comparison to 5.976 in. of the radial-bladed wheel initially provided in the Compressor Research Package.

The compressor design values are tabulated in Table C-1. The total-to-total pressure ratio is 2.30, and the total-to-static pressure ratio is 2.43; the speed is 38,500 rpm. The specific work is 45.5 hp/lb/sec. The weight flow is 0.611 lb/sec. The specific speed is

TABLE C-1

BACKWARD-CURVED COMPRESSOR IMPELLER DESIGN VALUES

	P_{TDT}, psia	P_{STATIC}, psia	T_{TOTAL}, °R	η (up to location)
Inlet (Outside Blade)	6.00	5.68	536	- -
Impeller Exit (Mean)	14.8	10.68	794	0.905
Diffuser Inlet (Core)	14.7	11.14	794	0.897
Diffuser Exit (Core)	14.7	13.51	794	- -
Scroll Inlet (Mean)	13.86	13.61	794	0.828
Scroll Exit (Mean)	13.8	13.74	794	0.821

0.1057. The backward-curved compressor impeller velocity diagram is shown in Figure C-1 and the diffuser velocity diagram is shown in Figure C-2. The rotor and the stator physical dimensions are shown in Figure C-3.

A stress analysis of the 6.442-in. diameter backward-curved impeller was performed. The disk stress analysis of the scaled impeller is shown in Table C-2 and is graphically shown in Figure C-4. Scale factors applied to experimentally determined blade stresses in the full-scale T76 second-stage impeller show that the blade stress levels in the backward-curved impeller are approximately one-half of those existing in the T76 impeller. The blade stress scale factor was derived as follows:

$$\text{Centrifugal stress} = (\text{density})\ (\text{radius})^2\ (\text{speed})^2$$

where

Turbocompressor speed = 38,500 rpm

TPE speed = 41,700 rpm

Both impellers are fabricated of Titanium Alloy Ti-6Al-4V density = 0.16 $lb/in.^3$. Thus,

$$\sigma_T = \frac{0.16}{0.16}\ (0.779)^2\ (0.923)^2\ \sigma_O$$

$$= 0.517 \times \sigma_O$$

where

σ_T = centrifugal blade stress for turbocompressor

and σ_O = centrifugal blade stress for T76 impeller

IMPELLER INLET (INSIDE BLADE)

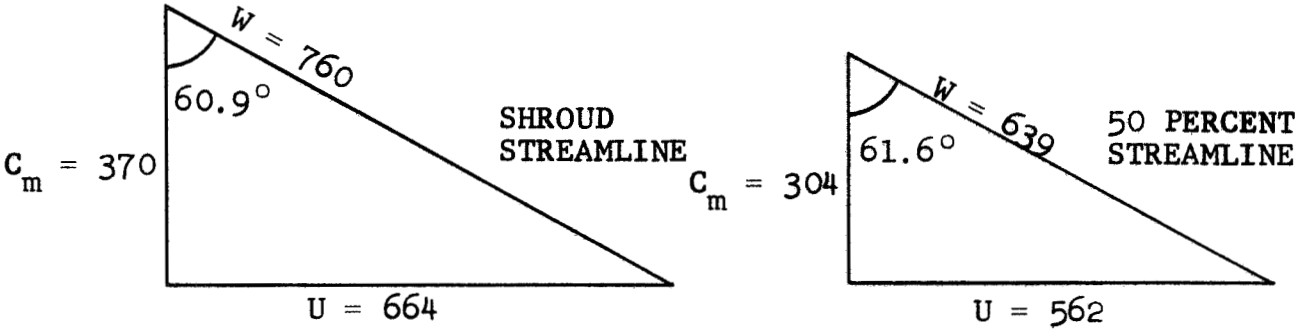

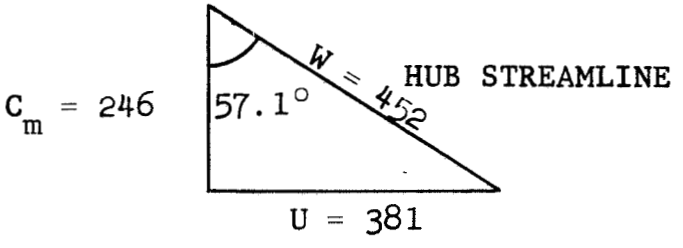

IMPELLER EXIT (MEAN VELOCITY INSIDE BLADE)

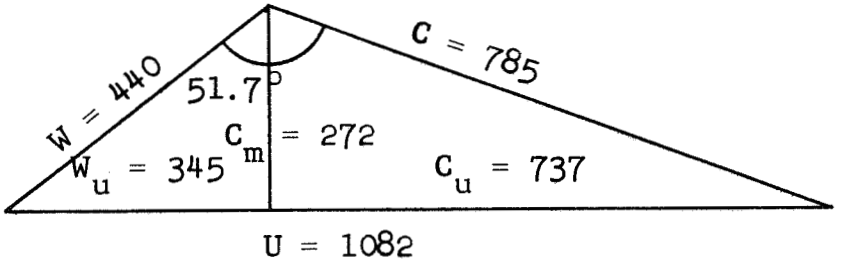

BACKWARD CURVED COMPRESSOR IMPELLER VELOCITY TRIANGLES
FIGURE C-1

A33317

DIFFUSER INLET (INSIDE BLADE)

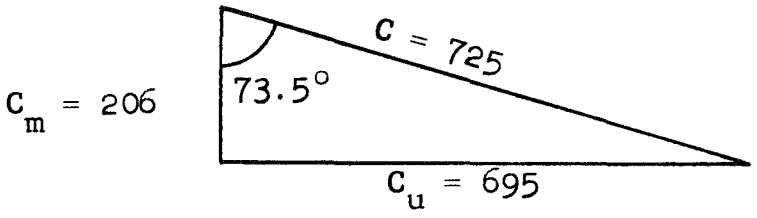

DIFFUSER EXIT (CORE VELOCITY INSIDE BLADE)

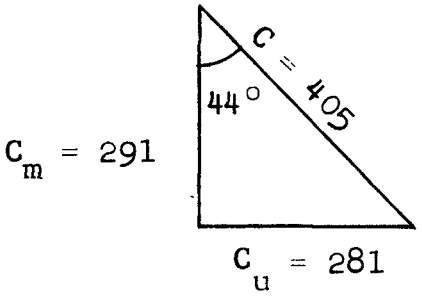

SCROLL INLET (MEAN VELOCITY)

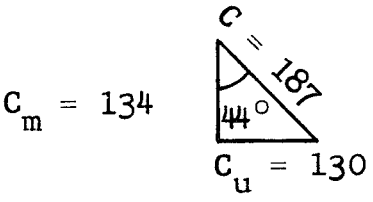

SCROLL EXIT MEAN VELOCITY 90 FT/SEC
YIELDING M_{EXIT} = .071

BACKWARD CURVED COMPRESSOR DIFFUSER VELOCITY TRIANGLES

FIGURE C-2

A33318

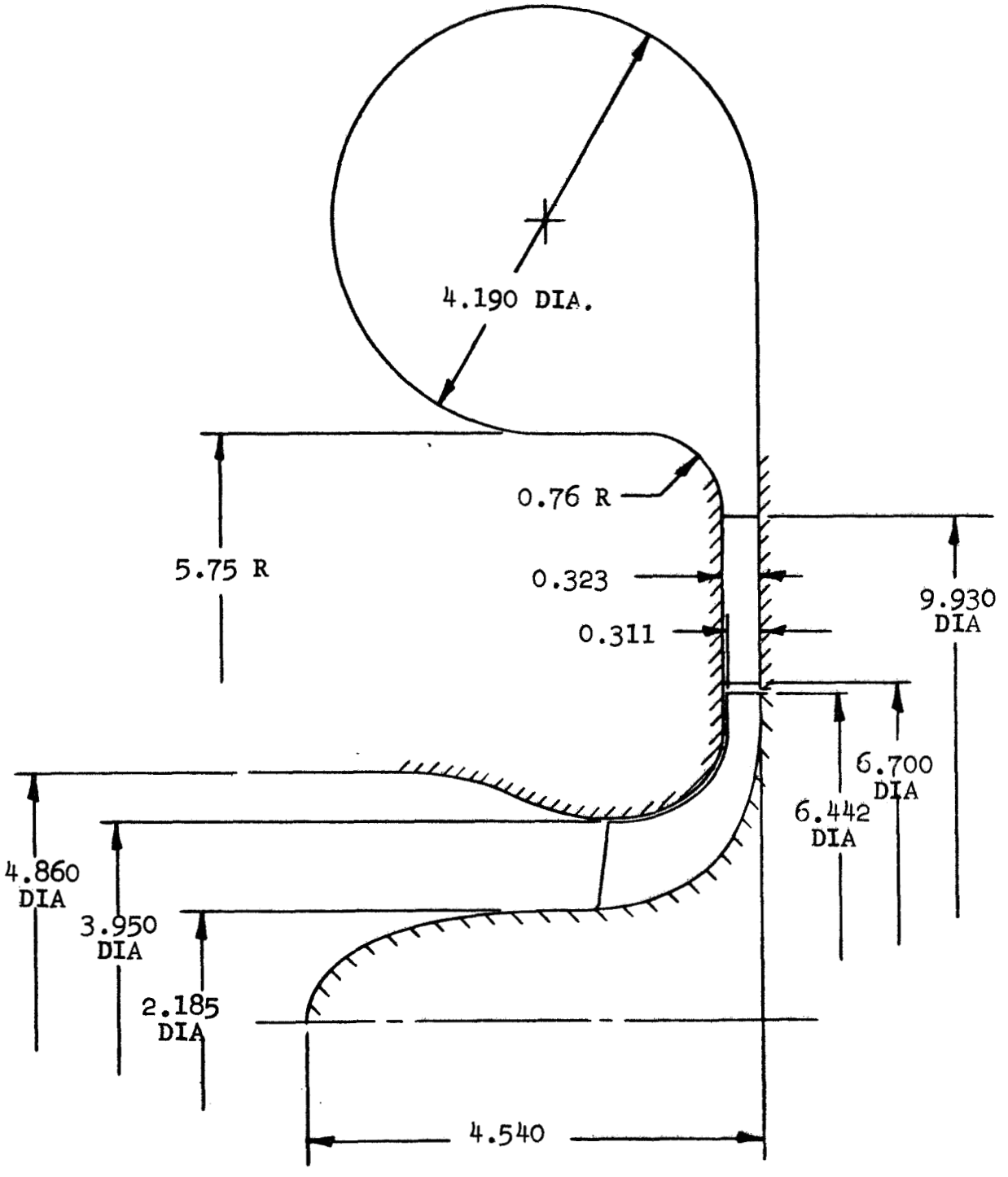

ROTOR AND STATOR PHYSICAL DIMENSIONS

FIGURE C-3

A33319

TABLE C-2

CALCULATED DATA FOR TITANIUM
BACKWARD-CURVED COMPRESSOR IMPELLER

Average tangential stress at 38,500 rpm	11,200 psi
Room-temperature burst-speed range (0.90 burst factor)	124,000 - 137,000 rpm
250°F burst-speed range (0.90 burst factor)	117,000 - 129,000 rpm
Room-temperature minimum disk yield speed	70,000 rpm
250°F minimum disk yield speed	66,000 rpm
Polar moment of inertia	0.015 in.-lb-sec^2
Diametral moment of inertia	0.010 in.-lb-sec^2
Weight	3.1 lb

NOTES: (1) CENTRIFUGAL STRESS ONLY
(2) MATERIAL = Ti - 6Al - 4V
(3) SPEED = 38,500 RPM
(4) SCALED FROM PN867520 USING A.779 SCALE FACTOR
(5) ALL STRESSES IN KSI
(6) AVERAGE TANGENTIAL STRESS = 11,200 PSI
(7) MAXIMUM TANGENTIAL STRESS = 35,600 PSI

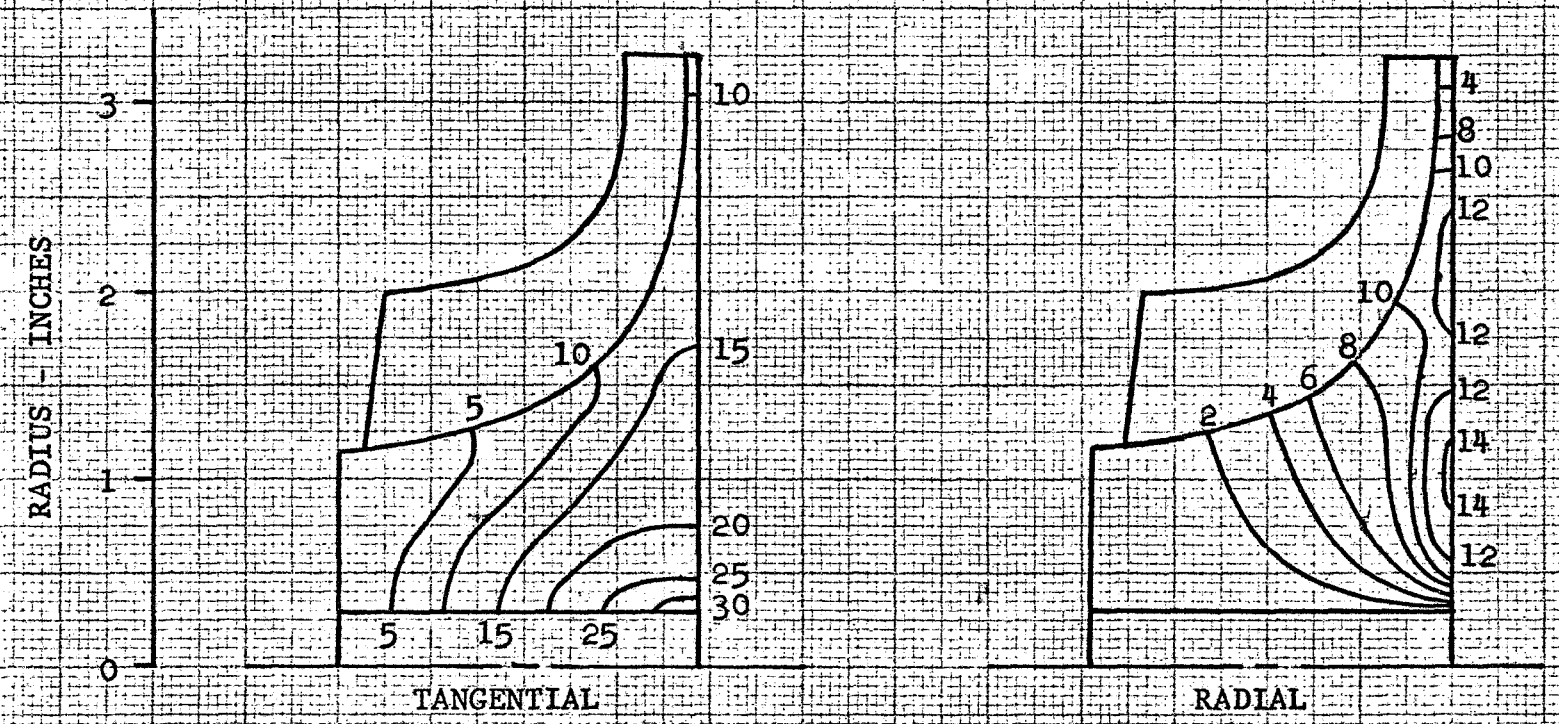

CALCULATED BY	3400	9-66	CENTRIFUGAL DISK STRESSES FOR BRAYTON COMPRESSOR	A33148
TRACED BY	FES	9-66		
CHECKED BY				
APPROVED BY			AiResearch Manufacturing Company of Arizona	
UNIT NO.				

P5109

FIGURE C-4

II. COMPRESSOR RESEARCH PACKAGE RETROFIT

The layout of the 6.442-in.-dia backward-curved compressor impeller, diffuser, and scroll, mounted on the existing NASA Compressor Research Package is shown in Drawing 699661. The scroll is fabricated of 347 Stainless Steel to minimize heat transfer by conduction from the scroll plenum section back along the shroud area toward the impeller inlet. The impeller is fabricated of titanium alloy 6Al-4V. The spinner, S/N 699625, is aluminum alloy 6061-T6. All other rotating parts are AlSl 4340 Steel, and all other stationary components are 347 Stainless Steel.

A steady-state thermal analysis of the compressor section of the retrofitted Compressor Research Package was performed. The cycle conditions for this analysis were that the impeller speed is 38,500 rpm, the inlet pressure (total) 6.0 psia, the inlet temperature 536°R, the system gas argon, the mass flow-rate is 0.61 lb/sec, and the compressor efficiency 83 percent. It was assumed that the compressor is perfectly insulated from ambient conditions. The other boundary conditions imposed were that the temperature of the main bearing housing was 145°F, and the temperature of the compressor-end bearing was 150°F at the inner race. The frictional heat generation in the compressor seal assembly was assumed to be 100 w.

The results of the thermal analysis are shown in Figure C-5. It is of interest to note the temperature gradient along the impeller shroud and the very small heating effect on the impeller-eye inlet gas. This analysis should prove useful during research package testing as an aid to determine heat balance for efficiency records.

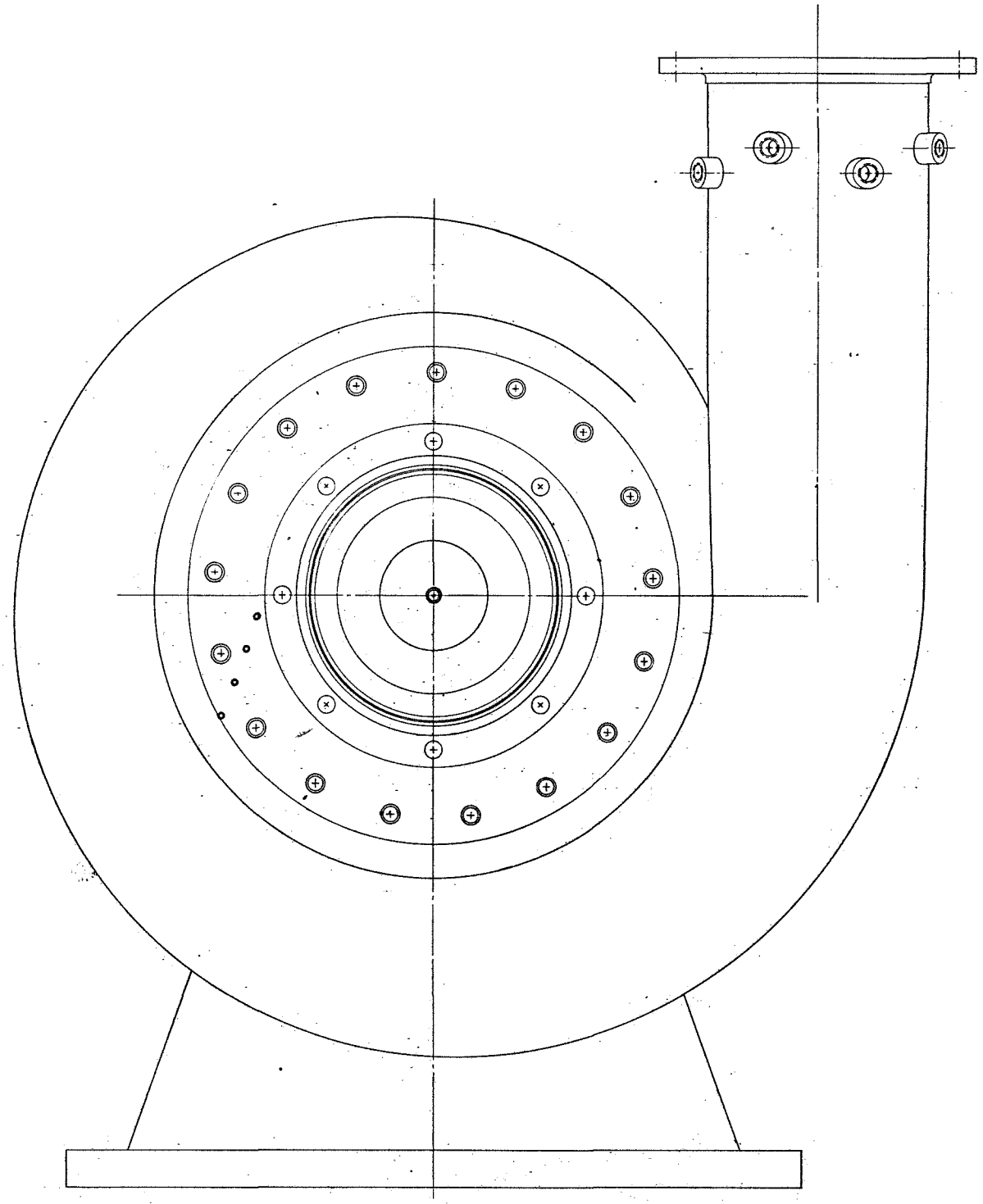

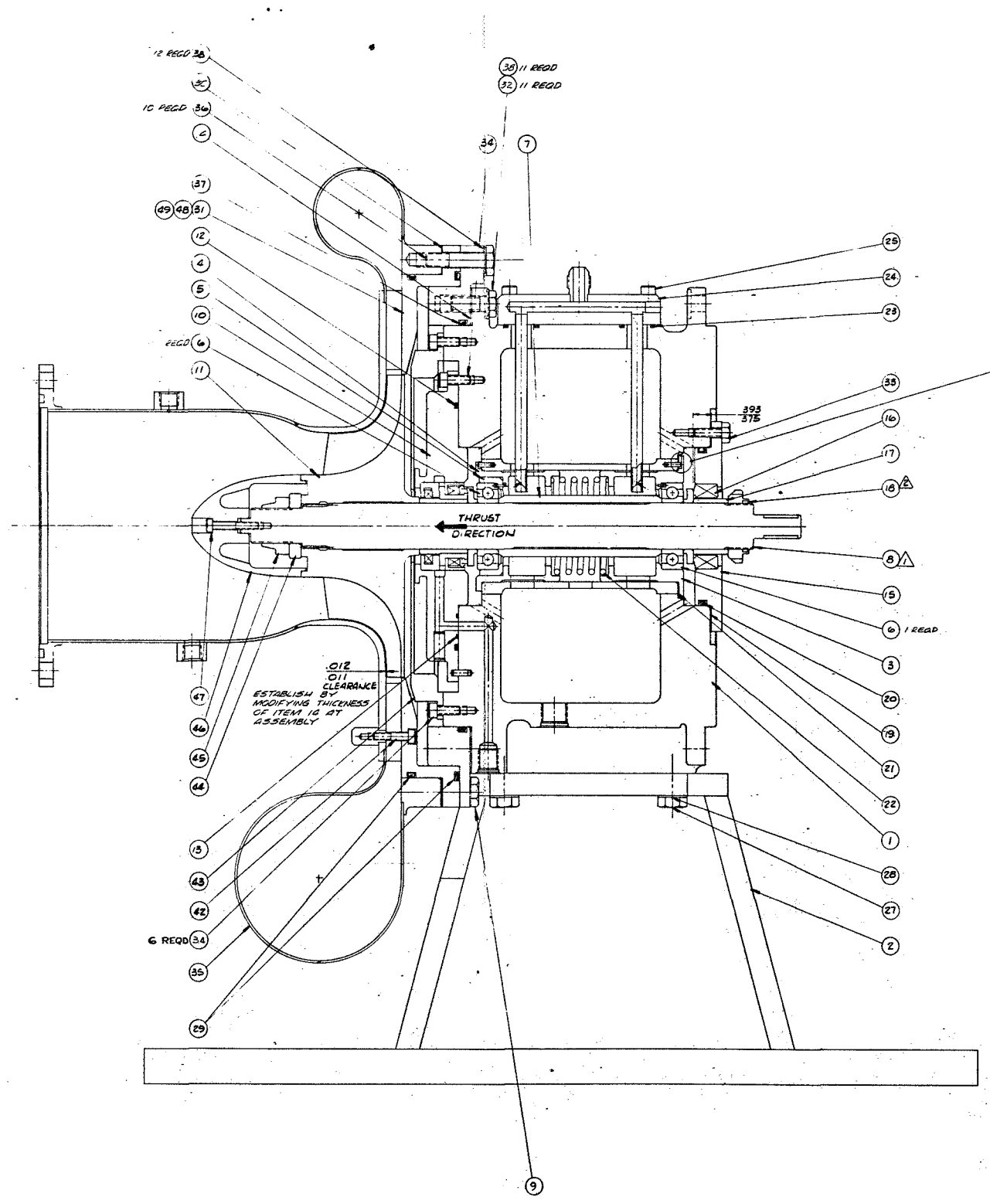

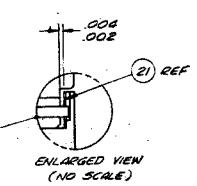

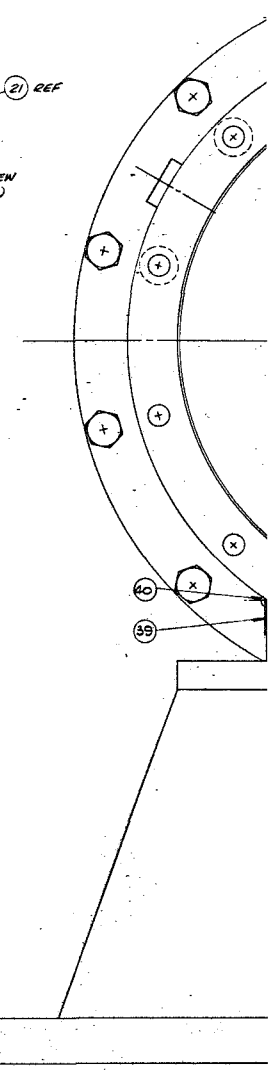

6. SIMILAR TO 369731

5. FOR TORQUE REQUIREMENT SEE AIRESEARCH SPEC. AP DEVELOPED FROM SELF-LO BE ADDED TO FASTENER MUST BE DETERMINED FASTENER.

4. LOCKWIRE PER MS 33540

△2 VENDOR ITEM: SEE APPLI SOURCE CONTROL DRAWI

△3 TIGHTEN NUT ITEM (18) O 300-350 IN-LBS TORQUE.

△1 APPLY △2 473-010-9001 L PRIOR TO ASSEMBLY.

699661

SHEET 1 OF 1

ZONE	LTR	REVISIONS DESCRIPTION	DATE	APPROVED
	A	ITEM REVISION - SEE E.O.	9/14/67	
	B	REVISED PARTS LIST (SEE E.O.)	9/6/67	

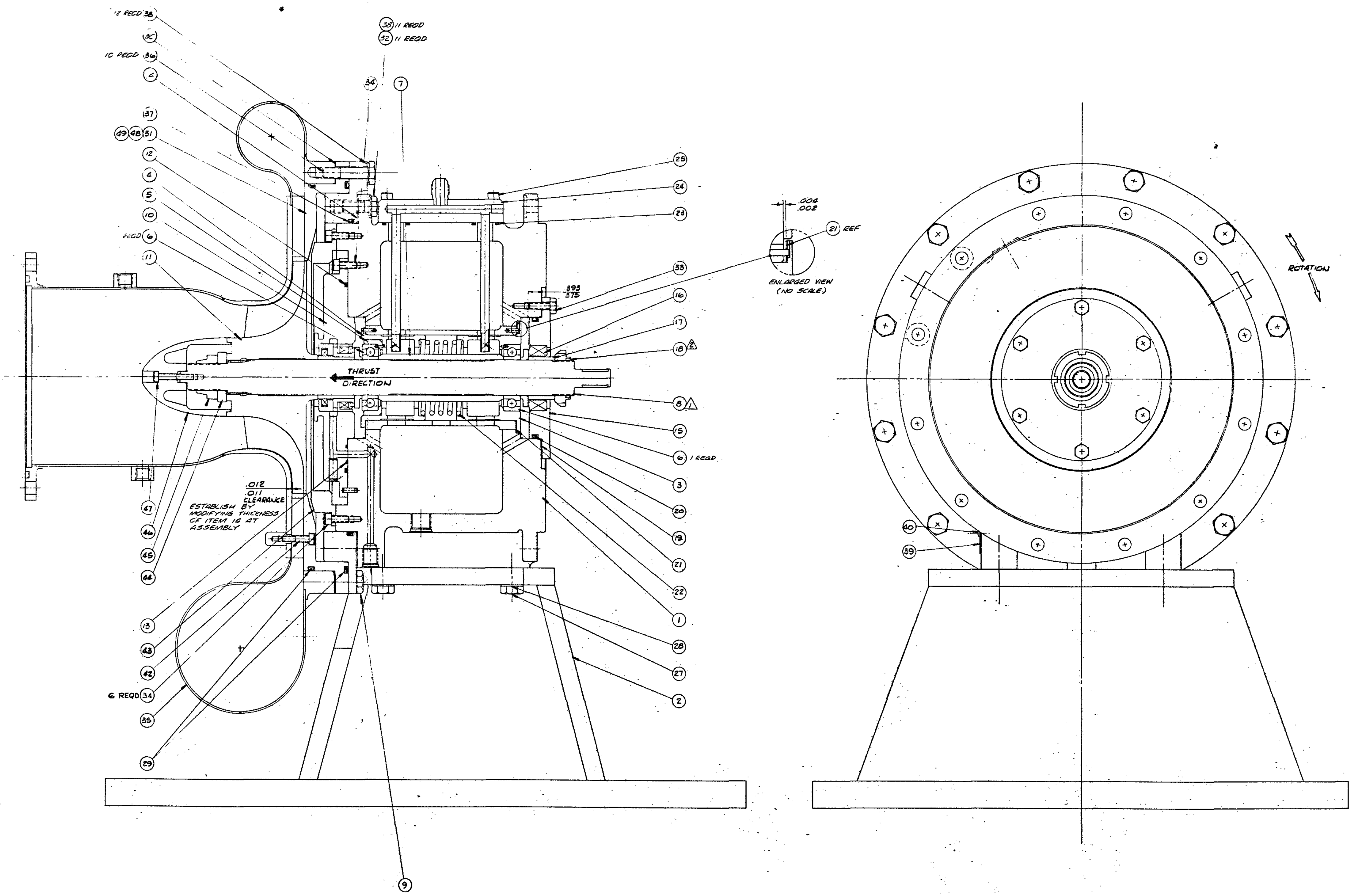

6. SIMILAR TO 369731

5. FOR TORQUE REQUIREMENT ON THREADED FASTENERS SEE AIRESEARCH SPEC. AF-349. THE FRICTION TORQUE DEVELOPED FROM SELF-LOCKING DEVICES IS TO BE ADDED TO FASTENER LOADING TORQUE AND MUST BE DETERMINED FOR EACH FASTENER.

4. LOCKWIRE PER MS33540

3 VENDOR ITEM: SEE APPLICABLE SPECIFICATION OR SOURCE CONTROL DRAWING.

2 TIGHTEN NUT ITEM (18) ON SHAFT ITEM (8) TO 300-350 IN-LBS TORQUE.

1 APPLY 1 473-010-9001 LUBE TO THDS OF NOTED ITEMS PRIOR TO ASSEMBLY.

APS-5327-R
Appendix C
Page 10

QTY REQD -3	QTY REQD -2	QTY REQD -1	ITEM NO.	PART NO.	DESCRIPTION	ZONE
1			49	699892-3	DIFFUSER ASSY SET, MATCHED	4
	1		48	699892-2	DIFFUSER ASSY SET, MATCHED	9
1	1	1	47	NAS1352C06LN16	SCREW	9
1	1	1	46	699625-1	SPINNER, COMPRESSOR	9
1	1	1	45	699635-1	NUT SELF LOCKING	9
1	1	1	44	699629-1	WASHER	9
1	1	1	43	699664-1	SHIELD	9
17	17	17	42	NAS1352C06LN12	SCREW	9
			41			
2	2	2	40	MS24630-2	SCREW	5
1	1		39	SEE NOTE 699660-1-2-3	IDENTIFICATION PLATE	5
23	23	23	38	AN960C516L	WASHER	9/5
1	1	1	37	MS17413-173	PACKING	9/5
10	10	10	36	AN5 H-12A	BOLT	9
1	1	1	35	699623-1	SCROLL ASS'Y, COMPRESSOR	9
8	8	8	34	MS24673-2	SCREW	8
6	6	6	33	AN3CH5A	SCREW	6
11	11	11	32	AN5 H-5A	BOLT	
		1	31	699892-1	DIFFUSER ASSY SET, MATCHED	9
			30			9
2	2	2	29	MS17413-275	PACKING, 'O' RING	9
4	4	4	28	AN960C616	WASHER	6
4	4	4	27	AN6CH10A	SCREW	6
			26			
4	4	4	25	MS24673-5	SCREW	6
1	1	1	24	369728	NOZZLE ASSEMBLY, OIL	6
2	2	2	23	MS29561-015	PACKING, "O" RING	6
1	1	1	22	111917	SPRING	6
AR	AR	AR	21	369743-1-2-3	SHIM, BEARING CARRIER	6
1	1	1	20	MS29561-235	PACKING	6
AR	AR	AR	19	369744-1-2-3	SHIM	6
1	1	1	18	525-577-9006	NUT	6
1	1	1	17	369723	SPACER	6
1	1	1	16	358319	SEAL, AIR-OIL	6
1	1	1	15	369727	CARRIER, SEAL	6
1	1	1	14	699628-1	SHIM	9
2	2	2	13	362-522-9002	SEAL	9
1	1	1	12	362506-9012	SEAL	9
1	1	1	11	699622-1	IMPELLER, COMPRESSOR	9
1	1	1	10	369753	SEAL ASSEMBLY, CARBON	9
2	2	2	9	AN5H7A	BOLT	5
1	1	1	8	699662-1	SHAFT ASSEMBLY, IMPELLER	6
1	1	1	7	369732	SPACER, BEARING	8
2	2	2	6	358313	BEARING, BALL	9
1	1	1	5	369733	MOUNT, BEARING, RESILIENT	9
1	1	1	4	369735	CARRIER, BEARING	9
1	1	1	3	369734	CARRIER, BEARING	6
1	1	1	2	699663-1	STAND ASSEMBLY, MOUNTING	6
1	1	1	1	369722	HOUSING ASSEMBLY, MAIN	6
-3	-2	-1	← ASSY			

LIST OF MATERIAL

REQD	NEXT ASSY	USED ON
1(-3)	FINAL	699660-3
1(-2)	FINAL	699660-2
1(-1)	FINAL	699660-1

SIGNATURES / DATES: DFT C. W. WARNER 5-21-67; CHK 4-21-67; 4-26-67; MATL E. Kornerand 4-26-67; STRESS 4-26-67; 4-27-67

UNLESS OTHERWISE SPECIFIED ON THIS DRAWING, FABRICATION OF THIS ITEM SHALL BE IN ACCORDANCE WITH AIRESEARCH SPECIFICATION SC-5535, STANDARD DRAWING INTERPRETATIONS.

AIRESEARCH MANUFACTURING COMPANY OF ARIZONA
A DIVISION OF THE GARRETT CORPORATION
PHOENIX, ARIZONA

DWG TITLE: COMPRESSOR ASSEMBLY, RESEARCH PACKAGE

SIZE J | CODE IDENT NO. 99193 | DWG NO. 699661

SCALE 1/1 | WT — | SHEET 1 OF 1

DWG NO. 699661 SHEET 1 OF 1

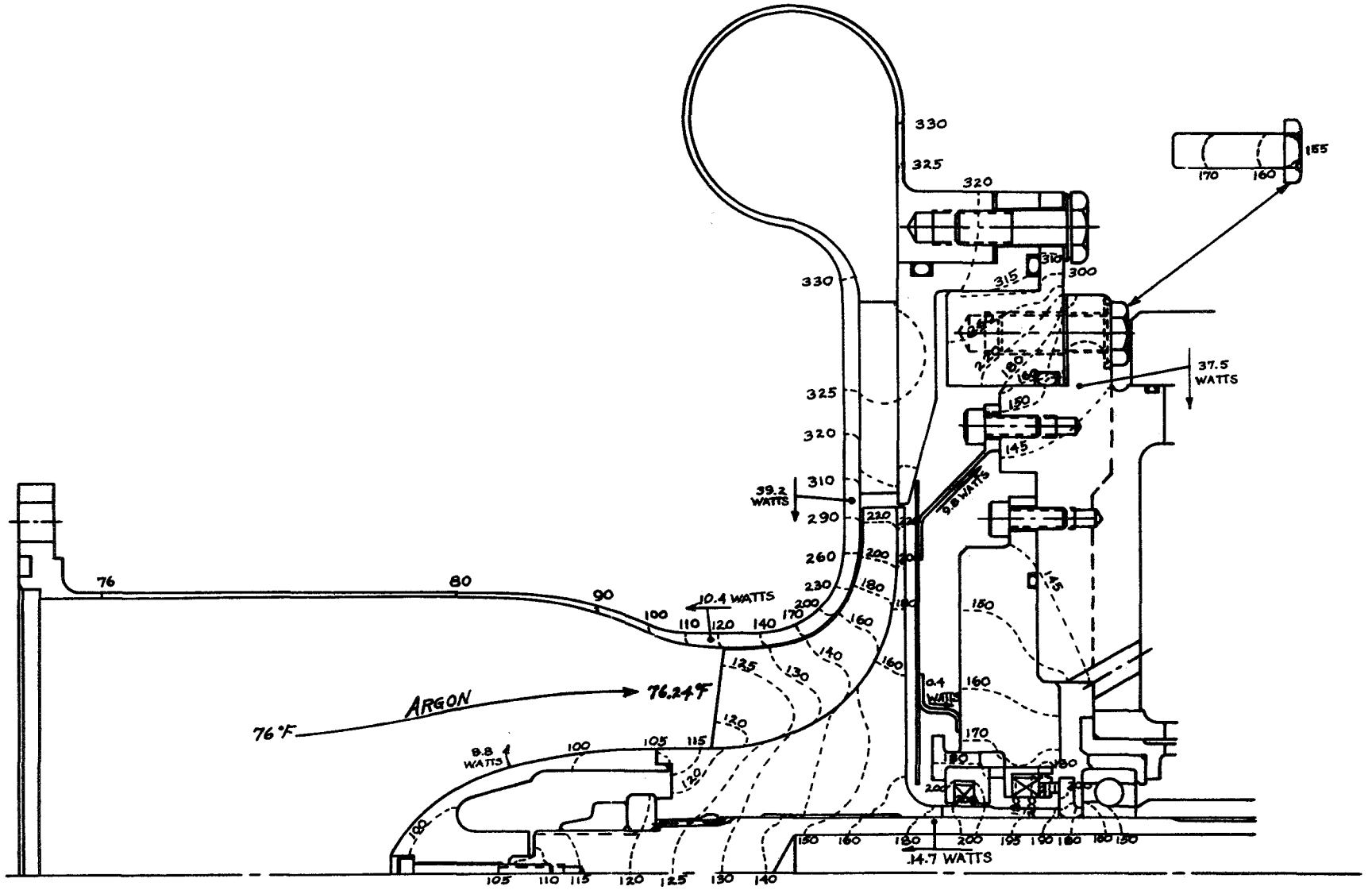

NASA - BRU COMPRESSOR RESEARCH PACKAGE

STEADY-STATE TEMPERATURES
(ISOTHERMAL LINES IN °F)

PERTINENT HEAT FLOWS (WATTS)

FIGURE C-5

APPENDIX D

DRAWINGS AND SCHEMATICS

1. Drawing 699220 BRU-R Lubrication and Cooling System Flow Schematic (Sheet 1 of 2)

2. Drawing 699190 Contacting-Type Carbon Nose Seal

3. Drawing 303913 Thermocouple Locations in the BRU-R

REVISIONS				
ZONE	LTR	DESCRIPTION	DATE	APPROVED

LEGEND	
CLEAN GAS	
OIL/GAS	
COOLING WATER	
CUSTOMER SUPPLIED	
COMPRESSED AIR	

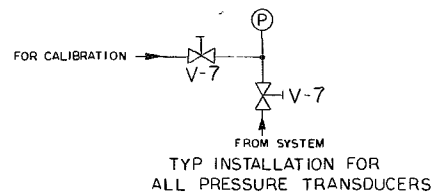

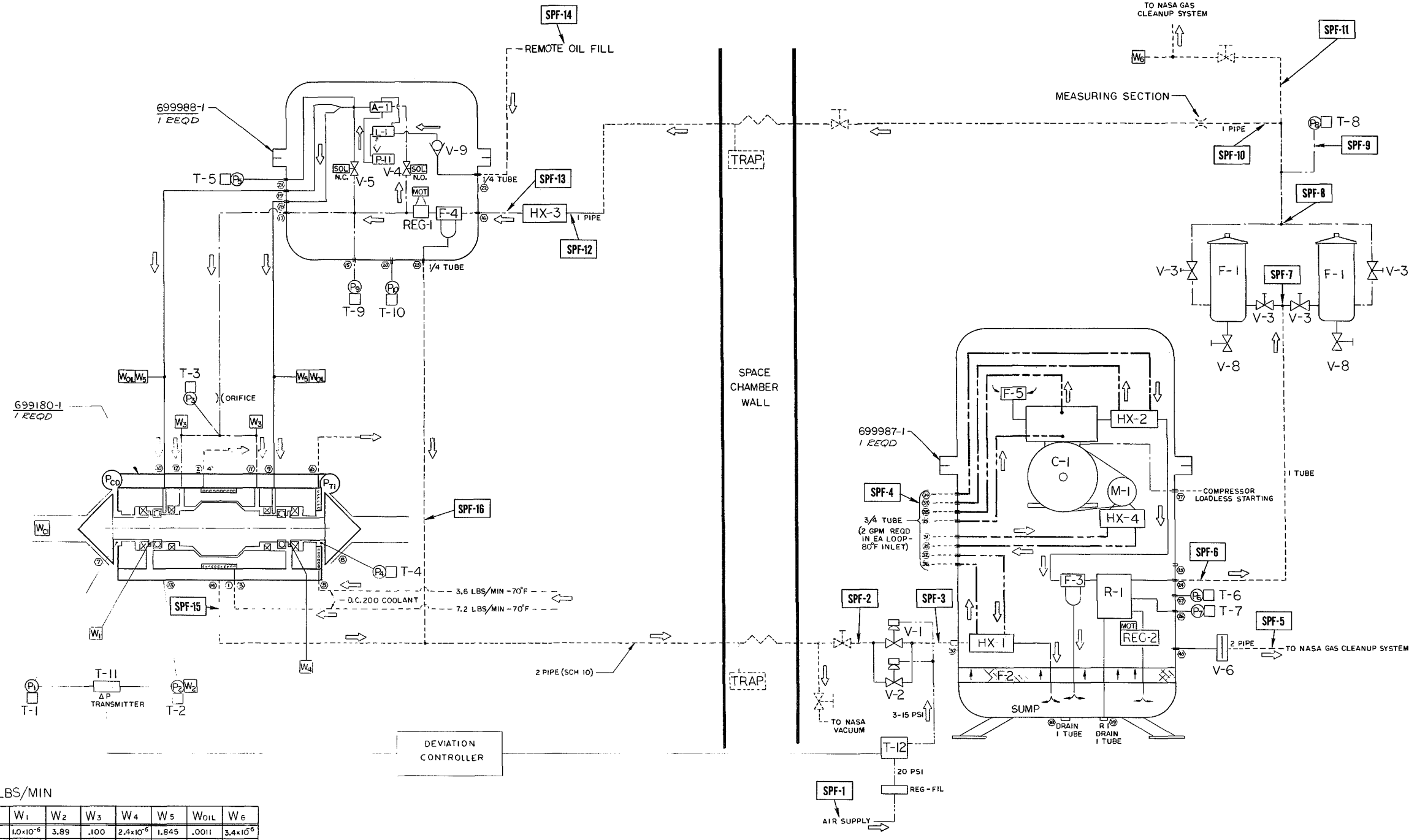

FLOW-LBS/MIN

KW	W_{C1}	W_1	W_2	W_3	W_4	W_5	W_{OIL}	W_6
2.25	25.2	1.0×10^{-6}	3.89	.100	2.4×10^{-6}	1.845	.0011	3.4×10^{-6}
6.0	47.6	2.0×10^{-6}	3.89	.100	8.5×10^{-6}	1.845	.0011	10.5×10^{-6}
10.5	79.2	8.0×10^{-6}	3.89	.100	20.0×10^{-6}	1.845	.0011	28.0×10^{-6}

PRESSURE-PSIA

KW	P_{CD}	P_{T1}	P_1	P_2	P_3	P_4	P_5	P_6
2.25	14.3	13.7	10.2	10.0	11.0	10.5	64.5	8.0
6.0	27.1	25.8	19.1	18.9	19.6	19.8	64.5	8.0
10.5	45.1	43.0	32.0	31.5	32.0	32.9	64.5	8.0

1. FOR ELECTRICAL SCHEMATIC SEE DWG # 304065-1

QUANTITY REQD	ITEM NO.	PART NO.	SYM	DESCRIPTION	CODE IDENT	MATERIAL AND SPECIFICATION	UNIT WT	ZONE
← ASSY				PARTS LIST				

"UNLESS OTHERWISE SPECIFIED ON THIS DRAWING, FABRICATION OF THIS ITEM SHALL BE IN ACCORDANCE WITH AIRESEARCH SPECIFICATION 503535, STANDARD DRAWING INTERPRETATIONS."

SIGNATURES	DATES
DR	5-24-68
CHK	10-17-68
MFG	
MATL	
STRESS	
AERO	
APPD	5-27-68
APPD	
DESIGN ACTIVITY APPD	10-21-68
OTHER ACTIVITY APPD	

REQD NEXT ASSY | USED ON | FINAL
HEAT TREATMENT | PROCESS
HARDNESS AND SPEC | BASIC AND SPEC

AIRESEARCH MANUFACTURING COMPANY OF ARIZONA
A DIVISION OF THE GARRETT CORPORATION
PHOENIX, ARIZONA

DWG TITLE
SCHEMATIC, SYSTEM, LUBRICATION AND COOLING, BRU-R

SIZE E | CODE IDENT NO. 99193 | DWG NO. 699220
SCALE NONE | WT | SHEET 1 OF 2

699220
REV

ZONE	LTR	REVISIONS DESCRIPTION	DATE	APPROVED
	A	ADDED RELEASE HOLES - SEE E.O.		

OPERATING CONDITIONS

MEDIUM	MONATOMIC GAS - MOLECULAR WEIGHT = 83.8
PRESSURE	SEE TABLE AT RIGHT
SPEED	36,000 RPM
LIFE	500 HRS MIN.
OVERSPEED	43,200 RPM FOR 5 MINUTES
MAX. LEAKAGE	SEE TABLE AT RIGHT
AMBIENT TEMP	400 °F

PRESSURES - PSIA

CONDITION	P_1	P_2	P_3
2.25 KW	10.0	10.2	10.5
6.0 KW	18.9	19.1	19.8
10.5 KW	31.5	32.0	32.9

LEAKAGE (MAX.)-LBS/MIN.

CONDITION	P_2 TO P_1	TEMP °R	P_3 TO P_1	TEMP °R
2.25 KW	.01270	760	.01770	960
6.0 KW	.01445	760	.03270	960
10.5 KW	.03410	810	.05310	960

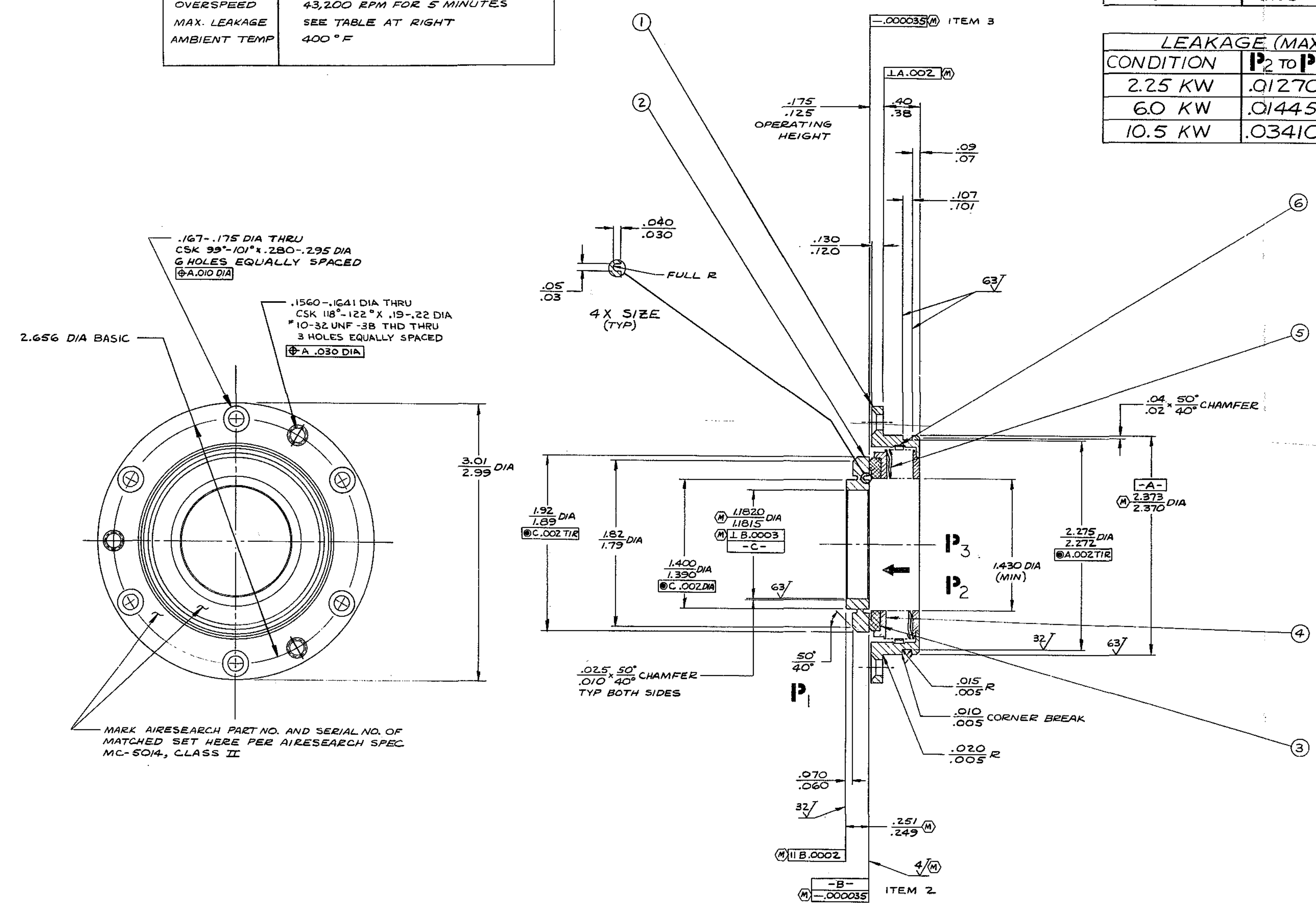

7. THE SEAL NOSE LOAD IN DIRECTION OF ARROW WILL BE 2.5 POUNDS AT .150 OPERATING HEIGHT.

6. THE SEAL ASSY WILL BE DESIGNED WITH A 52% TO 57% PRESSURE OVERBALANCE (IN DIRECTION OF ARROW).

5. THE FOLLOWING ITEMS MUST BE LISTED ON MEASURED DATA SHEET REQ'D BY AIRESEARCH CLASSIFICATION OF CHARACTERISTICS:
ROTOR (ITEM 2) MATERIAL AND HARDNESS
NOSE (ITEM 3) CARBON GRADE

4. VENDOR WILL PERFORM A LEAKAGE CHECK OF WELDED SEAL ASSY (EXCLUDING NOSE, ITEM 3), BY EVACUATING ASSY TO 25 INCHES OF MERCURY. ANY PERCEPTIBLE LEAKAGE, INDICATED BY A PRESSURE CHANGE, IN 5 MINUTES SHALL BE CAUSE FOR REJECTION.

3. ITEMS 2, 4 AND 5 SHALL BE STABILIZED AT 650°F.

2. BELLOWS SPRING RATE TO BE 10-30 LBS/IN. INSTRON CHARTS OF SPRING RATE WILL BE FURNISHED BY VENDOR FOR EACH SEAL.

1. A VIBRATION DAMPER MUST BE INCORPORATED AND WILL CONTACT AT LEAST 3 CONVOLUTIONS AT APPROX MID-SPAN OF BELLOWS AT OPERATING HEIGHT. AN ADDITIONAL DAMPER MAY BE INCORPORATED AT NOSE CARRIER AT VENDORS OPTION.

15. THESE PARTS TO BE MANUFACTURED, INSPECTED, STOCKED AND SOLD AS REPLACEMENT PARTS IN MATCHED SETS ONLY.

14. (C) DESIGNATES CRITICAL CHARACTERISTIC
(M) DESIGNATES MAJOR CHARACTERISTIC

13. PROCUREMENT SOURCE(S) PER ASL 222122

12. ALL DESIGN AND PART NUMBER CHANGES REQUIRE PRIOR AIRESEARCH APPROVAL.

11. ONLY THE ITEM DESCRIBED ON THIS DRAWING WHEN PROCURED FROM THE VENDOR(S) LISTED HEREIN IS APPROVED BY AIRESEARCH MANUFACTURING COMPANY OF ARIZONA, PHOENIX, ARIZONA FOR USE IN THE APPLICATION(S) SPECIFIED HEREON. A SUBSTITUTE ITEM SHALL NOT BE USED WITHOUT PRIOR TESTING AND APPROVAL BY AIRESEARCH MANUFACTURING COMPANY OF ARIZONA OR BY THE GOVERNMENT PROCURING ACTIVITY.

10. DRAWING REVISIONS FOR SUBSTITUTE ITEMS SHALL NOT BE MADE WITHOUT PRIOR APPROVAL BY AIRESEARCH MANUFACTURING COMPANY OF ARIZONA.

9. IDENTIFY PACKAGING WITH AIRESEARCH PART NUMBER.

8. PARTS PROCURED BY VENDOR PART NUMBER SHALL BE PROCURED IN ACCORDANCE WITH THIS AIRESEARCH SOURCE CONTROL DRAWING.

LIST OF MATERIAL

QUANTITY REQD	ITEM NO.	PART NO.	DESCRIPTION	MATERIAL AND SPECIFICATION
1	6		DAMPER	OPTIONAL -
1	5		BELLOWS ASSY	CRES - AMS 5548 (AM350)
1	4		CARRIER	INVAR - 42% NICKEL
1	3		NOSE	
1	2		ROTOR	
1	1		CASE	CRES-AMS 5646 (AISI 347)
-1		← ASSY		

	NEXT ASSY	USED ON
1(-1)	699671-2	699670-2
2(-1)	699181-1	699180-1

SIGNATURES / DATES: 8-23-67; 10-4-67; 10-4-67

CRITICAL ITEM

UNLESS OTHERWISE SPECIFIED ON THIS DRAWING, FABRICATION OF THIS ITEM SHALL BE IN ACCORDANCE WITH AIRESEARCH SPECIFICATION SC-5535, STANDARD DRAWING INTERPRETATIONS.

AIRESEARCH MANUFACTURING COMPANY OF ARIZONA
A DIVISION OF THE GARRETT CORPORATION
PHOENIX, ARIZONA

SEAL & ROTOR SET, MATCHED

SIZE E | CODE IDENT NO. 99193 | DWG NO. 699190 | REV A

SCALE 4/1 | SHEET 1 OF 1

PART NO. 303913-1

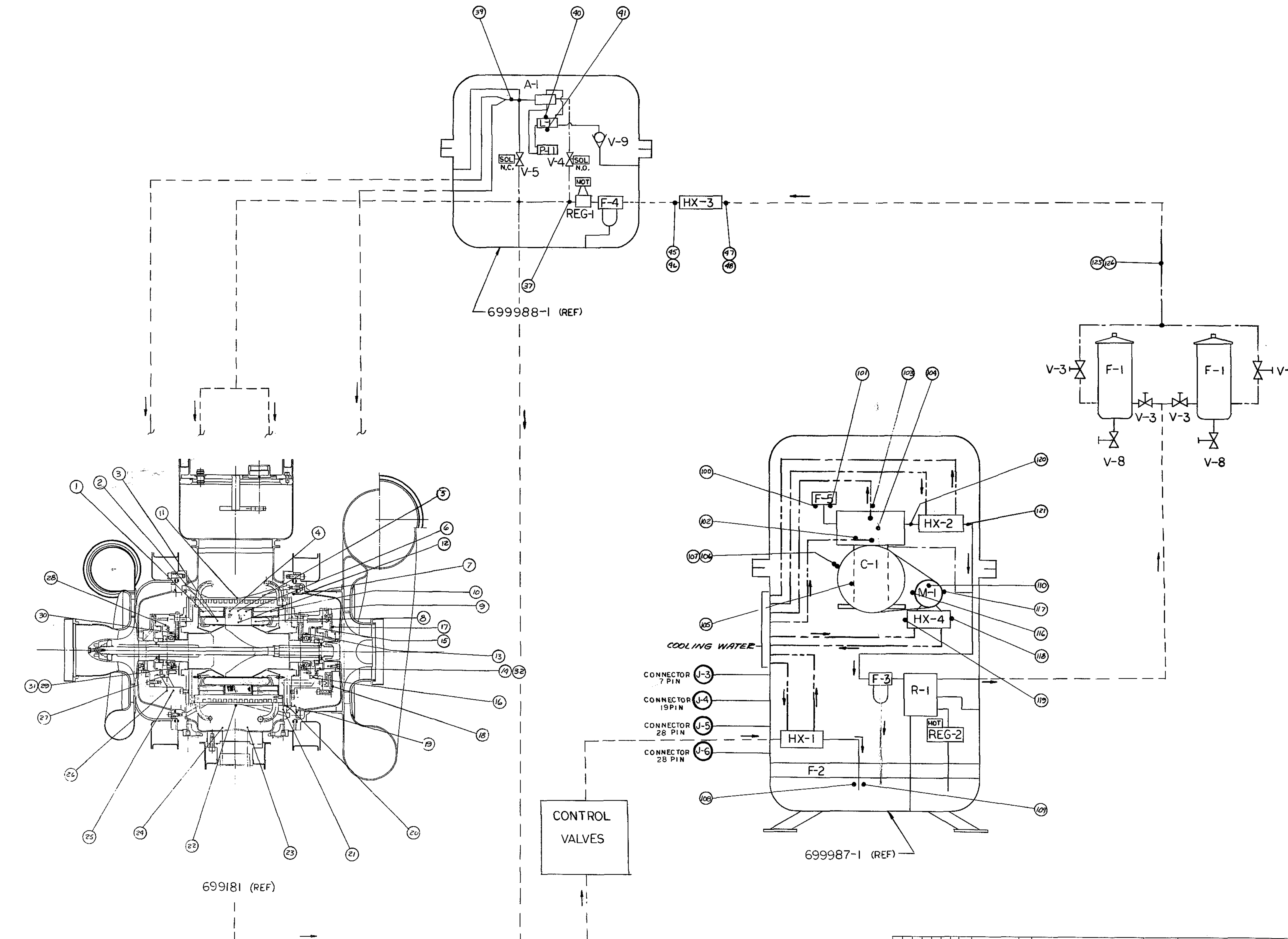

2. SHALL CONFORM TO AIRESEARCH SPEC SC6000 INTERPRETATION OF DRAWINGS.

1. NUMBERS DESIGNATED THUS (XX) REPRESENT THERMOCOUPLE LOCATION.

UNLESS OTHERWISE SPECIFIED ON THIS DRAWING, FABRICATION OF THIS ITEM SHALL BE IN ACCORDANCE WITH AIRESEARCH SPECIFICATION SC5535, STANDARD DRAWING INTERPRETATIONS.

AIRESEARCH MANUFACTURING COMPANY OF ARIZONA, A DIVISION OF THE GARRETT CORPORATION, PHOENIX, ARIZONA

SCHEMATIC, THERMOCOUPLE LOCATION, BRU-R

1(-1) 309065-1 | 699220-1 (NEXT ASSY | USED ON)

SIZE E | CODE IDENT NO. 99193 | DWG NO. 303913

SCALE NONE | SHEET 1 OF 1

BRAYTON CYCLE

FINAL REPORT DISTRIBUTION LISTS
FOR CONTRACT NAS 3-9428

NASA Lewis Research Center
21000 Brookpark Road
Cleveland, Ohio 44135
Attention:

Contract Manager (5 + reproducible)
Mail Stop 500-201

Brayton Project Office (25)
Mail Stop 500-201

H. O. Slone
Mail Stop 500-201

D. R. Packe
Mail Stop 500-201

R. E. English
Mail Stop 500-201

B. Lubarsky
Mail Stop 3-3

J. E. Dilley
Mail Stop 500-309

D. G. Beremand
Mail Stop 500-201

W. T. Wintucky
Mail Stop 500-201

V. Hlavin
Mail Stop 3-14

P. A. Thollot
Mail Stop 500-201

A. S. Valerino
Mail Stop 500-202

H. A. Shumaker
Mail Stop 77-2

W. L. Stewart
Mail Stop 77-2

W. J. Anderson
Mail Stop 23-2

L. P. Ludwig
Mail Stop 23-2

Library (2)
Mail Stop 60-3

Report Control Office
Mail Stop 5-5

Reliability and Quality Assurance Office
Mail Stop 500-111

Technology Utilization Office
Mail Stop 3-19

NASA Lewis Research Center
Plum Brook Station
Taylor Road
Sandusky, Ohio 44870
Attention:

J. C. Nettles
Mail Stop 1441-1

D. B. Fenn
Mail Stop 1441-1

R. C. Nussle
Mail Stop 1441-1

D. H. Baldwin
Mail Stop 1441-1

A. O. Ross
Mail Stop 1441-1

National Aeronautics and
Space Administration
Washington, D.C. 20546
Attention:

P. R. Miller
Code RNP

H. D. Rochen
Code RNP

NASA Scientific and Technical
Information Facility
Post Office Box 5700
College Park, Maryland 20740
Attention:

Acquisitions Branch
(SQT-34054)

NASA Ames Research Center
Moffett Field, California 94033
Attention: Library

NASA Flight Research Center
Post Office Box 273
Edwards, California 93523
Attention: Library

Jet Propulsion Laboratory
4800 Oak Grove Drive
Pasadena, California 91103
Attention: Library

NASA Langley Research Center
Langley Station
Hampton, Virginia 23365
Attention: Library

NASA Manned Spacecraft Center
Houston, Texas 77058
Attention: Library
A. Redding - EP-5

NASA Goddard Space FlightCenter
Greenbelt, Maryland 20771
Attention: Library

NASA Marshall Space Flight Center
Marshall Space Flight Center, Ala.
Attention: Library 35812

Aerojet-General Corporation
1100 West Hollyvale
Azusa, California 91702
Attention: Library

Aerospace Corporation
Post Office Box 95085
Los Angeles, California 91745
Attention: Library

AiResearch Manufacturing Co.
402 South 36th Street
Phoenix, Arizona 85034
Attention: Library
Lyle Six
R. Gildersleeve
B. B. Heath
D. Luther

AiResearch Manufacturing Co.
9851 Sepulveda Boulevard
Los Angeles, California 90009
Attention: Library

AiResearch Manufacturing Co.
2525 W. 190 Street
Torrance, California 90509
Attention: Library

Battelle Memorial Institute
505 King Avenue
Columbus, Ohio 43201
Attention: Library

Bendix Research Labs Division
Detroit, Michigan 48232
Attention: Library

Boeing Company
Aerospace Division
Post Office Box 3707
Seattle, Washington 98124
Attention: Library

Borg-Warner Corporation
Pesco Products Division
24700 North Miles Road
Bedford, Ohio 44146
Attention: Library

Bureau of Naval Weapons
Department of the Navy
Washington, D.C. 20025
Attention: Code RAPP

Continental Aviation and
Engineering Corporation
12700 Kercheval Avenue
Detroit, Michigan 48215
Attention: Library

Curtiss-Wright Corporation
Wright Aero Division
Main and Passaic Streets
Woodridge, New Jersey 07075
Attention: Library

General Dynamics Corporation
16501 Brookpark Road
Cleveland, Ohio 44142
Attention: Library

General Electric Company
Mechanical Technology Laboratory
R&D Center
Schenectady, New York 12301
Attention: Library

General Electric Company
Space Division
Cincinnati, Ohio 45215
Attention: Library

General Electric Company
Re-entry and Environmental Sys. Div.
3198 Chestnut Street
Philadelphia, Pa. 19104
Attention: Library

General Motors Corporation
Indianapolis, Indiana 46206
Attention: Library

Hughes Aircraft Corporation
Centinda and Teale Avenue
Culver City, California 90230
Attention: Library

Institute for Defense Analyses
400 Army-Navy Drive
Arlington, Virginia 22202
Attention: Library

Lear Siegler, Inc.
3171 S. Bundy Drive
Santa Monica, California 90406
Attention: Library

Lockheed Missiles and Space Co.
Post Office Box 504
Sunnyvale, California 94088
Attention: Library

McDonnell-Douglas Astronautics Co.
5301 Bolsa Avenue
Huntington Beach, California
Attention: Library 92647

McDonnell-Douglas Astronautics Co.
3000 Ocean Park Boulevard
Santa Monica, California 90406
Attention: Library

Massachusetts Institute of
Technology
Cambridge, Massachusetts 02139
Attention: Library

Mechanical Technology Incorporated
968 Albany-Shaker Road
Latham, New York 12110
Attention: Library

North American Rockwell Corp.
Space Division
12214 Lakewood Boulevard
Downey, California 90241
Attention: Library

Northern Research and
Engineering Co.
219 Vassar Street
Cambridge, Massachusetts 02139
Attention: Library

Power Information Center
University of Pennsylvania
3401 Market Street, Room 2107
Philadelphia, Pensylvania 19104

Solar
Division of International Harvester
2200 Pacific Highway
San Diego, California 92112
Attention: Library

Space Systems Division
Los Angeles Air Force Station
Los Angeles, California 90045
Attention: Library

Sundstrand Denver
2480 West 70 Avenue
Denver, Colorado 80221
Attention: Library

TRW Accessories Division
23555 Euclid Avenue
Cleveland, Ohio 44117
Attention: Library

TRW Systems
One Space Park
Redondo Beach, California 90278
Attention: Library

U.S. Army Engineer R&D Labs
Gas Turbine Test Facility
Fort Belvoir, Virginia 22060
Attention: W. Crim

United Aircraft Corporation
Pratt & Whitney Aircraft Div.
400 Main Street
East Hartford, Conn. 06108
Attention: Library

United Aircraft Research Lab
East Harford, Conn. 06108
Attention: Library

Westinghouse Electric Corp.
Astronuclear Laboratory
Post Office Box 10864
Pittsburgh, Pennsylvania 15236
Attention: Library

Williams Research
Walled Lake, Michigan 48088
Attention: Library